THE SEDIMENT BUDGET OF A HIGHLY ERODIBLE CATCHMENT. THE RIVER ISÁBENA (EBRO BASIN, CENTRAL PYRENEES)

BALANÇ DE SEDIMENT D'UNA CONCA ALTAMENT EROSIONABLE. EL RIU ISÀBENA (CONCA DE L'EBRE, PIRINEU CENTRAL)

JOSÉ ANDRÉS LÓPEZ TARAZÓN

THE SEDIMENT BUDGET OF A HIGHLY ERODIBLE CATCHMENT. THE RIVER ISÁBENA (EBRO BASIN, CENTRAL PYRENEES)

BALANÇ DE SEDIMENT D'UNA CONCA ALTAMENT EROSIONABLE. EL RIU ISÀBENA (CONCA DE L'EBRE, PIRINEU CENTRAL)

PhD Thesis

Tesi Doctoral

PhD presented by

JOSÉ ANDRÉS LÓPEZ TARAZÓN

to obtain his Doctoral Degree by the University of Lleida

Memòria presentada per

JOSÉ ANDRÉS LÓPEZ TARAZÓN

per optar al títol de Doctor per la Universitat de Lleida

Departament de Medi Ambient i Ciències del Sòl

Universitat de Lleida

The PhD Supervisor:

El Director de la Tesi:

Dr. Ramon J. Batalla

Departament de Medi Ambient
i Ciències del Sòl
Universitat de Lleida

The PhD Co-Supervisor:

El Co-Director de la Tesi:

Dr. Damià Vericat

Àrea d'Hidrologia
Centre Tecnològic Forestal
de Catalunya

Lleida, 17 de Gener de 2011

Note

This file contains papers that have been revised and modified according to the comments made by the referees. Results of the work have not changed after the revisions and publication, although some figures and tables have been redrawn.

Als que estan però, sobretot, als que marxaren

AGRAÏMENTS

Qui hauria dit fa 6 anys, quan vaig arribar a Lleida amb un munt de dubtes sobre la meva vàlua per fer una Enginyeria Superior, que estaria escrivint aquestes línies d'agraïment a tots aquells sense els quals no hauria pogut fer la present tesi. Per cert, no m'hauria imaginat mai que seria tan difícil escriure això, com puc expressar la meva gratitud?

Primer que res vull donar les gràcies (i quasi bé disculpes per tots els mals de cap que els he donat) a les persones més importants per la consecució d'aquesta tesi. Ells dos foren els que m'ajudaren a descobrir la meva vocació i tenir clar el que vull ser de gran: els meus directors (i amics), Ramon Batalla i Damià Vericat. Qui s'hauria pensat Ramon, arran d'aquella visita que vaig fer al teu despatx als inicis de 2006 per demanar-te una idea per fer el projecte final de carrera, que a finals de 2010 hauríem fet aquesta tesi. Moltes gràcies a tots dos per la ingent quantitat d'hores que m'heu dedicat (al camp i al despatx), tan des de Lleida com des de la llunyania (ja sigui a Gales, a Nova Zelanda o a qualsevol lloc del mon), la quantitat de mals de cap que haureu tingut per culpa meva, la quantitat de "deadlines" que no he complit i m'heu sabut tolerar, el número de bolis vermells que haureu gastat corregint els abstracts, papers, informes que us enviava i el gran recolzament que m'heu donat en aquells moments de "bajón" (que hi han hagut, i uns quants) i tantes altres coses que no he sabut expressar en paraules i gràcies a les quals he pogut fer açò que teniu entre mans. Gràcies als dos de tot cor i, tant de bo, això es pugui mantenir durant molts anys.

Un altre que ha hagut d'aguantar carros i carretes ha sigut aquell que ha conviscut amb mi la major part del temps, tant al camp (anàvem els 2 plegats), com al laboratori (estem taula amb taula) com, fins i tot, a casa (compartint pis). Aquest és l'Álvaro Tena. La veritat és que no sé que dir-te a part de gràcies per tot el que m'has suportat: els meus "vinagres", les meves anades d'olla, les meves discussions sense solució final... Tot i això, també han hagut molts moments bons i crec que ens ho hem passat molt bé. Com els hi deia al Ramon i al Damià, moltes gràcies de tot cor i, ja saps que, per al que vulguis, ací em trobaràs. Per cert, hem d'anar pensat en el "first draft" del llibre sobre totes les anècdotes, històries i contratemps que ens han passat (de tots els colors) al

camp, així com un manual de tot el que no s'ha de fer quan treballes a un riu.... i ànims amb la tesi, que no et queda res!

Com oblidar-me de la resta del grup RIUS: Cristina, Laura, Gemma, Jordi, David. No m'hauria pas pensat mai que podríem arribar a ser tanta gent treballant en Geomorfologia fluvial (i derivats) a la Universitat de Lleida i el Centre Tecnològic Forestal de Catalunya. Gràcies a tots per suportar-me (i el que us queda per suportar) i ajudar-me en tot el que heu pogut. Per la meva part, espero haver-vos ajudat en alguna cosa (si no ho he fet més és perquè no he pogut) i poder continuar ajudant-vos d'ara estant. Dintre d'aquest grup, i encara que no l'he citat abans, voldria destacar especialment al Carles Balasch, que és una de les persones més destacades de RIUS (encara que no sé si ell n'és conscient); moltes gràcies Carles pel teu suport, per tot el que m'has ensenyat durant aquest anys i per tota l'ajuda que m'has donat de manera totalment altruista; espero poder continuar treballant i col·laborant amb tu.

Moltes son les institucions i organismes que m'han permès treballar durant els últims 4 anys: l'Agència de Gestió d'Ajuts Universitaris i de Recerca (AGAUR, Generalitat de Catalunya) que mitjançant l'ajut FI per la contractació de personal investigador novell (co-finançat amb el Fons Social Europeu) m'ha donat un sou amb el que viure i, posteriorment amb les beques BE per fer estades de recerca fora de Catalunya, em finançà l'estada de recerca a Melbourne; la Confederació Hidrogràfica de l'Ebre (CHE) i el seu "Sistema Automàtico de Información Hidrológica" (SAIH) que em permeteren instal·lar els meus aparells a les seves infraestructures i em donaren tota mena de suport i dades necessàries i imprescindibles per la consecució d'aquesta tesi; el Ministerio de Ciencia e Innovación (MICINN) que mitjançant el seu programa CICYT vaig poder incrementar la meva formació al participar en 2 projectes de recerca a l'Ebre ("Diseño y aplicación de crecidas generadoras como estrategia de reequilibrio hidro-sedimentario en ríos regulados" acrònim FF3 i "Desarrollo y experimentación de un sistema de crecidas de mantenimiento en cascada con base en criterios físicos y económicos para la mejora hidrosedimentaria del bajo Ebro y sus principales afluentes" acrònim FF4); el Centre Tecnològic Forestal de Catalunya que m'acollí i em donà totes les facilitats possibles (i més) durant els mesos que vaig passar allà. A tots ells, moltes gràcies per la vostra col·laboració.

Tampoc puc deixar d'agrair a la Universitat de Lleida, i al Departament de Medi Ambient i Ciències del Sòl, que em donaren un lloc on fer la tesi. Gràcies Pedro per permetre'm entrar al laboratori d'Agrometeorologia al 2006; gràcies Clara per arreglar tota la paperassa que t'he fet arribar i sol·lucionar-me tots els problemes que t'he portat i sempre amb un somriure a la cara (si no fos per tu, no sé que seria de nosaltres); gràcies Montse per aconseguir-me tot allò que t'he demanat durant aquests temps. Gràcies a tots aquells del DMACS/UdL que, d'una manera o un altra, m'heu suportat aquests anys i m'heu ajudat a realitzar aquesta tesi.

I would like to thank to the SESAM group and the people of the University of Potsdam too. Thanks a lot for making me part of this group and trust me to develop my PhD Thesis on the framework of the SESAM. Special thanks to: Prof. Axel Bronstert who allowed me to do a 2-month research stay on the University of Potsdam at Golm and Till Francke, who spent (and continues spending) a lot of his time teaching me how to deal with not-enough-good-data to obtain good results. Thanks a lot Till for your help and support (at least now, you know that 2 am is a good time to sample at the field).

The group led by Patrick Lane and Gary Sheridan of the Department of Forest and Ecosystem Science of the University of Melbourne let me to develop my longest research stay with them. Special thanks to Hugh Smith (my former supervisor during my stay) that initiated me in the fingerprinting topic and introduced me into the big city of Melbourne (despite my bad English). Thanks a lot to Phil Noske and Chris Sherwin for sharing with me their office and Pat Michael, Peter, Jane, Rachel for considering me as part of their group.

Special thanks are also given to Chris Gibbins for his help and support during my thesis. Thanks Chris for introducing me into the eco-geomorphology topic and for being prepared to spent a night sampling at the field with Ramon and me during your holidays; thanks a lot for reviewing all the documents we have sent you during these years. I hope to continue working with you at the projects you share with us and in all the new projects we could get together.

Moltes gràcies també a tots aquells companys i amics que m'ajudaren durant la durada de la meva tesi (principalment des del punt de vista personal), encara que no fossin

conscients del que feren: Silvia Pérez, Nacho, Ana, Silvia Gómez, Cristina Lafragüeta, Jorge (Gargallo), Jorge (Iñesta), Quique, Sabina, Nuria... i tants altres que desgraciadament no em vindran al cap i no sortiran a aquestes línies. Voldria agrair especialment a Alberto Sánchez, company de laboratori durant el meu primer any de tesi i amb ajuda del qual vaig poder instrumentar la conca (durant el més dur de l'estiu) i tirar endavant molta feina (durant el més dur del hivern; te'n recordes del "trenca-gels"?). Llàstima que sigui tan tossut i no s'hagi volgut dedicar a la recerca... (no tot anaven a ser paraules maques, no Alberto?).

Donar les gràcies també a totes aquelles persones que han suggerit canvis, retocs o millores de l'esborrany de tesi, així com als revisors externs (Joan Estrany i Joaquim Farguell) i al conjunt de membres del tribunal (titulars i suplents) per l'interès mostrat per aquest treball i la seva col·laboració per a què hagi arribat al final (especialment a Joan Verdú i Xavier Úbeda).

Abans d'acabar, agrair i demanar disculpes a tots aquells que m'ajudaren i que, per culpa de la meva mala memòria, no sortiran a aquests paràgrafs.

Per últim (però no menys important), voldria donar les gràcies a aquells que sempre m'han recolzat, encara que després de tants anys no tinguin clar que és el que faig: els meus pares, el meu germà, la meva cunyada i els meus nebots. Gràcies per haver-me donat suport per damunt de tots els inconvenients (les dificultats econòmiques, la llunyania...) i per haver entès que el que faig és el que m'agrada, malgrat que no hagi sigut mai capaç d'explicar bé en què treballo. Gràcies per haver-me aixecat en aquells moments difícils, de soledat, de "bajón", de llunyania... que els han hagut (i molts). Gràcies per haver tolerat la meva fredor habitual, el no trucar per telèfon quasi bé mai (tot i que sempre us tenia en ment), la meva absència a moltes celebracions familiars, els meus oblits de dates importants... I, sobre tot, gràcies per, malgrat tot, estar orgullosos de mi. Si d'alguna cosa n'estic segur és de que, sense vosaltres, no hauria sigut capaç de fer aquesta tesi.

INDEX

ANNEX 1

1. Introduction

2. Suspended sediment model development

Francke, T., López-Tarazón, J.A., Schröder, B., 2008. Estimation of suspended sediment concentration and yield using linear models, random forests and quantile regression forests. *Hydrological Processes*, **22**: 4892-4904.

ANNEX 2

1. Introduction

2. Suspended sediment model application

Francke, T., López-Tarazón, J.A., Vericat, D., Bronstert, A., Batalla, R.J., 2008. Flood-based analysis of high-magnitude sediment transport using a non-parametric method. *Earth Surface Processes and Landforms*, **33**: 2064-2077.

CHAPTER 1
INTRODUCTION

INDEX CHAPTER 1: INTRODUCTION

Figure captions

Table captions

Table 1.1. Scheme of the thesis and associated papers

Table 1.2. Instantaneous maximum discharge (Qc_i) registered and estimated by the Gumbel method for different return periods at the Capella gauging station for the period 1945-2009.

1. INTRODUCTION

1.1. State of the art

1.1.1. The sediment transfer in a river basin

Rivers are very complex natural systems which transfer water and sediments from erosion (e.g., headwaters) to sedimentation zones (e.g., floodplains, estuaries, deltas) and ultimately to seas and oceans (Williams and Wolman, 1984). The morphology of a fluvial section is the result, at the long-term, of the erosion, transport and sedimentation processes during competent events (i.e., floods) of different magnitude and frequency. According to these processes and their associated fluvial dynamics, a river basin can be divided in a simple way, in three zones (Fig. 1.1) (Schumm, 1977; Kondolf and Matthews, 1993; Kondolf, 1994):

a) **Sediment generation zone** (e.g., headwaters): the section of the catchment that is essentially characterised by erosion processes (sediment production). Sediment delivery is controlled by different factors such as climate, lithology, relief, vegetation cover, soil, physical properties and land uses.

b) **Sediment transport zone** (e.g., transition zones, channel networks): the catchment area in which at-a-section sediment transport and downstream sediment transfer process in the drainage network are predominant.

c) **Sedimentation zone** (e.g., lowlands, floodplains, estuaries and deltas): the section of the basin that is characterised by sedimentation processes. Channel networks lose competence when valley opens, sediments are then deposited developing floodplains and ultimately nourishing deltas and oceans.

Walling (2006) recently reported that sediment transfer is: (a) important for understanding and modelling the global denudation cycle (e.g., Gregor, 1970), (b) essential to global geochemical cycling (e.g., Meybeck, 1994), (c) crucial for the functioning of coastal ecosystems and the evolution of deltas (e.g., Morton, 2003), and

(d) vital due to its role as a pathway for the transfer of pollutants and nutrients from terrestrial to coastal and marine systems. Flow regime and sediment supply to the channel are the main factors controlling the dynamics of the fluvial system, however these may be significantly altered by human activities and climate change.

In this context, in natural unaltered streamcourses, there exists a dynamic balance between water and sediment transport. Human activities are the origin of numerous modifications in the fluvial systems, causing the breakup of this dynamic balance. Such modifications alter basic hydraulic and morpho-sedimentary processes at different scales that in turn may affect the habitat of aquatic species and the stability of infrastructures. After these modifications happen, riverchannels and floodplains may need long time to get a dynamic balance that is adjusted to the new conditions (Petts, 1984).

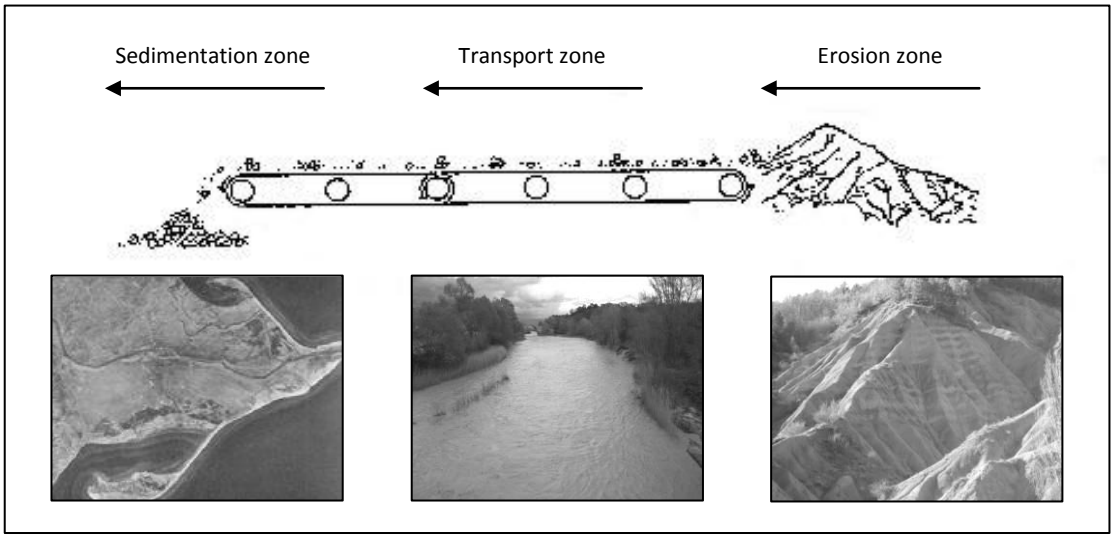

Figure 1.1. The conveyor belt transfer simile: erosion, transport and deposition zones in a fluvial basin (after Schumm, 1977). Bottom photographs exemplify main fluvial features in such zones: (right) badlands where high rates of erosion control the sediment production in the headwaters of a fluvial catchment; (centre) plane bed channel section where sediment is mainly transferred to downstream reaches during competent flood events (Source: Damià Vericat, 2006); and (left) delta nourished with sediment providing from transfer zones (Source: Solé-Sabaris, 1958).

1.1.2. Characterization of high erodible surfaces

It is well known that high erodible surfaces (e.g., badlands) may represent the main sediment sources of some catchments, despite of being a small proportion of the total basin's area. This is the case of the Isábena, where a badland strip located in the middle part of the basin, representing <1% of its total area, have been identified as the main sediment producer (Francke et al., 2008a, 2008b; López-Tarazón et al., 2009; López-Tarazón et al., 2010a, 2010b, 2010c). The term badland refers to areas of unconsolidated sediment or poorly consolidated bedrock with little or no vegetation, which are useless for agriculture because of their intensely dissected landscape (Gallart et al., 2002). Badlands develop in many climatic regions on a wide range of substrata (Bryan and Yair, 1982; Howard, 1994), but extensive badland development is usually associated with unconsolidated or poorly cemented materials. The main factor controlling badland formation is the particular physicochemical properties of surface materials, which are the basis for the interaction of weathering and erosion processes (Campbell, 1989). Lithology is probably of greater importance than tectonics, climate, topography, or land use (Gerits et al., 1987; Imeson and Verstraten, 1988; Campbell, 1989; Calvo-Cases et al., 1991). Geomorphological processes in the Mediterranean region have an important anthropogenic component because of long-term human occupation of the area; badlands that develop in such regions are characterized by both strong climatic contrast and considerable human influence (Fairbridge, 1968). Much of the literature on badland geomorphology has emphasized that erosion occurs primarily by overland flow processes, and has focused on the influence of different material properties or surface covers on erosion rates. Eocene marls are the most important erodible rock substratum (the main sediment source area) in the Central Pyrenees (Beguería, 2005), where badland landscapes are widespread (more than a hundred morphologies were mapped) and hydrologically disconnected between them. The extension of these badlands is very variable, from some hundred square metres to a few square kilometres. Badlands are frequently considered to be landscapes that are characteristics of dryland areas. Semi-arid badlands are frequent throughout the Mediterranean, the better-known examples being located in various parts of Spain and southern Italy (Alexander, 1982; López-Bermúdez and Romero-Díaz, 1989; Calvo-Cases and Harvey, 1996; Solé-Benet et al., 1997; Piccarreta et al., 2006; Desir and Marín, 2007). Nevertheless, they also occurred in wetter areas where high topographic

gradients, bedrock weakness and high intensity rainstorms coexist. Sub-humid badlands develop in areas, usually mountainous in character, with annual precipitation around 700 mm, and with frequent storms during the summer (Gallart et al., 2002; Nadal-Romero and Regüés, 2010). These badlands probably should be much younger than arid or semi-arid types (Gallart et al., 2002; García-Ruiz and López-Bermudez, 2009).

1.1.3. Sediment transport and impacts on reservoirs

Sediment transport is a non-lineal process both in time and in space; it varies as a function of different factors as the distribution of the precipitation along the basin, the availability of sediment at the source areas and the distance between them and the outlet of the catchment (Williams, 1989). In this context, and owing to the modelling of these processes, it is essential the study of the magnitude, the frequency and the relations between the sediment sources (i.e., erosive processes at the slopes) and the sediment transport downstream (i.e., drainage network), with the objective of determining sediment transport patterns and residence time of the sediment within the catchment.

Reservoirs suffer siltation worldwide. This process is controlled by the contribution of sediment from rivers that drain into them. Siltation worsens in areas draining non-consolidated and highly erodible sediments under intense and contrasted climatic conditions, as in the case of the Mediterranean mountains, where long dry periods are followed by high intensity storms. In those regions, most of the sediment is generated during low-duration but high-intensity thunderstorms, creating high erosion rates which in turn produces high density flows (i.e., non-Newtonian, laminar and uniform flows with very low particle settling velocities; Newson, 1989) in fluvial courses downstream (Fig. 1.2). Such episodes are often restricted to small mountain torrents from localised storms triggering mass movements (e.g., Clotet et al., 1988; Batalla et al., 1999), although they have also been reported for large rivers, such as the Yellow River (Li et al., 1997), where maximum suspended sediment concentrations can reach 700 g l^{-1} (Xu, 1997). Moreover, river-channel dynamics control sediment transport in the basin and the sediment input to the reservoirs, since determine the sediment availability at given moments of the year and during floods and base-flows (Lambert and Walling, 1988; Walling et al., 1998; Walling et al., 1999).

Reservoir siltation problems compound their negative impacts on both environmental and socio-economical issues. The first is focused mainly on macrophyte communities (Clarke and Wharton, 2001), invertebrate biodiversity (Scullion, 1983) and fish populations (Acornley and Sear, 1999), whilst the latter refers especially to reservoir sedimentation, that causes water quality problems and, especially, a progressive reduction in dam impoundment capacity, which creates serious problems for water management (Valero-Garcés et al., 1999). Loss of storage capacity may threaten domestic water supply and economic activities such as irrigation, hydropower production, nuclear power production and coastal tourism.

Figure 1.2. High density flow observed at the Capella gauging station (outlet of the Isábena basin) during a flood in April 2008.

Understanding siltation process and acting over it consequences require the quantitative analysis of different aspects related to sediment transport (e.g., seasonality and magnitude of the sediment export) and its modelling en relation to the basin's hydrology (e.g., hydro-sedimentological response). This is the theoretical framework of the present PhD Thesis, that has been developed at the Isábena catchment. This river drains into the Barasona reservoir, that is the responsible of the irrigation of more than 100,000 ha of land in Aragon and Catalunya. The reservoir suffers acute siltation problems (Fig. 1.3) since its construction in the 1930s (e.g., Avendaño et al., 1997a; Avendaño et al., 1997b; Valero-Garcés et al., 1997; Navas et al., 1998). This process is related to the fine

sediment contribution that is mostly originated from Eocene marls (e.g., badlands) located in the middle part of the basin despite representing less than 1% of the total basin area (Francke et al., 2008a, 2008b; López-Tarazón et al., 2009).

Engineering works during 1990s to release sediment through the dam bottom outlets resulting in around 9 hm^3 (1 hm^3 = $1x10^6$ m^3) of sediment being sluiced through the dam (Palau, 1998; Avendaño et al., 2000). Nowadays the reservoir capacity equals that of 1993 (76 hm^3) (Mamede, 2008). The reservoir siltation process is a fact that puts on risk cyclically the water resources and, therefore requires a continuous attention from the water authorities.

Figure 1.3. Evolution of the siltation in the Barasona Reservoir. Images illustrate the changes at the same section between September 2001 (left) and November 2007 (right). Left image was taken by Ramon J. Batalla in 2001.

1.2. Framework of the thesis

The case of the River Isábena has come to the attention of scientists since the later 1990s. In particular, researchers at the University of Lleida undertook several studies mainly focused on badland characterization and changes in land use (e.g., Fargas et al., 1997; Poch and Martínez-Casasnovas, 1997; Martínez-Casasnovas and Poch, 1998; Serrat and Martínez-Casasnovas, 1998). Soon after, RIUS, the Fluvial Dynamics Research Group of the University of Lleida and the Forest Technology Centre of Catalonia, led by Dr. Ramon J. Batalla, started the study of the hydro-sedimentogical dynamics of the catchment. Firstly the research was directed to evaluate the hydrological response of the catchment, together with the hydraulics, grain size

distribution and sediment entrainment; the work generated a PhD Thesis (Verdú, 2003) and several publications (e.g., Verdú et al, 2004; Verdú et al, 2006a, 2006b). Later, suspended sediment transport and dynamics were the focus of the work. This objective was pursued within the frame of the SESAM Project (Sediment Export from large Semi-Arid catchments: Measurements and Modelling), funded by German DFG-Deutsche Forschungsgemeinschaft. From 2005 to 2009, members of the University of Lleida, the Forest Technology Centre of Catalonia, the University of Potsdam (Germany), the German Research Centre for Geosciences-GFZ (Germany), have been conducting research in three mesoscale dryland catchments in Spain and Brazil, aiming at monitoring and modelling water and sediment fluxes from the sources to the deposition areas. Within this context, three PhD Thesis have been developed in the Isábena catchment on the framework of this project; one dedicated to the modelling of the suspended sediment deposition and movement in the Barasona reservoir (Mamede, 2008); a second focused on water and sediment generation in the source areas and at a landscape scale (Francke, 2009); and, finally, the present work, that is embedded in the complementary work of the SESAM project, and whose objectives are described in the following section. Results obtained by the SESAM research team have been published in international journals; specifically for the Isábena catchment main papers are Mamede et al., (2005), Francke et al., (2008 a, 2008b), López-Tarazón et al., (2009) and López-Tarazón et al., (2010a, 2010b and 2010c).

1.3. Objectives and structure

The aim of the present PhD Thesis is to measure, monitor and model the suspended sediment transport of the River Isábena, a river that frequently undergoes high density fluxes before draining into the Barasona reservoir (see location maps in section 2). The conceptual model used in this PhD has been based in the sediment budget approach described by Dietrich and Dunne (1978). Suspended sediment modelling has been based in the non-parametric *Random Forests* and *Quantile Regression Forests* statistical tools presented by Francke et al. (2008a and 2008b). Special attention has been given to the temporal and spatial sediment transport variability in relation to (a) the distribution and intensity of rainfall events and (b) the storage of fine sediment in the channel network between competent flood events. (Fig. 1.4; Table 1.1).

To meet the aim, 4 interrelated specific objectives have been derived which link with the different chapters of this PhD Thesis:

(O.1) *Calculation of the suspended sediment yield at the outlet of the basin*. Sediment yield has been calculated following a *black-box* approach based on discharge and suspended sediment data obtained continuously at a 15 minute frequency at the Capella gauging station (EA047), located at the outlet of the Isábena basin (results presented in Chapter 3).

(O.2) *To study the relation between rainfall, hydrology and sediment transport*. A characterization of the precipitation patterns of the catchment has been developed and correlated to water and sediment export calculations (O.1) at the outlet of the basin. (Chapter 4).

(O.3) *To estimate in-channel suspended sediment storage between flood events.* The spatial and temporal variations of the in-channel sediment storage were studied following the methodology described by Lambert and Walling (1988). Chapter 5 describes the role of the bed-channel as a controller of the sediment transport at the outlet of the basin (O.1).

(O.4) *To calculate the suspended sediment budget of the basin*. The quantification and evaluation of the hydrological and sedimentological dynamics of the main sub-basins in relation to the basin outlet has been analysed coupling field data and statistical modelling (Chapter 6).

According to the possibility given by the Doctorate Programme of the University of Lleida, the Thesis is presented in papers format. The document has been divided in 7 chapters, containing a total of 4 papers (published, accepted, in press or submitted) (Table 1.1). Each chapter has an introduction in which the specific objectives of this are described. **Chapter 1** gives a general introduction (state of the art) on sediment transport and dynamics; introduces the aim and the specific objectives of the thesis and, finally, describes the study area although all the papers contain a proper description of the study reach. **Chapter 2** introduces the methodology of the thesis (i.e., fieldwork design, sampling and monitoring, laboratory work, data calculation and modelling).

Chapter 3 (related to O.1) contains the first SCI published paper assessing the sediment yield of the Isábena basin, explaining the suspended sediment transport and its dynamics following a *black-box* model approach. **Chapter 4** (related to O.2 and containing the second published SCI paper) reports on the hydro-sedimentological response of the catchment by identifying the rainfall, runoff and sediment transport relations. **Chapter 5** (related to O.3 and containing an accepted SCI paper) describes the role of in-channel suspended sediment storage on the total sediment transport at the outlet of the basin. **Chapter 6** (related to O.4 and containing a submitted SCI paper) estimates the sediment budget of the River Isábena, calculating the contribution of each of the main sub-basins to the total sediment load of the Isábena basin by coupling field data and non-parametric statistical techniques (*Random Forests* and *Quantile Regression Forests).* Finally, **Chapter 7** presents the general discussion and conclusions of the Thesis.

Complementary, as additional information to improve the understanding of the whole Thesis, 2 more papers have been included as annexes (**Annex 1** and **Annex 2**). They have been considered as fundamental to complete this volume because they develop and explain the statistical non-parametric statistical techniques used to model the continuous sedigraphs for the Isábena basin. They have not been embedded in the main body of the present volume and are not meant to be considered for evaluation here, since both they have been previously used by the first author as part of his PhD Thesis.

Table 1.1. Scheme of the thesis and associated papers

Chapter	Key words	Paper Status
1. Introduction	- Suspended sediment transport, high suspended sediment concentrations	
2. Methods	- Turbidimeter, re-suspension cylinder, modelling	
3. Sediment transport	- Suspended sediment load, specific yield, hysteresis	-published
4. Hydro-sedimentological response	- Rainfall, runoff, floods, sediment transport	-published
5. In-channel sediment transport	- Badlands, channel storage, re-suspension cylinder	-accepted, in press
6. Sediment budget	- Sediment yield, sediment budget, statistical techniques	-submitted
7. Discussion and conclusions		
Annex 1. Model development	- Random Forests, Quantile Regression Forests	-published
Annex 2. Model application	- Random Forests, Quantile Regression Forests	-published

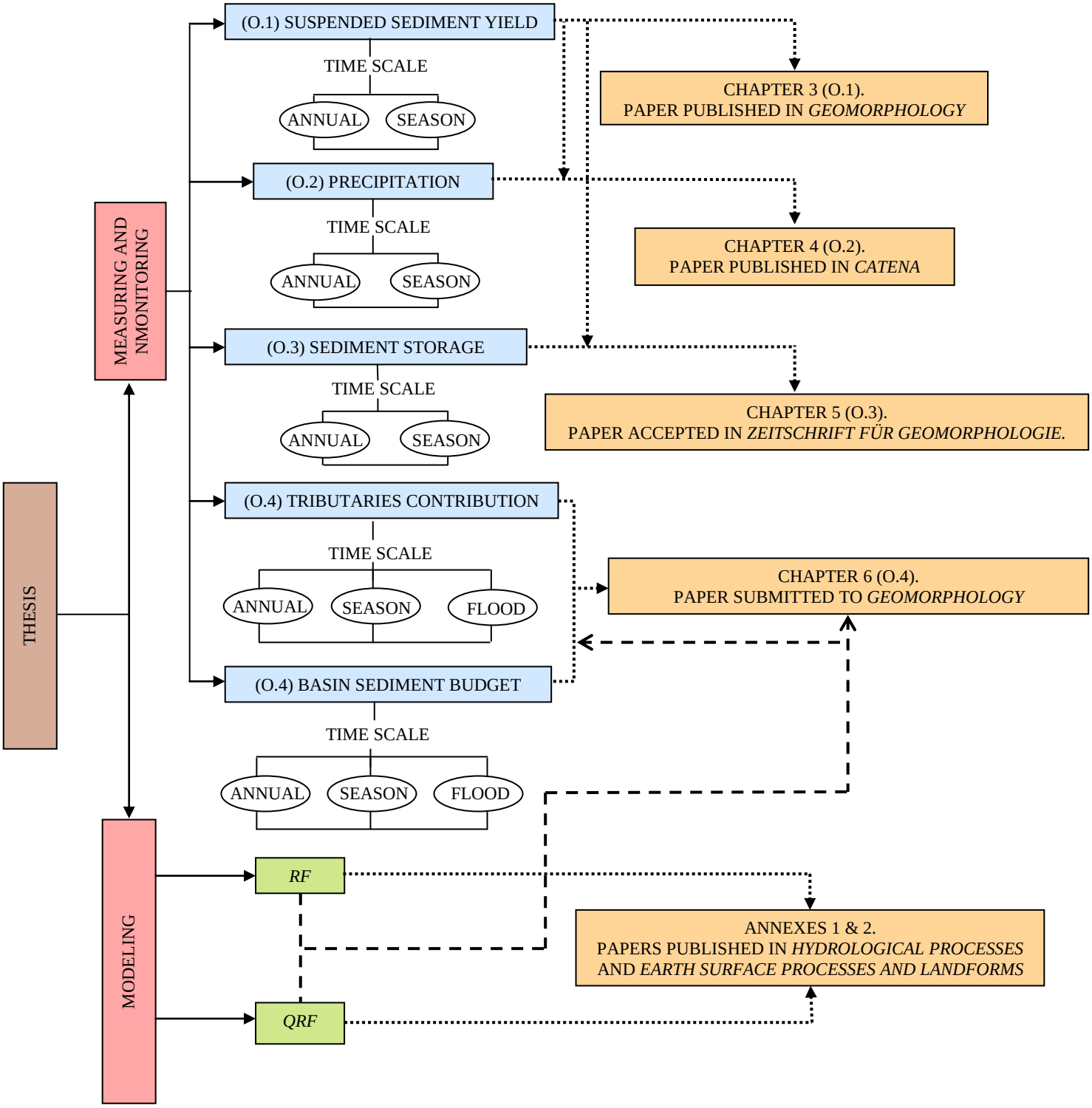

Figure 1.4. Interactions between the main objectives and sediment transport processes of the Thesis; timescales at which they have been studied, its location in the present volume and the publications they have generated are also included.

2. THE ISÁBENA BASIN

2.1. Location

The River Isábena is the main tributary of the River Ésera; both constitute some of the most important tributaries of the Cinca basin, in turn the second largest tributary of the River Ebro (Fig. 1.5). The Isábena basin is located in the north-east part of the Iberian Peninsula, at the Southern Central Pyrenees (Fig. 1.5). Despite of displaying purely Pyrenean climate features, the river shows a rain-snow fed regime, with a very high inter-annual irregularity and remarkable discharge variations.

The Isábena drains an area of 445 km^2 (0.48% of the Ebro basin). The mean annual discharge estimated at the outlet of the basin (Capella gauging station, EA047) for the entire period of record (1945-2009) is 4.1 $m^3 s^{-1}$ (0.96% of the Ebro mean discharge). The mean annual water yield for the same period is 177 hm^3, a value that represents ~1.5% of the Ebro basin's total runoff (López-Tarazón et al., 2009). Elevation varies from 450 m a.s.l. at the catchment outlet to 2,720 m a.s.l. in the northern part (Fig. 1.6). The basin is not hydraulically regulated at all (i.e., its hydrological regime is determined just by natural factors), empowering this way the interests of its study.

In the headwaters the river flows through limestones in the Pyrenees, creating deep canyons as the "Congosto de Obarra". In its middle course, ca. 30 km upstream from the basin's outlet (near the village Puebla de Roda), the river receives the input of water and sediment from the Villacarli torrent, that drains the southern side of the Turbón massif (2,492 m a.s.l.). From this point, the river flows through Tertiary materials widening its channel, until it drains into the River Ésera in the village of Graus. The total length of the river's mainsteam is around 50 km (Verdú, 2003). The catchment can be divided in 5 main sub-basins (Fig. 1.6): Cabecera (146 km^2, representing the 33% of the total catchment area), Villacarli (42 km^2, 9%), Carrasquero (25 km^2, 6%), Ceguera (28 km^2, 6%) and Lascuarre (45 km^2, 10%). The rest of the catchment is formed by small creeks that flow only after rainfall events.

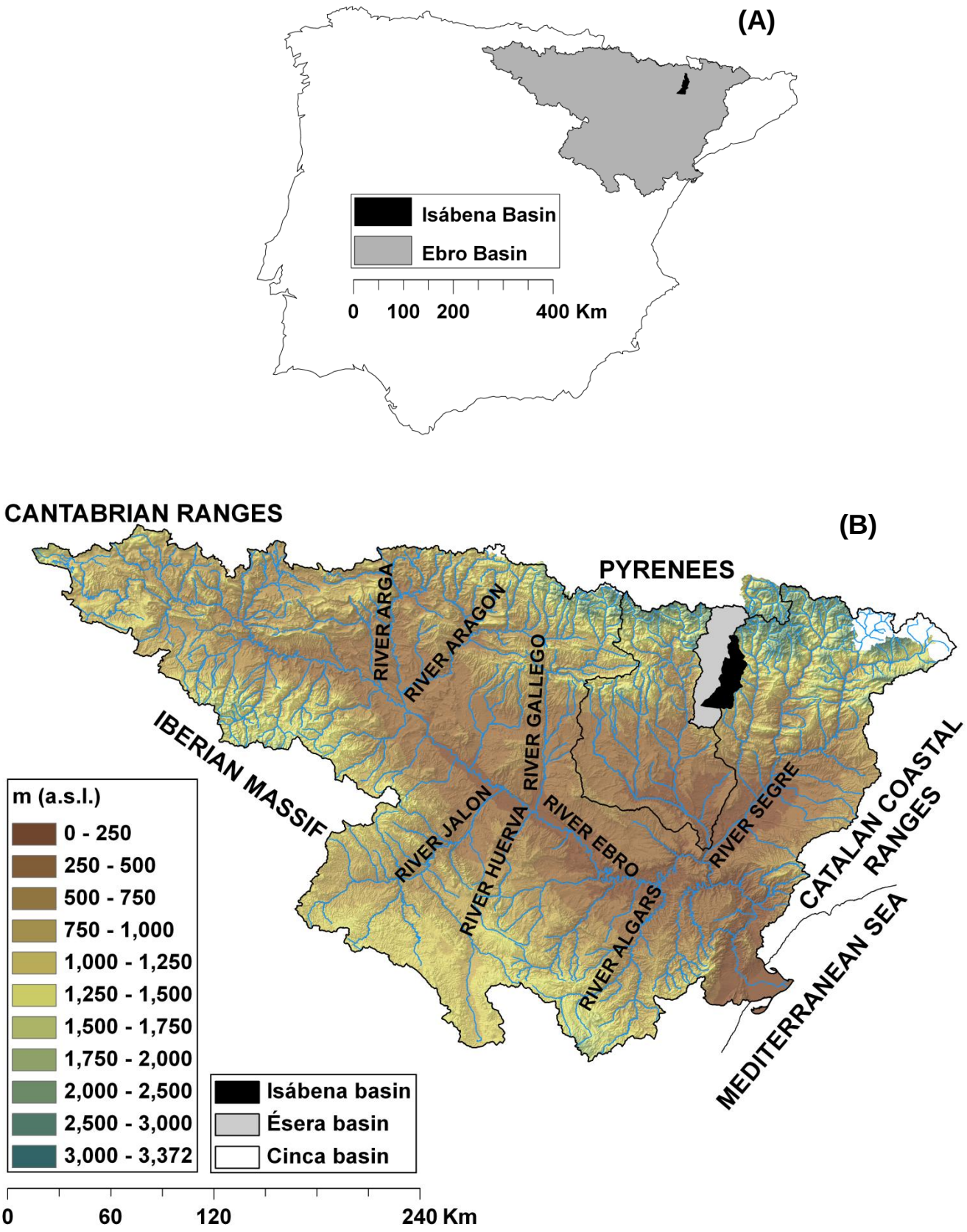

Figure 1.5. A) The Isábena in the Ebro basin and in the Iberian Peninsula. B) Location of the Isábena, the Ésera and the Cinca catchments within the Ebro river basin.

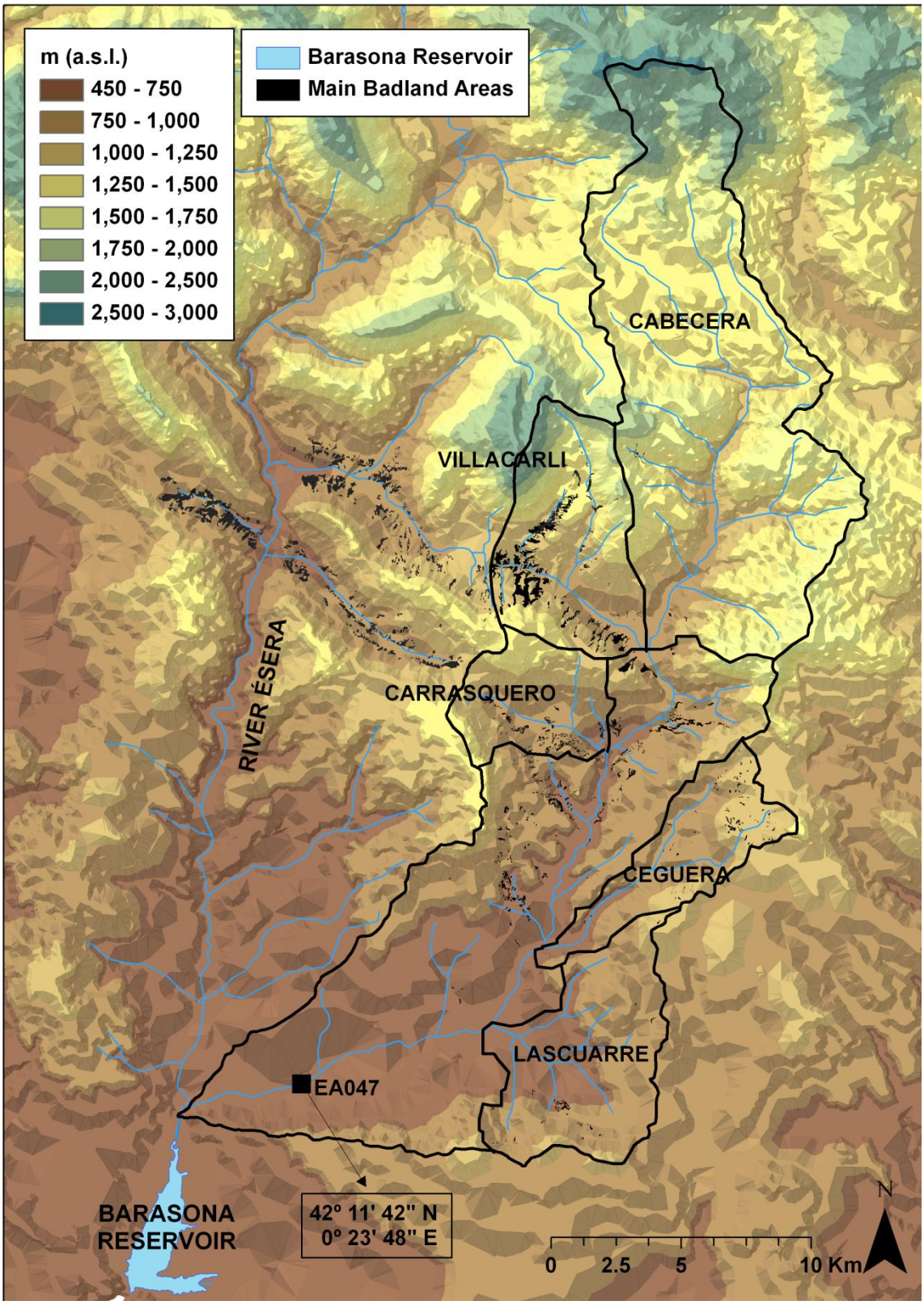

Figure 1.6. The Isábena basin and its main sub-basins.

2.2. Physical characteristics

2.2.1. Climate

The climate of the Isábena catchment is typical of Mediterranean mountainous areas (pure Mediterranean in his continental variant; Verdú et al., 2006a). The main characteristic is the important thermal contrast, with cold and dry winters and hot and stormy summers, with frequent thunderstorms.

Climatically, the basin can be subdivided into two main areas: i) *the south:* representing all the area located south from the Turbón massif, being warmer and drier (i.e., dry Mediterranean climate) than the rest of the basin; and ii) *the north*: part of the basin located north of this massif, purely Pyrenean, with the typical climatic characteristics of the southern side of the Pyrenees (Verdú et al., 2006a). These features are enhanced by the altitudinal variability, varying from a sub-mediterranean climate in the southern-lower part to a sub-alpine climate since the 1,600 m a.s.l. It is also remarkable the high bioclimatic contrasts due to the aspect and the "screen effect" that mountains create over the depressions, generating a high variability in temperature and precipitation even in very close areas.

Mean precipitation varies from 450 mm in the lower part to the 1600 mm in the summits (Fig. 1.7; source: CHEBRO, 1996). The mean annual precipitation for the whole basin is 767 mm, with monthly maximum values of ranging from 75-90 mm in May and June. The minimum rainfall values are registered historically in July (i.e., 46 mm); the higher rainfall intensities occur in summer and autumn due to frequent thunderstorms, when maximum intensities can reach values higher than 70 mm h^{-1}. Rainfall variability was deeply analyzed by López-Tarazón et al., (2010) for the period of interest for the present thesis (2005-2009). The average rainfall for this period was 719 mm, with a marked variability between years (723 mm during the 2005-06 hydrological year, 624 mm for the 2006-07, 737 mm for the 2007-08 and 792 mm for the 2008-09 hydrological year). This interannual variability can be seen in the figure 1.8, where the mean annual isohyetal lines have been plotted for each hydrological year.

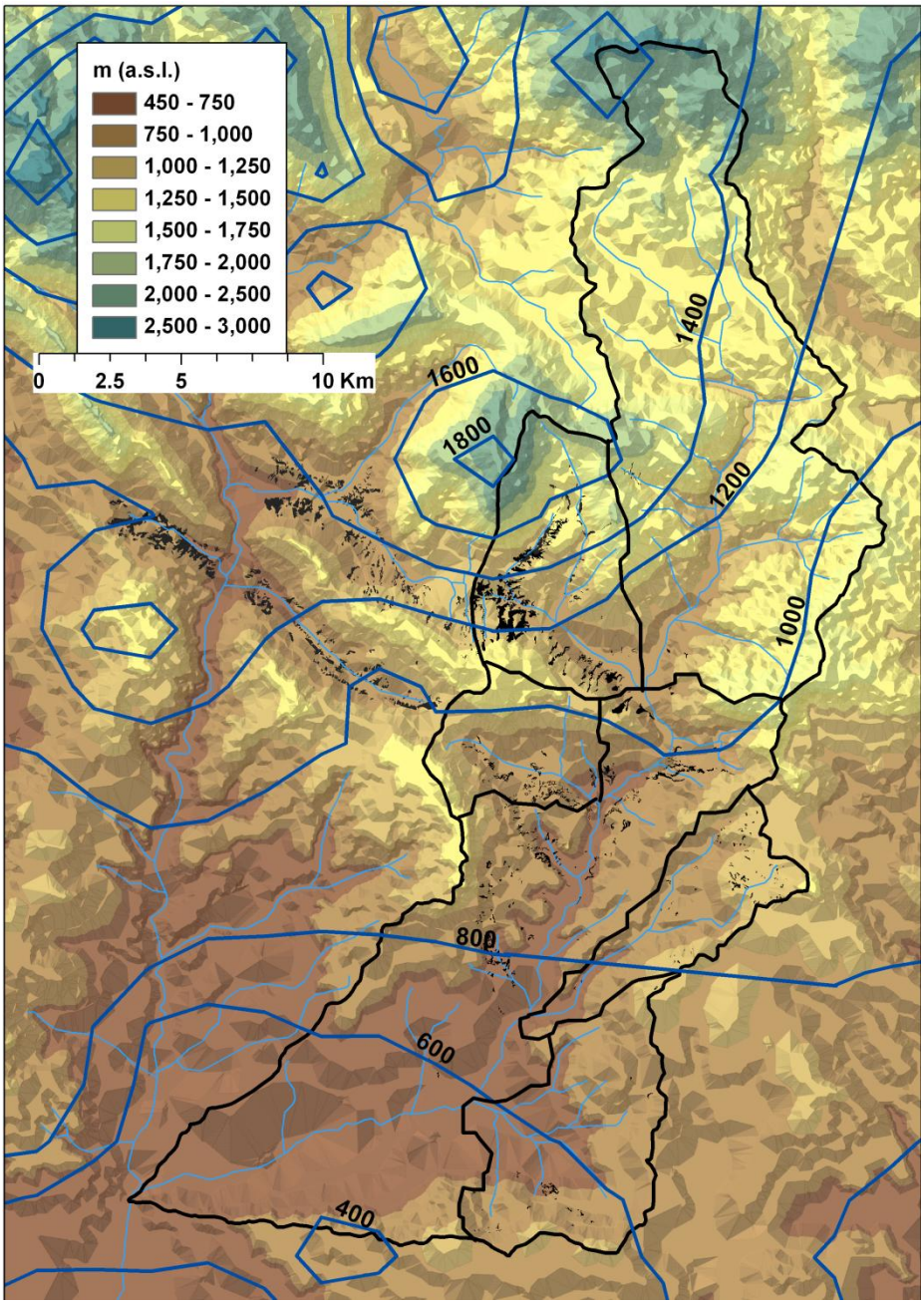

Figure 1.7. Mean annual isohyetal lines for the Isábena basin for the entire data record. The values over the lines represent the precipitation in mm (Source: CHEBRO, 1996).

Mean annual temperature in the catchment varies from 11ºC to 14ºC in the southern part, and from 9ºC to 11ºC in the northern part. Maximum mean values are registered in July and August (21ºC - 22ºC respectively), while minimum mean values are registered in January and December (2ºC - 4ºC respectively). Frosts can appear from September to May, being December, January and February the months with the highest freezing probabilities.

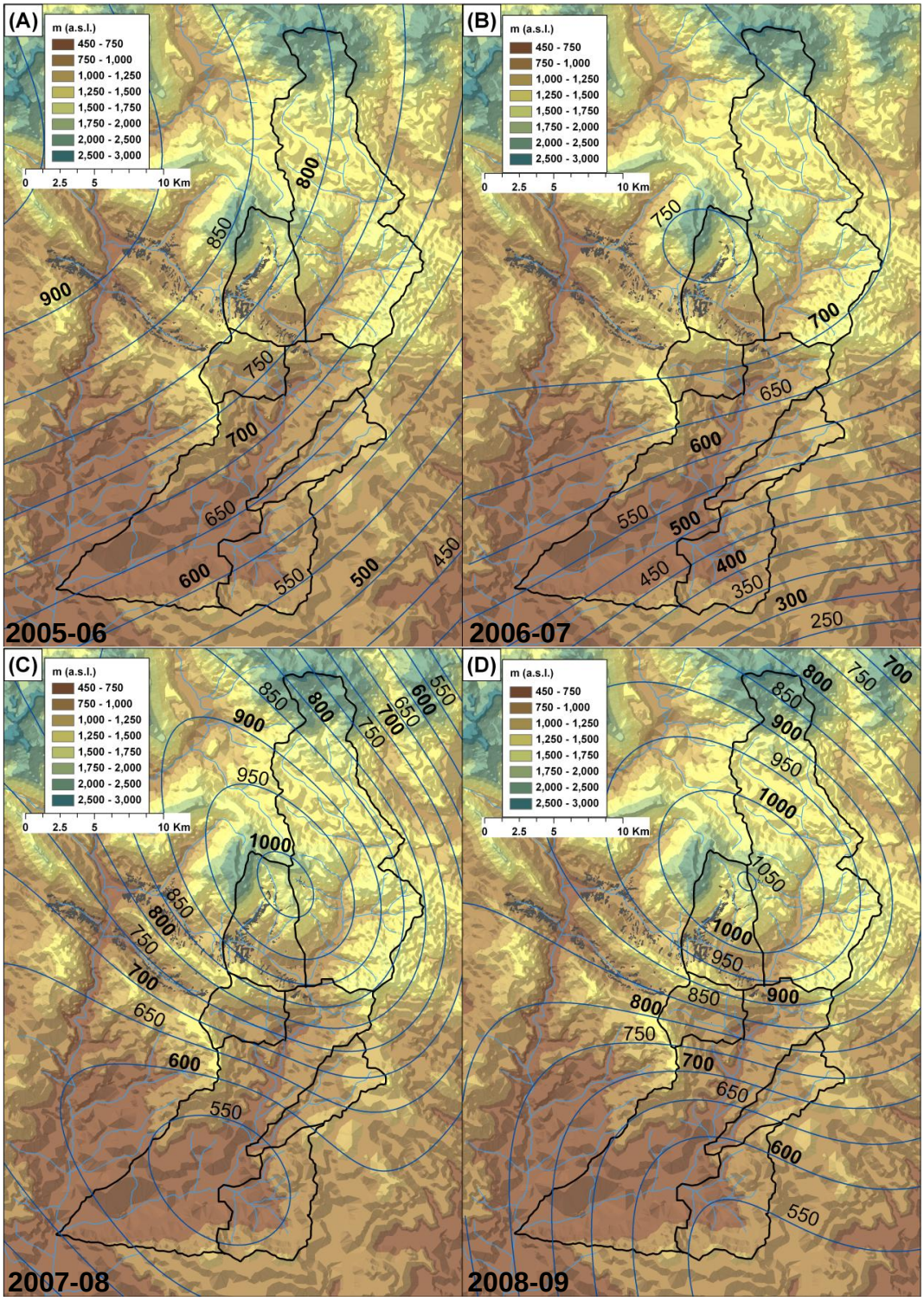

Figure 1.8. Mean annual isohyetal lines for the Isábena catchment for the hydrological years 2005-06 (A), 2006-07 (B), 2007-08 (C) and 2008-09 (D). Values over the lines represent the precipitation in mm.

2.2.2. Geology and geomorphology

The Isábena catchment belongs to the Tremp-Graus geological basin that is a wide depression closed between high mountains with general east-west aspect. Morphologically, the basin is included in the Pyrenean and sub-Pyrenean ranges. The Figure 1.9 shows the distribution of the different lithologies present in the catchment.

In the upper part of the basin (i.e., headwaters) the river flows through narrow valleys excavated on Cretaceous limestones (i.e., calcareous rocks) originating the prominent relief of the zone. Erosion has left the calcareous materials, partially karstified, at the highest levels of the massifs, with the later Eocene marls shaping run-down reliefs. These Pre-Pyrenean ranges are discontinuous, with very steep and fractionated slopes, due to its karstic modelling. At the north-east of the catchment the Palaeozoic materials appear, corresponding to the so-called axial zone of the Pyrenees (Verdú, 2003). The southern part of the Isábena belongs to the structural unit Southern Pre-Pyrenean; it is composed by Secondary age materials, mainly Cretaceous chalks (forming very rugged reliefs) together with Tertiary clay rocks and conglomerates.

The Isábena valley links two different morpho-structural sectors. At the right side the intra-Pre-Pyrenean depression appears, formed by the Lierp valley and the Merli corridor through the Jordal ranges. At the left side there is the Sis range, which delimites the eastern boundary of the basin. Usually, in the middle part of the basin, the landscape shows badland structures that have been identified as the most important source of sediment during storm periods, despite representing less than 1% of the total basin area (Francke et al., 2008a, 2008b; see location in Fig. 1.6).

Geomorphologically, different erosion pediments can be distinguished, in which the hydrographical network has been inserted, generating gullies which delimit surfaces, with slopes between 10-20%. Those surfaces are located at the mean altitude of the basin and currently are occupied by crop fields and pastures. The river is inserted over calcilutites, coinciding with the zones showing the highest slopes. Active incision/accretion processes have not been observed in the main watercourses during the last 10 years (Verdú et al., 2006b), so the more contemporary active geomorphologic

processes are mass movements and, especially, fluvial erosion on slopes and in the badlands.

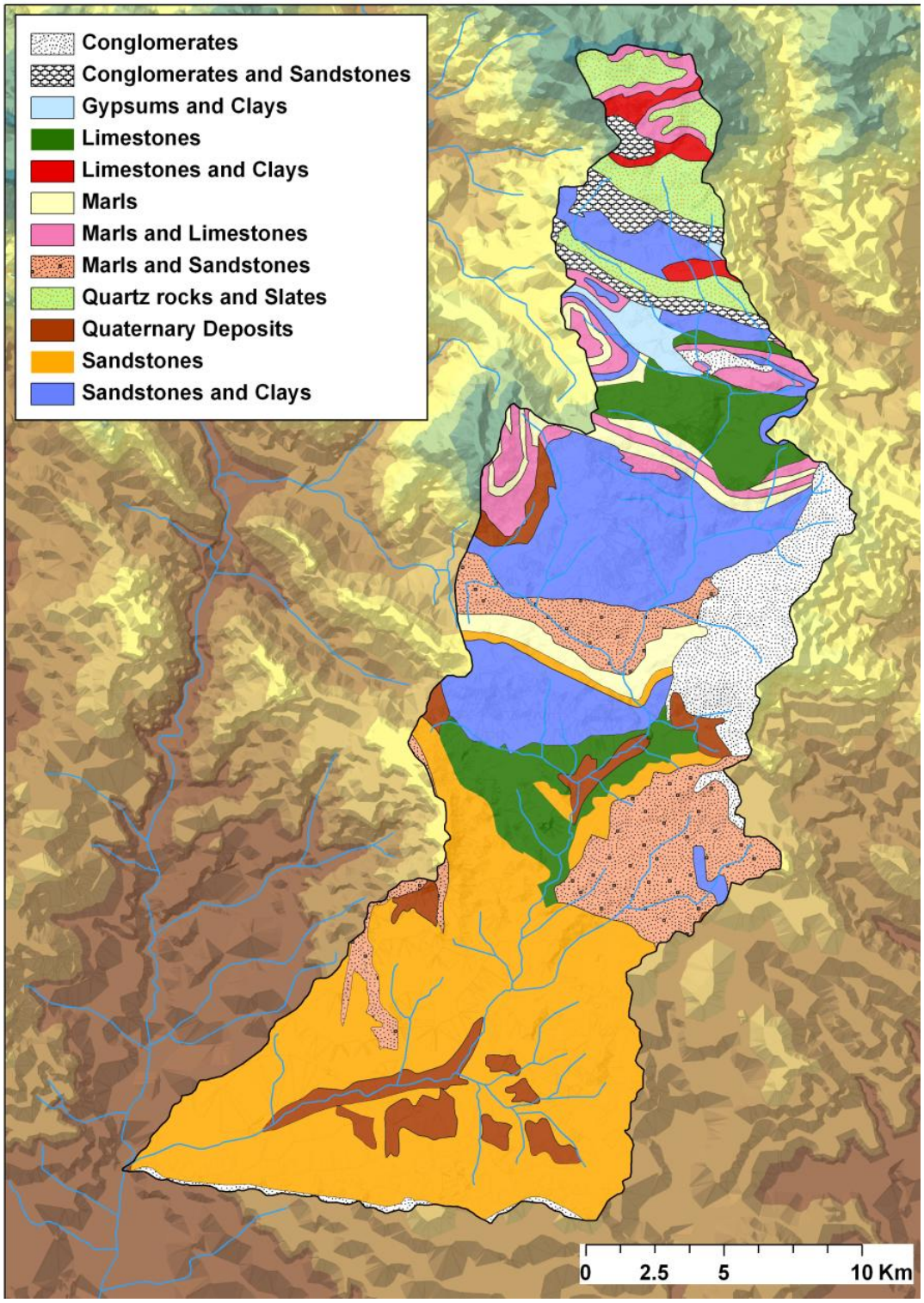

Figure 1.9. Lithology of the Isábena catchment (Source: CSIC, 2000).

2.2.3. Soils

The soils of the Isábena are developed over calcilutites, limestones, sandstones, and conglomerates, placed in stratums dipped to the south-southwest. Soils are poorly developed (Martínez-Casasnovas and Poch, 1998), an issue that can be translated into an absence of diagnosis horizons. They can be classified as Xerorthents (Soil Survey Staff, 1996) with silt loam texture and low organic content (< 2%). The soils are rather thin, well drained, with a limited capacity of water retention and with a moderate/low structural stability. The most eroded soils are those present in the badlands and in the agricultural zones, where sheet and rill water erosion is very active (Fig. 1.10).

Figure 1.10. Example of sheet and rill water erosion in the Isábena basin during the flood occurred the April 18th, 2008.

2.2.4. Vegetation and land uses

The vegetation in the Isábena basin reflects its intrinsic climatic variability and the typical contrasts between north and south facing locations (shady and sunny, respectively). Climax vegetation of the central and lower parts of the basin are the

forests of *Quercus ilex ballota* with *Pinus halepensis* in the sunny places and woodland of *Quercus faginea* in the shady places; currently its extension is very reduced and scattered giving way to the more degraded vegetation structures, as shrublands and dry pastures. There are some plantations of pine forests, mainly of *Pinus halepensis*, *Pinus nigra* and *Pinus sylvestris* in the southern part. There is a plentiful of abandoned crop lands, where shrublands in different transitional states appear, predominating species as *Buxus sempervirens*, *Quercus coccifera*, *Thymus vulgaris*, *Rosmarinus officinalis* and *Echinospartum horridum*. Most of these lands are used to feed flocks of sheep and goat during spring and autumn (Serrat and Martínez-Casasnovas, 1998). In the northern part, the climax vegetation is forests of *Pinus sylvestris,* from 600 m a.s.l. to 1,600 m a.s.l., where gives way to *Pinus uncinata*. Deciduous forests are represented mainly by *Quercus faginea*, *Betula pendula* and *Fraxinus sp*., frequently forming mixed forests with *Abies sp.* and *Pinus uncinata*. There are some pastures distributed along the basin, spread by man in the interest of the livestock activities. The predominant species on the high quality pastures are *Festucion supinae*, *Festuca nigrescens*, *Festuca ovina*, *Festuca eskia* and *Cares sempervirens*.

Forest management is mainly based in the exploitation of conifers in the northern part and pastures or cynegetic purposes at the scattered and dry forests of the southern part. Agricultural areas are mainly located at the lower Isábena, especially rain-fed cereals (barley, wheat and sunflowers) and forage for the cattle; some permanent crops (almond and olive trees) can be found in the lower parts as well. Meadows and pastures are the only agricultural activity in the northern part. It is also notable the important changes in the land use occurred during the last 50 years, with the abandoning of many former agricultural areas and the subsequent natural reforestation, a common phenomena in the whole of the Pyrenees (Gallart and Llorens, 2004).

2.2.5. Hydrology

The fluvial dynamics and the hydrology of the Isábena catchment can be described at the catchment scale, by means of the data registered at the Capella gauging station (EA047; see location in Fig. 1.6), the unique official gauging section present at the basin. It was constructed by the Ebro Water Authorities (hereafter CHE) during the 1940s, starting the data acquisition during the 1945-1946 hydrological year.

The hydrology of the basin is characterised by a rain-snow fed regime, with maximum discharge peaks occurring during spring due to the snowmelt at the headwaters, and minimum levels occurring in summer (August and September), usually delayed in relation to the period with less precipitation (July and August). Nevertheless, maximum discharges belong to autumn, with for instance historical mean values above 40 $m^3 s^{-1}$ in October and November during the 1960s. Mean annual discharge for the entire period of record (1945-2009) is 4.1 $m^3 s^{-1}$, with and standard deviation (σ) of 2.2 $m^3 s^{-1}$. Figure 1.11 represents the monthly discharge (mean, maxima and minima) for the whole data series.

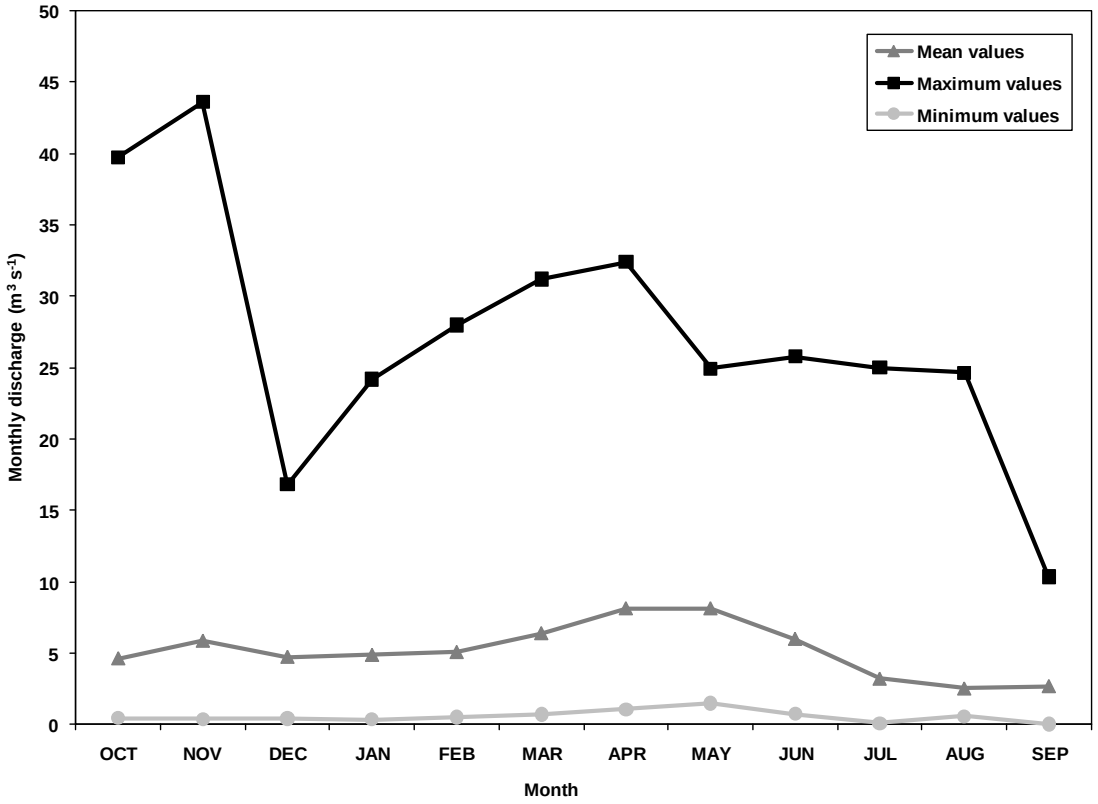

Figure 1.11. Monthly discharge registered in the Isábena basin during the period 1945-2009.

Mean annual water yield is 177 hm^3 (σ = 92 hm^3). Figure 1.12 shows the evolution of the water yield for the period 1945-2009 at EA047. It can be observed that the 1960s and the 1970s are the wettest decades, with the most of the years above the mean, while the 1980s and the 2000s are the driest, with the most of the water yield values below the long-tem average.

Table 1.2 presents the largest floods registered at the EA047 and the respective return periods estimated by the Gumbel method for the period 1951-2009. In addition, the estimated discharges using this method are presented. The two highest floods ever registered, with peak discharges higher than 300 m^3 s^{-1}, are the responsible of the deviation of the Gumbel adjustment to this value for the relatively low return periods (35-100 years). This statistical adjustment creates that the estimated instantaneous maximum discharge for a return period of 2 years is almost 100 m^3 s^{-1}, a value just exceeded in 10 floods during the last 65 years. This fact illustrates the variable hydrological response of the basin, which usually shows relatively low flows despite having a very wide channel and floodplain (up to 200 m at some locations), indicating that historically very large floods have happened (larger than currently), as in the case of the years 1963 and 1966.

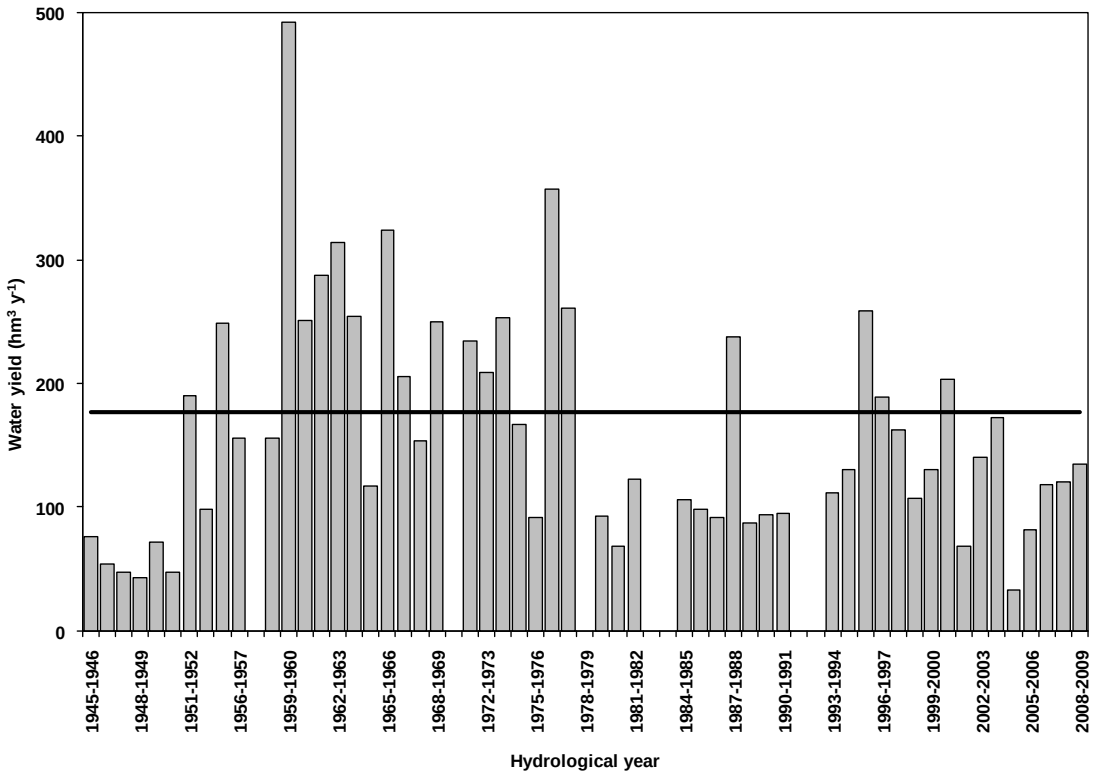

Figure 1.12. Annual water yield of the Isábena basin for the record period (1945-2009). The black line represents the mean water yield of the whole period (i.e., 177 hm^3).

Table 1.2. Instantaneous maximum discharge (Qc_i) registered and estimated by the Gumbel method for different return periods at the Capella gauging station for the period 1945-2009.

Qc_i registered ($m^3 s^{-1}$)	Date of flood	Return Period	Qc_i estimated ($m^3 s^{-1}$)
-	-	100	374.9
370.0	August 3rd, 1963	94	-
-	-	50	325.7
321.2	November 9th, 1966	48	-
281.5	December 18th, 1997	27	-
-	-	25	276.4
252.0	July 23rd, 1965	18	-
-	-	10	211.4
190.6	January 1st, 1977	8	-
163.2	April 23rd, 1971	5	-
-	-	2	97.1
-	-	1	47.9

2.2.6. Sediment generation and main sources

The Isábena together with the Ésera basin (Fig. 1.5 and 1.6), experiences intense erosion phenomena due to overland flow that ultimate causes the sediment siltation of the Barasona Reservoir, where both rivers drain into. The dam was constructed in the earlies 1930s with an original capacity of 71 hm^3, and it was further enlarged in 1972 reaching a total capacity of 92 hm^3. The reservoir supplies water mainly to the Aragón and Catalunya Canal, irrigating more than 70,000 ha of land. For almost 75 years the reservoir has been progressively silting up at a rate of between 0.3 and 0.5 hm^3 of sediment deposited per year (Francke et al., 2008a). Engineering works undertaken during the 1990s to alleviate the problem resulting in around 9 hm^3 of sediment being sluiced through the dam bottom outlets (Palau, 1998; Avendaño et al., 2000). Despite of that, sluicing represented a mere 30% of the total sediment volume accumulated in the reservoir estimated, at that time, in 28 hm^3 (Alcázar and Ferrán, 1998). Nowadays, the reservoir capacity equals that of 1993 (76 hm^3), when the engineering works started (Mamede, 2008).

Some studies demonstrated that a 25% of the catchment area that closes the reservoir has a high or very high risk of generating sediment (i.e., land erosion; Fargas et al., 1997). Such zones are mainly in the middle part of the basin, in a stripe located at the

south of the Turbón massif. In the particular case of the Isábena catchment, this area is included in the sub-basins of Villacarli and Carrasquero (Fig. 1.6). The stripe consists in valleys excavated over Eocene marls with sandstones in the watersheds. The marls come to the surface in badland structures, with a very high contact surface, making them the largest sediment producers (Fig. 1.13).

Figure 1.13. Example of two different typologies of badlands present at the Isábena basin.

Some other works, related with remote sensing and modelling of water erosion risks (Serrat and Martínez-Casasnovas, 1998), corroborated the results obtained by Fargas et al. (1997), regarding to the high risk of sediment emission in the badlands located in the middle part of the Isábena basin (Fig. 1.6). The badland dynamics and characterisation showed that those zones are the main sediment sources in the reservoir catchment (Poch and Martínez-Casasnovas, 1997; Martínez-Casasnovas and Poch, 1998). The sediment generated by the badlands was estimated by those authors in 0.6 hm^3 y^{-1} (similar to values reported by Francke et al., 2008a); the main part of these materials (around 0.5 hm^3 y^{-1}) is rapidly incorporated into the drainage network, through the numerous torrents that drain the middle regions of the Ésera and the Isábena basin (Fig. 1.6), finally being accumulated downstream in the reservoir (Martínez-Casasnovas and Poch, 1998). This data coincides with the work done by Valero-Garcés *et al*. (1997) who measured suspended sediment concentrations in different parts of the Isábena basin, confirming that the main source of sediment is located in its middle reaches.

Furthermore, the analysis of some orthophotographs at different dates in the badland stripe allowed estimating its growth towards not eroded zones at a rate of 4.6 ha y^{-1}; the advance of the badlands is produced by a headwaters expansion to the marls (Penella, 1997, Martínez-Casasnovas and Poch, 1998). At the agricultural areas scale (southern part of the Isábena basin), the application of the USLE model (Wischmeier and Smith, 1978) allowed estimating soil loss due to agricultural activities (Martínez-Casasnovas and Poch, 1998). Results showed that around the 70% of the agricultural soils have losses higher than 20 t ha^{-1} y^{-1} due to sheet and rill water erosion.

3. REFERENCES

Acornley, R.M., Sear, D.A., 1999. Sediment transport and siltation of brown trout (*Salmo Trutta* L.) spawning gravels in chalk streams. *Hydrological Processes*, **13**: 447–458.

Alcázar, J., Ferrán, I., 1998. La vegetación de ribera de los ríos Ésera y Cinca en el tramo afectado por el vaciado del embalse de Joaquín Costa. *Limnética*, **14**: 73-82.

Alexander, R.W., 1982. Difference between 'calanchi' and 'biancane' badlands in Italy. In: Bryan, R., Yair, A., (eds): *Badlands geomorphology and piping*, Norwich: Geo Books, 71–88.

Avendaño, C., Cobo, R., Sanz, M.E., Gómez, J.L., 1997a. Capacity situation in Spanish reservoirs. *Proceedings of the Nineteenth Congress on Large Dams,* **74** (53): 849-862.

Avendaño, C., Sanz, M.E., Cobo, R., Gómez, J.L., 1997b. Sediment yield at Spanish reservoirs and its relationships with the drainage basin area. *Proceedings of the Nineteenth Congress on Large Dams*, **74** (54): 863-874.

Avendaño, C., Sanz, M.E., Cobo, R., 2000. State of the art of reservoir sedimentation management in Spain. In: *Proceedings of the International Workshop and Symposium on Reservoir Sedimentation Management*, Tokyo, Japan, pp. 27-35.

Batalla, R.J., De Jong, C., Ergenzinger, P., Sala, M., 1999. Field observations on hyperconcentrated flows in mountain torrents. *Earth Surface Processes and Landforms*, **24**: 247–253.

Beguería, S., 2005. *Erosión y fuentes de sedimento en la cuenca del embalse de Yesa (Pirineo Occidental): ensayo de una metodología basada en teledetección y análisis de SIG*. Zaragoza: Instituto Pirenaico de Ecología (CSIC), pp. 158.

Bryan, R., Yair, A., 1982. Perspectives on studies of badland geomorphology. In: Bryan, R. and Yair, A. (eds): *Badland geomorphology and piping*, Norwich: Geobooks, 1–12.

Calvo-Cases, A., Harvey, A.M., Paya-Serrano, J., 1991. Processes interactions and badland development in SE Spain. In: Sala, M., Rubio, J.L., García-Ruiz, J.M., (eds): Soil erosion studies in Spain, Logroño, *Geoforma*, 75–90.

Calvo-Cases, A., Harvey, A.M., 1996. Morphology and development of selected badlands in southeastern Spain: implications on climate changes. *Earth Surface Processes and Landforms*, **21**: 725–35.

Campbell, I.A., 1989. Badlands and badland gullies. In: Thomas, D.S.G., (ed): *Arid zone geomorphology*, London: Belhaven, 159–83.

CHEBRO, 1996. Mapa "Isoyetas Medias Anuales" 1:50000, 1996. URL:http://www.oph.chebro.es/ContenidoCartoClimatologia.htm (accessed May 5th, 2010).

Clarke, S.J., Wharton, G., 2001. Sediment nutrient characteristics and aquatic macrophytes in lowland English rivers. *The Science of the Total Environment*, **266**: 103–112.

Clotet, N., Gallart, F., Balasch, J.C., 1988. Medium term erosion rates in a small scarcely vegetated catchment in the Pyrenees. *Catena supplement* **13:** 37-47.

CSIC/IRNAS, 2000. Mapa de suelos (Clasificacion USDA, 1987), 1:1 Mio, Sevilla, SEISnet-website, URL:http://leu.irnase.csic.es/mimam/seisnet.htm (accessed 3 Jul. 2006)

Desir, G., Marín, C., 2007. Factors controlling the erosion rates in a semi-arid zone (Bardenas Reales, NE Spain). *Catena*, **71:** 31–40.

Dietrich, W. E., Dunne, T., (1978). Sediment budget for a small catchment in mountainous terrain, *Zeitschrift für Geomorphologie*, **29**: 191-206

Fairbridge, R.W., 1968. *Encyclopedia of geomorphology*. Stroudsburg, PA: Dowden, Hutchinson and Ross.

Fargas, D., Martínez-Casasnovas, J.A., Poch, R.M., 1997. Identification of critical sediment source areas at regional level. *Physics and Chemistry of the Earth*, **22**: 355-359.

Francke, T., 2009. Measurement and Modelling of Water and Sediment Fluxes in Meso-Scale Dryland Catchments. Unpublished PhD Thesis, Universität Potsdam, Germany.

Francke, T., López-Tarazón, J.A., Schröder, B., 2008a. Estimation of suspended sediment concentration and yield using linear models, random forests and quantile regression forests. *Hydrological Processes*, **22**: 4892-4904.

Francke, T., López-Tarazón, J.A., Vericat, D., Bronstert, A., Batalla, R.J., 2008b. Flood-based analysis of high-magnitude sediment transport using a non-parametric method. *Earth Surface Processes and Landforms*, **33**: 2064-2077.

Gallart, F., Llorens, P., 2004. Observations on land cover changes and water resources in the headwaters of the Ebro catchment, Iberian Peninsula. *Physics and Chemistry of the Earth*, **29**: 769-773.

Gallart, F., Solé, A., Puigdefábregas, J., Lázaro, R., 2002. Badland systems in the Mediterranean. In: Bull, L.J. and Kirkby, M.J., (eds): *Dryland rivers: hydrology and geomorphology of semi-arid channels*, Chichester, Wiley, 299–326.

García-Ruíz, J.M., López-Bermudez, F., 2009. Un caso especial: badlands y sufosión. In: Sociedad Española de Geomorfología, (ed): *Erosión del suelo en España*, Zaragoza: SEG, 239–72.

Gerits, J.J.P., Imeson, A.C., Verstraten, J.M., Bryan, R.B., 1987. Rill development and badland regolith properties. *Catena Supplement*, **8**: 141–60.

Gregor, C.B., 1970. Denudation of the continents. *Nature*, **228:** 273–275.

Howard, A.D. 1994: Badlands. In: Abrahams, A.D., Parsons, A.J., (eds): *Geomorphology of desert environments*, London: Chapman and Hall, 213–42.

Imeson, A.C., Verstraten, J.M., 1988. Rills on badland slopes: a physico-chemically controlled phenomenon. *Catena Supplement*, **12**: 139–50.

Kondolf, G.M., Matthews, W.V.G., 1993. *Management of coarse sediment in regulated rivers of California*. University of California Water Resources Center, Davis, California.

Kondolf, G.M., 1994. Geomorphic and environmental effects of instream gravel mining. *Landscape and Urban Planning*, **28**: 225-243.

Lambert, C.P., Walling, D.E., 1988. Measurement of channel storage of suspended sediment in a gravel-bed river. *Catena*, **15**: 65-80.

Li, W., Qi, P., Sun, Z., 1997. Deformation of river bed and the characteristics of sediment transport during hyper-concentrated flood in the Yellow River. *International Journal of Sediment Research*, **12** (3): 72–79.

López-Bermudez, F., Romero-Díaz, M.A., 1989. Piping erosion and badland development in south-east Spain. *Catena Supplement Band*, **14**: 59–73.

López-Tarazón, J.A., Batalla, R.J., Vericat, D., 2010a. In-channel sediment storage in a highly erodible catchment: the River Isábena (Ebro Basin, Southern Pyrenees). *Zeitschrift für Geomorphologie* (accepted, in press).

López-Tarazón, J.A., Batalla, R.J., Vericat, D., Balasch, J.C., 2010b. Rainfall, runoff and sediment transport relations in a mesoscale mountainous catchment: the River Isábena (Ebro basin). *Catena*, **82**: 23-34.

López-Tarazón, J.A., Batalla, R.J., Vericat, D., Francke, T., 2009. Suspended sediment transport in a highly erodible catchment: The River Isábena (Southern Pyrenees). *Geomorphology*, **109**: 201-221.

López-Tarazón, J.A., Batalla, R.J., Vericat, D., Francke, T., 2010c. The balance of sediment in a highly dynamic catchment. An estimation based on field data and non-parametric statistics (in preparation, to be submitted to *Geomorphology*).

Mamede, G., 2008. Reservoir sedimentation in dryland catchments: modelling and management. Unpublished PhD Thesis, Universität Potsdam, Germany.

Mamede, G.L., Bronstert, A., Francke, T., Muller, E.N., De Araujo, J.C., Batalla, R.J., Guntner, A., 2005. 1D Process-based modelling of reservoir sedimentation: a case study for the Barasona reservoir in Spain. In: Rui, M.L.F., Alves, E.C.T.L., Leal, J.G.A.B, Cardoso, A.H. (eds.): *River Flow 2006*. Taylor and Francis, London, vol. 2, pp. 1585-1595, ISBN 0-415-40814-8.

Martínez-Casasnovas, J.A., Poch, R.M., 1998. Estado de conservación de los suelos de la cuenca del embalse de Joaquín Costa. *Limnética*, **14**: 83 - 91.

Meybeck, M., 1994. Origin and variable composition of present day riverborne material. *Material Fluxes on the Surface of the Earth*, 1994. National Academy of Sciences, pp: 61–73.

Morton, R.A., 2003. *An Overview of Coastal Land Loss: with Emphasis on the Southeastern United States*. U.S. Geological Survey. Open File Report 03-337.

Nadal-Romero, E., Regüés, D., 2010. Geomorphological dynamics of subhumid mountain badland areas – weathering, hydrological and suspended sediment transport processes: A case study in the Araguás catchment (Central Pyrenees) and implications for altered hydroclimatic regimes. *Progress in Physical Geography*, **34**(2): 123-150.

Navas, A., Valero, B., Machín, J., Walling, D., 1998. Los sedimentos del embalse Joaquín Costa y la historia de su depósito. *Limnética*, **14**: 93-112.

Newson, M.D., 1989. Flood effectiveness in river basins: progress in Britain in a decade of drought. In: Beven, K., Carling, P. (eds.): *Floods: Hydrological, Sedimentological and Geomorphological Implications*. Geomorphology in Environmental Planning, vol. 1. John Willey and sons publications, Chichester, UK, pp. 151–171.

Palau, A., 1998. Estudio limnológico del ecosistema fluvial afectado por los vaciados del embalse de Barasona. Limnética, **14**: 1-15.

Penella, M.E., 1997. Caracterización de badlands y análisis de su dinámica mediante estudio multitemporal de fotografías aéreas y SIG en Campo (Huesca). Unpublished Master Thesis, University of Lleida, Spain.

Petts, G.E., 1984. *Impounded Rivers. Perspectives for Ecological Management*. Wiley, New York, 326 pp.

Piccarreta, M., Faulkner, H., Bentivenga, M., Capolongo, D., 2006. The influence of physico-chemical material properties on erosion processes in the badlands of Basilicata, southern Italy. *Geomorphology*, **81**: 235–51.

Poch, R.M., Martínez-Casasnovas, J.A., 1997. Prevention of reservoir siltation in large watersheds: from sediment source identification to the design of soil conservation measures. *Journal of Soil and Water Conservation*, **52**: 285-286.

Schumm, S.A., 1977. *The fluvial system*. John Wiley & Sons, New York.

Scullion, J., 1983. Effects of impoundments on downstream bed materials of two upland rivers in mid-Wales and some ecological implications. *Archiv für Hydrobiologie*, **96**: 329–344.

Serrat, N., Martínez-Casasnovas, J.A., 1998. Cartografía del riesgo de erosión hídrica en grandes cuencas hidrográficas mediante técnicas de teledetección y SIG. *Montes*, **54**: 27-35.

Soil Survey Staff, 1996. Keys to Soil Taxonomy, 7th ed. U.S. Government Printing Office, Washington, DC.

Solé-Benet, A., Calvo-Cases, A., Cerdà, A., Lázaro, R., Pini, R., Barbero, J., 1997. Influences of micro-relief patterns and plant cover on runoff related to processes in badlands from Tabernas (SE Spain). *Catena*, **31**: 28–38.

Solé-Sabarís, L., 1958. Geografia de Catalunya. Barcelona: Aedos, 3 vol.

Valero-Garcés, B., Navas, A., Machín, J., 1997. Sediment deposition in the Barasona reservoir (central Pyrenees, Spain): temporal and spatial variability of sediment yield and land use impacts. *Human Impact on Erosion and Sedimentation*, IAHS Publ. no. **245**: 241-249.

Valero-Garcés, B., Navas, A., Machín, J., Walling, D., 1999. Sediment sources and siltation in mountain reservoirs: a case study from the Central Spanish Pyrenees. *Geomorphology*, **28**: 23-41.

Verdú, J.M., 2003. Análisis y modelización de la respuesta hidrológica y fluvial de una extensa cuenca de montaña mediterránea (río Isábena, Pre-Pirineo). Unpublished PhD Thesis, Universitat de Lleida, Spain. URL: http://www.tdx.cat/TDX-0630107-193135.

Verdú, J.M., Batalla, R.J., Martínez-Casasnovas, J.A., 2006a. Estudio hidrológico de la cuenca del río Isábena (Cuenca del Ebro). I: Variabilidad de la precipitación. *Ingeniería del Agua*, **13**(4): 321-330.

Verdú, J.M., Batalla, R.J., Martínez-Casasnovas, J.A., 2006b. Estudio hidrológico de la cuenca del río Isábena (Cuenca del Ebro). II: Respuesta hidrológica. *Ingeniería del Agua*, **13**(4): 331-343.

Verdú, J., Martínez-Casasnovas, J.A., García-Hernández, N., 2004. Respuesta hidrológica de la cuenca del río Isábena (Huesca) a los cambios en la vegetación y los usos del suelo en la década de los noventa. *Lucas Mallada*, **11**: 213-228.

Walling, D.E., 2006. Human impact on land-ocean sediment transfer by the world's rivers. *Geomorphology*, **79**: 192-216.

Walling, D.E., Owens, P.N., Leeks, G.J.L., 1998. The role of channel and floodplain storage in the suspended sediment budget of the River Ouse, Yorkshire, UK. *Geomorphology*, **22**: 225-242.

Walling, D.E., Owens, P.N., Leeks, G.J.L., 1999. Rates of contemporary overbank sedimentation and sediment storage on the floodplains of the main channel systems of the Yorkshire Ouse and River Tweed, UK. *Hydrological Processes*, **13**: 993-1009.

Williams, G.P., 1989. Sediment concentration versus water discharge during single hydrologic events in rivers. *Journal of Hydrology*, **111**: 89-106.

Williams, G.P., Wolman, M.G., 1984. *Downstream effects of dams on alluvial rivers*. USGS Proffesional paper 1986.

Wischmeier, W.H., Smith, D.D., 1978. Predicting rainfall erosion losses - A guide to conservation planning. USDA Agriculture Handbook num. 537. US Government Printing Office. Washington, DC.

Xu, J., 1997. The optimal grain size composition of suspended sediment of hyperconcentrated flow in the middle Yellow River. *International Journal of Sediment Research*, **12** (3): 170–176.

CHAPTER 2

METHODS

INDEX CHAPTER 2: METHODS

Figure captions

Figure 2.1. General map of the Isábena catchment, showing locations of the main badlands areas (source of fine sediment), the Barasona Reservoir and all the monitoring stations.

Figure 2.2. (A) Outside view of the Capella gauging station (EA047). (B) Detail of the interior of the EA047 with the measuring and sampling equipments.

Figure 2.3. (A) Electromagnetic current meter Valeport 801 adapted to a depth-integrated suspended sediment sampler DH-74. (B) Detail of the electromagnetic current meter Valeport 801.

Figure 2.4. (A) Electronic automatic sampler ISCO 3700; (B) Crane used to operate the manual samplers; (C) Cable suspended depth-integrating USGS DH-74; (D) Cable suspended depth-integrating USGS DH-59.

Figure 2.5. (A) Location of the turbidimeter at the EA047; (B) McVann ANALITE NEP-9350; (C) Endress+Hausser Turbimax W CUS41.

Figure 2.6. (Initial) sampling design at the EA047 (flood registered in April 2006).

Figure 2.7. Examples of the instrumentation installed at the monitored sub-basins: (A) Cabecera, (B) Carrasquero, (C) Villacarli, (D) Ceguera and (E) Lascuarre. Note that the capacitive water stage sensors (Trutrack WT-HR) are installed inside the grey PVC tubes.

Figure 2.8. Campbell ARG100 tipping-bucket rain gauges installed at (A) Villacarli and (B) Roda de Isábena.

Figure 2.9. Flux diagram of the instrumentation, the works done during the Thesis and the interactions between all of them to achieve the main research goals.

Figure 2.10. (A) Filtering equipment; (B) Decanting equipment; (C) Examples of filters after processing; (D) Sediment in plates resulting after decanting.

Figure 2.11. (A) Rating curve of the McVann ANALITE NEP-9350 turbidimeter; (B) Rating curve of the Endress+Hausser Turbimax W CUS41 turbidimeter.

Figure 2.12. (A) Rating curve (i.e., *h/Q*) of the Capella gauging station after modelling with HEC-RAS©; (B) Rating curve (i.e., *h/Q*) of the Lascuarre measuring section after modelling with WinXSPro©. Black dots at both figures represent the gauges done.

Table captions

Table 2.1. Summary of the different monitoring stations and their instrumentation.

1. INTRODUCTION

This chapter describes the fieldwork design, sampling and monitoring, the laboratory work and the calculation methods undertaken to meet the aim of the present PhD Thesis. All together constitutes the bases to provide the data and, ultimately, to establish the sediment budget and the sediment yield of the Isábena basin. Specifically, section 2.1 presents the criteria that we used to select the Isábena basin and sub-basins to carry out the present thesis. Section 2.2 exposes the hydrological and suspended sediment monitoring network used in the research; field instrumentation is described as well as the techniques employed to sample during floods and low flow conditions. Section 3 describes the laboratory techniques applied to process water and sediment samples to each set of data. Finally section 4 presents data process and the calculation methods employed to obtain the final data sets.

2. FIELDWORK DESIGN, SAMPLING AND MONITORING

2.1. Study basins selection criteria

In the current context in which regulation of Mediterranean rivers is such intense and siltation of reservoirs becomes problematic, together with the scarcity of studies regarding that topic, the River Isábena basin (i.e., a representative Pyrenean Mediterranean catchment) offers an optimum setting to analyze sediment transport dynamics and the geomorphology of a non-regulated streamcourse located upstream of a reservoir threatened by historical siltation problems. Results derived from the present work are meant to be useful for the Water Authorities to implement more efficient reservoir management programmes, as well as to provide a starting point to develop attenuation techniques of sediment siltation (i.e., temporal sediment traps, regular sediment pass-through practices). Besides that, the frequent presence of high density flows (e.g., hyper-concentrated flows) draining the Isábena basin (e.g., a mesoscale mountainous catchment) may allow the study and quantification of the role played by such flows as controllers of the sediment transport, sediment yield, channel morphology and bed-material dynamics in such dynamic geomorphic environments.

Regarding to the instrumented sub-basins of the basin, the selection criteria was based mainly on 2 facts: a) the 5 sub-basins are the unique that show permanent flow over time in the Isábena, despite 2 of them (e.g., Ceguera and Lascuarre) can be dried up during the driest months (i.e., summer); b) all of them present some badland zones on their surface areas, so they may be the main sediment producers of the basin; Cabecera can be considered as an exception, because it doesn't have any badland formation. Besides that, the selected sub-catchments are the same that these selected by Verdú (2003).

2.2. Discharge, suspended sediment and rainfall measurements

To carry out the present work, three basic measurements were undertaken at different monitoring sections: discharge, suspended sediment transport and rainfall. Initially, in 2005, monitoring efforts were focused in the Capella gauging station, located at the outlet of the basin (e.g., EA047, Fig. 2.1), with the objective of quantifying the total suspended sediment load that eventually would be deposited into the Barasona Reservoir, following a *black-box* model approach.

At this monitoring station, discharge is measured by the Ebro Water Authorities at a 15 minutes frequency. Real time water stage and discharge data are available online (www.saihebro.com). Frequent direct flow gauges were performed during flood and base flow conditions with the objective to populate the entire range of water stages in the rating curve (i.e., relation between water stage and discharge) of the station, reducing its uncertainties and associated extrapolation errors. Gauges were performed by means of an electromagnetic current meter Valeport 801 adapted to a depth-integrated suspended sediment sampler DH-74 (Fig. 2.3). All gauges have been statistically analysed together to develop the water stage/discharge rating curve of the gauging station, using this rating curve instead of the official one to obtain the discharge values.

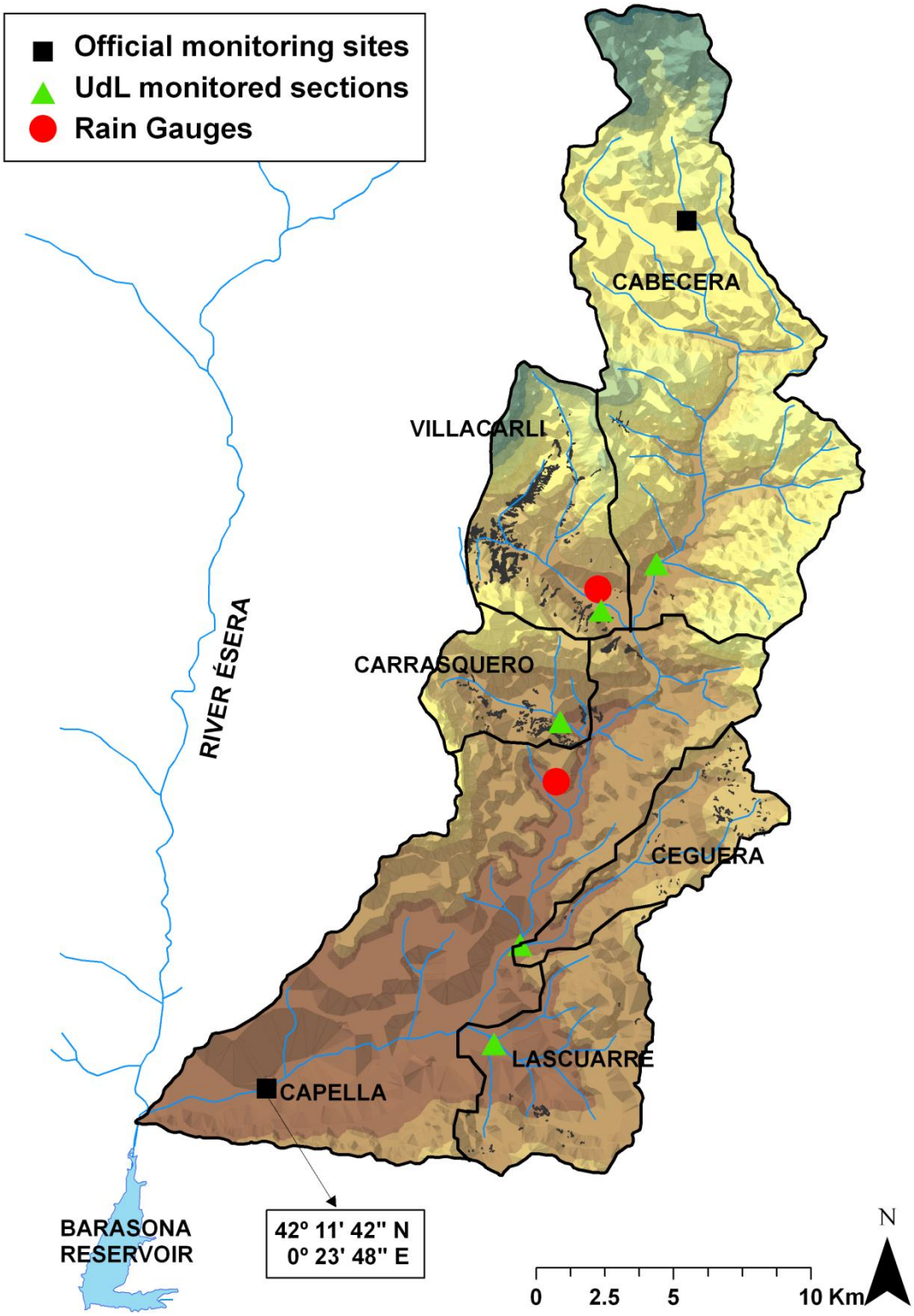

Figure 2.1. General map of the Isábena catchment, showing locations of the main badlands areas (source of fine sediment), the Barasona Reservoir and all the monitoring stations.

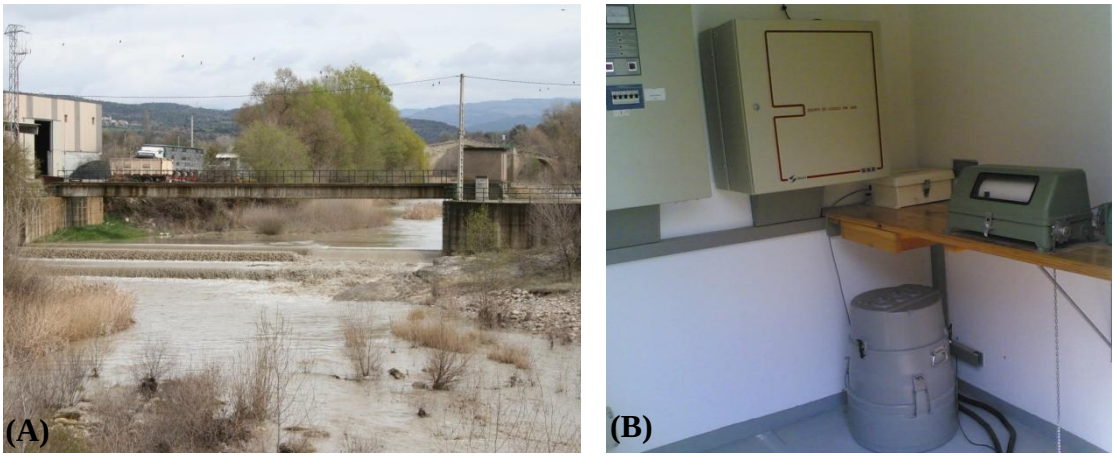

Figure 2.2. (A) Outside view of the Capella gauging station (EA047). (B) Detail of the interior of the EA047 with the measuring and sampling equipments.

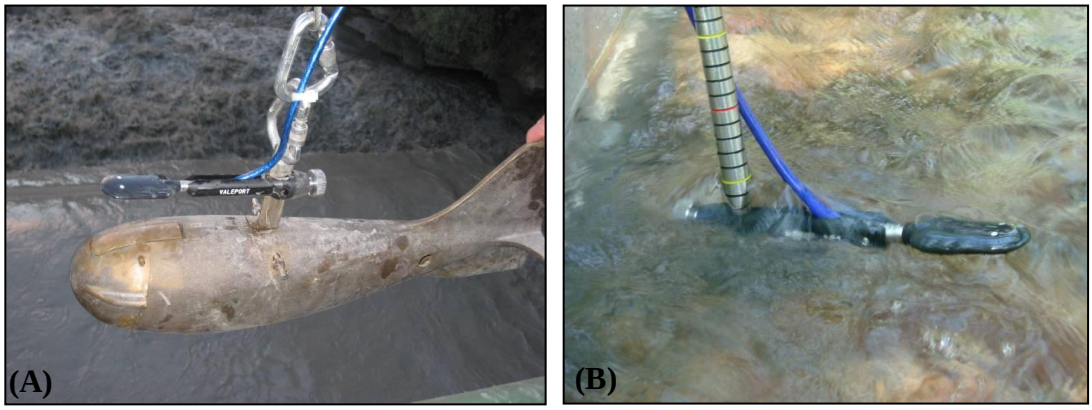

Figure 2.3. (A) Electromagnetic current meter Valeport 801 adapted to a depth-integrated suspended sediment sampler DH-74. (B) Detail of the electromagnetic current meter Valeport 801.

Sampling of suspended sediment transport at the catchment outlet can be divided in relation to: a) direct techniques and b) indirect techniques.

a) Direct techniques. This type of techniques is based on collecting water samples directly from the river. The collection can be done by means of automatic and/or manual samplers. The automatic sampler installed at Capella was an electronic ISCO 3700 sampler (Fig. 2.4). The sampler was programmed to sample during floods from a previously determined water stage. It samples up to 24 bottles of 1 litre at a predetermined time frequency (e.g., usually 1 h). Water samples were also obtained manually during low flow and flood conditions. The cable-suspended, depth-integrating

USGS DH manual samplers (e.g., DH-59, DH-74) were operated from bridges using a manual crane (Fig. 2.4). Samples were taken from different points (locations) across the section every 15-30 min during floods while a single sample from the middle point of the cross section was obtained during low-flow conditions. The bottles are filled up to the 75-90% of its total capacity (1 litre), depending on the sampling conditions (e.g., water stage). Finally, all samples were labelled, stored in bottles previously cleaned with deionised water and brought to the laboratory to be processed.

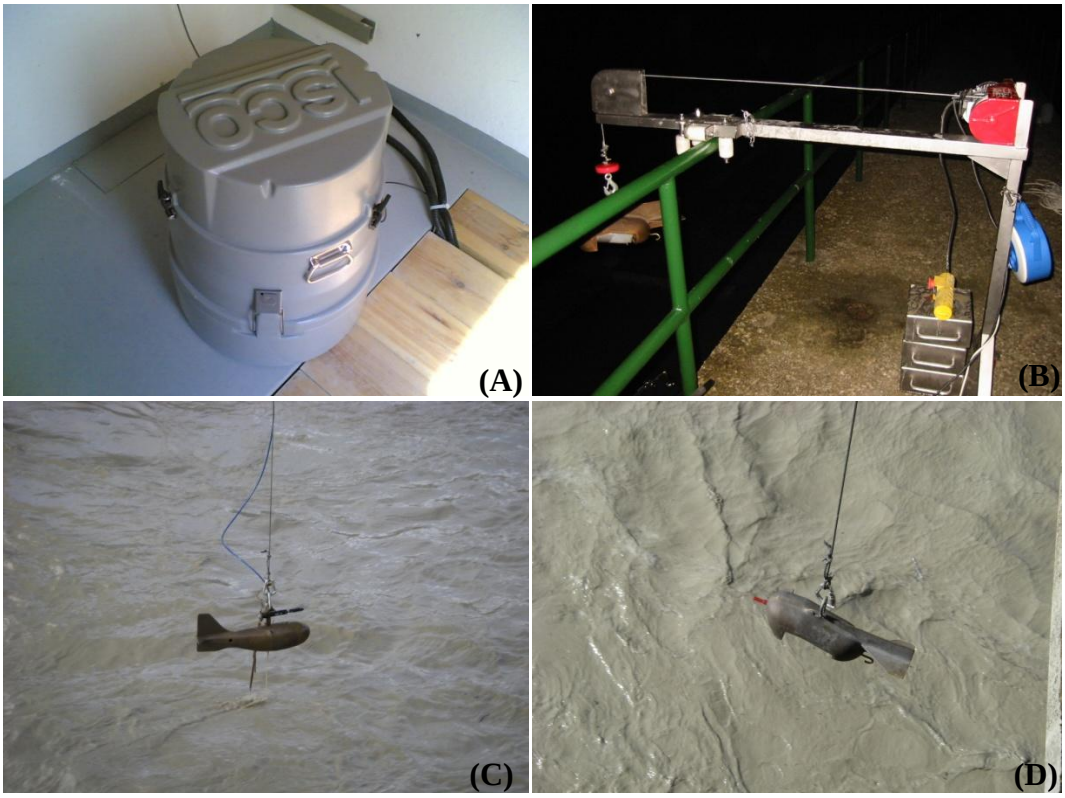

Figure 2.4. (A) Electronic automatic sampler ISCO 3700; (B) Crane used to operate the manual samplers; (C) Cable suspended depth-integrating USGS DH-74; (D) Cable suspended depth-integrating USGS DH-59.

b) Indirect techniques. Indirect techniques consist in obtaining the suspended sediment concentration by means of the transformation of another variable. Suspended sediment concentration was derived from turbidity records obtained, initially, by a low-range turbidimeter McVann ANALITE NEP-9350 (measuring range 0-3000 NTU ≈ 3 g l^{-1}) that was replaced in November 2007 by a high range back-scattering Endress+Hausser Turbimax WCUS41 turbidimeter (range up to 300 g l^{-1}) (Fig. 2.5). Water turbidity is an expression of the optical property of the water that causes light to be scattered and absorbed rather than transmitted in straight lines trough the sample; it

can be defined as the reduction of transparency of a liquid caused by the presence of undissolved matter (i.e., clays, soluble organic composites, plankton, microorganisms, etc) being, this way, the opposite of clarity (Lawler, 2005). Turbidity is measured in Nephelometric Turbidity Units (NTU); these units do not have direct transformation to concentration, but they can be converted into suspended sediment concentration by means of a calibration with water and sediment samples taken simultaneously and at the same place where the turbidimeter is installed. Turbidimeters were installed, in the EA047 (Capella Station), at the left bank of the river, in the same place were the intake of the ISCO was placed (Fig. 2.5). The turbidity probes were linked to a Campbell CR-510 data-logger. Turbidity sampling was set up at 1-min intervals while the logging was at 15-min intervals (thus recording the average value of the samples between log intervals).

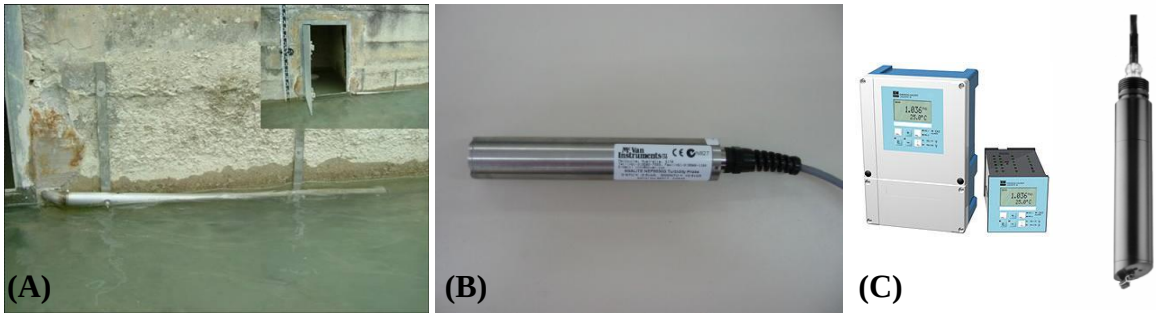

Figure 2.5. (A) Location and installation of the turbidimeter at the EA047; (B) McVann ANALITE NEP-9350; (C) Endress+Hausser Turbimax WCUS41.

Together with discharge and suspended sediment transport, rainfall was continuously monitored at 2 places in the Isábena basin (e.g., EA047 at the outlet and Les Paules at headwaters; Fig. 2.1). Rainfall was measured by means of tipping-bucket rain gauges that the Ebro Water Authorities manages. These rain gauges register accumulated values of rainfall every 15 minutes.

With this set of instruments, we started to gather data in a continuous way on discharge, suspended sediment concentration and rainfall to obtain a first estimation of the suspended sediment loads flowing through the Capella monitoring section. The optimum sampling design at Capella monitoring station (EA047) during that period is summarized in the example plotted in the Figure 2.6. During low-flows, water turbidity was continuously measured by the turbidity probes, and some manual samples were taken weekly and fortnightly. During floods, when hyper-concentrated conditions are

present, and to avoid gaps on the turbidity record, automatic and manual samples were taken at a fixed time frequency to calibrate the turbidimeters and to get data to rebuilt sedigraphs when the turbidimeters were out of range (e.g., no NTU was recorded). Initial sampling design improved substantially when a high-range turbidimeter was installed; once it was calibrated and once we tested that it was never out of range, we decided to stop the automatic sampling (i.e., ISCO 3700), and keeping further just with the manual sampling during and between floods.

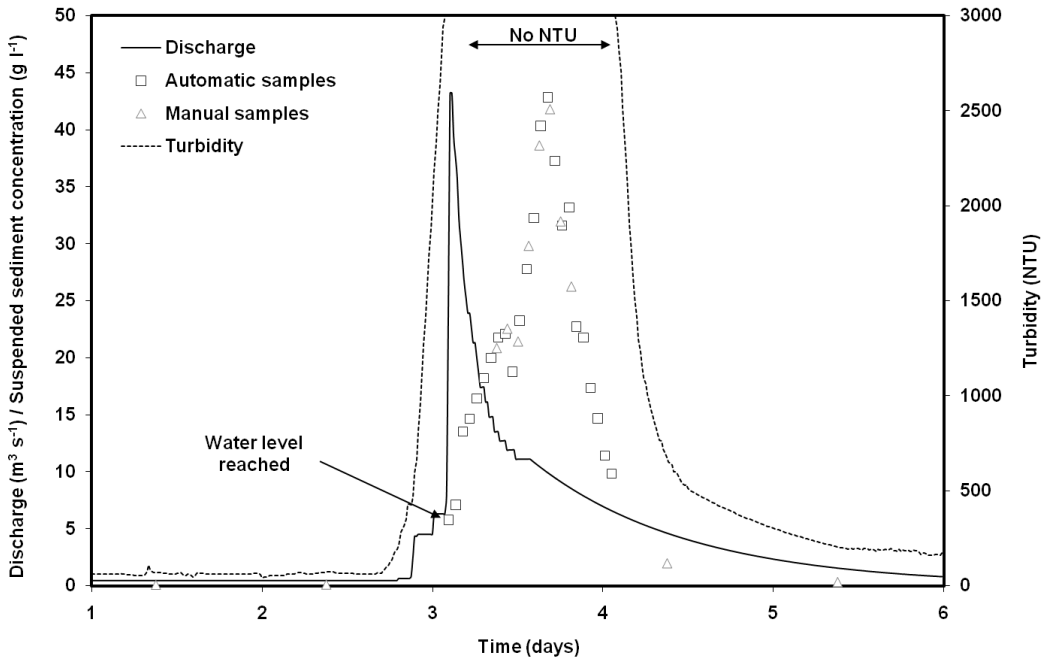

Figure 2.6. (Initial) sampling design at the EA047(flood registered in April 2006).

Additionally to the outlet monitoring station, 8 new stations were set up and used (Fig. 2.1). In 2007, after taking consciousness of the enormous suspended sediment transport of the Isábena basin we decided to increase and update the instrumentation in the basin (i.e., new equipments, increment in the spatial and temporal resolution of the measurements), not only to control the sediment yield at the main catchment outlet, but to estimate sediment load discharged from the main sub-basins. For this purpose we monitored the main five sub-basins of the catchment (i.e., Cabecera, Villacarli, Carrasquero, Ceguera and Lascuarre), at their confluence with the Isábena mainstem; there we started to measure discharge and sediment transport; in addition, we installed two more tipping-bucket rain gauges at the Villacarli and Carrasquero sub-basins where, hypothetically, most of the sediment is generated (Fig. 2.1). All instrumentation at these stations is the same and follows identical designs and sampling strategies

Discharge is measured by means of capacitive water stage sensors/loggers (Trutrack WT-HR) installed at suitable cross sections in the sub-catchments (i.e., in river constriction below bridges were available) (Fig. 2.7).

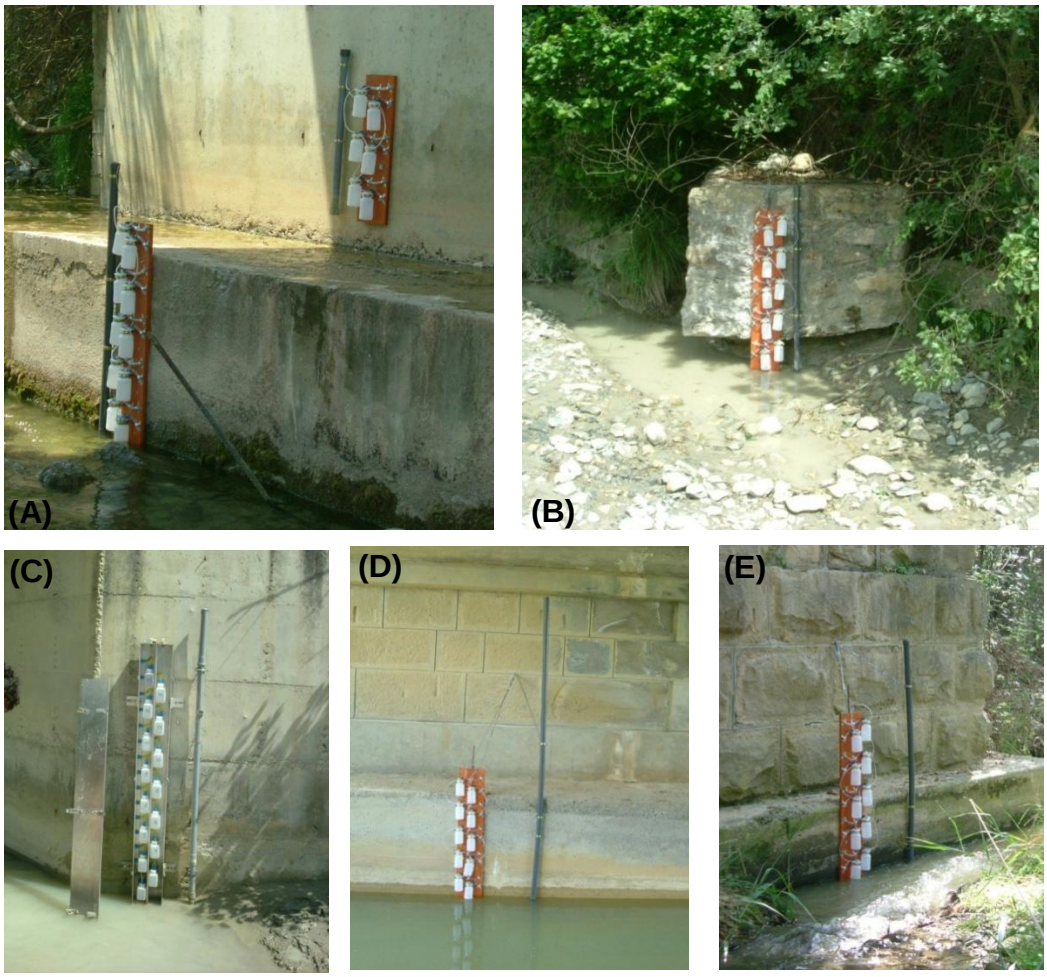

Figure 2.7. Examples of the instrumentation installed at the monitored sub-basins: (A) Cabecera, (B) Carrasquero, (C) Villacarli, (D) Ceguera and (E) Lascuarre. Note that the capacitive water stage sensors (Trutrack WT-HR) are installed inside the grey PVC tubes.

Flow was recorded at a 5-min interval and was later converted into discharge by means of the derived water stage-discharge rating curves of each location. To derive these rating curves, repeated discharge measurements (e.g., gauges) were made at each tributary using an electromagnetic flow meter Valeport 801 (Fig. 2.3b) and completed with cross section surveys (Geodimeter total station).

Suspended sediment was sampled by means of water stage samplers at the sub-basins (Fig. 2.7). These samplers were hand-made built based on the original design by Schick

(1967). These samplers are designed to take 0.5-l bottles at different water stages during the rising limb of the flood event. During the recession, the bottles are filled up, although the design avoids water recirculation, and no samples are taken. In addition, manual samples were taken in 1-litre-bottles during flood events (mainly during the recession period) and routinely (weekly or fortnightly) during low flows. As in the case of Capella, all samples were labelled, stored in bottles previously cleaned with deionised water and brought to the laboratory to be processed.

To complete the rainfall record across the basin we installed two Campbell ARG100 tipping-bucket rain gauges in Villacarli (Villacarli sub-basin, Fig. 2.1) and in Roda de Isábena (located downstream of the Carrasquero sub-basin measuring section; Fig. 2.1). Both of them were connected to a Campbell CR-200 data-logger, setting-up the measurements at 1-min intervals (Fig. 2.8).

Figure 2.8. Campbell ARG100 tipping-bucket rain gauges installed at (A) Villacarli and (B) Roda de Isábena.

Table 2.1 summarizes the different monitoring stations set up and used in this thesis, providing the list of instrumentation for each of these. More information about the instrumentation can be found at papers contained in **Chapter 3**, **4** and **6**.

Table 2.1. Summary of the different monitoring stations and their instrumentation.

Monitoring station	Discharge	Suspended sediment	Rainfall
Capella	Official gauging station	ISCO 3700 / Turbidimeters	Tipping bucket
Cabecera	Trutrack WT-HR	Water stage sampler	N/A
Villacarli	Trutrack WT-HR	Water stage sampler	Tipping bucket
Carrasquero	Trutrack WT-HR	Water stage sampler	N/A
Ceguera	Trutrack WT-HR	Water stage sampler	N/A
Lascuarre	Trutrack WT-HR	Water stage sampler	N/A
Les Paules	N/A	N/A	Tipping bucket
Roda de Isábena	N/A	N/A	Tipping bucket

Figure 2.9 presents a flux diagram of the instrumentation, the works done during the Thesis and the interactions between all of them.

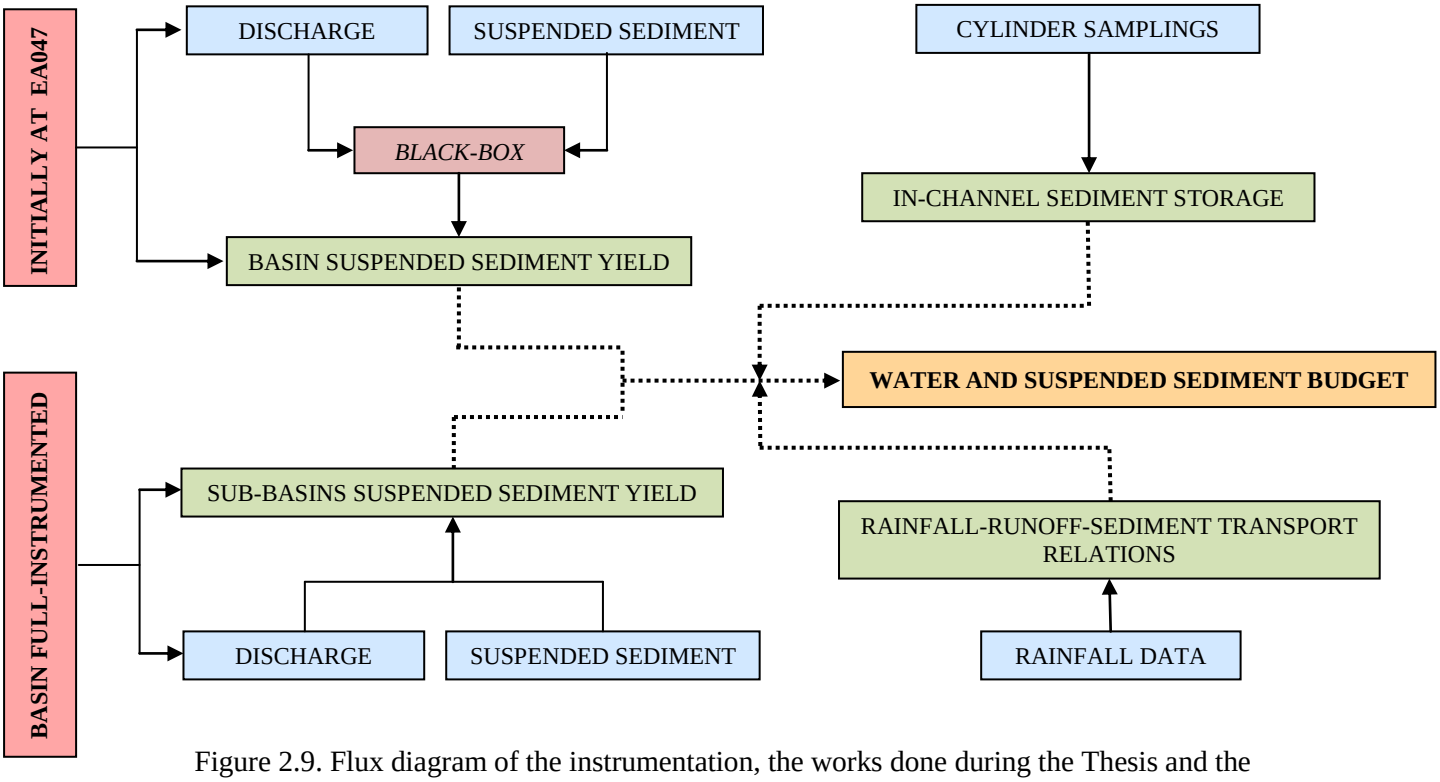

Figure 2.9. Flux diagram of the instrumentation, the works done during the Thesis and the interactions between all of them to achieve the main research goals.

3. LABORATORY WORK

Laboratory work consisted mostly in processing the almost 2000 water and sediment samples collected during the fieldwork (e.g., automatic and manual samples everywhere in the catchment). Samples were vacuum filtered in cellulose and glass microfiber filters (Millipore, 0.045 mm pore size) when concentrations were (approximately) below 2 g l^{-1}; samples with higher concentrations were decanted (for more information see paper in **Chapter 3**). In both cases, water volume was simultaneously measured. Finally, all samples were oven-dried for 24 h at a constant 60ºC and weighted to determine the suspended sediment concentration. Figure 2.10 shows the equipment used to filter and decant the samples and some examples of the resulting filters and decanting plates. Suspended sediment concentration (*SSC*, g l^{-1}) was calculated for each water sample following the equation:

$$SSC = P_n/V$$

where, P_n represents the neat weight of the sediment retained in the filter (in g) and V represents the water volume of the sample (in l). Organic matter content in the samples was visually examined and found negligible so no explicit process was made.

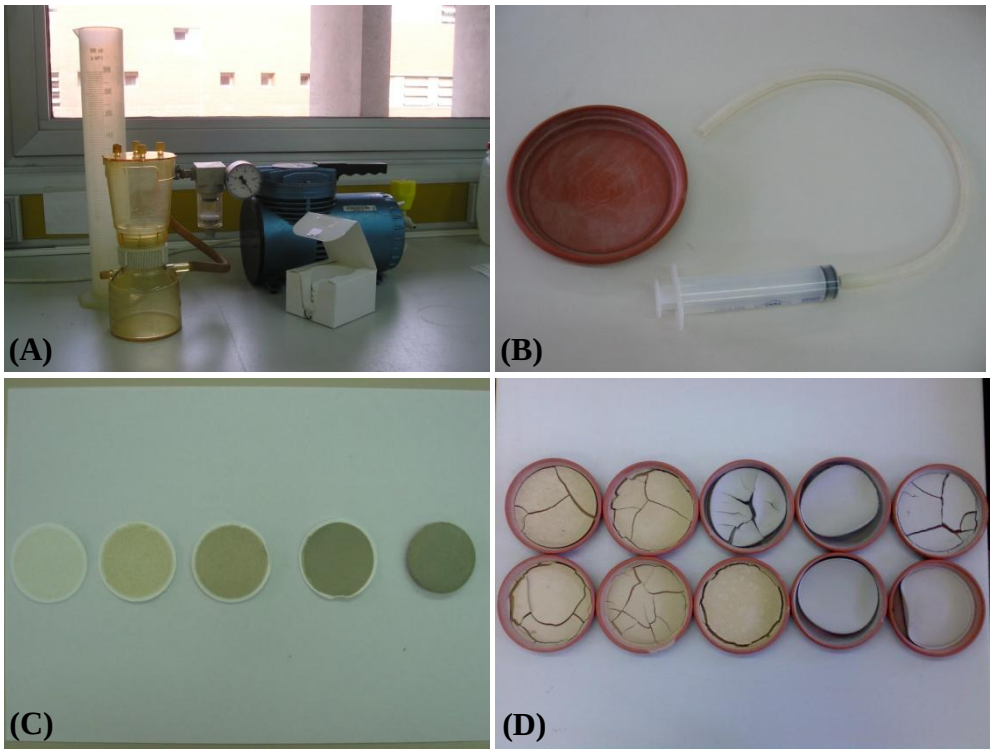

Figure 2.10. (A) Filtering equipment; (B) Decanting equipment; (C) Examples of filters after processing; (D) Sediment in plates resulting after decanting.

Turbidity was transformed in suspended sediment concentration by means of a calibration procedure for each turbidimeter. Turbidity records were firstly clean after identifying and correcting anomalous values. Corrections were done by deleting the erroneous values and creating new data by interpolating between the closer correct values. Anomalous values could be the result of a series of malfunctioning situations, including (a) the turbidimeter being out of range, (b) the blind effect (i.e., low turbidity measurements because of the presence of a bio-film on the lens or an extended period of high suspended sediment concentrations), (c) fouling from algae development and other phenomena, such as bubbles or density discontinuities (e.g., Lawler, 2005; Lawler et al., 2006). Once the turbidity data records are revised and corrected, a rating curve between pair of values of turbidity (e.g., NTU) and suspended sediment concentration (e.g.,

SSC) was obtained. In the case of the McVann ANALITE NEP-9350 turbidimeter, the statistically significant rating curve was $SSC=(0.0012*NTU) + 0.0605$ ($N = 490$; $r^2 = 0.82$; $p<0.001$), while in the case of the Endress+Hausser Turbimax WCUS41 turbidimeter, two separate rating curves were obtained (e.g., Nadal-Romero et al., 2008). For sediment concentrations below 40 g l^{-1}, a polynomial regression was the best fit to the data, yielding an equation of the form $SSC=(0.1436*NTU^2)+(1.9673*NTU)$ ($N= 145$; $r^2=0.96$; $p<0.01$), whereas for higher sediment concentration values, a linear regression yielded the highest coefficient of determination: $SSC=(5.7738*NTU)+1.9608$ ($N=6$; $r^2=0.94$; $p<0.01$). The rating curves obtained for both turbidimeters are shown in Figure 2.11.

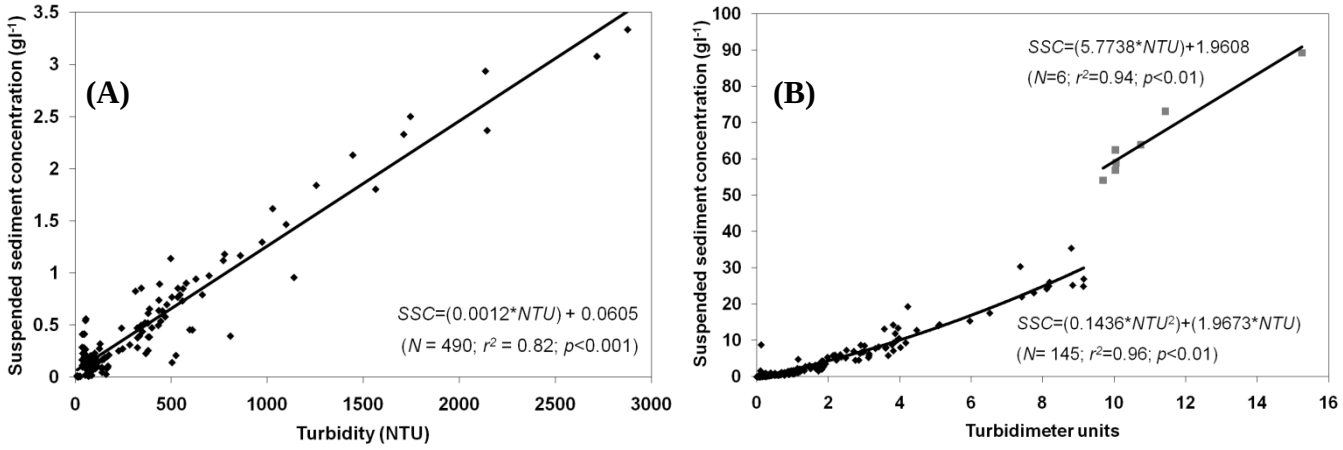

Figure 2.11. (A) Rating curve of the McVann ANALITE NEP-9350 turbidimeter; (B) Rating curve of the Endress+Hausser Turbimax WCUS41 turbidimeter.

Discharge (Q in m^3 s^{-1}) was calculated at every section using the velocity/surface method. Velocity and depth were measured at several vertical points (from 2 to 10) in section by means of an electromagnetic current meter (e.g., Valeport 801, see Fig. 2.3). Bed-area and slope were derived from the topographical surveys carried out at all the measuring sections by means of a Geodimeter total station. Discharge is calculated following the equation:

$$Q=V\times A$$

where V represents the velocity in m s^{-1} and A the bed surface in m^2. Once discharge was calculated, the rating curves (i.e., relation between water level and discharge) of each section were estimated. The rating curve of the Capella gauging station and

Lascuarre measuring section are shown in Figure 2.12 as an example. These calculations were done and validated by means of the software HEC-RAS© (developed by the USACE) and WinXSPro© (developed by the USDA). Both software applications calculate the discharge by means of the Manning's equation, having as a bases topographical information and grain-size distribution data (i.e., grain-size samplings were done at each section) to estimate the roughness coefficient *n*. The Manning equation is expressed as follows:

$$V = \left(R^{2/3} \times S^{1/2}\right)/n$$

where V represents the velocity in m s^{-1}, R the hydraulic radius in m, S is the dimensionless longitudinal slope of the section and n is the roughness coefficient in mm^{-1} calculated following the equation (Strickler, 1923). Discrepancies between sampled and modelled values lower than the 5% were found at all monitoring sections.

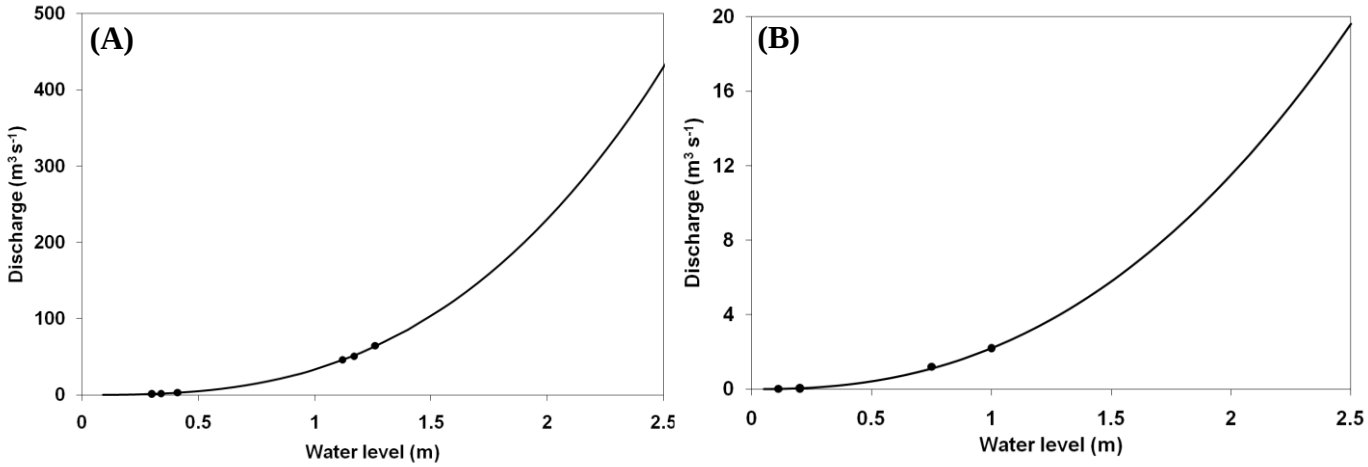

Figure 2.12. (A) Rating curve (i.e., *h*/*Q*) of the Capella gauging station after modelling with HEC-RAS©; (B) Rating curve (i.e., *h*/*Q*) of the Lascuarre measuring section after modelling with WinXSPro©. Black dots at both figures represent the gauges done.

4. DATA PROCESS

Suspended sediment load is often estimated using the Flow Duration Curve Approach developed by Walling (1984). Although this method is appropriated in catchments where there is a positive statistically significant relation between discharge and suspended sediment concentration, it cannot be applied in catchments where suspended

sediment is not directly related to driving forces, presenting enormous variability related to the supply of fine sediment to the channel network. This is the case of the River Isábena where for a given discharge (e.g., *Q*), suspended sediment concentrations (e.g., *SSC*) can oscillate up to 6 orders of magnitude. Then, the use of the traditional rating curve method (Walling, 1984) was not feasible because of the lack of statistical significance in the relationship between *Q* and *SSC* over the study period (for more details see the paper in chapter 3). Although once the high range turbidimeter was installed, this problem was overcome because of all ranges of transport were recorded and sedigraphs were obtained, a methodology was required for preliminar periods in which the low range turbidity meter was in operation (2005-2007). The strategy adopted for this period was:

- (a) Periods where $SSC > 3$ g l^{-1}: these periods occurred mainly during floods, with concentrations above the detection limit of the low-range turbidimeter. In these cases the suspended sediment load was obtained by using an interpolation method (Phillips et al., 1999; Rovira and Batalla, 2006); this method assumes that an instantaneous sample concentration is representative of the intersampling period between samples. Altogether, the interpolation method was used for 556 samples, with resulting SSC values multiplied by the discharge to obtain the total load of a given period.

- (b) Periods where $SSC < 3$g l^{-1}: these represented the most of the time during the study period. For these periods, continuous turbidity data were available at a time resolution of 15-min. In this case, the sediment load has been obtained by multiplying *Q* and the estimated *SSC* (i.e., transformed *SSC* from turbidity records) for each 15-min interval. Finally, both sets of results were added together to obtain the total sediment load for the studied periods.

Since the installation of the high-range backscatter Endress+Hausser Turbimax WCUS41 turbidimeter (November 2007), (b) was the only methodology used since the upper measuring range of the turbidimeter was never more exceeded.

Continuous sedigraphs were produced for the studied sub-catchments by using some statistical techniques (e.g., *Random Forests*, *Quantile Regression Forests*). This methodology is not fully explained at this point since there are 3 chapters of the present

volume dedicated to this topic. However a brief summary is given here (for more information see **Chapter 6**, **Annex 1** and **Annex 2)**: sedigraphs were estimated (at 15-min resolution, a high temporal frequency, predetermined by the maximum resolution of our rainfall and discharge data.) for all sites using Random Forest and Quantile Regression Forest models (hereafter *RF* and *QRF* respectively) allowing, this way, the calculation of sediment yields from ancillary data.

The *QRF* (Meinshausen, 2006) is a non-parametric multivariate regression technique that builds on *RF* regression tree ensembles (Breiman et al., 1984). Regression trees (i.e., CARTs, Breiman et al., 1984) are constructed by recursive data partitioning, which can include both categorical and continuous data from ancillary datasets. *RF* and *QRF* employ an ensemble of these trees, each one grown on a random subset of the training data. In *RF*, model estimates are based on the mean of all tree predictions, whereas *QRF* employs the whole distribution of tree predictions and hence, offers the possibility to assess the accuracy and precision of model estimates (Meinshausen, 2006). The advantage of both *RF* and *QRF* is their ability to perform favourably when dealing with nonlinearity, imply no assumptions about the distribution of the data and are robust and capable of handling non-additive behaviour and non-Gaussian data, which makes these techniques particularly suited for *SSC* modelling (see more details in Francke et al., 2008a; 2008b). Model building and statistical analyses were conducted using the statistic software R (R-Team Development Core, 2006) with the Random Forest (Liaw and Wiener, 2002) and quantregForest (Meinshausen, 2007) packages.

Finally, the amount of fine sediment stored in the channel bed of the Isábena was also determined using the method developed by Lambert and Walling (1988) (for more information see **Chapter 5**). Field data provided information on the amount of sediment stored on the bed of the channel at specific sites that could be subsequently extrapolated to hydraulically and morphologically equivalent areas. Sediment storage is commonly temporarily and spatially variable, and may be remobilized during high flow periods. The sampling of sediment storage was done at four different cross-sections located in the lower part of the basin. Sampling sections were selected based on a) their location downstream from the main tributaries to include the total discharge and sediment transport from the basin and b) their representativeness of the morphological characteristics of the lower Isábena mainstem channel (i.e., riffle-pool system in typical

low gradient gravel-bed river). That work allowed us to obtain sediment storage data over a determinate period which could be compared with measurements of sediment exports from the catchment.

5. REFERENCES

Breiman, L.M., Friedman, J., Olshen, R., Stone, C., 1984. *Classification and regression trees.* Wadsworth: Belmont, CA.

Francke, T., López-Tarazón, J.A., Schröder, B., 2008a. Estimation of suspended sediment concentration and yield using linear models, random forests and quantile regression forests. *Hydrological Processes*, **22**: 4892–4904.

Francke, T., López-Tarazón, J.A., Vericat, D., Bronstert, A., Batalla, R.J., 2008b. Flood-based analysis of high-magnitude sediment transport using a non-parametric method. *Earth Surface Processes and Landforms*, **33**: 2064–2077.

Lambert, C.P., Walling, D.E., 1988. Measurements of channel storage of suspended sediment in a gravel-bed river. *Catena*, **15**: 65–80.

Lawler, D.M., 2005. Turbidimetry and nephelometry. In: Worsfold, P.J., Townshend, A., Poole, C.F. (eds): *Encyclopedia of Analytical Science*. Elsevier, 2nd ed., 343-351.

Lawler, D.M., Petts, G.E., Foster, I.D.L., Harper, S., 2006. Turbidity dynamics during spring storm events in an urban headwater river system: the Upper Tame, West Midlands, UK. *Science of the Total Environment*, **360**: 109–126.

Liaw, A., Wiener, M., 2002. Classification and Regression by randomForest. *R News*, **2**(3): 18-22.

Meinshausen, N., 2006. Quantile Regression Forests. *Journal of Machine Learning Research*, 7: 983-999.

Meinshausen, N., 2007. quantregForest: Quantile Regression Forests; R package version 0.2-2.

Nadal-Romero, E., Latron, J., Martí-Bono, C., Regüés, D., 2008. Temporal distribution of suspended sediment transport in a humid Mediterranean badland area: the Araguás catchment, central Pyrenees. *Geomorphology*, **97**: 601–616.

Phillips, J.M., Webb, B.W., Walling, D.E., Leeks, G.J.L., 1999. Estimating the suspended sediment loads of rivers in the LOIS study area using infrequent samples. *Hydrological Processes*, **13:** 1035–1050.

R-Team Development Core, 2006. R: a Language and Environment for Statistical Computing. R Foundation for Statistical Computing: Vienna.

Rovira, A., Batalla, R.J., 2006. Temporal distribution of suspended sediment transport in a Mediterranean basin: the lower Tordera (NE Spain). *Geomorphology*, **79**: 58–71.

Schick, A.P., 1967. Gerlach troughs, overland flow traps. Field methods for the study of slope and fluvial processes. *Revue de Géomorphologie Dynamique*, **4**: 170-172.

Strickler, A., 1923. Beiträge zur Frage der Geschwindigheitsformel und der Rauhigkeitszahlen für Strome, Kanale und Geschlossene Leitungen. *Mitteilungen des Eidgenössischer Amtes für Wasserwirtschaft*, Bern, Switzerland, 16 pp.

Verdú, J., 2003. Análisis y modelización de la respuesta hidrológica y fluvial de una extensa cuenca de montaña mediterránea (río Isábena, Pre-Pirineo). Unpublished PhD Thesis, Universitat de Lleida, Spain. URL: http://www.tdx.cat/TDX-0630107-193135.

Walling, D.E., 1984. Dissolved loads and their measurements. In: Hadley, R.F., Walling, D.E, (eds): *Erosion and sediment yield: Some methods of measurements and modelling*. Geo Books, London; 111-177.

CHAPTER 3

SEDIMENT TRANSPORT

INDEX CHAPTER 3: SEDIMENT TRANSPORT

Figure captions in the paper

Figure 1. A) Location of the Isábena catchment in the Iberian Peninsula. B) Location of the Cinca, Ésera, and Isábena basins in the Ebro Basin (85,000 km^2). C) The Isábena catchment: location of the study reach.

Figure 2. Scatter plot of the relation between *Q* and *SSC* in the Isábena for the 3-year study period. Note that up to five orders of magnitude of *SSC* can be observed for the same range of discharges; the high scatter implies that no statistically significant relations exist between the two variables, either for the whole period or for each of the study years.

Figure 3. A) Hidrological regime of the River Isábena for the study period. The grey line represents the mean discharge for the complete period. Some floods include Q_i, where *i* means the return period of the floods. B) Mean monthly discharge for the study period.

Figure 4. Discharge and suspended sediment concentration at the Capella gauging station (i.e., EA47, Fig. 1).

Figure 5. Seasonal and annual distribution of rainfall, runoff, suspended sediment load, and specific sediment yield in the Isábena catchment.

Figure 6. Examples of the *Q*/*SSC* counterclockwise hysteretic patterns found in the River Isábena: a) 2 December 2005 (CC1); b) 14 May 2007 (CC1); c) 14 October 2005 (CC2) and d) 6 September 2006 (CC2) (see text for more details and discussion).

Figure 7. Monthly statistically significant relationships between rainfall (both in the headwaters and the outlet) and the suspended sediment load at the outlet of the Isábena catchment (Figure 1).

Figure 8. Suspended sediment load and runoff frequency curves for the study period and the individual years in the River Isábena.

Table captions in the paper

Table 1. Water samples obtained during the study period in the River Isábena

Table 2. Annual and mean hydrological values for the entire study period in the Isábena catchment.

Table 3. Summary of the main characteristics of the floods recorded during the study period in the River Isábena.

Table 4. Flood discharge data for the entire study period in the River Isábena.

Table 5. Flood suspended sediment data for the entire study period in the River Isábena.

Table 6. Seasonal and annual hydrology and suspended sediment load for the study period (2005-2008) in the River Isábena.

1. INTRODUCTION

This chapter describes the sediment transport processes and dynamics of the River Isábena at different temporal scales. For this purpose we present a paper analysing the sediment transport measured at the outlet of the Isábena basin, at the Capella gauging station (EA047). The paper is presented maintaining its original structure; its format has been adapted to the general format of the present volume.

Specifically, the paper was published by *Geomorphology* in March 2009; it reports on the suspended sediment transport and dynamics of the Isábena catchment during a 3-year period (May 2005 – May 2008) at different temporal scales (seasonal and annual), presenting the sediment yield of this period as well (related to Objective 1). The paper results were obtained following a *black-box* model approach and are focused on the measurements done at the outlet of the basin. This paper also gives a first insight on the on-going geomorphological processes, most of them related with the in-channel suspended sediment storage. Paper evaluation helped to revise the objectives of the thesis, especially the firm need of measuring transport along the basin (main tributaries) and refining the fieldwork practices, increasing sampling during and between floods.

2. SEDIMENT TRANSPORT

López-Tarazón, J.A., Batalla, R.J., Vericat, D., Francke, T., 2009. Suspended sediment transport in a highly erodible catchment: The River Isábena (Southern Pyrenees). *Geomorphology*, 109: 201-221.

Suspended sediment transport in a highly erodible catchment: The River Isábena (Southern Pyrenees)

Abstract

Understanding and quantifying sediment load is important in catchments draining highly erodible materials that eventually contribute to siltation of downstream reservoirs. Within this context, the suspended sediment transport and its temporal dynamics have been studied in the River Isábena (445 km^2, south-central Pyrenees, Ebro basin) by means of direct sampling and turbidity recording during a 3-year dry period. The average flood-suspended sediment concentration was 8 g l^{-1}, with maximum instantaneous values above 350 g l^{-1}. The high scatter between discharge and suspended sediment concentrations (up to five orders of magnitude) has not permitted the use of rating curve methods to estimate the total load. Interpolation techniques yielded a mean annual sediment load of 184,253 t y^{-1} for the study period, with a specific yield of 414 t km^{-2} y^{-1}. This value resembles those reported for small torrents in nearby mountainous environments and is the result of the high connectivity between the badland source areas and stream courses, a fact that maximises sediment conveyance through the catchment. Floods dominated the sediment transport and yield. However, sediment transport was more constant through time than that observed in Mediterranean counterparts; this can be attributed to the role of base flows that entrain fine sediment temporarily stored in the channel and force the river to carry high sediment concentrations (i.e., generally in the order of 0.5 g l^{-1}), even under minimum flow conditions.

Keywords: suspended sediment transport, specific yield, reservoir sedimentation, interpolation, hysteresis, River Isábena.

1. INTRODUCTION

Research on reservoir sedimentation, surface water quality, sediment dynamics in the river-estuary-coast interface, continental denudation processes, and sediment budgets together with the ecological impacts of channel engineering and sediment exploitation emphasises the need for a better understanding of sediment transport and dynamics in a variety of catchments and rivers. Quantifying sediment load is especially important in catchments draining highly erodible materials (e.g., soft marls: Mathys et al., 2005) that exacerbate siltation problems in downstream reservoirs (e.g., Valero-Garcés et al., 1999). Once sediments reach the reservoirs, siltation becomes a long-term socio-economical problem because it reduces water storage capacity. This, in turn, may threaten domestic water supply and economic activities such as irrigation, hydropower production, nuclear power production, and coastal tourism.

Siltation is a severe phenomenon in areas experiencing variable climatic conditions (such as the Mediterranean mountains) with long dry periods and storms of high rainfall intensity, where runoff occurs over highly erodible unconsolidated sediments on bare slopes (i.e., badlands on marls, mudstones or shales). Under such conditions, erosion rates are very high, creating large suspended sediment concentrations in the river network that reach the lowland areas and the reservoirs (Francke et al., 2008a). Such episodes are not uncommon in mountain regions (e.g., Clotet et al., 1988), although they are often restricted to small mountain torrents from localised storms triggering mass movements (e.g., Batalla et al., 1999). High density flows have also been reported for large rivers, such as the Yellow River (Li et al., 1997), where maximum suspended sediment concentrations can reach 700 g l^{-1} (Xu, 1997).

Suspended sediment data are also essential for the calibration and validation of numerical models that aim to reproduce past soil erosion and sediment dynamics and to generate reliable data for management purposes (e.g., Mamede et al., 2006, Francke et al., 2008a). Despite its high scientific and management importance, sediment transport studies are scarce and frequently limited because of technical difficulties inherent to measuring in situ suspended sediment concentrations (*SSC*) with sufficiently high frequency and the subsequent estimation of sediment loads. Total sediment loads are

typically extrapolated from infrequent sample data to a range of discharges, a process that carries a degree of uncertainty (e.g., Ferguson, 1986; Asselman, 2000; Horowitz et al., 2001; Horowitz, 2003). Researchers have developed a series of statistical techniques (e.g., rating curves, interpolation) to estimate sediment loads based on discrete sampling (e.g., Walling, 1977; Williams, 1979; Phillips et al., 1999). The rating curve method describes the average relation between discharge (*Q*) and *SSC* (Horowitz, 2003), although it may not be applicable to highly dynamic fluvial environments because of the high scatter of data and the consequent poor relationship between *Q* and *SSC* nor to catchments experiencing wide ranges of sediment concentrations. Interpolation techniques have been used frequently to overcome these statistical problems (e.g., Phillips et al., 1999), as well as to derive continuous sedigraphs from real *SSC* data. One way to deal with these methodological issues is the use of turbidity probes (e.g., optical backscatter type) to obtain continuous records of water turbidity as a surrogate measurement of *SSC*.

The objective of this paper is to analyse suspended sediment dynamics and loads in a highly erodible fluvial environment (the River Isábena) during a dry 3-year period. Analyses were undertaken at different timescales comparing the contribution of base flows and floods to the annual sediment yield, describing the seasonality of suspended sediment transport in relation to rainfall and runoff in the catchment, and studying the factors that explain the variability of the river's suspended sediment response.

2. STUDY AREA

2.1. Rationale

The River Isábena is a mesoscale mountainous catchment (445 km^2) located in the southern central Pyrenees (Fig. 1). The river experiences frequent floods, a characteristic that keeps sediment transport rates relatively high; instantaneous *SSC* occasionally attains 300 g l^{-1}. The main sources of fine sediment are badland areas on marls that occupy < 1% of the catchment area (Francke et al., 2008a, Alatorre et al., 2008). The river flows into the River Ésera a few hundred metres upstream from the Barasona Reservoir (Fig. 1). The Barasona Reservoir was built in 1932 and re-grown in the 1970s. This reservoir experiences acute siltation problems (e.g., Avendaño et al.,

1997a, b; Navas et al., 1998). Consequently, and in order to ensure water supply to 70,000 ha of irrigated land, more than 9 hm^3 (1 $hm^3 = 1\times10^6$ m^3) of sediment located near the dam were sluiced down between 1995 and 1997 (Palau, 1998; Avendaño et al., 2000).

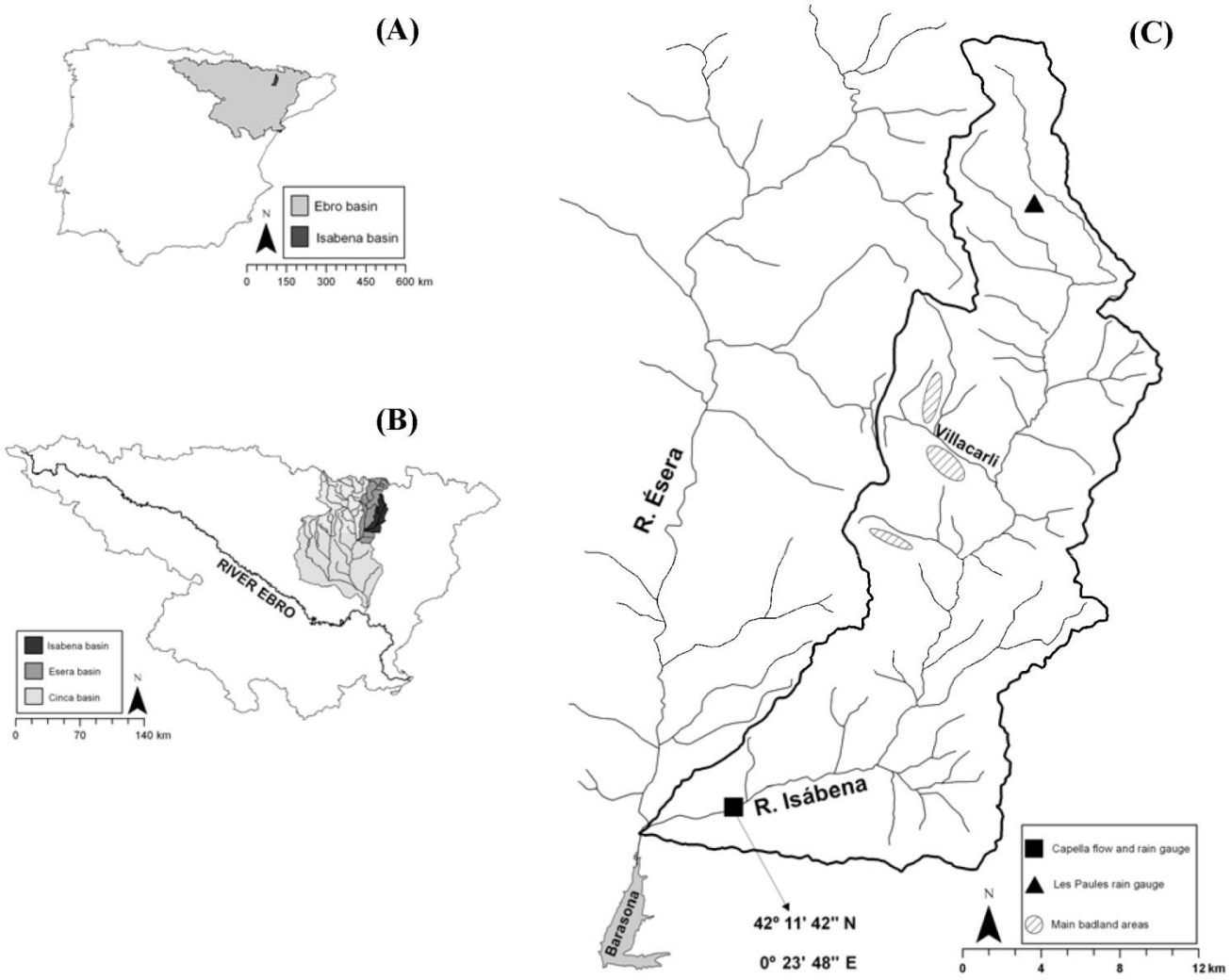

Figure 1. A) Location of the Isábena catchment in the Iberian Peninsula. B) Location of the Cinca, Ésera, and Isábena basins in the Ebro Basin (85,000 km^2). C) The Isábena catchment: location of the study reach.

2.2 The Isábena basin

The Isábena basin is located in the southern central Pyrenees (Ebro basin, NE Iberian Peninsula; Fig. 1). The river drains an area of 445 km^2 (0.48% of the Ebro basin) upstream of the confluence with the River Ésera. The River Ésera is the main tributary of the Cinca, in turn the second largest river flowing into the Ebro (Fig. 1). The Isábena

is not regulated, though its main course experiences occasional gravel mining. The basin has an altitude between 650 and 2720 m asl. Mean temperature is 10ºC in the Pyrenean zone (i.e., northern part of the basin) and 12.5ºC in the southern Mediterranean area (i.e., lowermost part of the basin). Mean annual rainfall is 767 mm, with seasonal maximum during spring and autumn. The basin shows a clear altitudinal rainfall gradient with mean values around 450 mm y^{-1} in the valley bottom and more than 1600 mm y^{-1} on the summits (Verdú et al., 2006a).

In the headwater parts of the catchment the river flows through narrow valleys excavated on Cretaceous limestones. Dissolution processes have left the calcareous materials at the highest levels of these massifs partially karstified, with the later Eocene marls shaping run-down reliefs (Verdú et al., 2006a). Usually the Eocene marls have badland structure, being the most important source of sediment during storm periods, but representing < 1% of the total area (Francke et al., 2008a; see location in Fig. 1). In its lower part, the basin is mainly composed of Cretaceous chalks together with Tertiary clay rocks and conglomerates. From a geomorphologic point of view, active incision/accretion processes have not been observed in the main watercourses during the last 10 years (Verdú et al., 2006b), so the more contemporary active geomorphologic processes are mass movements and, especially, fluvial erosion on slopes and in the badlands. The soils of the Isábena basin are rather thin and developed over calcilutites, limestones, sandstones, and conglomerates; they can be classified as Xerorthents (Soil Survey Staff, 1996), with silt loam texture and low organic content (< 2%).

The hydrology of the basin is characterized by a rain-snow regime, with floods typically occurring in spring from snowmelt and, especially, in late summer and autumn as a consequence of localised thunderstorms. Minimum flow (0.20 m^3 s^{-1} during the study period) occurs in summer, but the river never dries up. Generally absolute maxima occur in autumn: for example, 321 m^3 s^{-1} during the November 1966 flood and 281 m^3 s^{-1} during the December 1997 flood (Q_{43} and Q_{25}, respectively, estimated from the instantaneous maximum discharge by the Gumbel method for the period 1951-2005). However, the largest peak ever recorded at the basin outlet took place in summer (August 1963), reaching 370 m^3 s^{-1} (Q_{86}). The mean annual discharge at the basin outlet for the entire period of record (1945-2008) was 4.1 m^3 s^{-1} (σ = 2.2 m^3 s^{-1}, where σ is the

standard deviation of the observations). The mean annual water yield is 177 hm^3 (σ = 92 hm^3), a value that represents ~ 1.5% of the Ebro basin total runoff.

3. METHODS

3.1. Field measurements

Water discharge is continuously recorded by the Ebro Water Authorities (CHE) at the Capella gauging station (EA47), located at the outlet of the Isábena catchment and upstream of the confluence with the River Ésera and the Barasona Reservoir (Fig. 1). Water stage is recorded every 15 min and then transformed into discharge. Rainfall is measured by tipping-bucket rain gauges operated by the CHE at the basin headwaters (Les Paules) and at the outlet (Capella) (Fig. 1). Real-time rainfall and runoff data are available at the Automatic Hydrologic Information System (SAIH) of the Ebro river basin (www.saihebro.com).

Table 1. Water samples obtained during the study period in the River Isábena

Year	Manual samples (baseflows)[a]	Manual samples (floods)[b]	US DH59 samples[c]	Automatic samples (base flows)[d]	Automatic samples (floods)[e]
2005-2006	47	13	0	101	200
2006-2007	34	38	30	66	374
2007-2008	45	30	20	183	181
Complete period	126	81	50	350	755

[a] Depth-integrated manual samples taken during base flows.
[b] Depth-integrated manual samples taken during floods.
[c] Samples taken with a cable-suspended, depth-integrating US DH59 sampler during floods.
[d] ISCO samples taken during base flows.
[e] ISCO samples taken during floods.

Suspended sediment transport has been monitored between May 2005 and May 2008 at EA47 by means of (*i*) automatic water sampling, (*ii*) manual sampling (together, hereafter called direct sampling), and (*iii*) turbidity measurements (indirect sampling). Automatic water samples were obtained by means of an ISCO 3700 sampler (ISCO), mostly during floods but also during some base flows to study SSC variability. In addition, depth-integrated manual water samples were collected weekly and during baseflows but also during particular floods (for more details see Table 1). Altogether, 1362 water samples (i.e., 257 manual and 1105 automatic) were taken during the monitoring period, covering almost the entire range of discharges (0.3 to 87.1 $m^3 s^{-1}$, discharges accounting for 98.1% of the time in the flow duration curve of the study

period). Furthermore, turbidity was recorded with an optical ANALITE NEP9350 turbidimeter (range 0-3000 NTU ≅ 3 g l^{-1}) that was substituted by a high range back-scattering Endress+Hauser Turbimax W CUS41 turbidimeter (range up to 300 g l^{-1}) in November 2007. The turbidity probes were linked to a Campbell CR-510 data logger. Turbidity sampling was set up at 1-min intervals while the logging was at 15-min intervals (thus recording the average value of the samples between log intervals).

The spatial variability of the SSC in the monitoring section was examined by means of intensive sampling carried out during floods that occurred in September 2006 (peak discharge of 16 m^3 s^{-1}, $Q_{0.6}$) and April 2008 (peak discharge of 68 m^3 s^{-1}, $Q_{1.3}$). The cross section was surveyed for suspended sediment at 3 verticals at points evenly distributed across the section, with a cable-suspended, depth-integrating US DH59 sampler. Spatial variability was calculated as the average deviation from the mean of all samples. Overall, 50 samples were taken, with these indicating that the average spatial variability was 9%, ranging from 4 to 14%. In addition, 49 depth-integrated samples were obtained manually during different floods at a vertical located at the centre of the cross section. These samples were collected exactly at the same time that the ISCO was sampling in order to calibrate the ISCO values. Results indicate that the variability is on average < 14% (3 to 21%).

One-litre water samples were processed in the laboratory. Samples were filtered by means of 1.2 μm cellulose and glass microfibre filters for samples with concentrations < 2 g l^{-1}; samples with higher concentrations were decanted. Samples were dried in an oven for 24 h at a constant 60ºC. Filters and decanted samples were subsequently weighted to determine the suspended sediment concentration (g l^{-1}).

3.2. Data computation

3.2.1. Sampling design and turbidity calibration

The sampling design was developed to obtain a continuous record of SSC based on turbidity data and direct water samples. Direct samples were used both for calibration purposes and to complement turbidity measurements above 3 g l^{-1} (i.e., upper measuring range limit of the ANALITE NEP9350 turbidimeter), a value that was equalled or

exceeded 9% of the time between May 2005 and November 2007 (91% of the *SSC* < 3 g l^{-1}).

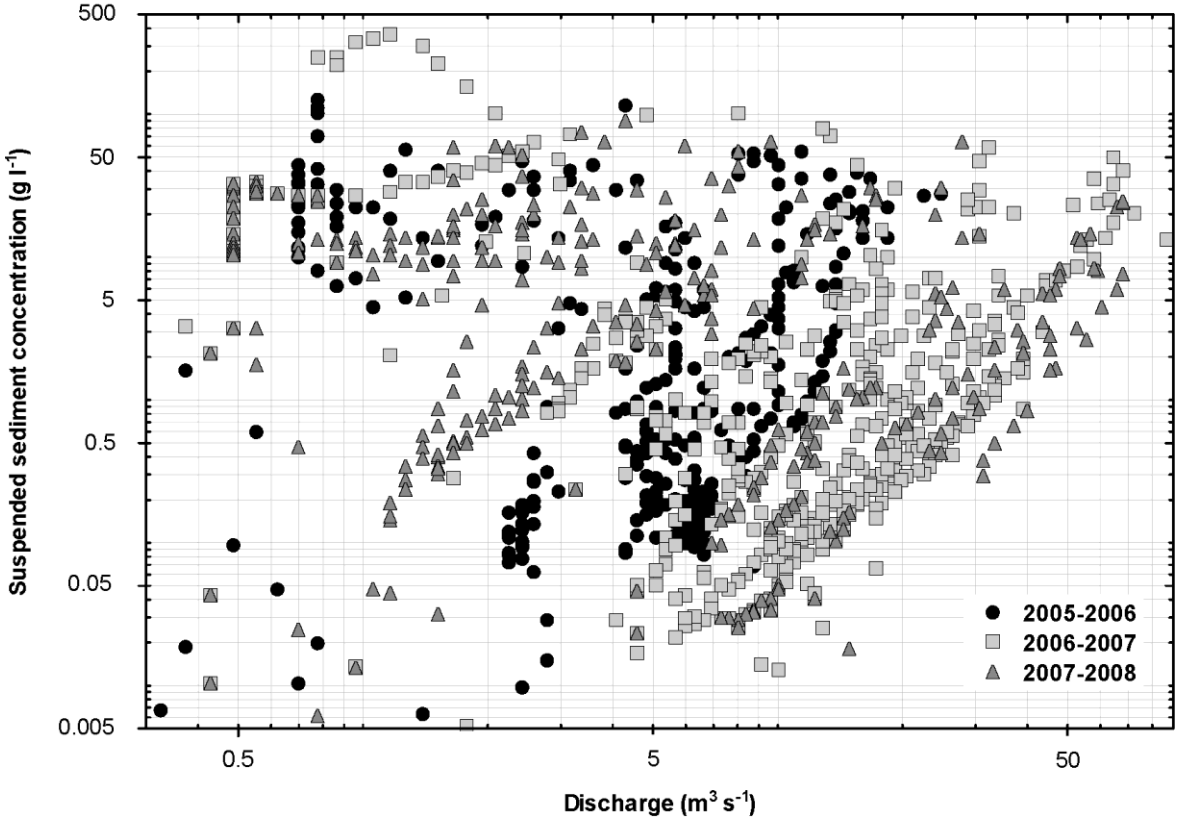

Figure 2. Scatter plot of the relation between *Q* and *SSC* in the Isábena for the 3-year study period. Note that up to five orders of magnitude of *SSC* can be observed for the same range of discharges; the high scatter implies that no statistically significant relations exist between the two variables, either for the whole period or for each of the study years.

Turbidity data were transformed to *SSC* through a calibration process. First, anomalous values were identified and corrected. Correction was done by deleting the erroneous values and creating new data by interpolating between the closer correct values. Anomalous values could be the result of a series of malfunctioning situations, including (*i*) the turbidimeter being out of range, (*ii*) the blind effect (i.e., low turbidity measurements because the presence of a biofilm on the lens or an extended period of high *SSC*), (*iii*) fouling from algae development and other phenomena, such as bubbles or density discontinuities (e.g., Lawler, 2005; Lawler et al., 2006). Once the turbidity data records were reviewed and corrected, a rating curve between pair values of NTU and *SSC* was obtained. In the case of the ANALITE NEP 9350 turbidimeter, the

statistically significant rating curve is *SSC*=(0.0012*NTU) + 0.0605 (N = 490, r^2 = 0.82, p < 0.001), while in the case of the Endress+Hauser Turbimax W CUS41 back scattering turbidimeter, two separate rating curves have been obtained (e.g., Nadal-Romero et al., 2008). For sediment concentrations below 40 g l^{-1}, a polynomial regression was the best fit to the data, yielding an equation of the form *SSC*=(0.1436*NTU^2) + (1.9673*NTU) (N = 145, r^2 = 0.96, p < 0.01), whereas for higher *SSC* values a linear regression yielded the highest coefficient of determination; *SSC*=(5.7738*NTU) + 1.9608 (N = 6, r^2 = 0.94, p < 0.01).

3.2.2 Suspended sediment computation

The use of the rating curve method (Walling, 1984) was not feasible because of the lack of statistical significance in the relationship between *Q* and *SSC* over the study period (Fig. 2). To overcome this limitation, sediment load has been estimated in two different ways:

(i) Periods where *SSC* > 3 g l^{-1} (i.e., 8% of the time in the first year, 16% in the second year, and 1% in the third year). These periods occurred mainly during flood peaks with concentrations above the detection limit of the low-range turbidimeter. In these cases the suspended sediment load was obtained by means of the interpolation method (Phillips et al., 1999; Rovira and Batalla, 2006); this method assumes that an instantaneous sample concentration is representative of the intersampling period between samples. Altogether, the interpolation method was used for 556 samples, with resulting *SSC* values multiplied by the discharge to obtain the total load of a given period.

(ii) Periods where *SSC* < 3 g l^{-1} (i.e., most of the time during the study period). For these periods, continuous turbidity data were available at a time resolution of 15 min. In this case, the sediment load has been obtained by multiplying *Q* and the estimated *SSC* (i.e., transformed *SSC* from turbidity records) for each 15-min interval. Finally, both sets of results were added together to obtain the total sediment load for the studied periods.

Suspended sediment dynamics during floods have been studied by examining hysteretic loops (e.g., Williams, 1989) and the seasonal transport patterns. Hysteretic analysis

relates *Q* and *SSC* to look for specific patterns of sediment transport; results have been interpreted in the context of rainfall data (see location of rainfall gauges in Fig. 1). Flood runoff volume has been taken as just the quick flow that was separated from the base-flow component by means of a simple visual technique based on the breakpoints detected on the logarithmic falling limb (e.g., Maidment, 1993).

Table 2. Annual and mean hydrological values for the entire study period in the Isábena catchment.

Period	Yield (hm^3)	σ^a	Specific yield ($hm^3\ km^{-2}\ y^{-1}$)	σ^a	Discharge[b] ($m^3\ s^{-1}$)	σ^a	Specific discharge[c] ($l\ s^{-1}\ km^{-2}$)	σ^a
2005-2006	59.13	-	0.13	-	1.88	2.25	4.23	5.06
2006-2007	135.67	-	0.31	-	4.30	6.64	9.68	14.94
2007-2008	88.13	-	0.20	-	2.79	6.37	6.28	14.33
Complete period	94.00[d]	39	0.21[e]	0.09	2.99	5.56	6.72	12.49

[a] Standard deviation
[b] Mean discharge
[c] Mean specific discharge
[d] Mean water yield
[e] Mean specific water yield

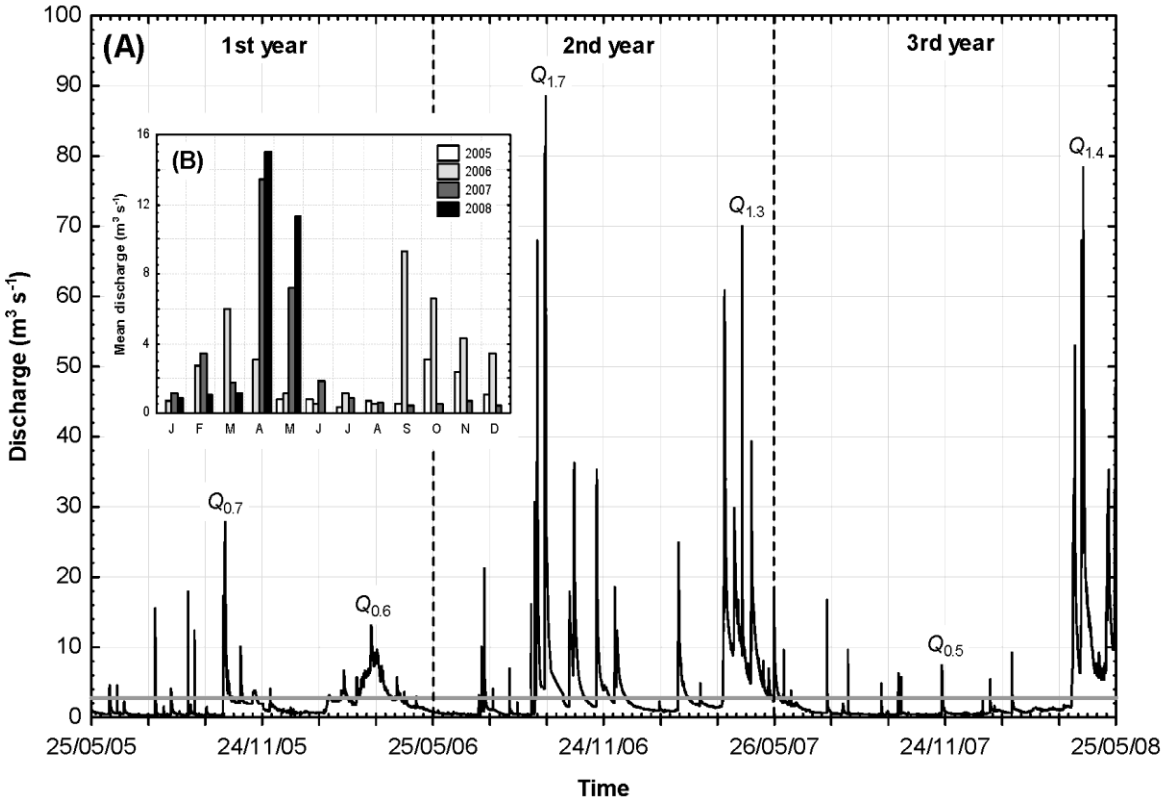

Figure 3. (A) Hidrological regime of the River Isábena for the study period. The grey line represents the mean discharge for the complete period. Some floods include Q_i, where *i* means the return period of the floods. (B) Mean monthly discharge for the study period.

4. RESULTS AND DISCUSSION

4.1. Hydrology

Runoff at EA47 for the whole study period (May 2005–May 2008) was 283 hm^3, yielding a mean annual value of 94 $hm^3\ y^{-1}$ (σ = 39 $hm^3\ y^{-1}$; i.e., 212 mm y^{-1}) (see Table 2 for more details). Annual runoff for each of the studied years was below the long-term mean (i.e., 177 $hm^3\ y^{-1}$ for the period 1945-2008; σ = 92 $hm^3\ y^{-1}$). A year was considered to be very dry if annual runoff was lower than the long-term mean annual value minus one σ (i.e., 85 $hm^3\ y^{-1}$). Within this context, the first and the third years can be classified as very dry, while the second year can be considered simply as dry because annual runoff is only slightly lower (i.e., 0.5 σ) than the long-term mean annual value. No clear seasonal patterns in runoff were observed: winter, autumn, and spring were the wettest seasons during the first, second, and third years, respectively. Mean annual discharge (Fig. 3) was 2.99 $m^3\ s^{-1}$ (σ = 1.23 $m^3\ s^{-1}$), and mean specific discharge was 6.73 $l\ s^{-1}\ km^{-2}$ (σ = 2.77 $l\ s^{-1}\ km^{-2}$)

A total of 80 floods distributed through the study period were analysed (Tables 3 and 4). Mean flood discharge during the first year was 4.2 $m^3\ s^{-1}$, 11.2 $m^3\ s^{-1}$during the second year, and 12.9 $m^3\ s^{-1}$ during the third year. Maximum instantaneous discharge ranged from 29.0 $m^3\ s^{-1}$ (observed on 15 October 2005) to 88.8 $m^3\ s^{-1}$ (23 September 2006), values associated with recurrence intervals of 0.7 and 1.7 years (Fig. 3), respectively (i.e., $Q_{0.7}$ and $Q_{1.7}$).

Table 3. Summary of the main characteristics of the floods recorded during the study period in the River Isábena.

Year	Peak Discharge$_{min}$ ($m^3\ s^{-1}$)[a]	Peak Discharge$_{max}$ ($m^3\ s^{-1}$)[b]	Return period (y)[c]	Water yield (hm^3)[d]	Annual water yield (%)[e]
2005-2006	1.17	28.97	0.7	16.50	27.9
2006-2007	2.09	88.81	1.7	73.21	53.9
2007-2008	0.70	78.74	1.5	43.23	49.1
Complete period	0.70	88.81	1.7	73.21	46.7

[a] Minimum peak discharge
[b] Maximum peak discharge
[c] Return period of the maximum peak discharge calculated by Gumbel's methodology for the period 1945-2005
[d] Water yield of annual highest flood
[e] Percentage of the annual water yield corresponding to floods

4.2. Sediment transport

A total of 73 floods were sampled during the study period (Table 5; note that no *SSC* data are available for seven floods for which only hydrology has been analysed). Figure 4 shows discharge and *SSC* derived from the turbidity record and the suspended sediment samples for the entire study period.

Statistically significant relationships between *Q* and *SSC* were neither found for the complete period nor for individual years or even seasons. The *SSC* may be up to 5 orders of magnitude for the same *Q* (Fig. 2). The high degree of scatter between the two variables is usually related to seasonal causes and to hysteretic effects, either from exhaustion of sediment or dilution during flood events (e.g., Walling, 1977) and because of the increase in sediment availability from coupled zones. The scatter also indicates that *SSC* is not fully hydraulically dependent (i.e., it does not increase as discharge increases during floods), a fact that may indicate that fine sediment may also be available and easily removed, even during base flows. The role of in-channel storage of sediment has been identified as one of the main controls on suspended sediment transport during interflood periods of stable flow (e.g., Walling and Amos, 1999; Smith and Dragovich, 2008); this phenomenon is the subject of ongoing investigations in the River Isábena (Francke et al., 2008b).

Mean *SSC* for the study period (estimated as the mean of all measurements including base flows and floods) was 0.63 g l^{-1} (σ = 3.92; *CV* = 622 %, where *CV* is the coefficient of variation of the observations) for a mean sampled discharge of 3.38 m3 s^{-1} (σ = 5.63 m^3 s^{-1}; *CV* = 167 %). Mean flood *SSC* (estimated as the mean of the measured concentrations during floods) was 5.42 g l^{-1} (σ = 7.54 g l^{-1}; *CV* = 139 %) in the first year, 10.81 g l^{-1} (σ = 24.83 g l^{-1}; *CV* = 230 %) in the second, and 6.95 g l^{-1} (σ = 12.72 g l^{-1}; *CV* = 193 %) in the third (see Table 5 for flood scale characteristics). Maximum instantaneous *SSC* reached 357 g l^{-1} during the flood that occurred on 13 July 2006. Instantaneous *SSC* obtained during base-flow conditions were remarkably high, with a mean of 0.45 g l^{-1} (σ = 2.75 g l-1; *CV* = 611 %), a minimum of 0.002, and a maximum of 130 g l^{-1}.

Table 4. Flood discharge data for the entire study period in the River Isábena.

Flood	Q_{mean} [a] (m^3/s)	Q_{peak} [b] (m^3/s)	Total runoff (hm^3)	Flood	Q_{mean} [a] (m^3/s)	Q_{peak} [b] (m^3/s)	Total runoff (hm^3)
13.06.05 [c]	2.57	4.08	0.13	**08.12.06** [d]	5.99	12.37	4.37
14.06.05 [c]	2.00	4.58	0.42	**22.01.07** [d]	1.47	2.25	0.18
21.06.05 [c]	2.07	4.58	0.06	**12.02.07** [d]	9.42	24.92	4.48
28.06.05 [c]	1.00	1.52	0.04	**07.03.07** [d]	2.91	4.84	0.29
29.06.05 [c]	1.32	2.25	0.14	**31.03.07** [d]	8.89	18.58	1.97
01.08.05 [c]	3.67	15.56	0.28	**02.04.07** [d]	31.71	60.87	6.65
18.08.05 [c]	2.88	4.08	0.14	**12.04.07** [d]	18.20	29.83	6.36
19.08.05 [c]	2.06	3.61	0.27	**21.04.07** [d]	27.88	70.93	1.08
05.09.05 [c]	3.17	17.95	0.11	**30.04.07** [d]	10.32	14.99	0.52
08.09.05 [c]	0.89	1.79	0.07	**01.05.07** [d]	11.45	39.31	12.05
12.09.05 [c]	4.12	12.37	0.11	**14.05.07** [d]	5.76	8.05	0.41
25.09.05 [c]	0.76	1.17	0.03	**19.05.07** [d]	4.55	6.98	0.77
26.09.05 [c]	0.91	1.52	0.03	**25.05.07** [e]	8.63	18.58	1.45
12.10.05 [c]	6.36	17.33	0.65	**04.06.07** [e]	2.67	3.39	0.07
14.10.05 [c]	11.96	24.92	1.50	**05.06.07** [e]	4.48	9.64	0.20
15.10.05 [c]	12.54	28.97	2.23	**12.06.07** [e]	2.23	3.84	0.17
31.10.05 [c]	6.38	10.06	0.87	**21.07.07** [e]	5.62	16.72	0.49
02.12.05 [c]	2.33	4.08	0.34	**12.08.07** [e]	2.82	9.64	0.09
29.01.06 [c]	2.14	3.18	2.01	**17.09.07** [e]	1.55	4.84	0.11
16.02.06 [c]	4.09	6.64	1.41	**23.09.07** [e]	0.52	0.70	0.06
04.03.06 [c]	3.97	5.70	1.08	**24.09.07** [e]	0.54	0.87	0.08
19.03.06 [c]	9.71	13.90	3.46	**04.10.07** [e]	1.42	3.61	0.05
17.04.06 [c]	3.61	5.70	0.76	**05.10.07** [e]	2.17	6.32	0.05
07.05.06 [c]	1.80	2.98	0.36	**08.10.07** [e]	2.32	5.70	0.07
13.07.06 [d]	1.29	3.18	0.11	**21.11.07** [e]	3.88	8.43	0.64
16.07.06 [d]	2.40	10.06	0.23	**03.01.08** [e]	1.26	2.79	0.10
19.07.06 [d]	3.34	21.25	1.25	**11.01.08** [e]	1.89	5.40	0.28
29.07.06 [d]	1.33	4.08	0.15	**16.01.08** [e]	1.14	1.65	0.18
15.08.06 [d]	1.39	6.98	0.14	**04.02.08** [e]	4.11	9.22	0.20
23.08.06 [d]	0.87	2.09	0.09	**08.04.08** [e]	13.93	31.59	3.10
07.09.06 [d]	4.08	16.13	0.15	**10.04.08** [e]	30.48	53.01	4.96
10.09.06 [d]	0.91	2.79	0.08	**17.04.08** [e]	24.92	67.96	5.34
11.09.06 [d]	14.19	30.70	0.47	**19.04.08** [e]	34.60	78.74	12.05
13.09.06 [d]	28.90	67.96	5.88	**07.05.08** [e]	7.44	9.22	0.98
22.09.06 [d]	37.40	80.36	3.37	**10.05.08** [e]	6.34	6.98	1.13
23.09.06 [d]	27.27	88.81	6.18	**13.05.08** [e]	6.66	7.68	0.94
18.10.06 [d]	11.06	17.95	2.88	**14.05.08** [e]	14.28	18.58	2.24
23.10.06 [d]	12.96	36.29	7.19	**16.05.08** [e]	23.20	32.50	2.82
16.11.06 [d]	11.09	35.32	5.13	**17.05.08** [e]	22.60	35.32	1.20
06.12.06 [d]	7.85	18.58	0.78	**23.05.08** [e]	27.95	46.98	4.18

[a] Mean flood discharge
[b] Flood peak discharge
[c] 2005-2006
[d] 2006-2007
[e] 2007-2008

Table 6 summarises the seasonal hydrology and suspended sediment transport results. The suspended sediment yield (hereafter *SSY*) was 552,760 t for the entire study period, a value that represents an average of 184,253 t y^{-1}, giving a specific sediment yield of 414 t km^{-2} y^{-1}. Floods are responsible of the majority of the *SSY* in the catchment (91%

of the annual yield, on average). No linear relation was found between the annual runoff and the *SSY*. Data suggest that a small increment in the annual runoff can trigger a large increment in the *SSY*. For instance, during the third year, annual runoff was 50% higher than that in the first year, while the *SSY* was 2.5 times higher. This may be related to the relatively high runoff activity during the second year (e.g., 30 floods) when snowmelt processes may have caused a large sediment contribution that was not completely exported but retained in the channel until floods occurred in the third year. Suspended sediment yield during the second year was almost twice the annual average yield (i.e., 250,292 t).

A seasonal pattern in *SSY* was not evident. The highest *SSY* was observed in autumn, summer, and spring during the first, second, and third years, respectively (Fig. 5). The seasonal highest *SSY* correlated well with periods of high rainfall. The seasonal pattern for minimum *SSY* was spring (first year) and autumn (second and third), but in this case no direct relationship was observed with rainfall or runoff. The case of autumn 2006 is especially remarkable because it was one of the wettest seasons of the whole study period but accounted for a very low *SSY* (Fig. 5). This may indicate that an exhaustion phenomenon occurred after a summer season with a very high sediment load.

Specific sediment yield in the Isábena averaged 414 t km^{-2} y^{-1} (with a maximum of 550 t km^{-2} y^{-1} in 2006-2007). This is in the same order of magnitude as those reported for the Ésera basin (1,250 km^2, including the Isábena catchment) by Sanz-Montero et al. (1996) estimated from the Barasona Reservoir sedimentation data (350 t km^{-2} y^{-1}). de Vente et al. (2006) reported data on sediment yield for 44 Mediterranean basins, within which the Isábena would fall within the moderate to high values. For comparison, Batalla et al. (1995) reported specific yield of 32 t km^{-2} y^{-1} in the River Arbúcies, a 106 km^2 catchment located in the Catalan Coastal Ranges (i.e., similar latitude as the Isábena) but on granite lithology and almost complete forest cover. In the same region, Rovira and Batalla (2006) reported values in the order of 50 t km^{-2} y^{-1} for the 900 km^2 Tordera catchment. Notably, values obtained in the Isábena were observed during dry years, well below the average rainfall-runoff activity in the catchment. A crude direct extrapolation of the 3-year *SSY* to the mean runoff value for the period 1945-2008 can be done. This extrapolation is tentative and can be biased at some degree. The total yield estimated for the period 1945-2008 would be representative of a scenario with

medium to dry hydrological years, being a conservative estimate that provides a minimum long-term suspended sediment yield estimate. The extrapolation yields a value of 750 t km^{-2} y^{-1}. Most studies that showed a similar range of *SSY* are restricted to small mountainous catchments (<1 km^2), where sediment eroded off the slopes is readily available to be transported and exported out of the catchment during floods. Mathys et al. (2005) and Gallart et al. (2005) worked on small Mediterranean basins with similar lithological characteristics to the Isábena (i.e., on extremely erodible marls and presence of badlands). Mathys et al. (2005) reported 800 t km^{-2} y^{-1} for the Brusquet catchment, a 1 km^2 basin located in the French Alps; Gallart et al. (2005) presented an average of 535 t km^{-2} y^{-1} for the Ca l'Isard basin (1.3 km^2 in the southeastern Pyrenees).

Most sediment in the Isábena catchment comes from bare areas. These badlands in the Isábena occupy <1% of the basin area (i.e., <4 km^2; Francke et al., 2008a) so the reported specific yields would fit with those from small catchments with a much higher percentage of badland areas. The only difference is likely to be the timing and duration of sediment export. While in mountainous areas any sediment produced is ready to be exported, in medium-size catchments like the Isábena this process may take longer (months to years). Connectivity between badland areas and the stream channel in the Isábena catchment is very high. In addition, no sustained accretion has been observed during the study period, suggesting that (at the year scale) sediment conveyance from the sources throughout the catchment is also very high and that the river has to work at almost full capacity to be able to export all available sediment. Most of the badlands are located in the Villacarli subcatchment (see location in Fig. 1), a 44-km^2 basin draining the eastern part of the catchment (for more details on tributary characteristics see Francke et al., 2008a). Catchments in the range of 10-100 km^2 seem to have valley and hydraulic characteristics that optimize flow depth, energy slope, and velocity to maximize flood power and hence sediment transport capacity (Baker and Costa, 1987, in Newson, 1989). Costa (1987) added that maximum flood peaks originate from an optimal combination of basin morphology, physiography, and storm intensity. Although a long-term sediment yield estimation for the Villacarli basin is not available yet, preliminary field observations indicate that *SSC*s during floods are very similar to those registered in Capella (EA47), thus supporting the idea of efficient sediment conveyance in the catchment and the hypothesis that certain catchment sizes optimise sediment transport during floods. Such catchments also provide maximum likelihood of

noncohesive sediment gravity flows, debris flows, and other forms of high density fluids and hyperconcentrated sediment transport mechanisms (Newson, 1989).

Table 5. Flood suspended sediment data for the entire study period in the River Isábena.

Flood	SSC_{mean} [a] (g/l)	SSC_{max} [b] (g/l)	Total *SSL* [c] (t)	Flood	SSC_{mean} [a] (g/l)	SSC_{max} [b] (g/l)	Total *SSL* [c] (t)
13.06.05 [d g]	1.17	1.86	154	**08.12.06** [e i]	0.17	1.87	999
14.06.05 [d h]	1.95	12.77	1,247	**22.01.07** [e]	No data	No data	No data
21.06.05 [d h]	25.14	54.96	1,239	**12.02.07** [e i]	1.91	77.90	13,532
28.06.05 [d g]	0.99	1.75	37	**07.03.07** [e g]	1.58	6.31	461
29.06.05 [d g]	1.84	5.51	287	**31.03.07** [e h]	1.85	10.03	5,386
01.08.05 [d i]	2.86	4.85	796	**02.04.07** [e g]	0.82	1.63	6,124
18.08.05 [d g]	2.79	4.73	426	**12.04.07** [e i]	0.34	2.16	2,627
19.08.05 [d g]	1.47	2.58	416	**21.04.07** [e h]	4.18	12.09	5,785
05.09.05 [d h]	29.12	111.81	5,371	**30.04.07** [e g]	1.43	5.60	863
08.09.05 [d g]	1.79	3.97	145	**01.05.07** [e g]	0.21	0.70	2,884
12.09.05 [d g]	4.65	7.83	691	**14.05.07** [e g]	0.50	0.98	68
25.09.05 [d g]	2.41	3.49	62	**19.05.07** [e g]	1.56	2.95	1,213
26.09.05 [d g]	0.45	0.60	11	**25.05.07** [f i]	0.36	3.12	574
12.10.05 [d h]	24.56	51.70	21,397	**04.06.07** [f g]	1.13	1.25	84
14.10.05 [d h]	12.62	51.88	20,846	**05.06.07** [f]	No data	No data	No data
15.10.05 [d j]	2.21	9.26	7,116	**12.06.07** [f g]	0.66	1.20	109
31.10.05 [d i]	0.97	4.37	934	**21.07.07** [f i]	17.99	58.31	9,821
02.12.05 [d g]	1.25	3.16	462	**12.08.07** [f h]	19.84	62.13	2,714
29.01.06 [d g]	0.25	1.14	531	**17.09.07** [f h]	13.18	50.82	1,744
16.02.06 [d h]	1.62	17.13	2,974	**23.09.07** [f i]	0.45	1.19	25
04.03.06 [d g]	0.63	11.06	907	**24.09.07** [f i]	0.62	1.93	49
19.03.06 [d i]	1.82	24.76	8,182	**04.10.07** [f g]	0.51	1.62	39
17.04.06 [d]	No data	No data	No data	**05.10.07** [f i]	24.06	56.87	1,441
07.05.06 [d i]	1.35	5.78	529	**08.10.07** [f h]	9.65	16.97	691
13.07.06 [e h]	152.12	357.74	14,388	**21.11.07** [f i]	6.48	54.74	6,897
16.07.06 [e]	No data	No data	No data	**03.01.08** [f j]	4.39	8.66	437
19.07.06 [e i]	2.39	8.98	5,919	**11.01.08** [f h]	9.49	58.89	3,049
29.07.06 [e g]	1.35	3.36	180	**16.01.08** [f g]	2.11	9.54	391
15.08.06 [e]	No data	No data	No data	**04.02.08** [f h]	42.59	89.18	8,987
23.08.06 [e]	No data	No data	No data	**08.04.08** [f i]	13.73	63.88	54,001
07.09.06 [e h]	50.61	99.63	9,616	**10.04.08** [f i]	4.40	14.45	25,318
10.09.06 [e]	No data	No data	No data	**17.04.08** [f j]	2.98	24.23	30,739
11.09.06 [e i]	1.26	3.24	558	**19.04.08** [f j]	1.26	7.33	23,332
13.09.06 [e i]	12.80	56.90	86,430	**07.05.08** [f i]	0.06	0.20	63
22.09.06 [e i]	8.99	48.65	45,767	**10.05.08** [f i]	0.02	0.09	27
23.09.06 [e h]	1.71	13.21	20,083	**13.05.08** [f g]	0.08	0.25	80
18.10.06 [e i]	0.61	5.36	1,769	**14.05.08** [f j]	1.08	3.89	2,562
23.10.06 [e i]	0.40	2.55	4,438	**16.05.08** [f i]	1.41	6.58	4,654
16.11.06 [e i]	0.31	7.11	3,789	**17.05.08** [f h]	3.61	9.69	4,621
06.12.06 [e g]	1.12	3.43	1,169	**23.05.08** [f i]	2.85	10.06	13,269

[a] Mean flood suspended sediment concentration
[b] Max flood suspended sediment concentration
[c] Total flood suspended sediment load
[d] 2005-2006
[e] 2006-2007
[f] 2007-2008
[g] Counterclockwise hysteretic loop group 1 (CC1)
[h] Counterclockwise hysteretic loop group 2 (CC2)
[i] Clockwise hysteretic loop (C)
[j] No hysteresis

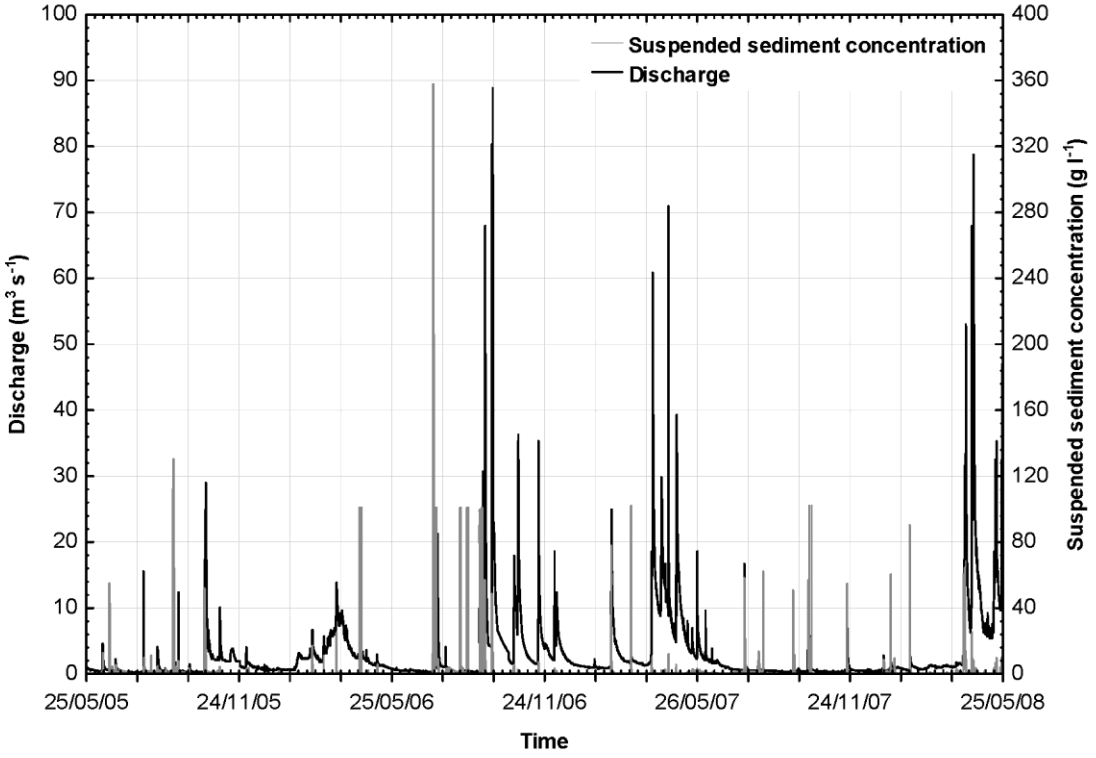

Figure 4. Discharge and suspended sediment concentration at the Capella gauging station (i.e., EA47, Fig. 1).

Table 6. Seasonal and annual hydrology and suspended sediment load for the study period (2005-2008) in the River Isábena.

Season	Precipitation at headwaters[a] (mm)	Precipitation at the outlet [b] (mm)	Water yield (hm^3)	Floods *SSL* [c] (10^3 t)	Baseflows *SSL* [d] (10^3 t)	Total *SSL* [e] (10^3 t)	SSS Yield[f] (t km^{-2} y^{-1})
Spring 05	127	74	2.45	2.96	1.54	4.50	101
Summer 05	184	245	4.25	7.92	6.19	14.11	127
Autumn 05	225	221	17.13	50.76	4.31	55.07	495
Winter 06	122	74	24.62	12.59	2.82	15.41	139
Spring 06	132	83	12.42	0.53	0.89	1.42	13
Summer 06	431	321	28.85	182.94	8.38	191.32	1,720
Autumn 06	201	126	38.19	12.16	1.73	13.89	125
Winter 07	130	43	17.71	19.38	0.92	20.30	183
Spring 07	291	240	56.87	20.33	9.13	29.46	265
Summer 07	127	128	5.08	14.35	5.05	19.40	175
Autumn 07	124	45	4.40	9.07	1.03	10.10	91
Winter 08	129	77	7.92	12.86	1.86	14.72	132
Spring 08	371	265	63.10	158.66	4.40	163.06	2,443
May 05 - May 06 [g]	745	675	59.13	74.76	15.65	90.41	203
May 06 - May 07 [g]	1017	703	135.67	234.05	16.24	250.29	562
May 07 - May 08 [g]	833	565	88.13	195.72	16.35	212.07	477

[a] Les Paules rainfall gauge (see Fig. 1 for location)
[b] Capella gauging station (see Fig. 1 for location)
[c] Suspended sediment load during floods
[d] Suspended sediment load during baseflows
[e] Total suspended sediment load
[f] Specific suspended sediment yield
[g] Total values for the complete year

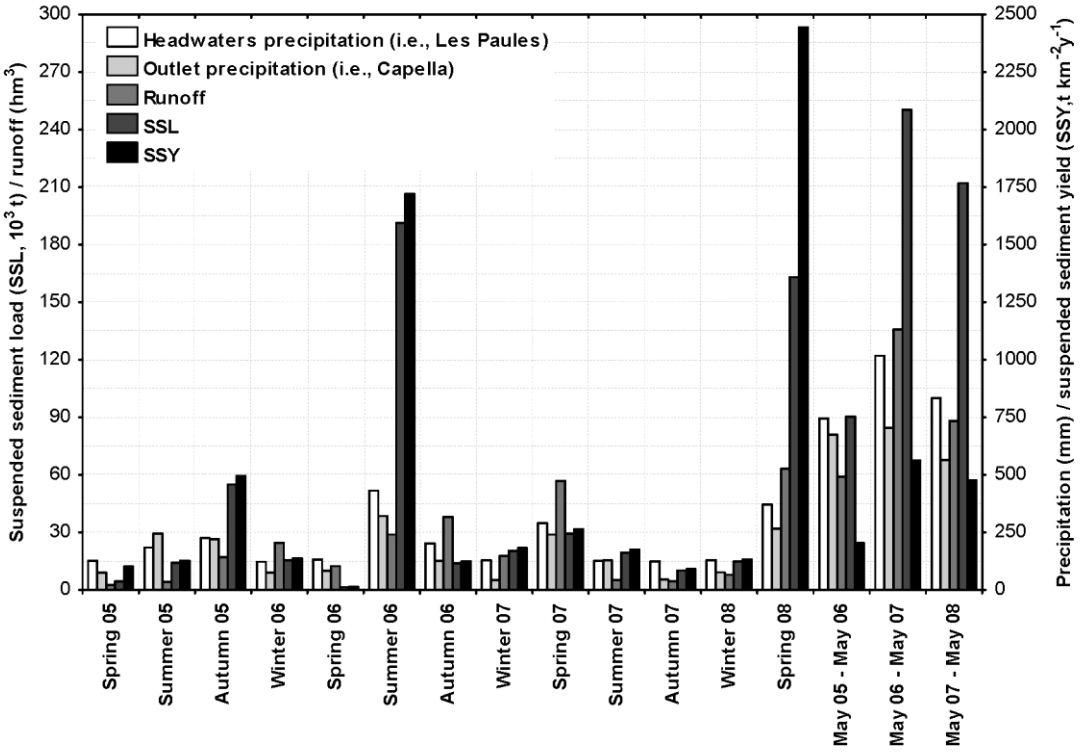

Figure 5. Seasonal and annual distribution of rainfall, runoff, suspended sediment load, and specific sediment yield in the Isábena catchment.

4.3. Sediment dynamics

The sediment dynamics in the River Isábena have been studied through the analysis of hysteretic loops for the 73 floods with available sediment data (Table 5). The hysteretic analysis has been carried out using the conceptual framework first reported by Williams (1989). Hysteretic loops can be clockwise or counterclockwise. In natural catchments, these two types of hysteresis are explained by the relative position of sediment sources within the catchment in relation to surface runoff. In general, clockwise loops are caused by sediment accumulated near the catchment outlet, while counterclockwise loops are related to sources supplying sediment from remote places. In the case of the Isábena, a dominance of counterclockwise loops has been observed: (*i*) 57% of the analysed floods were counterclockwise, (*ii*) only 37% were clockwise, and (*iii*) the remaining 6% did not show hysteresis. Counterclockwise behaviour would theoretically mean that sediment is generated in headwater areas and that the peak of *SSC* would reach the outlet much later than flow peak. However, in the case of the Isábena, observations indicate that it is not always as simple as this, with two different groups of counterclockwise loops found:

(i) A group of 25 floods (34% of the total) that follow the typical counterclockwise characteristics (hereafter called CC1 floods). These floods were characterised by rainfall events located in the headwaters as well as over the main sediment sources (badlands). The runoff volume of such floods was usually high, but the sediment load relatively low (illustrative examples of this were observed during the 2 December 2005 and 14 May 2007 floods; Tables 4 and 5; Fig. 6).

(ii) A group of 17 floods (23% of the total) that responded to a rainfall evenly distributed along the whole basin and with variable sediment sources (hereafter CC2 floods). The runoff volume of these floods was relatively low, but the sediment load very high (e.g., floods of 14 October 2005 and 6 September 2006; Tables 4 and 5; Fig. 6).

No seasonal patterns were found, with the exception of spring, where CC1 floods dominated (11 CC1 floods versus 4 CC2 floods). The temporal distribution of rainfall between headwaters and the outlet was quite different between the CC2 floods and so cannot be used to explain the distinct flow-sediment relations (Fig. 6); however, in general terms, rainfall peaks tended to occur first in the headwaters, followed by a second peak at the outlet several hours later.

The clockwise phenomenon was found preferentially when rainfall was mostly located near the catchment outlet, with runoff likely triggering the movement of sediment accumulated in the channel during the previous seasons and with little or no contribution from nearby tributaries. For instance, this was the case of the clockwise-dominated floods (hereafter C floods) that occurred in autumn 2006 and spring 2008. The group of floods followed the wettest season in the study period (i.e., summer 2006) and produced a very high sediment load, likely causing an important sediment accumulation in the channel near the outlet. These processes were first observed by Becker (2007) who reported a channel erosion of 2300 t of sediment in the 5-km river reach upstream from the outlet during the last flood of summer 2006. Another set of floods of this type occurred in spring 2008 following a year with very little rainfall. During such periods, sediment is typically deposited in the drainage network by small floods and base flows and is ready to be transported when larger floods occur. We

hypothesize that the behaviour of the catchment expressed by hysteretic loops can be interpreted in the relation to the inchannel sediment storage (30 km separates Villacarli and the outlet; see Fig. 1). At the flood scale, the river channel controls the transport of sediment, occasionally acting as the main source of sediment (e.g., C and CC2 loops) and other times as a sink (e.g., CC1 loops).

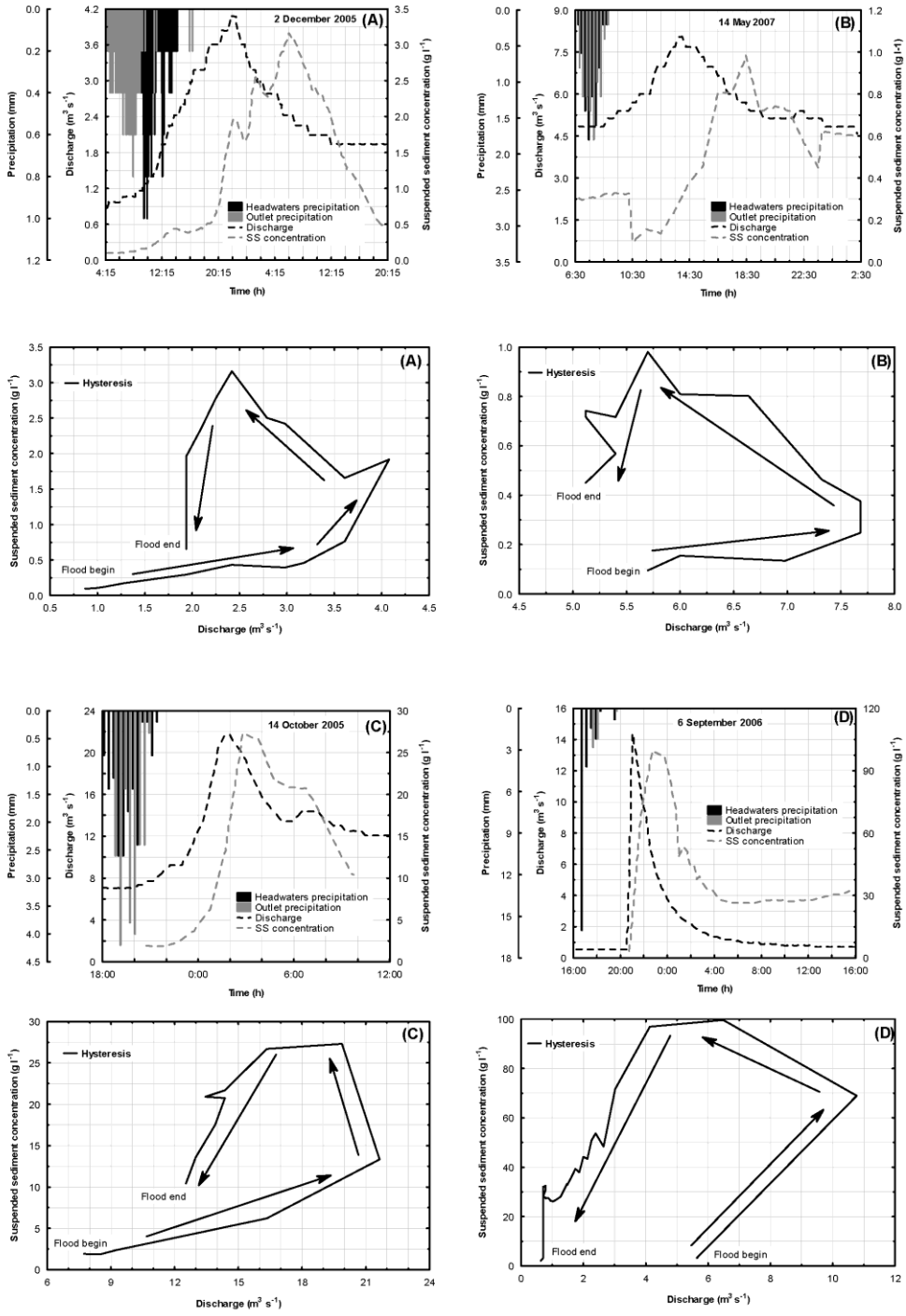

Figure 6. Examples of the *Q*/*SSC* counterclockwise hysteretic patterns found in the River Isábena: (A) 2 December 2005 (CC1); (B) 14 May 2007 (CC1); (C) 14 October 2005 (CC2) and (D) 6 September 2006 (CC2) (see text for more details and discussion).

It has been found that in highly erodible catchments with similar lithology to the Isábena, the suspended sediment transport follows a temporal pattern that can be related to the availability of the sediment throughout the year. Erosion processes and subsequent sediment transport downstream are subjected to strong seasonal controls such as freezing and thawing that control weathering in winter and to intense rainfall events that trigger erosion in summer (e.g., Clotet and Gallart, 1986; Balasch et al., 1992; Gallart et al., 2005). Although such temporal patterns have not been observed in the Isábena, a rainfall-dependent *SSY* is evident (Fig. 7).

The frequency curves presented in Fig. 8 show that runoff is much more constant through time than suspended sediment load; the latter exhibiting a somewhat exponential pattern. As such, half of the sediment load was transported during 3% of the time, while 80% of the load was transported, on average, during 10% of the time. A breakpoint can be visually established at around 65% of the load. Above this point, sediment transport becomes more constant (with the exception of the third year). Other studies in the Mediterranean area have shown that for basins with sizes comparable to the Isábena, 90% of the suspended load is transported during 10% of the time (Batalla et al., 1995; Rovira and Batalla, 2006). Recently, Estrany et al. (2009) reported that 90% of the load was transported in just 1% of the time in a small agricultural catchment on the island of Mallorca. Other studies carried out in large basins but under severe human impacts (e.g., River Colorado >350,000 km^2; River Ebro >85,000 km^2) found that almost all the suspended load is transported between 10% and 50% of the time, depending on the runoff characteristics of the year (Wolman and Miller, 1960, and Vericat and Batalla, 2006, respectively). Overall, the Isábena load frequency curves indicate that, as expected, floods are the most important feature in terms of sediment yield. This illustrates both the torrential character of this mesoscale catchment and the continuous availability of sediment, whether it is primarily confined in badlands or stored within the drainage network. Results also indicate that the Isábena has a more constant sediment transport in comparison with its regional counterparts. This is illustrated by the high *SSC*s typically observed during base flows (e.g., mean *SSC* = 0.45 g l^{-1}). In other words, overall sediment yield is strictly dependent upon floods, but base flows, and even daily fluctuations in the flow and small floods play remarkably important roles in the export of sediment from the catchment.

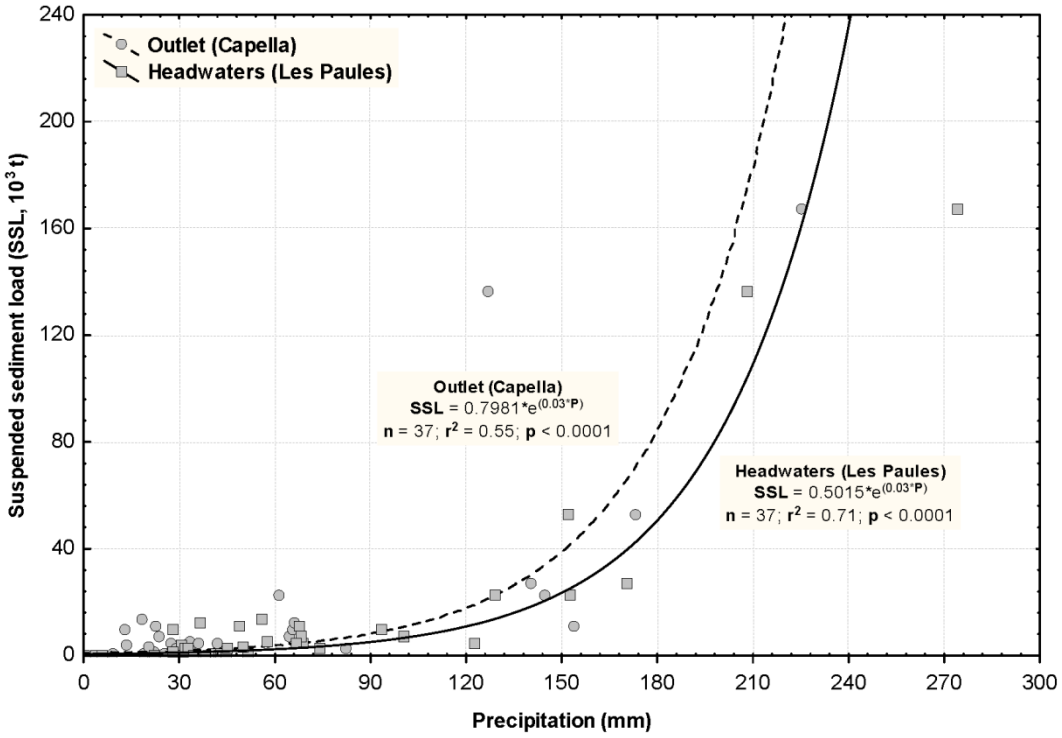

Figure 7. Monthly statistically significant relationships between rainfall (both in the headwaters and the outlet) and the suspended sediment load at the outlet of the Isábena catchment (Fig. 1).

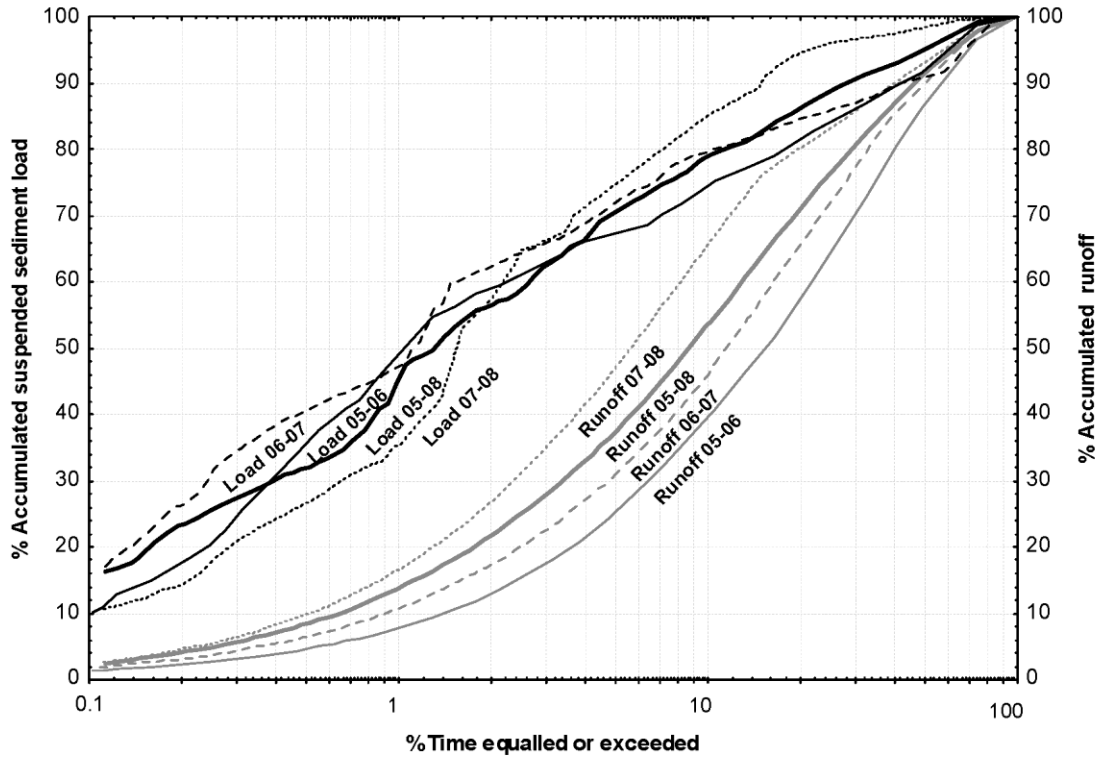

Figure 8. Suspended sediment load and runoff frequency curves for the study period and the individual years in the River Isábena.

5. CONCLUSIONS

This paper reports on the suspended sediment yield and temporal variability in the River Isábena for the period May 2005 to May 2008. The catchment drains regions of highly erodible sediments located in badlands that occupy < 1% of the area. The main conclusions of the study are as follows:

(*i*) Suspended sediment concentrations span five orders of magnitude, occasionally attaining instantaneous values in excess of 300 g l^{-1}. Concentrations do not show a direct relationship with flow discharge (i.e., they are not solely hydraulically dependent). This indicates that the rating curve method is not appropriate to estimate the suspended sediment load in this type of catchment, where sediments sources are not uniformly distributed and temporal in-channel sediment storage exerts an important control on sediment yield.

(*ii*) Mean specific sediment yield of the catchment in the dry period studied is high (414 t km^{-2} y^{-1}), approaching that reported for small mountain torrents in similar Mediterranean environments. This may be seen as a direct consequence of the high connectivity between the source areas (i.e., badlands) and the stream courses at the annual scale, which maximises sediment conveyance through the catchment, causing the river to be working at or close to full sediment transport capacity for most of the year.

(*iii*) A high rainfall-dependent transport has been observed. High suspended sediment concentrations appear only with significant rainfalls, with highest loads observed in the wettest seasons (e.g., autumn 2005, summer 2006, and spring 2008).

(*iv*) Floods dominate the sediment transport and yield. However, sediment transport is much more constant through time than observed in other Mediterranean basins; this can be attributed to the role of baseflows and even small discharge fluctuations that entrain fine sediment stored in the channel and force the river to carry high sediment concentrations (i.e., typically in the order of 0.5 g l^{-1}, even under minimum flow conditions).

(*v*) Results from the hysteretic analysis show that counterclockwise floods predominate, which can be grouped into two. The first is a group (CC1 floods) that shows typical counterclockwise characteristics as a response to rainfall events concentrated in the headwaters. These floods are characterised by high runoff but low sediment load. The second group (CC2 floods) shows atypical counterclockwise characteristics as a response to evenly distributed rainfall events, giving low runoff but very high sediment load. The channel controls the sediment transfer between the sources and the outlet, acting sometimes as the main source of sediment (CC2 floods) and others as sink (CC1 floods).

The Isábena represents one-third of the catchment area of the Barasona Reservoir. The suspended sediment load for the entire 3-year period exceeds 550,000 t. Assuming a dry density of the sediment of 1.52 g cm^{-3} (Mamede, 2008), the total load transported by the Isábena to the reservoir can be estimated at around 0.36 hm^3, a value that represents more than 0.4% of the original reservoir capacity and more than 4% of the total sediment sluiced down during maintenance operations carried out in the 1990s (ca. 9 hm^3). The sediment load transported by the River Isábena, in addition to that transported by the Ésera, explains the historical siltation of the Barasona reservoir. Our study gives a reliable estimation of the sediment load and its temporal dynamics, and it underlines the importance of quantifying the suspended sediment transport in mesoscale catchments in mountainous areas that may help to inform future management actions to decrease the siltation of reservoirs.

Acknowledgements

The first author has a grant funded by the Catalan Government and the European Social Fund. Research has been carried out within the framework of the project "Sediment Export from Large Semi-Arid Catchments: Measurements and Modelling" (SESAM), funded by the Deutsche Forschungsgemeinschaft (DGF). The authors wish to thank the Ebro Water Authorities for their permission to install the equipment at the Capella gauging station and for providing hydrological data. Authors are indebted to Chris Gibbins who undertook a helpful revision of the paper and the two anonymous referees whose comments greatly improved the manuscript.

REFERENCES

Alatorre, L.C., Beguería, S., Vicente-Serrano, S.M., 2008. Identificación de zonas con erosión activa y áreas de riesgo en un paisaje de cárcavas sobre margas. In: Benavente, J., Gracia, F. J., (Eds.), *Trabajos de Geomorfología en España, 2006-2008*. SEG, Cádiz, pp., 141-144

Asselman, N.E.M., 2000. Fitting and interpretation of sediment rating curves. *Journal of Hydrology*, **234**: 228-248.

Avendaño, C., Cobo, R., Sanz, M.E., Gómez, J.L., 1997a. Capacity situation in Spanish reservoirs. *I.C.O.L.D. Proceedings of the Nineteenth Congress on Large Dams*, **74**(53): 849-862.

Avendaño, C., Sanz, M.E., Cobo, R., Gómez, J.L., 1997b. Sediment yield at Spanish reservoirs and its relationships with the drainage basin area. *I.C.O.L.D. Proceedings of the Nineteenth Congress on Large Dams*, **74**(54): 863-874.

Avendaño, C., Sanz, M.E., Cobo, R., 2000. State of the art of reservoir sedimentation management in Spain. In: *Proceedings of the International Workshop and Symposium on Reservoir Sedimentation Management*, Tokyo, Japan, pp. 27-35.

Baker, V.R., Costa, J.E., 1987. Flood power. In: Mayer, L., Nash, D. (Eds.), *Catastrophic Flooding, The Binghamton Symposia in Geomorphology*. International Series 18, Allen and Unwin, Boston, Massachusetts, pp. 1-24.

Balasch, J.C., Castelltort, F.X., Llorens, P., Gallart, F., 1992. Hydrological and sediment dynamics network design in a Mediterranean mountainous area subject to gully erosion. In: Bogen, J., Walling, D.E., Day, T. (Eds.), *Erosion and Sediment Transport Monitoring Programmes in River Basins.* IAHS Publication 210, Wallingford, UK ,pp. 433-442.

Batalla, R.J., Sala, M., Werrity, A., 1995. Sediment budget focused in solid material transport in a subhumid Mediterranean drainage basin. *Zeitschrift für Geomorphologie*, **39**(2): 249-269.

Batalla, R.J., De Jong, C., Ergenzinger, P., Sala, M., 1999. Field observations on hyperconcentrated flows in mountain torrents. *Earth Surface Processes and Landforms*, **24**: 247-253.

Becker, A., 2007. Quantification of the temporal storage at characteristic cross-sections at the Isábena River in the Pre-Pyrenees of Spain. M. S. thesis, Universität Potsdam, Germany.

Clotet, N., Gallart, F., 1986. Sediment yield in a mountainous basin under high Mediterranean climate. *Zeitschrift für Geomorphologie, Supplement Band*, **60:** 205-216.

Clotet, N., Gallart, F., Balasch, C., 1988. Medium-term erosion rates in a small scarcely vegetated catchment in the Pyrenees. *Catena Supplement*, **13:** 37-47.

Costa, J.E., 1987. Hydraulics and basin morphometry of the largest flash floods in the conterminous United States. *Journal of Hydrology*, **93**(3/4): 313-338.

de Vente, J., Poesen, J., Bazzoffi, P., Van Rompaey, A., Verstraeten, G., 2006. Predicting catchment sediment yield in Mediterranean environments: the importance of sediment sources and connectivity in Italian drainage basins. *Earth Surface Processes and Landforms*, **31:** 1017-1034.

Estrany, J., Garcia, C., Batalla, R.J. (in press): Suspended sediment transport in a small Mediterranean agricultural catchment. *Earth Surface Processes and Landforms*.

Ferguson, R.I., 1986. River loads underestimated by rating curves. *Water Resources Research*, **21:** 74-76.

Francke, T., López-Tarazón, J.A., Vericat, D., Bronstert, A., Batalla, R.J., 2008a. Flood-based analysis of high-magnitude sediment transport using a non-parametric method. *Earth Surface Processes and Landforms*, **33**: 2064-2077.

Francke, T., Mamede, G., López-Tarazón, J.A., Batalla, R.J., 2008b. Assessment of sediment yield and reservoir siltation using non-parametric regression and numerical modelling. European Geosciences Union General Assembly, Vienna, Austria. *Geophysical Research Abstracts*, 10, SRef-ID: 1607-7962/gra/EGU2008-A-06723.

Gallart, F., Balasch, J.C., Regüés, D., Soler, M., Castelltort, F., 2005. Catchment dynamics in a Mediterranean mountain environment: the Vallcebre research basins (southeastern Pyrenees). II: Temporal and spatial dynamics of erosion and stream sediment transport. In: García, C., Batalla, R.J. (Eds.), *Catchment Dynamics and River Processes: Mediterranean and Other Climate Regions*. Developments in Earth Surface Processes, Publication 7, Elsevier, Amsterdam, The Nederlands, pp. 17-29.

Horowitz, A.J., 2003. An evaluation of sediment rating curves for estimating suspended sediment concentrations for subsequent flux calculations. *Hydrological Processes*, **17**: 3387-3409.

Horowitz, A.J., Elrick, K.A., Smith, J., 2001. Estimating suspended sediment and trace element fluxes in large river basins: methodological considerations as applied to the NASQAN programme. *Hydrological Processes*, **15**: 1107-1132.

Lawler, D.M., 2005. Spectrophotometry: turbidimetry and nephelometry. In: Townshend, A. (Ed.), *Encyclopedia of Analytical Science*, 2nd ed. Academic Press, Elsevier, Amsterdam, The Nederlands, pp. 343-351.

Lawler, D.M., Petts, G.E., Foster, I.D.L, Harper, S., 2006. Turbidity dynamics during spring storm events in an urban headwater river system: the Upper Tame, West Midlands, UK. *Science of the Total Environment*, **360**: 109-126.

Li, W., Qi, P., Sun, Z., 1997. Deformation of river bed and the characteristics of sediment transport during hyper-concentrated flood in the Yellow River. *International Journal of Sediment Research*, **12**(3): 72-79.

Maidment, D.R., 1993. Handbook of Hydrology. McGraw-Hill, New York.

Mamede, G., 2008. Reservoir sedimentation in dryland catchments: modelling and management. Unpublished PhD Thesis, Universität Potsdam, Germany.

Mamede, G.L., Bronstert, A., Araújo, J.C., Batalla, R.J., Güntner, A., Francke, T., Müller, E.N., 2006. 1D process-based modelling of reservoir sedimentation: a case reservoir in Spain. *Proceedings of the International Conference on Fluvial Hydraulics* (River Flow 2006) 2, 1585-1594.

Mathys, N., Klotz, S., Esteves, M., Descroix, L., Lapetite, J.M., 2005. Runoff and erosion in the Black Marls of the French Alps: observations and measurements at the plot scale. *Catena,* **63**: 261-281.

Nadal-Romero, E., Latron, J., Martí-Bono, C., Regüés, D., 2008. Temporal distribution of suspended sediment transport in a humid Mediterranean badland area: the Araguás catchment, central Pyrenees. *Geomorphology*, **97**: 601-616.

Navas, A., Valero, B., Machín, J., Walling, D., 1998. Los sedimentos del embalse Joaquín Costa y la historia de su depósito. *Limnética*, **14**: 93-112.

Newson, M.D., 1989. Flood effectiveness in river basins: progress in Britain in a decade of drought. In: Beven, K., Carling, P. (Eds.). *Floods: Hydrological, Sedimentological and Geomorphological Implications*. Geomorphology in Environmental Planning. John Willey and sons publications 1, Chichester, UK, pp. 151-171.

Palau, A. 1998. Estudio limnológico del ecosistema fluvial afectado por los vaciados del embalse de Barasona. *Limnética,* **14**: 1-15

Phillips, J.M., Webb, B.W., Walling, D.E., Leeks, G.J.L., 1999. Estimating the suspended sediment loads of rivers in the LOIS study area using infrequent samples. *Hydrological Processes*, **13**: 1035-1050.

Rovira, A., Batalla, R.J., 2006. Temporal distribution of suspended sediment transport in a Mediterranean basin: the lower Tordera (NE Spain). *Geomorphology*, **79**: 58-71.

Sanz-Montero, M., Cobo-Rayán, R., Avendaño-Salas, C., Gómez-Montaña, J., 1996. Influence of the drainage basin area on the sediment yield to Spanish reservoirs. In: *Proceedings of the First European Conference and Trade Exposition on Control Erosion*, International Erosion Control Association IECA, Sitges, Spain.

Smith, H.G., Dragovich, D., 2008. Sediment budget analysis of slope-channel coupling and in-channel sediment storage in an upland catchment, southeastern Australia. *Geomorphology*, **101**: 643-654

Soil Survey Staff, 1996. Keys to Soil Taxonomy, 7th ed. U.S. Government Printing Office, Washington, DC

Valero-Garcés, B. L., Navas, A., Machín, J., Walling, D. 1999. Sediment sources and siltation in mountain reservoirs: a case study from the central Spanish Pyrenees. *Geomorphology*, **28**: 23-41.

Verdú, J.M., Batalla, R.J., Martínez-Casasnovas, J.A., 2006a. Estudio hidrológico de la cuenca del río Isábena (Cuenca del Ebro). I: Variabilidad de la precipitación. *Ingeniería del Agua*, **13**(4): 321-330.

Verdú, J.M., Batalla, R.J., Martínez-Casasnovas, J.A., 2006b. Estudio hidrológico de la cuenca del río Isábena (Cuenca del Ebro). II: Respuesta hidrológica. *Ingeniería del Agua*, **13**(4): 331-343.

Vericat, D., Batalla, R.J., 2006. Sediment transport in a large impounded river: the lower Ebro, NE Iberian Peninsula. *Geomorphology*, **79:** 72-92.

Walling, D.E., 1977. Limitations of the rating curve technique for estimating suspended sediment loads, with particular reference to British rivers. In: *Erosion and solid matter transport in inland waters*. Proceedings of the Paris Symposium on Hydrological Forecasting, IAHS Publication 122, Wallingford, Oxfordshire, UK, 34-48.

Walling, D.E., 1984. Dissolved loads and their measurements. In: Hadley, R.F., Walling, D.E. (Eds.), *Erosion and Sediment Yield: Some Methods of Measurements and Modelling*. Geo Books, London.

Walling, D.E., Amos, C.M., 1999. Source, storage and mobilisation of fine sediment in a chalk stream system. *Hydrological Processes*, **13**(3): 323-340.

Williams, G.P., 1989. Sediment concentration versus water discharge during single hydrologic events in rivers. *Journal of Hydrology*, **111**(1–4): 89-106.

Williams, R.P., 1979. Sediment Discharge in the Santa Clara River Basin, Ventura and Los Angeles Counties, California. *Water-Resources Investigations* 78-79, U.S. Geological Survey, Tallahassee, Florida.

Wolman, M.G., Miller, W.P., 1960. Magnitude and frequency of forces in geomorphic processes. *Journal of Geology*, **68:** 54-74.

Xu, J., 1997. The optimal grainsize composition of suspended sediment of hyperconcentrated flow in the middle Yellow River. *International Journal of Sediment Research*, **12**(3): 170-176.

CHAPTER 4

HYDRO-SEDIMENTOLOGICAL RESPONSE

INDEX CHAPTER 4: HYDRO-SEDIMENTOLOGICAL RESPONSE

Figure captions in the paper

Figure 1. A) Location of the Isábena, Ésera and Cinca catchments in the Ebro basin. B) General map of the Isábena catchment, showing locations of the main badland areas and field instrumentation. Codes of the instrumented sites are also cited in the text.

Figure 2. A) Flow regime of the study period. The grey line represents the mean discharge for the 2007-2008 hydrologic year (i.e., 3.87 $m^3 s^{-1}$). Some floods include Q_i, where *i* represents the return period of the floods. B) Mean monthly discharge for the hydrological year 2007-2008.

Figure 3. Discharge and suspended sediment concentration at the Capella gauging station (i.e., EA047, Fig. 1b) during the study period.

Figure 4. Monthly total precipitation and mean runoff coefficient for the study period in the Isábena catchment.

Figure 5. Scatter plot of the relation between total runoff and total suspended sediment load for the 34 studied floods. Note the differences on magnitude between the spring floods and the floods of the rest of the year; highest runoff and sediment loads were observed during that season.

Figure 6. Discharge and suspended sediment concentration of selected floods taken for the linearity analysis: A) 4th October 2007 (precipitation = 14.68 mm); B) 4th February 2008 (precipitation = 16.81 mm); C) 2nd June 2008 (precipitation = 15.28 mm); D) 18th September 2008 (precipitation = 12.64 mm). In all cases, the precipitation recorded in P030 (rain gauge located at headwaters, Fig. 1b) and in EA047 (rain gauge located near the outlet, Fig. 1b) has been plotted as an example of the rainfall data of each event.

Table captions in the paper

Table 1. Flood variables and associated abbreviations used in the statistical analysis of the rainfall-runoff-suspended sediment transport relations.

Table 2. Detailed description of the floods analysed in the paper (see Table 1 for abbreviations and units of the variables). Bold values are maximum values of each variable while italics indicate the minimum values.

Table 3. A) Pearson correlation matrix between rainfall and runoff variables (n = 34); B) Equations of the rainfall-runoff relations after the application of the backward stepwise multiple regression, together with the β coefficients (see Table 1 for abbreviations).

Table 4. A) Pearson correlation matrix between rainfall and suspended sediment transport variables (n = 34); b) Equations of the rainfall-suspended sediment transport relations after the application of the backward stepwise multiple regression, together with the β coefficients (see Table 1 for abbreviations).

Table 5. Pearson correlation matrix between runoff and suspended sediment transport variables (n = 34) (see Table 1 for abbreviations).

Table 6. Description of the Kinetic Energy and Stream Power resulting from the selected floods (see Table 1 for abbreviations).

Table 7. Main hydrological and sedimentary characteristics of the selected flood events (see Table 1 for abbreviations).

1. INTRODUCTION

This chapter describes the hydro-sedimentological response of the Isábena catchment by examining the relations between the energy inputs (rainfall) and the runoff and sediment generated by this energy; for this purpose we present a published paper analysing this issue. Paper is presented maintaining its original structure; its format has been adapted to the general format of the present volume.

The paper was published by *Catena* in July 2010; it examines the relations between rainfall, runoff and suspended sediment transport in the Isábena basin during a quasi-average hydrological year (2007 – 2008). The paper also includes an analysis of the different hydrological and sedimentary responses of the catchment to a similar rainfall (related to Objective 2). These analysis were carried out by means of statistical techniques (Pearson correlation matrix and backward stepwise multiple regressions). The main results show very low correlations between rainfall intensity and the hydrological and sedimentological responses. The non-linear hydrosedimentary response is also reflected in the wide range of runoff coefficients and sediment loads that have been observed in response to similar amounts of precipitation.

2. HYDRO-SEDIMENTOLOGICAL RESPONSE

López-Tarazón, J.A., Batalla, R.J., Vericat, D., Balasch, J.C., 2010. Rainfall, runoff and sediment transport relations in a mesoscale mountainous catchment: the River Isábena (Ebro basin). *Catena*, 82: 23-34.

Rainfall, runoff and sediment transport relations in a mesoscale mountainous catchment: the River Isábena (Ebro basin)

Abstract

This paper examines the relations between rainfall, runoff and suspended sediment transport in the Isábena basin during a quasi-average hydrological year. The Isábena is a mesoscale river basin that drains a mountainous area comprising patches of highly erodible materials (badlands). The paper includes an analysis of the different hydrological and sedimentary responses of the catchment to a similar rainfall. Thirty-four floods were studied, with a very variable response observed. Runoff coefficients ranged from 0.32% to 33%. The sedimentary response was also highly variable, with maximum suspended sediment concentrations (*SSC*) oscillating between < 0.1 and 90 g l^{-1} and flood sediment loads varying from 27 to 54,000 t per hydrological event. Most sediment load was concentrated in spring when competent floods occur frequently. Pearson correlation matrix and backward stepwise multiple regression indicate that the hydrological response of the catchment is strongly correlated with total precipitation, event duration, and rainfall of the previous days. Very low correlation was observed with rainfall intensity. The relation between rainfall and sediment transport followed the same trend. Sediment variables (e.g., total load and *SSC*) were significantly correlated with variables such as total rainfall and rainfall over the previous days, although the significance level was lower in comparison with the runoff related variables. There was again no correlation between sediment variables and rainfall intensity. On-going research in the area suggests that, apart from rainfall, factors such as sediment availability in the badlands and accumulation of sediment in the channels influences the river's sedimentary response. The non-linear hydrosedimentary response is reflected in the wide range of runoff coefficients and sediment loads that have been observed in response to similar amounts of precipitation.

Keywords: rainfall, runoff, sediment transport, floods, mesoscale catchment, River Isábena, Ebro basin, southern Pyrenees.

1. INTRODUCTION

It is well known that the variability of many hydrological and geomorphological processes in catchments located in Mediterranean mountainous areas is related to the high temporal and spatial variability of rainfall and evapotranspiration and the spatial variability of soil characteristics (Seeger et al., 2004). As a result, it is difficult to find general rules that explain or predict how rainfall generates runoff, erosion and sediment transport (Lorente et al., 2000; García-Ruiz, et al., 2000; Gallart et al., 1998). There remains a lack of studies examining the relation between the rainfall input and the sediment output, especially in medium to large (i.e., hereafter mesoscale) catchments, where water conveyance maximises energy losses and reduces the potential of the rainfall and the runoff to erode and transport materials downstream.

The hydrological response of a catchment is the combination of several location specific factors (e.g., water storage in the soil, antecedent soil moisture, land use, and topography), and can therefore be characteristic of that catchment, but it is also related to individual rainfall events (Latron et al., 2008). The study of hydrographs and runoff volumes (essentially storm-flow volume) has been a classic approach in catchment hydrology for decades. Hewlett and Hibbert (1967) and Woodruff and Hewlett (1970) studied rainfall-runoff relations at the event scale to define a factor of catchment hydrological response at the annual scale. Hewlett et al. (1977, 1984) and Hewlett and Bosch (1984) used this approach to demonstrate the negligible role of rainfall intensity on the magnitude of the hydrological response of forested catchments. Cappus (1960) explored the relation between storm-flow coefficient (i.e., ratio between storm-flow and rainfall volume), rainfall depth and baseflow to illustrate the hydrological role of saturated areas within a catchment. Taylor and Pearce (1982) concluded that storm-flow volume always correlates with rainfall amount. The scale effect of the runoff coefficient was investigated by Cerdan et al. (2004), while Peters et al., (2003) explored the relations between storm-flow, rainfall depth, water table and soil moisture dynamics. Recently, Angulo-Martínez and Beguería (2009) estimated the rainfall erosivity from daily precipitation records of the Ebro basin (Spain), but results did not show clear differences between calculation methods. Most results owe to studies in humid temperate conditions; in drier climates (i.e., Mediterranean regions), relations may only

be appropriate for short wet periods during the year. During dry periods, there is appreciable variability in rainfall-runoff relations (Beven, 2002), as a function of the antecedent wetness of the catchment, the storm duration and the pattern of rainfall intensities.

In Mediterranean mountainous regions, non-linear relations (i.e., defining the linearity in statistical terms) between rainfall and runoff can be seen at the event scale due to the combination of the high seasonality of the climate and the generally high spatial heterogeneity of the environment. A number of the studies providing examples of the non-linearity of the hydrological response in small Mediterranean catchments have been carried out in the Iberian Peninsula. For instance, Ávila (1987) investigated the seasonal hydrological response of a very small catchment; Piñol et al. (1997) showed the non-linearity of the rainfall-runoff relations during a wetting-up period in two paired research catchments; Ceballos and Schnabel (1998) found two different rainfall-runoff relations, depending on the existence of saturated conditions in the valley bottom; finally, long-term (> 20 years) studies in the Vallcebre research area, provided insights into several aspects of catchment hydrology (e.g., Gallart et al., 2002; Gallart et al., 2005 a, b; Latron and Gallart, 2007; Latron et al., 2008).

Erosion, and thus subsequent sediment transport in alluvial channels, is the main geomorphic consequence of the runoff resulting from rainfall inputs in river basins. Kinetic energy from the precipitation transforms inevitably to stream power in the drainage network that will ultimately be responsible for the transportation of solid matter to the basin outlet. The occurrence and intensity of erosion and sediment transport will depend on the hydroclimatic and geomorphologic characteristics of the basin, together with the availability of sediment within the catchment.

The transport of fine material in suspension is the major transferring mechanism of particulate material in streams worldwide (Webb et al., 1995), typically attaining more than 90% of the annual load in alluvial streams (Meade et al., 1990). For this reason, total sediment yields are often based purely on suspended load data (Wood, 1977). In addition, research on sediment transport in catchments draining highly erodible materials (e.g., soft marls, badlands) has become of interest due to the possibility of

setting maximum thresholds and magnitudes of sediment transport in fluvial systems, and also allowing model calibration and validation in extremely active geomorphic environments, together with the interest for management purposes (i.e., reservoir siltation; e.g., Mamede et al., 2006; Francke et al., 2008b; López-Tarazón et al., 2009). Badlands are considered to be characteristic of arid regions, but they also occur in wetter climates with high intensity storm events such as in the Mediterranean (Gallart et al., 2002), where rainfall mostly occurs in the form of high intensity storm events. Vegetation growth is limited no longer by water availability but by the high erosion rates and freezing on north exposed slopes (Regüés et al., 2000). This is the case for the Isábena that drains extensive areas of badlands shaping run-down reliefs that have been identified as the main source of the sediment deposited in the downstream Barasona reservoir (Valero-Garcés et al., 1999, Francke et al, 2008b).

Literature provides case studies of the linkages between rainfall components (e.g., total precipitation, intensity, and precipitation of the previous days) and the suspended sediment transport, but studies are generally carried out in a micro (or plot) scale; while some of them have been developed in mountainous environments (e.g., Yair and Enzel, 1987; Regüés and Gallart, 2004; Seeger et al., 2004; Nadal-Romero et al., 2008), most describe processes in agricultural areas (e.g., Martínez-Casasnovas et al., 2002; Ramos and Martínez-Casasnovas, 2006; Arnáez, et al., 2007; Ramos and Martínez-Casasnovas, 2007; Marques et al., 2008; Estrany et al., 2009). Studies of rainfall-runoff-fine sediment transport relations at larger scales are scarce.

The aim of this paper is to investigate the rainfall-runoff-sediment transport relations and to assess the linearity of the hydrological and sedimentary response of the Isábena river basin, a highly dynamic Mediterranean mountainous catchment located in the Southern Pyrenees. Moreover, this work intends to improve our understanding of the factors that control sediment transport patterns and loads in mesoscale catchments.

2. STUDY AREA

The Isábena basin is located in the Southern Central Pyrenees (Ebro basin, NE Iberian Peninsula). Together with the Ésera, the Isábena is one of the major tributaries of the River Cinca, in turn one of the largest catchments in the Ebro basin (Fig. 1a). The catchment area is 445 km^2, 0.48% of the total area of the Ebro basin. The river flows from the Central Pyrenean Range, at 2720 m a.s.l., to the confluence with the River Ésera at 650 m a.s.l. The Isábena is not regulated at all, though its main channel experiences occasional gravel mining. Mean temperature is 10ºC in the northern part of the basin and 12.5ºC in the southern area. Mean annual rainfall is 767 mm, ranging from 1600 mm y^{-1} at the headwaters to 450 mm y^{-1} in the valley bottom (Verdú et al., 2006), with seasonal maxima during spring and autumn.

Dominant materials in the basin headwaters are Cretaceous limestones that, at the highest altitudes, are partially karstified. The presence of late Eocene marls is significant, usually having a badland drainage pattern, representing < 1% of the total basin area, but being the most important sediment source in the catchment (Francke et al., 2008b; see location in Fig. 1b). In the lower part, the basin is mainly composed by Cretaceous chalks together with Tertiary clay rocks and conglomerates. The soils of the Isábena basin are rather thin and developed over calcilutites, limestones, sandstones, and conglomerates; they can be classified as Xerorthents (Soil Survey Staff, 1996), with silt loam texture and low organic content (< 2%).

The vegetation in the Isábena basin reflects its intrinsic climatic variability and the typical contrasts between sunny and shady places. Climax vegetation of the central and lower parts of the basin are the forests of *Quercus ilex ballota* with *Pinus halepensis* in the sunny places and woodland of *Quercus faginea* in the shady places; in the northern part, the climax vegetation is forests of *Pinus sylvestris* and *Pinus uncinata*. It is notable that important changes in the land use occurred during the last 50 years, with the abandoning of most parts of the agricultural areas and the subsequent reforestation (Gallart and Llorens, 2004).

The hydrology of the basin is characterised by a rainy-snowy regime. Floods typically occur in spring (due to the snowmelt) and, especially, in late summer and autumn as a consequence of localised thunderstorms. Minimum flows (~ 0.20 $m^3 s^{-1}$) typically occur in summer, but the river never dries up. Absolute maximum flows normally occur in autumn; however, the largest peak ever recorded at the basin outlet (i.e., Capella gauging station, EA047, see Fig. 1b) took place in summer (August 1963), reaching 370 $m^3 s^{-1}$ (a discharge with a return period of 86 years, calculated from the series of annual maximum instantaneous discharges by the Gumbel method for the period 1951-2008). The mean annual discharge at the basin outlet for the entire period of record (1945-2008) is 4.1 $m^3 s^{-1}$ (P_{10} = 2.14 $m^3 s^{-1}$ and P_{90} = 8.21 $m^3 s^{-1}$, where P_i is the i percentile of the observations). The mean annual water yield is 177 hm^3 (P_{10} = 68 hm^3 and P_{90} = 259 hm^3, 1 hm^3 = 1x10^6 m^3), a value that represents ~1.5% of the Ebro basin's total runoff.

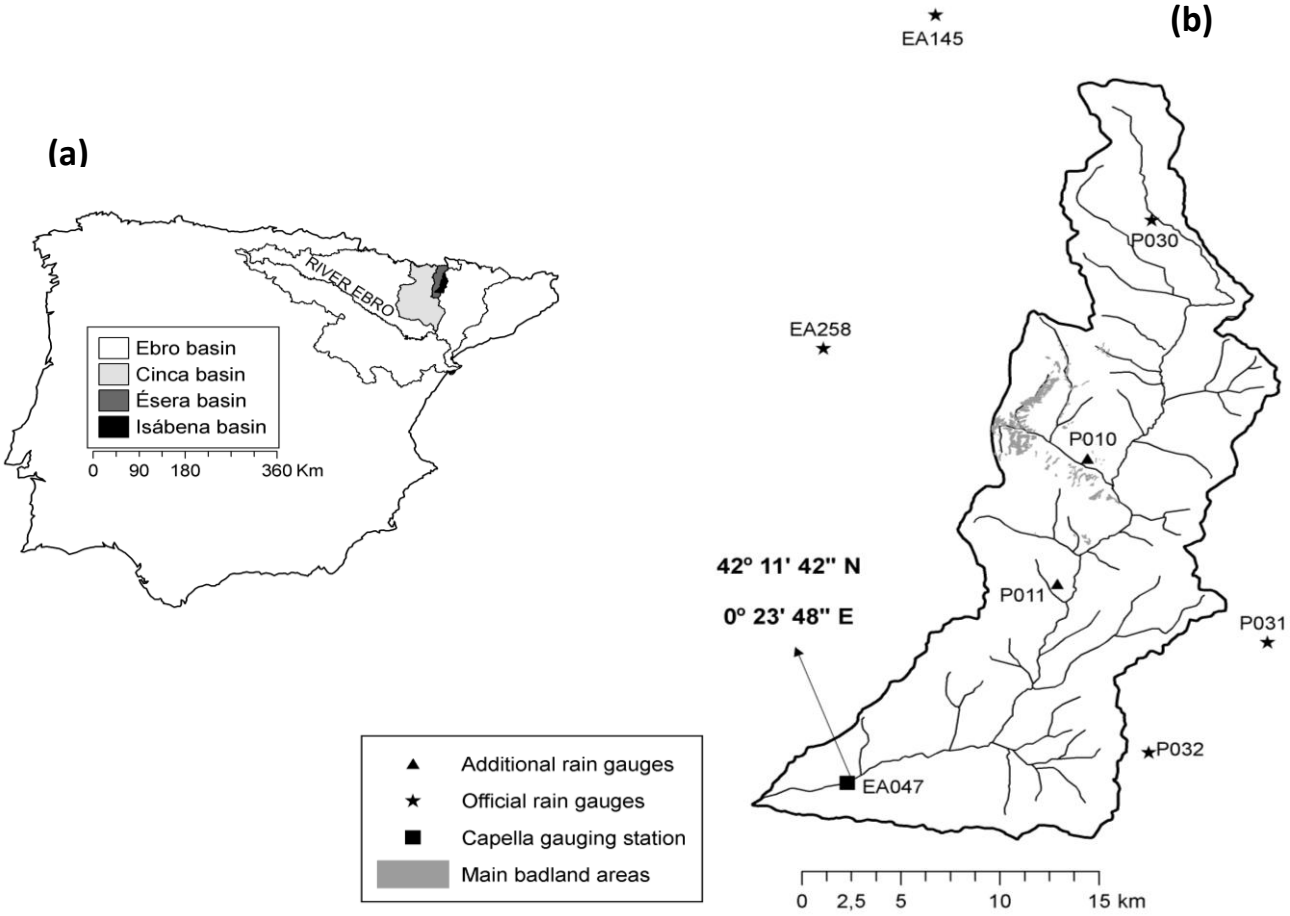

Figure 1. A) Location of the Isábena, Ésera and Cinca catchments in the Ebro basin. B) General map of the Isábena catchment, showing locations of the main badland areas and field instrumentation. Codes of the instrumented sites are also cited in the text.

3. METHODS

3.1. Field monitoring

The Isábena basin has been monitored since 2005 with the general aim of examining the suspended sediment transport dynamics in a highly active hydrological and sedimentary fluvial environment. Since then, instrumentation has been continuously updated (i.e., new equipment, increases in spatial and temporal resolution of measurements) to improve the understanding of the hydrological and sediment transport response of the catchment. Extensive details are given in López-Tarazón et al. (2009) and here we present a technical summary relevant for the purpose of the paper.

Rainfall is measured by the Ebro Water Authorities (hereafter CHE) by means of 2 tipping-bucket rain gauges located in Les Paules (P030; Fig. 1b) and Capella (EA047; Fig. 1b). To complete the rainfall record, we installed two Campbell ARG100 tipping-bucket rain gauges in Villacarli in 2006 (P010; see location in Fig. 1b) and in Roda de Isábena in 2007 (P011; Fig. 1b). Both of them were connected to a Campbell CR-200 data-logger, setting-up the measurements at 1-min intervals. Due to the size of the basin and the uneven distribution of the existing rain gauges within the catchment, four additional tipping-bucket rain gauges located out of the basin but very close to it (Casallera, P031; Castigaleu, P032; Eriste, EA145; and Campo, EA258; see location in Fig. 1b) were incorporated to improve the quality of the precipitation record. All the rain gauges operated by the CHE (P030, EA047, P031, P032, EA145 and EA258) register accumulated values of rainfall every 15 min. The rain gauging network was established trying to incorporate land use and rainfall spatial heterogeneities. This network is composed by public and private rain gauges. Rain gauges are located at high (P030 and EA145) and low altitudes (EA047 and P032), at the main badland strip in the basin (P010 and EA258), at forested areas (P030), at principal agricultural areas (EA047) and at the stretch where the river decreases its slope and the valley platform changes, starting widening (P011).

Water discharge is continuously recorded at the Capella gauging station (i.e., EA047), located near the outlet of the basin (Fig. 1b) and operated by the CHE. Water stage is

measured every 15 min and then transformed into discharge by means of the calibrated rating curve obtained through periodic flow measurements, especially during floods under high suspended sediment concentrations, that the authors have carried out since 2005. Figure 2 shows the hydrological regime of the study period.

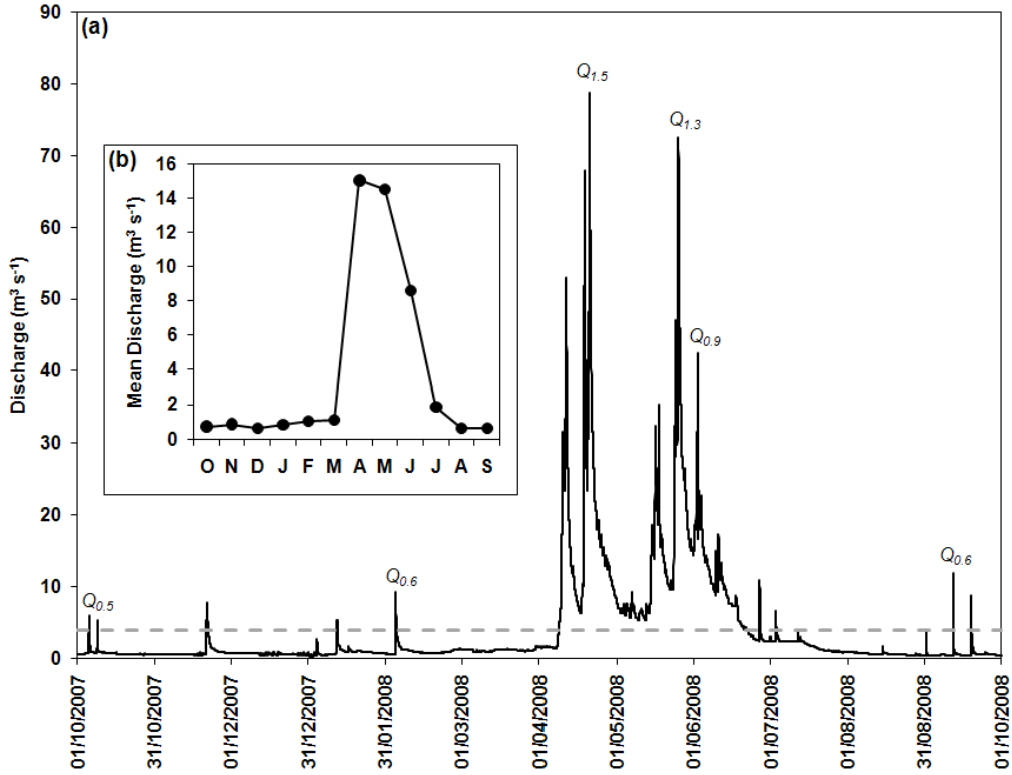

Figure 2. A) Flow regime of the study period. The grey line represents the mean discharge for the 2007-2008 hydrologic year (i.e., 3.87 $m^3 s^{-1}$). Some floods include Q_i, where i represents the return period of the floods. B) Mean monthly discharge for the hydrological year 2007-2008.

Suspended sediment transport is recorded as turbidity using a high-range backscattering Endress+Hauser Turbimax W CUS41 turbidimeter (with a measuring range up to 300 g l^{-1}). The turbidity probe is linked to a Campbell CR-510 data logger. Turbidity reading was set up at 5 s intervals while the logging recorded at 15 min intervals (thus recording the average value of the samples between log intervals). Turbidity records have been calibrated by means of suspended sediment concentrations obtained from water samples (for more details see López-Tarazón et al., 2009). A total of 428 water samples were obtained during the study period, 94 of them manually (by means of a cable-suspended depth-integrating US DH59 sampler) and 334 automatically (by means of an automatic water sampler ISCO 3700). Water samples taken during the monitoring period cover

almost the entire range of discharges, from 0.20 to 68 m^3 s^{-1}, values that account for >99% of the time on the flow duration curve of the study period. Figure 3 represents the discharge and the suspended sediment concentration during the 2007-2008 hydrological year.

3.2. Data computation

We selected the hydrological year October 2007 – September 2008 for the purpose of this particular paper. This period optimises the number of floods and the number of available precipitation series in the catchment. A total of 34 flood events were recorded during that year. With a total runoff of 122 hm^3, the study year can be considered relatively dry in comparison with the long term series (i.e., average of 177 hm^3 since 1945) but humid within our own recording period (i.e., 2005-2006 with 89 hm^3 and 2006-2007 with 117 hm^3). We have considered flood events as those in which discharge exceeded 1.5 times the baseflow at the beginning of the rainfall event (as per Garcia Ruiz et al., 2005). For each event, quick flow has been separated from the baseflow component by means of a simple visual technique based on the breakpoints detected on the logarithmic falling limb of the hydrograph (e.g., Hewlett and Hibbert, 1967; Maidment, 1993). The flood events have been subsequently characterised using three groups of variables (Table 1):

(1) The rainfall associated with each event was characterised by its (a) duration (*Dur*, minutes), (b) total precipitation (*Ptot*, mm), (c) maximum rainfall intensity over a 15-min period (*Imax15*, mm h^{-1}), (d) maximum rainfall intensity over a 30-min period (*Imax30*, mm h^{-1}), (e) kinetic energy of the maximum rainfall intensity over a 30-min period (*EcI30*, Mj mm ha^{-1} h^{-1}, after Brown and Foster, 1987) and (f) the precipitation accumulated during the previous 1 and 7 days (*P1d* and *P7d*, mm). The *EcI30* was calculated with the following equations:

$$EF = 0.29[1 - 0.72 \times \exp(-0.05 \times I)] \quad (1)$$

$$EcI30 = ((\sum EF \times P)Ix) \quad (2)$$

where, *EF* if the kinetic energy estimated from Brown and Foster (Mj ha^{-1} mm^{-1}), *I* is rainfall intensity over a 30-min period (mm h^{-1}), *P* is the accumulated precipitation over

a 30-min period (mm) and *Ix* is the maximum 30-min rainfall intensity of the event (mm h^{-1}).

(2) The runoff generated by the rainfall was described by (a) the total runoff volume of the flood (*Tr*, hm^3), (b) the peak discharge (*Qp*, $m^3\ s^{-1}$), (c) the mean flood discharge (*Qm*, $m^3\ s^{-1}$), (d) the baseflow at the start of the flood (*Qb*, $m^3\ s^{-1}$), and (e) the storm-flow coefficient (*RC*), calculated as the relation between the total amount of precipitation and the total runoff volume (after subtracting the baseflow) of each flood.

(3) The sediment transport observed in each event was characterised by (a) the mean suspended sediment concentration (*SSCmean*, g l^{-1}), (b) the maximum suspended sediment concentration (*SSCmax*, g l^{-1}), and (c) the total suspended sediment load (*TL*, t), estimated by multiplying discharge (*Q*) and the estimated suspended sediment concentration (*SSC*) (i.e., *SSC* transformed from the turbidity record) for each 15-min interval. For more details see López-Tarazón et al. (2009).

(4) Finally, the stream power was calculated using the formulation proposed by Leopold et al. (1964):

$$\Omega = \gamma \times Q \times s \qquad (3)$$

where, Ω is the stream power (W m^{-1}), γ is the specific weight of the water (9,810 N m^{-3}), *Q* is the mean discharge of the flood ($m^3\ s^{-1}$) and *s* is the slope of the channel (mm mm^{-1}).

Table 1. Flood variables and associated abbreviations used in the statistical analysis of the rainfall-runoff-suspended sediment transport relations.

Rainfall related variables		**Runoff related variables**	
Dur	Duration of the event (min)	*Tr*	Total flood runoff volume (hm^3)
Ptot	Total precipitation (mm)	*Qp*	Flood peak discharge ($m^3\ s^{-1}$)
Imax15	Maximum 15' rainfall intensity (mm h^{-1})	*Qm*	Mean flood discharge ($m^3\ s^{-1}$)
Imax30	Maximum 30' rainfall intensity (mm h^{-1})	*Qb*	Baseflow at the beginning ($m^3\ s^{-1}$)
EcI30	Kinetic energy of the maximum 30' rainfall intensity (Mj mm $ha^{-1}\ h^{-1}$)	*RC*	Storm-flow coefficient (%)
P1d	Antecedent precipitation 1 day before (mm)	**SST[a] related variables**	
P7d	Antecedent precipitation 7 days before (mm)	*SSCmean*	Mean flood SSC[b] (g l^{-1})
		SSCmax	Maximum flood SSC[b] (g l^{-1})
		TL	Total suspended sediment load (t)

[a] Suspended sediment transport
[b] Suspended sediment concentration

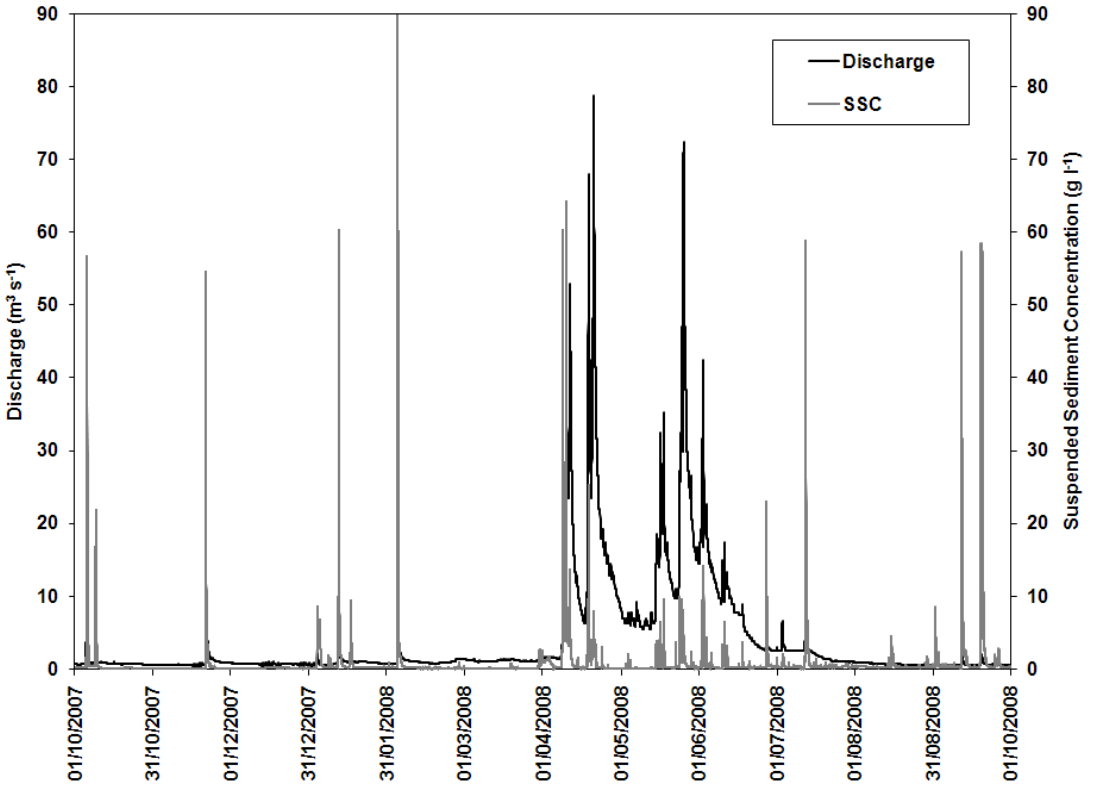

Figure 3. Discharge and suspended sediment concentration at the Capella gauging station (i.e., EA047, Fig. 1b) during the study period.

A continuous surface for the rainfall data has been calculated using *Spline* interpolation. This method adjusts the study surface to the input rainfall data using polynomial methods and least-squares (e.g., Sherman and Salter, 1975; Guenni and Hutchinson, 1998; Tait et al., 2006; Suprit and Shankar, 2007). The interpolation procedure was performed by means of ESRI© ArcMap™ 9.2 (*Spline* tool with an output cell size of 25 m^2). We assume that the selected method may give relatively high uncertainties, caused by the high variability of rainfall both in time and space, and stressing the importance of having long data series with a dense spatial coverage (Angulo-Martínez et al., 2009).

In order to assess the relations between variables, a linear regression by a Pearson correlation matrix was used. After the evaluation of the correlations, a backward stepwise multiple regression was applied using the package Statistica 6.0©. We have considered the variables calculated from runoff and sediment transport observations as the dependent ones (i.e., *Tr, Qp, Qm, Qb, RC, SSCmean, SSCmax, TL*) while the independent variables were those related to precipitation (i.e., *Ptot, Dur, Imax15,*

Imax30, *EcI30*, *P1d*, *P7d*). Stepwise multiple regressions allow determining the most influential rainfall variables, on both runoff and suspended sediment transport.

A backward stepwise multiple regression is a discriminant function analysis where the model for discrimination is built step-by-step. It starts by including all the variables in the model and then, at each step, the variable that contributes least to the prediction of a group membership is eliminated. Thus, as a result of a successful discriminant function analysis, one would only keep the "important" variables in the model which are those that contribute the most to the discrimination between groups. The stepwise procedure is guided by an F value. This value indicates, for a given variable, its statistical significance in the discrimination between groups. In our case, an F value of 5 was set as a threshold for significance. The variables already introduced into the regression always have an $F > 5$, being concluded the process when no variable was susceptible to inclusion or elimination. The exact weight of each of the variables was evaluated by means of regression coefficients (β); the variables with the largest β values contribute most to the prediction. The regression coefficients measure the effect of a particular independent variable on the variation of the dependent variable and they are dimensionless parameters, so they may be directly compared (Gregory and Walling, 1973).

4. RESULTS AND DISCUSSION

4.1. Characterisation of the flood events

Of the 34 floods which occurred during the study period, four occurred in autumn, four in winter, eighteen in spring and eight in summer. Following the classification presented by López-Tarazón et al. (2009), 22 of the floods occurred during the wet season (autumn, late spring and late summer) and 12 in the dry season (winter, early spring and early summer). Table 2 summarizes the general characteristics of rainfall, discharge and suspended sediment transport associated with the observed floods and the variables used in the statistical analysis. The main characteristics of the flood events can be summarised as follows:

(1) The maximum amount of precipitation for a single event was 72.7 mm (during the 23 May 2008 event), being a very regular precipitation along the catchment, varying from 76 mm in EA047 and P010 to 87 mm in P030. The most of the events were relatively small in terms of magnitude: only 9 (25% of the events) were greater than the average rainfall value (17.1 mm), while the rest of the episodes were below the average.

(2) The maximum 15 min intensity ranged from 3.4 to 27.9 mm h^{-1}; the maximum 30 min intensity varied from 2.3 to 15.5 mm h^{-1}; the erosivity index *EcI30* ranged from 3.6 to 307.6 Mj mm ha^{-1} h^{-1}. These values show that most of the rainfall events were relatively low in intensity: only 12% exceeded 20 mm h^{-1} at 15 min interval, which is the minimum estimated value to consider the infiltration excess surface flow as "Hortonian overland flow" (Selby, 1982); 25% exceeded 10 mm h^{-1} at 30 min interval and the *EcI30* was greater than the average value (i.e., 59 Mj mm ha^{-1} h^{-1}) only in 29% of the events.

(3) The antecedent rainfall values were very variable, ranging from 0 to 19 mm and 64 mm of precipitation registered during the 1-day and the 7-days previous period, respectively.

(4) The total runoff volume generated by the rainfall varied between 0.05 and 15.8 hm^3, with a mean value of 1.8 hm^3. Peak discharge oscillated between 1.52 and 78.7 m^3 s^{-1} (representing a return period of 0.5 and 1.5 years, respectively). Only during 4 floods (12% of the total) the peak was greater than 50 m^3 s^{-1} (the value that represents the 1-year return period flood). Mean discharge ranged between 0.82 and 34.6 m^3 s^{-1}, while baseflow level fluctuated from 0.49 to 19.2 m^3 s^{-1}; all baseflows greater than 3 m^3 s^{-1} were recorded in spring, the wettest season of the study period.

(5) The direct runoff coefficient (after subtracting the baseflow previous to the event to the total water runoff) was also very variable, ranging from 0.32% to 33%, with a mean value of 6 %. All the coefficients higher than 10% were measured in spring, when the catchment was highly saturated due to antecedent rainfall and snowmelt. Figure 4 summarizes the monthly precipitation and the variation of the mean runoff coefficient for the study period.

(6) Mean suspended sediment concentration was 6 g l^{-1}, with observed values ranging from 0.02 to 42.6 g l^{-1}. A total of five floods (14.7%) had mean suspended sediment concentration greater than 10 g l^{-1}. Maximum flood sediment concentrations varied from 0.09 to 89.2 g l^{-1}; eight floods (23.5%) showed maximum concentrations greater than 50 g l^{-1}.

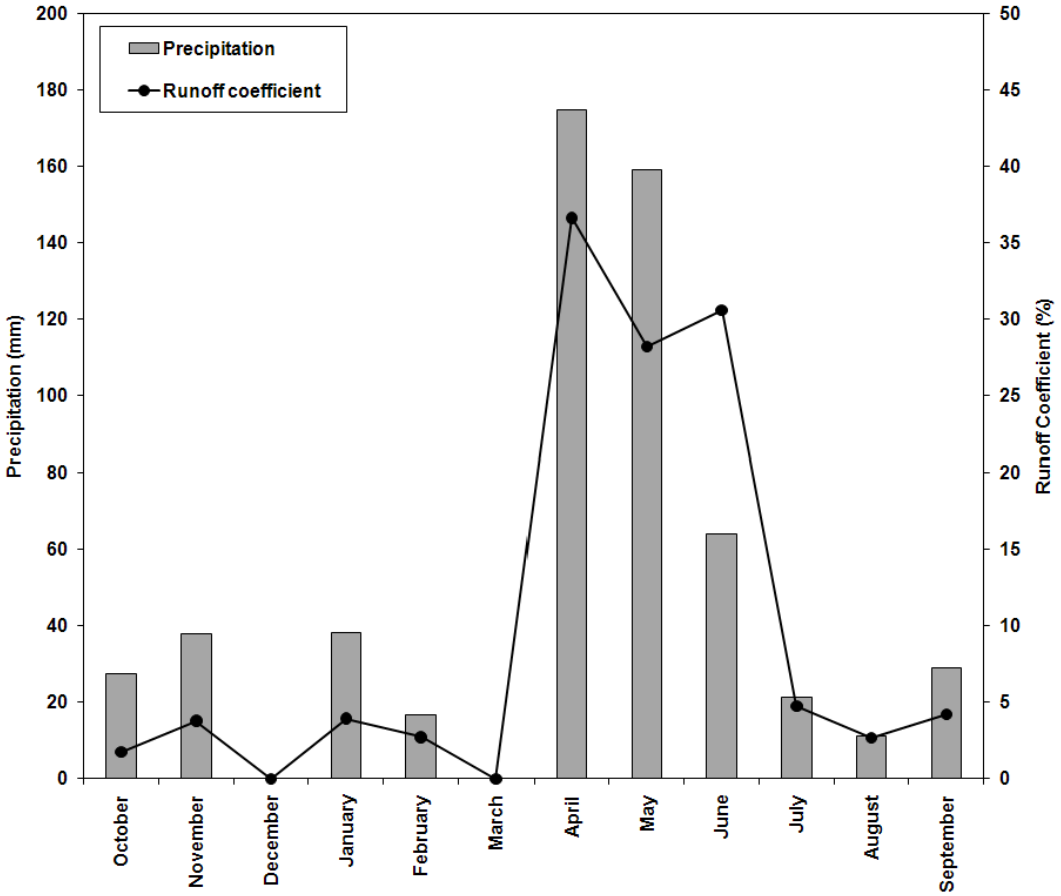

Figure 4. Monthly total precipitation and mean runoff coefficient for the study period in the Isábena catchment.

(7) The total suspended sediment load carried by 21 floods (61.8%) exceeded 1,000 t (representing a specific suspended sediment yield of 2.25 t km^{-2}), while 5 of them (14.7%) transported more than 10,000 t (i.e. 22.5 t km^{-2}). The maximum load during a single flood occurred the 8th of April 2008 and attained 54,000 t (i.e. 121 t km^{-2}). The load of this flood represented 25% of the total annual load and was generated by the second highest precipitation recorded during the study period (*Ptot* = 60 mm), creating a flood peak discharge of 32 m^3 s^{-1} and a total flood runoff volume of 3 hm^3. Floods

carried a total of 220,000 t during the study year; (this compares with the average for the period May 05-May 08 of around 180,000 t, López-Tarazón et al., 2009). These values illustrates the degree of geomorphic activity of the system and confirm the high sediment contribution and transport capacity of the River Isábena, mostly related to the availability of fine materials in the badland areas and its accumulations along the main channel (for more details and insights into these processes, see López-Tarazón et al., 2009).

Table 2. Detailed description of the floods analysed in the paper (see Table 1 for abbreviations and units of the variables). Bold values are maximum values of each variable while italics indicate the minimum values.

Flood event	Dur	Ptot	Imax15	Imax30	EcI30	P1d	P7d	Tr	Qp	Qm	Qb	RC	SSCmean	SSCmax	TL
04/10/2007	309	14.68	18.08	12.08	171.22	9.04	11.23	*0.05*	3.61	1.42	*0.49*	0.54	0.55	1.62	39
05/10/2007	274	4.11	6.44	3.92	5.57	14.68	24.13	*0.05*	6.32	2.17	0.70	1.88	24.06	56.85	1441
08/10/2007	69	8.56	16.30	11.68	54.87	0.05	26.30	0.06	5.70	2.32	0.63	1.24	9.65	16.97	691
21/11/2007	2470	37.80	6.15	5.15	50.89	1.45	1.52	0.64	8.43	3.88	0.56	3.24	6.48	54.74	6897
03/01/2008	1224	18.87	5.34	4.89	26.48	2.09	2.11	0.10	2.79	1.26	0.56	0.66	4.39	8.66	437
11/01/2008	1358	10.73	4.66	3.97	18.03	0.71	13.41	0.28	5.40	1.89	0.70	3.66	9.49	58.89	3049
16/01/2008	1264	8.59	4.10	3.09	5.32	1.32	13.56	0.18	1.65	1.14	0.87	1.14	2.11	9.54	391
04/02/2008	699	16.81	5.83	4.12	38.78	0.06	0.09	0.20	9.22	4.11	0.63	2.30	**42.59**	**89.18**	8987
08/04/2008	3887	60.04	12.37	9.20	128.97	0.63	5.52	3.10	31.59	13.93	2.25	9.71	13.73	63.88	**54001**
10/04/2008	1338	25.14	10.70	6.81	61.12	17.16	60.67	4.96	53.01	30.48	**19.22**	16.39	4.40	14.45	25318
17/04/2008	3046	48.54	9.34	7.30	103.93	0.02	30.71	5.34	67.96	24.92	6.64	18.13	2.98	24.23	30739
19/04/2008	2923	41.10	8.43	6.22	55.70	11.80	55.48	12.05	**78.74**	**34.60**	17.95	31.71	1.26	7.33	23332
07/05/2008	505	6.36	9.61	6.97	15.21	1.56	2.41	0.98	9.22	7.44	5.70	8.12	0.06	0.20	63
10/05/2008	2628	13.95	3.48	2.92	7.84	6.51	14.66	1.13	6.98	6.34	5.40	2.69	*0.02*	*0.09*	*27*
13/05/2008	1922	10.02	10.30	6.36	20.97	1.07	27.81	0.94	7.68	6.66	5.40	4.00	0.08	0.25	80
14/05/2008	916	21.84	9.26	6.49	30.38	2.18	32.03	2.24	18.58	14.28	6.32	12.83	1.08	3.89	2562
16/05/2008	1590	23.04	13.95	8.75	50.02	5.52	49.38	2.82	32.50	23.20	13.90	11.02	1.41	6.58	4654
17/05/2008	523	11.27	19.49	13.10	166.98	**18.96**	**64.27**	1.20	35.32	22.36	18.58	4.25	3.61	9.69	4621
23/05/2008	**7527**	**72.70**	23.15	**15.52**	**307.59**	7.51	48.89	**15.81**	72.45	31.54	10.06	**33.29**	1.56	10.06	31070
01/06/2008	1412	9.97	9.26	6.38	20.83	5.31	46.30	0.89	31.59	21.86	17.95	3.58	3.50	9.58	3348
02/06/2008	994	15.28	24.59	14.39	148.56	6.19	23.78	2.13	42.49	21.68	17.33	6.29	1.72	14.35	4425
03/06/2008	138	3.01	4.88	3.44	10.18	14.76	31.85	0.85	22.67	18.92	17.95	3.31	1.30	4.51	1108
09/06/2008	717	11.22	9.86	7.06	21.27	*0.00*	20.53	0.78	14.99	10.57	9.22	1.99	1.25	3.49	1014
10/06/2008	1646	9.39	7.32	5.43	20.57	11.58	16.65	2.89	17.33	11.21	9.22	12.26	0.90	6.60	2934
17/06/2008	217	3.00	9.37	4.92	7.38	4.01	15.83	0.10	8.82	8.14	7.32	0.77	1.12	2.44	112
27/06/2008	385	12.32	20.26	11.00	77.02	*0.00*	*0.00*	0.39	10.95	4.72	2.79	2.91	6.46	23.12	2731
01/07/2008	55	6.07	8.98	6.31	23.85	0.03	12.69	0.08	2.98	2.77	2.42	0.39	0.83	1.71	72
03/07/2008	294	7.86	15.12	13.14	146.42	0.25	11.49	0.34	6.64	3.73	2.42	3.41	1.26	2.19	452
12/07/2008	216	7.53	14.78	7.43	34.08	*0.00*	0.38	*0.05*	3.84	3.08	2.42	*0.32*	1.30	2.22	64
14/08/2008	1190	11.18	15.44	9.40	29.78	*0.00*	0.36	0.13	1.79	*0.82*	0.63	0.65	1.37	4.65	188
01/09/2009	*42*	*1.79*	*3.35*	*2.32*	*3.64*	0.11	1.71	0.06	4.08	1.10	*0.49*	4.20	4.54	8.62	227
11/09/2008	1182	11.36	19.46	10.90	43.79	*0.00*	13.16	0.14	11.88	1.40	*0.49*	1.76	6.11	57.42	1702
18/09/2008	460	12.64	**27.92**	15.46	95.12	*0.00*	11.47	0.17	8.82	2.72	0.63	2.35	19.42	58.50	3180
19/09/2008	55	3.10	10.28	5.11	11.77	12.64	20.08	*0.05*	*1.52*	1.00	0.78	0.75	23.45	57.42	1168
Average	1279	17.06	11.70	7.68	59.24	4.62	20.90	1.80	19.05	10.23	6.14	6.23	6.00	20.41	6504
SD[a]	1473	16.52	6.41	3.75	66.01	5.79	18.52	3.40	21.33	10.28	6.58	8.13	9.06	24.72	12095

[a] Standard Deviation

4.2. Relations between Rainfall and Runoff

Almost all the hydrological variables (*Tr*, *Qp*, *Qm* and *RC*) showed significant correlations ($p<0.01$, Table 3a) with the total precipitation (*Ptot*). No statistically

significant relations were found between the whole of the runoff related variables and the rainfall intensity factors (*Imax15* and *Imax 30*), whereas the hydrological response was strongly correlated with the antecedent precipitation, especially *P7d*, showing all the hydrological variables significant correlations with this variable. This behaviour indicates that the total amount of precipitation and the antecedent moisture conditions have an important role in determining the hydrological response of the catchment.

Table 3b shows the multiple regression equations derived in each case after the Pearson correlation analysis. These equations are presented here in a descriptive form as least squares fitted to the catchment data, and their use and interpretation should not be extended beyond the data limits from which they were derived. The multiple correlation coefficients perform around 0.8. The relative importance of the rainfall variables controlling the runoff response that were subsequently included in the modelled equations confirm the results obtained in the Pearson correlation analysis and can be summarised as follows:

(1) The hydrological response (with the exception of *Tr* and *RC*, where the main controlling variable was the duration of the flood and the total precipitation, respectively) was mostly explained by the precipitation of the 7 previous days. β coefficients of *P7d* varied from 0.36 to 0.81, a range that indicates that antecedent precipitation plays a distinct role over the different variables that form the hydrological response. As it was pointed out by the linear regression analyses, antecedent precipitation was more significant in relation to the baseflow observed at the beginning of the floods and in relation to the average discharge of the events.

(2) *Qp*, *Qm* and *RC* were significantly correlated with the total precipitation (*Ptot*), with β coefficients of 0.56, 0.38 and 0.64 respectively, showing also a positive correlation. Finally, *Tr* was influenced by the duration of the event (β = 0.71), but to a lower degree, since their equation coefficient was really small (0.002). This shows that total precipitation (including its duration), in addition to the antecedent wet conditions of the basin, controls the runoff response of the catchment to a given rainfall event.

Table 3. a) Pearson correlation matrix between rainfall and runoff variables (*n*=34); b) Equations of the rainfall-runoff relations after the application of the backward stepwise multiple regression, together with the β coefficients (see Table 1 for abbreviations).

a)

	Ptot	***Dur***	***Imax15***	***Imax30***	***EcI30***	***P1d***	***P7d***	***Tr***	***Qp***	***Qm***	***Qb***	***RC***
Ptot	1											
Dur	**0.89**	1										
Imax15	0.18	0.10	1									
Imax30	0.28	0.19	**0.96**	1								
EcI30	**0.63**	**0.56**	**0.69**	**0.80**	1							
P1d	-0.01	0.03	-0.03	-0.04	0.14	1						
P7d	0.28	0.30	0.14	0.19	0.14	**0.66**	1					
Tr	**0.79**	**0.82**	0.18	0.25	**0.57**	0.29	**0.57**	1				
Qp	**0.72**	**0.65**	0.21	0.28	**0.53**	0.38	**0.73**	**0.87**	1			
Qm	**0.58**	**0.54**	0.15	0.21	*0.43*	**0.50**	**0.83**	**0.78**	**0.94**	1		
Qb	0.16	0.18	0.09	0.11	0.19	**0.62**	**0.81**	**0.46**	**0.70**	**0.87**	1	
RC	**0.76**	**0.75**	0.11	0.19	**0.48**	0.28	**0.59**	**0.96**	**0.89**	**0.81**	**0.49**	1

Correlation is significant at the 0.01 level for bold numbers and 0.05 for italics.

b)

Equations	**β coefficients**				
Tr = -1.663 + 0.002*Dur* + 0.065*P7d*					
Qp = -6.969 + 0.725*Ptot* + 0.653*P7d*		*Tr*	*Qp*	*Qm*	*Qb*	*RC*
Qm = -2.173 + 0.235*Ptot* + 0.402*P7d*	*Dur*	0.712	------	------	------	------
Qb = 0.110 + 0.288*P7d*	*Ptot*	------	0.562	0.377	------	0.644
RC = -2.886 + 0.317 *Ptot* +0.178*P7d*	*P7d*	0.355	0.567	0.724	0.811	0.404

Table 4. a) Pearson correlation matrix between rainfall and suspended sediment transport variables (*n*=34); b) Equations of the rainfall-suspended sediment transport relations after the application of the backward stepwise multiple regression, together with the β coefficients (see Table 1 for abbreviations).

a)

	Ptot	***Dur***	***Imax15***	***Imax30***	***EcI30***	***P1d***	***P7d***	***TL***	***SSCmean***	***SSCmax***
Ptot	1									
Dur	**0.89**	1								
Imax15	0.18	0.10	1							
Imax30	0.28	0.19	**0.96**	1						
EcI30	**0.63**	**0.56**	**0.69**	**0.80**	1					
P1d	-0.01	0.03	-0.03	-0.04	0.14	1				
P7d	0.28	0.30	0.14	0.19	0.14	**0.66**	1			
TL	**0.87**	**0.71**	0.10	0.18	**0.49**	0.10	0.29	1		
SSCmean	-0.04	-0.15	-0.04	-0.11	-0.09	0.00	-0.22	0.10	1	
SSCmax	0.16	0.04	0.02	-0.03	-0.02	-0.11	-0.26	0.27	**0.86**	1

Correlation is significant at the 0.01 level for bold numbers.

b)

Equations	**β coefficients**			
		TL	*SSCmax*	*SSCmean*
TL = -4381.76 + 638.25*Ptot*	*Dur*	------	------	------
SSCmax = No regression	*Ptot*	0.872	------	------
SSCmean = No regression	*P7d*	------	------	------

(3) Surprisingly, rainfall intensity does not exert a major influence on any of the measured hydrology variables, indicating that, in the Isábena, the runoff generation and the overall hydrological response do not depend of the amount of rain falling per unit time. Bearing this in mind, the runoff generation in the Isábena basin for the study period seems to be better explained by the Dunne's theory, a theory that relates hydrological response with antecedent conditions and total precipitation (Dunne and Black, 1970) rather than to the rainfall intensity as indicated by the Horton's theory (Horton, 1933).

4.3. Relations between Rainfall and Sediment Transport

Table 4 summarizes the rainfall-suspended sediment transport relations. No significant relations were found between the peak and the average suspended sediment concentration and any of the rainfall variables, suggesting that there are other factors controlling the basin's instantaneous sedimentary response (i.e., sediment availability). As in the rainfall-runoff response, the total suspended load of the floods (*TL*) was correlated significantly with the total amount of precipitation (*Ptot*) and the duration of the rainfall event (*Dur*), while the erosivity index *EcI30* showed a much lower degree of correlation (Table 4a). The high correlation founded between *TL* and *Ptot* raises two interesting issues: a) the role of distant badland areas on the instantaneous river's sediment load at the catchment outlet; hypothetically, not all the sediment eroded by a given rainfall is exported out of the badland area and so, at least partly, is made available to the next rainfall event until the system become exhausted; and b) the role of the accumulated fines in the main channel that to reach the catchment outlet need to be entrained and removed not only by a single flood but by a succession of floods. This is illustrated in Figure 5, for the 34 floods that occurred during the study period. The figure shows the difference in magnitude between the spring floods and the floods of the rest of the year, a difference that suggests two important processes: first, that flood succession (i.e., eighteen were recorded during spring) generates the highest sediment loads, creating an exhaustion effect for the subsequent floods and seasons (see Figure 5); and second, the highest loads are produced, to a great extend, by highest runoff volumes. This latter indicates that such events are the only ones capable of entraining and resuspending the large amounts of sediment previously accumulated in the channel,

supplied from the badlands to the system through small events that not reach the basin outlet.

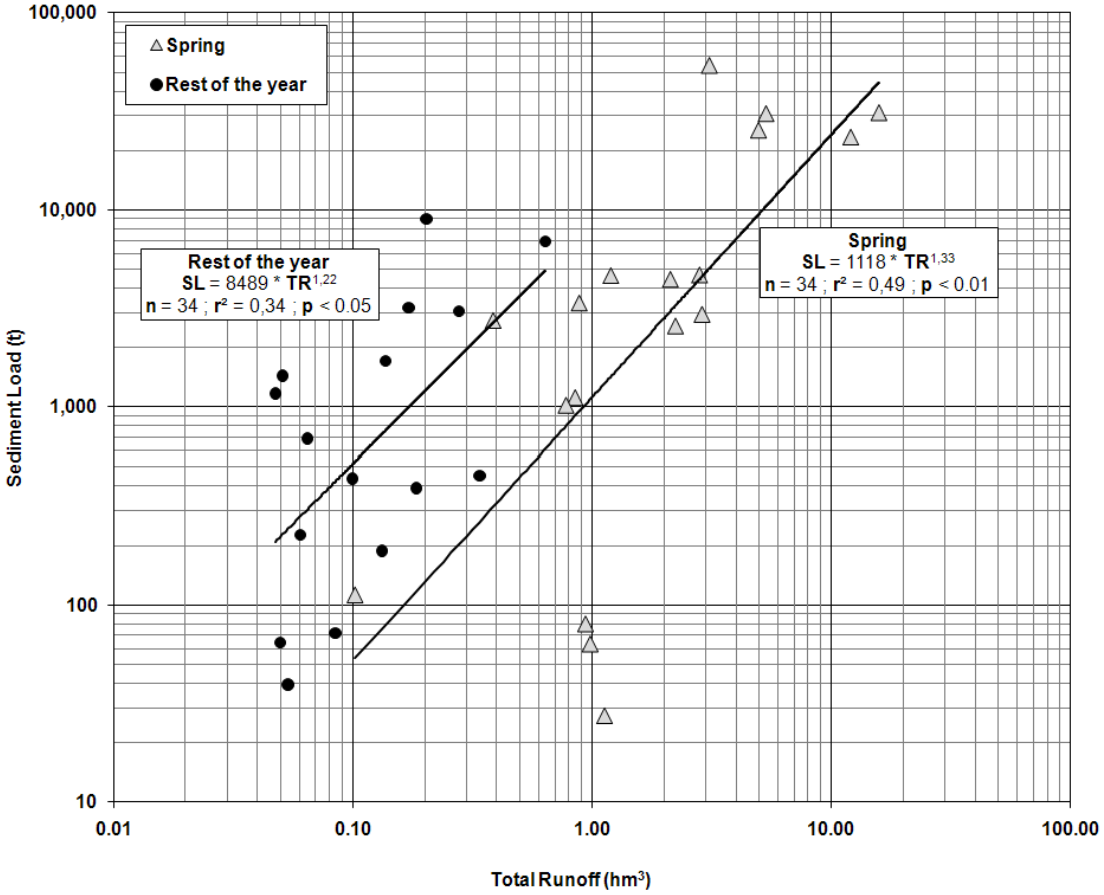

Figure 5. Scatter plot of the relation between total runoff and total suspended sediment load for the 34 studied floods. Note the differences on magnitude between the spring floods and the floods of the rest of the year; highest runoff and sediment loads were observed during that season.

In addition, the stepwise multiple regression analysis (Table 4b) shows that the total sediment load of the floods was controlled mainly by the total amount of precipitation of the individual events ($\beta = 0.87$, with an adjusted multiple correlation coefficient of $r^2 = 0.75$). As with the results from the Pearson correlation analysis, the variables associated with the suspended sediment concentration were not correlated at all with any of the rainfall variables. Table 5 shows the Pearson correlation matrix for the hydrologic and suspended sediment variables. The main hydrologic variables (*Tr*, *Qp*, *Qm* and *RC*) were correlated significantly with the total sediment load ($r^2 = 0.65$, 0.71, 0.59 and 0.67, respectively). However, there was no significant correlation between the

suspended sediment concentrations (*SSCmax* and *SSCmean*) and the rest of hydrological and sedimentary variables; this indicates the variety of the hydrosedimentary responses in the Isábena, a catchment in which small floods can create high suspended sediment concentrations (but not necessarily high loads) owing to the relative position of the sediment in the channel in relation to the measuring point at the catchment outlet. In contrast, largest floods may not attain high concentrations but carry large sediment loads due to the high runoff generated in the catchment and the flood duration.

Table 5. Pearson correlation matrix between runoff and suspended sediment transport variables (*n*=34) (see Table 1 for abbreviations).

	Tr	***Qp***	***Qm***	***Qb***	***RC***	***TL***	***SSCmean***	***SSCmax***
Tr	1							
Qp	**0.87**	1						
Qm	**0.78**	**0.94**	1					
Qb	**0.46**	**0.70**	**0.87**	1				
RC	**0.96**	**0.89**	**0.81**	**0.49**	1			
TL	**0.65**	**0.71**	**0.59**	0.22	**0.67**	1		
SSCmean	-0.19	-0.19	-0.28	-0.36	-0.20	0.10	1	
SSCmax	-0.14	-0.11	-0.25	-0.40	-0.14	0.27	**0.86**	1

Correlation is significant at the 0.01 level for bold numbers.

Most part of the rainfall energy remains in the catchment and is dissipated on hillslope erosion (e.g., particle detachment in bare areas); only a small part is transformed to energy available for the transport of sediment in the drainage network (see Table 6). The total rainfall energy associated with storm events occurred in the catchment during this relatively average hydrological year was 6.7×10^6 MJ; just an average 2% of this energy input (ranging from 0.04% to a maximum of 6%) is transformed to stream power (equating a total of 0.7×10^6 W) in the outlet of the basin, and subsequently made available to the channels to entrain and carry the sediment load. The annual sediment load attains 220,000 tones (i.e., 500 t km^{-2}); if the majority of the sediment is originated at the badlands (as on-going research in the area suggests us), this source areas represent less than 1% of the total basin area.

Altogether, the Isábena illustrates how a small proportion of the rainfall energy and the catchment area are sufficient to supply and transport a vast suspended sediment load. Our results help establish quantitative relations between energy input, energy expenditure and resulting geomorphic work (expressed as sediment transport) in a

relatively large river basin, not usually seen in the literature. It is also an insight into the amount of energy needed to rapidly denude a catchment that can be taken as an exponent of intense landscape instability.

Table 6. Description of the Kinetic Energy and Stream Power resulting from the selected floods (see Table 1 for abbreviations).

Flood event	Qm[a] ($m^3 s^{-1}$)	Dur[b] (s)	KE[c] (MJ)	Ω[d] ($W m^{-1}$)	Ωw[e] (W)	Ωw (MJ)	$\Omega w/KE$ (%)
04/10/2007	1.42	37,800	278,779	127	2,916	110	0.04
05/10/2007	2.17	23,400	41,256	194	4,456	104	0.25
08/10/2007	2.32	27,900	116,804	207	4,764	133	0.11
21/11/2007	3.88	163,800	388,725	346	7,967	1,305	0.34
03/01/2008	1.26	79,200	187,287	112	2,587	205	0.11
11/01/2008	1.89	146,700	123,706	169	3,881	569	0.46
16/01/2008	1.14	162,000	76,335	102	2,341	379	0.50
04/02/2008	4.11	49,500	199,494	367	8,439	418	0.21
08/04/2008	13.93	222,300	598,191	1,244	28,602	6,358	1.06
10/04/2008	30.48	162,900	258,745	2,721	62,583	10,195	3.94
17/04/2008	24.92	214,200	532,745	2,225	51,167	10,960	2.06
19/04/2008	34.60	348,300	399,125	3,089	71,042	24,744	6.20
07/05/2008	7.44	132,300	69,927	664	15,276	2,021	2.89
10/05/2008	6.34	178,200	116,007	566	13,017	2,320	2.00
13/05/2008	6.66	141,300	112,981	595	13,675	1,932	1.71
14/05/2008	14.28	156,600	228,022	1,275	29,320	4,592	2.01
16/05/2008	23.20	121,500	245,992	2,071	47,635	5,788	2.35
17/05/2008	22.36	53,100	204,144	1,996	45,910	2,438	1.19
23/05/2008	31.54	501,300	846,617	2,816	64,759	32,464	3.83
01/06/2008	21.86	40,500	100,214	1,951	44,884	1,818	1.81
02/06/2008	21.68	98,100	203,868	1,935	44,514	4,367	2.14
03/06/2008	18.92	45,000	42,279	1,689	38,847	1,748	4.13
09/06/2008	10.57	73,800	129,353	944	21,703	1,602	1.24
10/06/2008	11.21	257,400	108,838	1,001	23,017	5,925	5.44
17/06/2008	8.14	12,600	42,137	727	16,713	211	0.50
27/06/2008	4.72	81,900	181,053	421	9,691	794	0.44
01/07/2008	2.77	30,600	78,716	247	5,687	174	0.22
03/07/2008	3.73	90,900	144,532	333	7,659	696	0.48
12/07/2008	3.08	16,200	117,974	275	6,324	102	0.09
14/08/2008	0.82	162,000	133,456	73	1,684	273	0.20
01/09/2009	1.10	54,900	22,869	98	2,259	124	0.54
11/09/2008	1.40	98,100	149,400	125	2,875	282	0.19
18/09/2008	2.72	63,000	206,760	243	5,585	352	0.17
19/09/2008	1.00	47,700	46,289	89	2,053	98	0.21

[a] Flood mean discharge
[b] Total flood duration
[c] Rainfall kinetic energy (calculated with the same equations used for the *EcI30*)
[d] Stream power per unit channel width
[e] Total stream power

4.4. Assessing the linearity of the relations between Rainfall, Runoff and Sediment Transport

Our hypothesis is that relations between rainfall, runoff and suspended sediment transport are non-linear. To test this, we selected events (one per season) generated by similar precipitation but yielding a very different runoff and sediment transport

responses (events were on: 04/10/2007, 04/02/2008, 02/06/2008 and 18/09/2008; Fig. 6). Total precipitation (*Ptot*) varied between 12.6 mm and 16.8 mm (Table 7 displays a summary of the key data).

Table 7. Main hydrological and sedimentary characteristics of the selected flood events (see Table 1 for abbreviations).

Flood event	*Ptot* (mm)	*P7d* (mm)	*Imax30* (mm h^{-1})	*Qb* (m^3 s^{-1})	*Qm* (m^3 s^{-1})	*Qp* (m^3 s^{-1})	*RC* (%)	*Tr* (hm^3)	*SSCmean* (g l^{-1})	*SSCmax* (g l^{-1})	*TL* (t)
04/10/2007	14.68	11.23	12.08	0.49	1.42	3.61	0.54	0.05	0.55	1.62	39
04/02/2008	16.81	0.09	4.12	0.63	4.11	9.22	2.30	0.20	42.59	89.18	8987
02/06/2008	15.28	23.78	14.39	17.33	21.68	42.49	6.29	2.13	1.72	14.35	4425
18/09/2008	12.64	11.47	15.46	0.63	2.72	8.82	2.35	0.17	19.42	58.50	3180

Runoff Coefficient (*RC*) fluctuated considerably between events (from 0.54 to 6.29 %), highlighting the importance of antecedent conditions in the basin. Under dry conditions (*Qb* < 0.63 m^3 s^{-1} and *P7d* < 12 mm, e.g., 04/10/2007, 04/02/2008 and 18/09/2008) almost all the rainfall infiltrated and the runoff generation was very small (*Qp* between 3.61 and 9.22 m^3 s^{-1}, *Tr* between 0.05 and 0.20 hm^3 and *RC* between 0.54 and 2.35 %). Under wetter conditions (*Qb* > 17 m^3 s^{-1} and *P7d* > 23 mm, e.g., 02/06/2008) a high part of the precipitation (> 6%) generated runoff and thus contributed to erosion and sediment transport in the downstream channel (Fig. 6). Consequently, non-linear relations between rainfall and the catchment's sedimentary response can be established: the largest but less intense rainfall event (04/02/2008, *Ptot* = 16.8 mm, *Imax30* = 4.1 mm h^{-1}) generated the highest *SSCmean*, *SSCmax* and *TL*, while the smallest but most intense event (18/09/2008, *Ptot* = 12.6 mm, *Imax30* = 15.5 mm h^{-1}) produced a less intense response in terms of *SSCmax* and *SSCmean* (Table 7). This phenomenon may be discussed in relation to two main causes. First, under dry conditions (e.g., 18/09/2008) runoff took place on scattered impervious badlands and rocky areas, being most probably the only active runoff process in response to an intense storm (the highest precipitation and intensity values were recorded in P010, the rain gauge located closest to the badlands). The shape of the falling limb of the hydrograph (characterised by steps, not a smooth regular drop, Fig. 6d), the high suspended sediment concentrations associated with these conditions and the delay of the sedigraph in relation to the hydrograph, emphasise the predominance of this runoff generation and sediment delivery process, especially controlled by sediment contribution from badland areas

during this type of flood event (see badlands location in Fig. 1b). Second, the availability of fine sediment in the channel network allow low intensive rainfall events (e.g., 04/02/2008, Fig. 6b) to remove large amounts of fines from the channel, generating high suspended sediment concentrations in the outlet of the basin. This type of phenomenon generally occurred after a relatively long period without storms, within which the channel accumulated sediment.

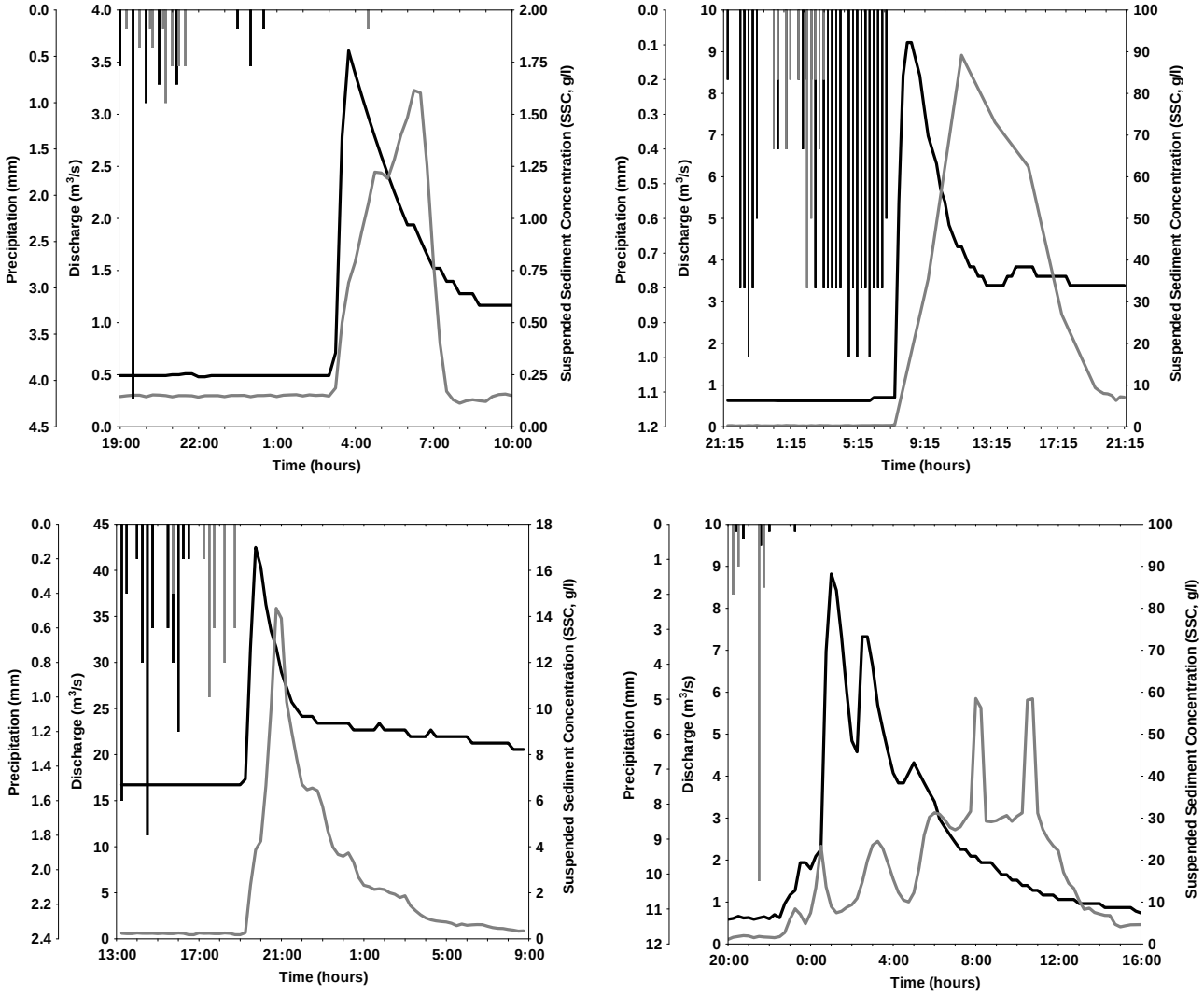

Figure 6. Discharge and suspended sediment concentration of selected floods taken for the linearity analysis: (a) 4th October 2007 (precipitation = 14.68 mm); (b) 4th February 2008 (precipitation = 16.81 mm); (c) 2nd June 2008 (precipitation = 15.28 mm); (d) 18th September 2008 (precipitation = 12.64 mm). In all cases, the precipitation recorded in P030 (rain gauge located at headwaters, Fig. 1b) and in EA047 (rain gauge located near the outlet, Fig. 1b) has been plotted as an example of the rainfall data of each event.

Such non-linear hydrological responses have been observed and reported in other Mediterranean catchments (e.g., Ceballos and Schnabel, 1998; Cosandey et al., 2005; Latron et al., 2008). As noted by Gan et al. (1997) and Francke et al. (2008a, 2008b), this phenomenon complicates the modelling of the hydrosedimentary of non-humid catchments because of the greater variability of the hydrological processes and the sedimentary responses associated with them.

5. SUMMARY AND CONCLUSIONS

This paper has examined the relations between rainfall, runoff and suspended sediment transport in the River Isábena basin during the hydrologic year 2007-2008. The analysis included an assessment of the linearity of the relations between the input of rainfall and the hydrological and sedimentary response. This catchment is particularly interesting because the River Isábena drains a region punctuated with areas of highly erodible sediments (i.e., badlands), that occupy a small portion of the basin but are the main sources of sediment (Francke et al, 2008b). This leads the catchment to carry very high suspended sediment loads during most flood events. At the annual scale, less than 2% of the rainfall energy is finally transformed to stream power and used in the drainage network to carry the sediment load (this value is less than 4% if we also consider pre and post-flood periods). Thirty four floods were recorded during the study period, generated from rainfall events that were mostly relatively small in magnitude (e.g., maximum precipitation was 72.7 mm). The hydrological response of the catchment was very variable: runoff coefficients ranged between 0.32% and 33% (just spring showed coefficients higher above 10%). The sedimentary response was also highly variable, with maximum suspended sediment concentrations varying from < 0.1 to 90 g l^{-1} and flood sediment loads varying between 27 and 54,000 t (i.e., 0.06 and 121 t km^{-2}, respectively). Within this context, the main conclusions of the paper can be drawn as follows:

(1) Pearson correlation matrix and backward stepwise multiple regression analysis showed that the hydrological response of the catchment is strongly related to the total amount of precipitation, the duration of the rainfall event and the rainfall of the previous days, especially that of the prior 7 days.

(2) Very low correlation was observed between the rainfall intensity and the selected hydrological variables, indicating that rainfall per unit time has little control on the hydrosedimentary response of the catchment.

(3) Rainfall-sediment transport relations mimic the general relation between rainfall and runoff. Selected sediment variables (especially the total load) are better correlated with the total amount of precipitation and the precipitation of the previous days, although the level of significance is lower in comparison with the hydrological variables. There was no correlation between the intensity of the rainfall and the sediment variables. Results suggest that, apart from the precipitation, factors such as the availability of fine sediment in the badlands and the temporal accumulation of sediment within the channel network influence the river's sedimentary response.

(4) The catchment displays a non-linear response between the input of rainfall and the hydrosedimentary characteristics. A wide range of runoff coefficients has been observed in response to similar amounts of precipitation. Variability can be attributed to the antecedent conditions of the basin, with floods with the highest runoff coefficients responding to the wettest antecedent conditions (in terms of previous precipitation and baseflow). In the case of the suspended sediment, the variability is even more pronounced, with high suspended sediment concentrations and loads that can be generated by either low or high intensity rainfall events.

Acknowledgements

The first author has a grant funded by the Catalan Government and the European Social Fund. Research has been carried out within the framework of the project "Sediment Export from Large Semi-Arid Catchments: Measurements and Modelling (SESAM)", funded by the *Deutsche Forschungsgemeinschaft* (DFG). The authors wish to thank the Ebro Water Authorities for the permission to install our measuring equipment at the Capella gauging station and for providing hydrological data. Authors are indebted to Chris Gibbins who undertook a helpful revision of the paper and the two anonymous referees whose comments greatly improved the manuscript.

REFERENCES

Angulo-Martínez, M., Beguería, S., 2009. Estimating rainfall erosivity from daily precipitation records: A comparison among methods using data from the Ebro basin (NE Spain). *Journal of Hydrology*, **379**(1-2):111-121.

Angulo-Martínez, M., López-Vicente, M., Vicente-Serrano, S.M., Beguería, S., 2009. Mapping rainfall erosivity at a regional scale: a comparison of interpolation methods in the Ebro Basin (NE Spain). *Hydrology and Earth System Sciences*, **13**:1907-1920.

Arnáez, J., Lasanta, T., Ruiz-Flaño, P., Ortigosa, L., 2007. Factors affecting runoff and erosion under simulated rainfall in Mediterranean vineyards. *Soil and Tillage Research*, **93**:324-334.

Àvila, A., 1987. Balanç d'aigua i nutrients en una conca d'alzinar al Montseny. PhD Thesis. Universitat de Barcelona, 173 pp.

Beven, K., 2002. Runoff generation in semi-arid areas. In: Bull, L.J., Kirkby, M.J., (Eds.), *Dryland Rivers*, John Wiley & Sons, Chichester, 57–105.

Brown, L.C., Foster, G.R., 1987. Storm erosivity using idealized intensity distributions. *Transactions of the American Society of Agricultural Engineers*, **30**:379-386.

Cappus P. 1960. Bassin expérimental d'Alrance. Étude des lois de l'écoulement. Application au calcul et à la prévision des débits. *La Houille Blanche* **A**, 493–520.

Ceballos, A., Schnabel, S., 1998. Hydrological behaviour of a small catchment in the dehesa landuse system (Extremadura, SW Spain). *Journal of Hydrology*, **210**:4-14.

Cerdan, O., Le Bissonnais, Y., Govers, G., Lecomte, V., van Oost, K., Couturier, A., King, C., Dubreuil, N., 2004. Scale effect on runoff from experimental plots to catchments in agricultural areas in Normandy. *Journal of Hydrology*, **299**:4–14.

Cosandey, C., Andréassian, V., Martin, C., Didon-Lescot, J.F., Lavabre, J., Folton, N., Mathys, N., Richard, D., 2005. The hydrological impact of the Mediterranean forest: a review of French research. *Journal of Hydrology*, **301**:235-249.

Dunne, T., Black, R.D., 1970. Partial area contributions to storm runoff in a small New England watershed. *Water Resources Research*, **6**(5):1296-1311.

Estrany, J., Garcia, C., Batalla, R.J., 2009. Suspended sediment transport in a small Mediterranean agricultural catchment. *Earth Surface Processes and Landforms*, **34**:929-940.

Francke, T., López-Tarazón, J.A., Schröder, B., 2008a. Estimation of suspended sediment concentration and yield using linear models, random forests and quantile regression forests. *Hydrological Processes*, **22**:4892-4904.

Francke, T., López-Tarazón, J.A., Vericat, D., Bronstert, A., Batalla, R.J., 2008b. Flood-based analysis of high-magnitude sediment transport using a non-parametric method. *Earth Surface Processes and Landforms*, **33**:2064-2077.

Gallart, F., Latron, J., Regüés, D., 1998. Hydrological and sediment processes in the research catchments of Vallcebre (Pyrenees). In: Boardman, J., Favis-Mortlock, D. (Eds.), *Modelling Erosion by Water*, NATO-ASI series 1-55, Springer, Berlin, 503-511.

Gallart, F., Llorens, P., Latron, J., Regüés, D., 2002. Hydrological processes and their seasonal controls in a small Mediterranean mountain catchment in the Pyrenees. *Hydrology and Earth System Sciences*, **6**(3):527-537.

Gallart, F., Llorens, P., 2004. Observations on land cover changes and water resources in the headwaters of the Ebro catchment, Iberian Peninsula. *Physics and Chemistry of the Earth*, **29**:769-773.

Gallart, F., Latron, J., Llorens, P., 2005a. Catchment dynamics in a Mediterranean mountain environment. The Vallcebre research basins (southeastern Pyrenees) I: hydrology. In: García, C., Batalla, R.J. (Eds.), *Catchment Dynamics and River Processes: Mediterranean and Other Climate Regions*. Developments in Earth Surface Processes, Publication 7, Elsevier, Amsterdam, The Nederlands, 1-16.

Gallart, F., Balasch, J.C., Regüés, D., Soler, M., Castelltort, F., 2005b. Catchment dynamics in a Mediterranean mountain environment: the Vallcebre research basins (southeastern Pyrenees). II: Temporal and spatial dynamics of erosion and stream sediment transport. In: García, C., Batalla, R.J. (Eds.), *Catchment Dynamics and River Processes: Mediterranean and Other Climate Regions*. Developments in Earth Surface Processes, Publication 7, Elsevier, Amsterdam, The Nederlands, 17-29.

Gan, T.Y., Dlamini, E.M., Biftu, G.F., 1997. Effects of model complexity and structure, data quality and objective functions on hydrologic modelling. *Journal of Hydrology*, **192**:81-103.

García-Ruiz, J.M., Martí-Bono, C., Arnáez-Vadillo, J., Beguería-Portugués, S., Lorente-Grima, A., Seeger, M., 2000. Las cuencas experimentales de Arnás y San Salvador

en el Pirineo Central Español: escorrentía y transporte de sedimento. *Cuadernos de Investigación Geográfica*, **26**:23-40.

García-Ruiz, J.M., Arnáez, J., Beguería, S., Seeger, M., Martí-Bono, C., Regüés, D., Lana-Renault, N., White, S., 2005. Runoff generation in an intensively disturbed, abandoned farmland catchment, Central Spanish Pyrenees. *Catena*, **59**:79-92.

Gregory, K.J., Walling, D.E., 1973. Drainage Basin Form and Process. A geomorphological approach. Edward Arnold (Publishers) Ltd., London, UK.

Guenni, L., Hutchinson, M.F., 1998. Spatial interpolation of the parameters of a rainfall model from ground based data. *Journal of Hydrology*, **212-213**:335-347.

Hewlett, J.D., Hibbert, A.R., 1967. Factors affecting the response of small watersheds to precipitation in humid areas. In: Sopper, W.E., Lull, H.W., (Eds.), *Forest Hydrology*, Pergamon, Oxford, 275–290.

Hewlett, J.D., Bosch, J.M., 1984. The dependence of storm flows on rainfall intensity and vegetal cover in South Africa. *Journal of Hydrology*, **75**:365–381.

Hewlett, J.D., Fortson, J.C., Cunningham, G.B., 1977. The effect of rainfall intensity on storm flow and peak discharge from forest land. *Water Resources Research*, **13**(2):259–266.

Hewlett, J.D., Fortson, J.C., Cunningham, G.B., 1984. Additional tests on the effect of rainfall intensity on storm flow and peak flow from wild-land basins. *Water Resources Research*, **20**(7):985–989.

Horton, R.E., 1933. The role of infiltration in the hydrologic cycle: EOS, Transactions. *American Geophysical Union*, **14**:446-460.

Latron, J., Gallart, F., 2007. Seasonal dynamics of runoff-contributing areas in a small Mediterranean research catchment (Vallcebre, Eastern Pyrenees). *Journal of Hydrology*, **335**:194-206.

Latron, J., Soler, M., Llorens, P., Gallart, F., 2008. Spatial and temporal variability of the hydrological response in a small Mediterranean research catchment (Vallcebre, Eastern Pyrenees). *Hydrological Processes*, **22**:775-787.

Leopold, L. B., Wolman, M. G., Miller, J.P., 1964. Fluvial Processes in Geomorphology. W.H. Freeman and Company, San Francisco, California, 522 pp.

López-Tarazón, J.A., Batalla, R.J., Vericat, D., Francke, T., 2009. Suspended sediment transport in a highly erodible catchment: The River Isábena (Southern Pyrenees). *Geomorphology*, **109**: 210-221.

Lorente, A., Martí-Bono, C., Beguería, S., Arnáez, J., García-Ruiz, J.M., 2000. La exportación de sedimento en suspensión en una cuenca de campos abandonados. Pirineo Central Español. *Cuaternario y Geomorfología*, **14**(1-2):21-34.

Maidment, D.R., 1993. Handbook of Hydrology. McGraw-Hill, New York.

Mamede, G.L., Bronstert, A., Araújo, J.C., Batalla, R.J., Güntner, A., Francke, T., Müller, E.N., 2006. 1D process-based modelling of reservoir sedimentation: a case reservoir in Spain. *Proceedings of the International Conference on Fluvial Hydraulics (River Flow 2006),* **2**:1585-1594.

Marques, M.J., Bienes, R., Pérez-Rodríguez, R., Jiménez, L., 2008. Soil degradation in Central Spain due to sheet water erosion by low-intensity rainfall events. *Earth Surface Processes and Landforms*, **33**:414-423.

Martínez-Casasnovas, J.A., Ramos, M.C., Ribes-Dasi, M., 2002. Soil erosion caused by extreme rainfall events: mapping and quantification in agricultural plots from very detailed digital elevation models. *Geoderma,* **105**:125-140.

Meade, R.H., Yuzyk, T.R., Day, T.J., 1990. Movement and storage of sediment in rivers of the United States and Canada. In: Wolman, M.G., Riggs, H.C. (Eds.), *Surface Water Hydrology,* The Geology of North America, vol. O-1. Geological Society of America: Boulder, Columbia, United States of America, 255–280.

Nadal-Romero, E., Latron, J., Martí-Bono, C., Regüés, D., 2008. Temporal distribution of suspended sediment transport in a humid Mediterranean badland area: The Araguás catchment, Central Pyrenees. *Geomorphology*, **97**:601-616.

Peters, N.E., Freer, J., Aulenbach, B.T., 2003. Hydrologic dynamics of the Panola Mountain Research Watershed, Georgia, USA. *Ground Water*, **41**(7):973–988.

Piñol, J., Beven, K., Freer, J., 1997. Modelling the hydrological response of Mediterranean catchments, Prades, Catalonia. The use of distributed models as aids to hypothesis formulation. *Hydrological Processes,* **11**:1287-1306.

Ramos, M.C., Martínez-Casasnovas, J.A., 2006. Trends in precipitation concentration and extremes in the Mediterranean Penedès-Anoia region, NE Spain. *Climatic Change*, **74**:457-474.

Ramos, M.C., Martínez-Casasnovas, J.A., 2007. Soil loss and soil water content affected by land leveling in Penedès vineyards, NE Spain. *Catena*, **71**:210-217.

Regüés, D., Gallart, F., 2004. Seasonal patterns of runoff and erosion responses to simulated rainfall in a badland area in Mediterranean mountain conditions

(Vallcebre, south-eastern Pyrenees). *Earth Surface Processes and Landforms*, **29**:755-767.

Regüés, D., Guárdia, R., Gallart, F., 2000. Geomorphic agents versus vegetation spreading as causes of badland occurrence in a Mediterranean subhumid mountainous area. *Catena*, **40**:173 -187.

Seeger, M., Errea, M.P., Beguería, S., Arnáez, J., Martí, C., García-Ruiz, J.M., 2004. Catchment soil moisture and rainfall characteristics as determinant factors for discharge/suspended sediment hysteretic loops in a small headwater catchment in the Spanish Pyrenees. *Journal of Hydrology*, **288**:299-311.

Selby, M.J., 1982. Hillslope materials and processes. Oxford University Press, 264 pp.

Sherman, R.J., Salter, P.M., 1975. An objective rainfall interpolation and mapping technique. *Hydrological Sciences Bulletin*, **20**(3):353-363.

Soil Survey Staff, 1996. Keys to Soil Taxonomy, 7th ed. U.S. Government Printing Office, Washington, DC.

Suprit, K., Shankar, D., 2007. Resolving orographic rainfall on the Indian west coast. *International Journal of Climatology*, **28**(5):643-657.

Tait, A., Henderson, R., Turner, R., Zheng, X., 2006. Thin plate smoothing spline interpolation of daily rainfall for New Zealand using a climatological rainfall surface. *International Journal of Climatology*, **26**(14):2097-2115.

Taylor, C.H., Pearce, A.J., 1982. Storm runoff processes and subcatchment characteristics in a New Zealand hill country catchment. *Earth Surface Processes and Landforms*, **7**:439–447.

Valero-Garcés, B. L., Navas, A., Machín, J., Walling, D., 1999. Sediment sources and siltation in mountain reservoirs: a case study from the Central Spanish Pyrenees. *Geomorphology*, **28**:23–41.

Verdú, J.M., Batalla, R.J., Martínez-Casasnovas, J.A., 2006. Estudio hidrológico de la cuenca del río Isábena (Cuenca del Ebro). I: Variabilidad de la precipitación. *Ingeniería del Agua*, **13**(4):321-330.

Webb, B.W., Foster, I.D.L., Gurnell, A.M., 1995. Hydrology, water quality and sediment behaviour. In: Foster, I., Gurnell, A., Webb, B. (Eds.), *Sediment and Water Quality in River Catchments*. John Wiley and Sons Ltd., Chichester, pp. 1-30.

Wood, P.A., 1977. Controls of variation in suspended sediment concentration in the River Rother, West Sussex, England. *Sedimentology*, **24**:437–445.

Woodruff, J.F., Hewlett, J.D., 1970. Predicting and mapping the average hydrologic response for the Eastern United States. *Water Resources Research*, **6**(5):1312–1326.

Yair, A., Enzel, Y., 1987. The relationships between annual rainfall and sediment yield in arid and semi-arid areas. The case of the Northern Negev. *Catena Supplement*, **10**:121-135.

CHAPTER 5

IN-CHANNEL SEDIMENT STORAGE

INDEX CHAPTER 5: IN-CHANNEL SEDIMENT STORAGE

Figure captions in the paper

Figure 1. (A) Location of the Isábena, Ésera and Cinca basins within the Ebro Basin. (B) Longitudinal profile of the River Isábena with the location of the monitoring sections. (C) Sketched map of the Isábena catchment, showing locations of main badland areas and a zoom to the location of the sampling sections.

Figure 2. Images of the sampling sections: a) S1, b) S2, c) S3 and c) S4. Main geomorphic characteristics of the sites (i.e. gravel-bed channel, bars, etc.) can be seen in the photographs. Photographs were taken mostly during low flows by the first and second authors in July-2007 (S1 and S4), November-2007 (S3) and April-2008 (S2). Arrow indicates flow direction.

Figure 3. Discharge and suspended sediment concentration of the Isábena River measured at the Capella gauging station (EA047; see Fig. 1c for location) over the study period (June 2007 – June 2008). The vertical dashed lines show the dates when the in-channel storage sampling was carried out.

Figure 4. Results obtained from the fine-grained sediment storage measurements at each season and for each sampling section (S1, S2, S3 and S4; see Fig. 1c for specific locations). (A) Results obtained for the first level of agitation (i.e. N1); (B) Results obtained after the second level of agitation (i.e. N2); (C) Average results for both agitation levels (see text for more details). In all cases, the black line represents the average value for all sampling sections and for each season.

Figure 5. Average sediment storage per unit length of channel for each sampling site (S1, S2, S3 and S4) and distance downstream from the first studied section (i.e. presented values for each site are based on the mean of results provided for both levels of agitation).

Figure 6. Comparison of the estimated seasonal sediment storage in the study reach, the sediment storage extrapolated to the whole channel, and the sediment yield and runoff for the study period in the Isábena basin.

Table captions in the paper

Table 1. Average seasonal fine sediment storage in the channel bed for each sampling site in the lower reach of the River Isábena (n = 5 for S1 and S3; n = 3 for S2 and S4; where n is the number of points in each sampling site; see Fig. 1c for location details), as determined by the two levels of bed disturbance (see text for further description).

Table 2. Total storage of fine-grained sediment in the channel bed of the lower part of the River Isábena for each sampling season. Sediment storage (calculated following equation 2) is presented in absolute terms (t) but also relatively to the channel length (t km-1). The maximum discharge registered in each season and its respective return period has been added as a reference of seasonal flood magnitude.

Table 3. Comparison of channel-bed sediment storage estimation in the River Isábena with the suspended sediment yield measured at the basin outlet (Capella gauging station, EA047, see Fig. 1c for location details).

1. INTRODUCTION

This chapter describes the role of in-channel sediment storage as a controller of the suspended sediment transport, acting sometimes as a deposition zone and other times being another sediment source at the outlet of the catchment. For this purpose the methodology developed by Lambert and Walling (1988) was used during different sampling campaigns along a year. The paper is presented maintaining its original structure; its format has been adapted to the general format of the present volume.

Specifically, the paper is accepted (in press, November 2010) to be published in *Zeitschrift für Geomorphologie*. The paper examines the in-channel sediment storage of a ~3-km channel length reach of the River Isábena during an average hydrological year (2007-2008). Total in-channel sediment storage for the study period was estimated at the 3-km sampled to be later extrapolated to the whole main 45 km channel length (related to Objective 4). In-channel storage shows both temporal and spatial trends. Results suggest that the fine-grained sediment stored in the channel may represent an important component of the suspended sediment budget of rivers draining highly erodible materials such as the River Isábena.

2. IN-CHANNEL SEDIMENT STORAGE

López-Tarazón, J.A., Batalla, R.J., Vericat, D., 2010. In-channel sediment storage in a highly erodible catchment: the River Isábena (Ebro Basin, Southern Pyrenees). *Zeitschrift für Geomorphologie* (accepted, in press).

In-channel sediment storage in a highly erodible catchment: the River Isábena (Ebro Basin, Southern Pyrenees)

Abstract

In-channel fine-sediment storage, especially in areas draining highly erodible materials, constitutes an important part of the sediment budget of a drainage basin. This phenomenon occurs when sediment production in the basin is greater than the river's transport capacity, resulting in large accumulations of fines along the river channel. In-channel sediment storage has been studied in a ~3-km channel length reach of the River Isábena during an average hydrological year (2007-2008). The River Isábena drains an area of 445-km^2. It is located at the Southern Pyrenees and the channel network flows through an area of extremely erodible materials producing an enormous amount of suspended sediment. Total in-channel sediment storage for the study period has been estimated at approximately 679 t, which equates to 0.32% of the annual suspended sediment load calculated at the basin's outlet. Sediment storage values obtained in the study reach have been extrapolated to the whole main channel length (45 km), resulting in a total storage of 9,810 t, representing the 4.7% of the annual total load. In-channel storage shows both temporal and spatial trends. In relation to the former, sediment is continuously accumulated during low-flows while the latter shows that sediment accumulation increases in the downstream direction. Results suggest that the fine-grained sediment stored in the channel may represent an important component of the suspended sediment budget of rivers draining highly erodible materials such as the River Isábena.

Keywords: In-channel sediment storage, suspended sediment transport, sediment yield, badlands, River Isábena, Southern Pyrenees, Ebro Basin.

1. INTRODUCTION

The transport of fine sediment in suspension through river systems is commonly an intermittent process, with sediment transfer occurring primarily during flood events. Sediment is often stored in the channel bed and floodplains between transport episodes (Wilson et al., 2004). Storage of fine-grained sediment frequently represents an important component of the sediment budget of a drainage basin and in many cases the quantity of sediment stored in intermediate channel locations can be even larger than the mean sediment export from the basin (e.g., Trimble, 1983; Walling, 1983; Phillips, 1991; Owens et al., 1997). This phenomenon is especially remarkable in areas draining highly erodible materials, whose sediment production is typically greater than the transport capacity of the river, resulting in large accumulations of fines along the main channel and tributaries (e.g., Walling and Amos, 1999; López-Tarazón et al., 2009; López-Tarazón et al., 2010). As a consequence, in-channel sediment storage may complicate the interpretation of downstream sediment yields in terms of sediment source and availability, by attenuating the record of sediment delivery from hillslopes and sediment transfer within the upstream drainage basin (Walling et al., 1998).

Besides the limited information available on in-channel sediment storage and its role in controlling suspended sediment transport in river systems, channel-bed sedimentation warrants investigation for other reasons. Sediment deposition reduces pore water fluxes and the rate of hyporheic exchange (e.g., Wood and Armitage, 1997; Packman and Mackay, 2003) and alters habitat quality and biodiversity; such impacts have been reported for fish spawning by Acornley and Sear (1999), for macroinvertebrates by Quinn et al. (1992) and for macrophyte communities by Clarke and Wharton (2001). In addition, transient sediment accumulations may increase sediment loads during floods, both locally and downstream, therefore changing sediment dynamics (i.e., high-density flows increase flood intensity thus flow competence to entrain and transport larger bed-materials and higher sediment loads) and sediment transport rating curves.

Despite the crucial role of sediment storage for the development of sediment budgets, little attention has been paid to this process in large river basins. Most studies have been developed in small catchments (generally <100 km^2), e.g., Loughran et al. (1992),

Owens et al. (1997), Walling and Amos (1999), Hodgkins et al. (2003), and Smith and Dragovich (2008), but very few have attempted to quantify sediment storage in larger areas (100-10000 km^2). Notable exceptions include Lambert and Walling (1988), Jordan and Slaymaker (1991), Phillips (1991), Meade (1994), Walling et al. (1998) and Collins and Walling (2007).

The main objective of this paper is thus to examine the in-channel sediment storage dynamics and its influence on the suspended sediment load over a hydrologically average year in the River Isábena (NE Iberian Peninsula). The River Isábena drains highly erodible sediments in a mesoscale Mediterranean mountainous catchment located in the Southern Pyrenees and flows into the Barasona Reservoir. The work follows previous papers on sediment transport processes recently published (López-Tarazón et al., 2009; López-Tarazón et al., 2010) and provides relevant information for establishing sediment budgets in drainage basins experiencing intense geomorphic activity.

2. STUDY AREA

2.1. Physical setting

The Isábena is a 445 km^2 catchment located in the NE of the Ebro Basin (Southern Pyrenees), and comprises ca. 0.5% of the Ebro basin total area (Fig. 1a). The River Isábena flows into the Barasona Reservoir together with the River Ésera, both tributaries of the River Cinca, which is the second most important tributary of the Ebro (Fig. 1a). The Isábena basin is not regulated, so its flow regime is natural. Historically, the main channel and some tributaries underwent gravel extraction.

The altitudinal range of the Isábena varies from 650 to more than 2700 m a.s.l. (Fig. 1b). Climatically, the basin belongs to the Mediterranean domain, with notable variations in temperature (i.e., mean temperature of 10ºC in the northern part and 12.5 ºC in the southern zone) and precipitation (i.e., mean annual precipitation of 1600 mm in headwaters and 450 mm in the lower part). Mean annual precipitation in the basin is around 767 mm, with seasonal maxima reached in spring and autumn (López-Tarazón et al., 2009).

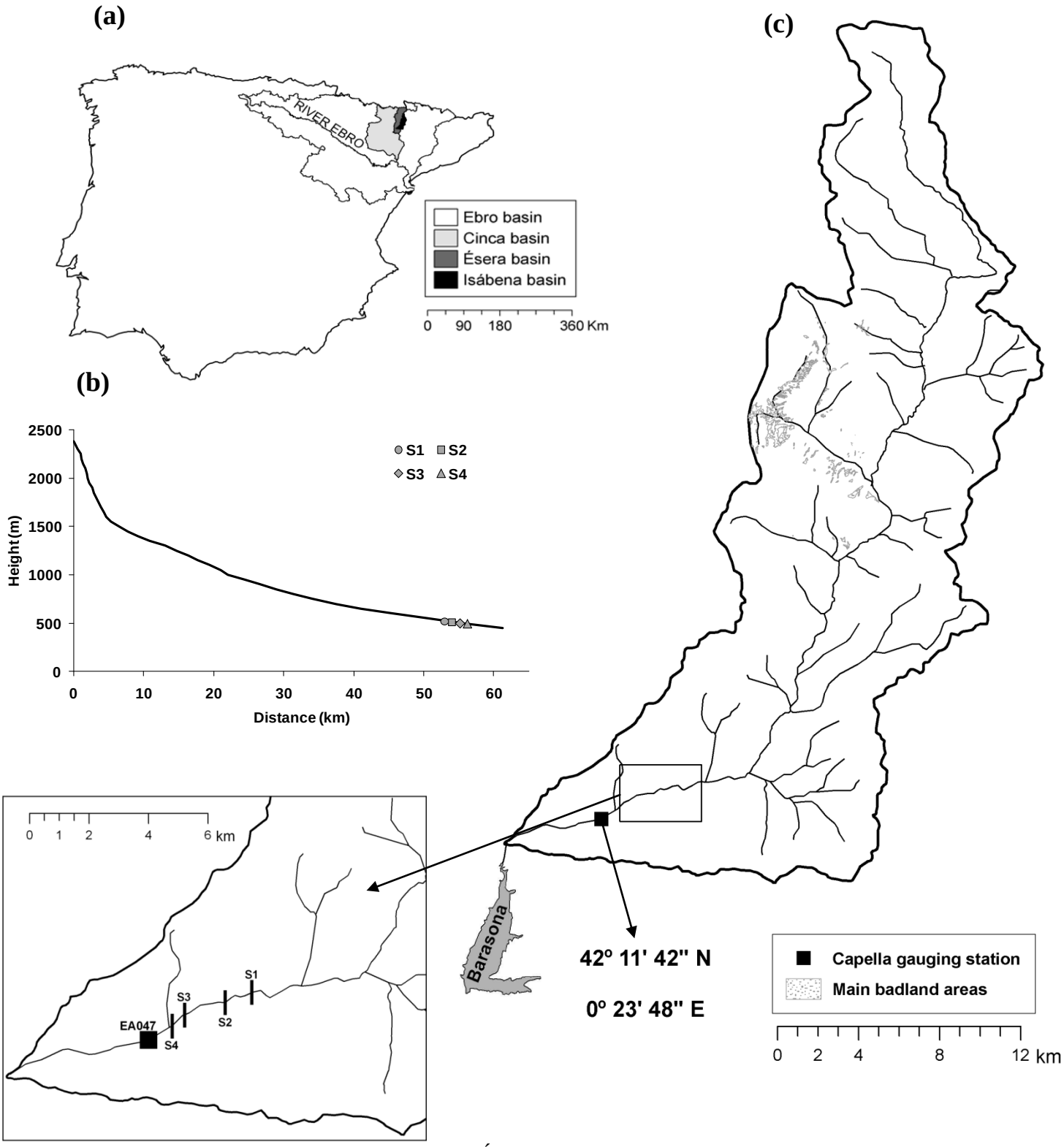

Figure 1. (A) Location of the Isábena, Ésera and Cinca basins within the Ebro Basin. (B) Longitudinal profile of the River Isábena with the location of the monitoring sections. (C) Sketched map of the Isábena catchment, showing locations of main badland areas and a zoom to the location of the sampling sections.

The basin has a nivo-pluvial regime with notable inter and intra-annual variations. Minimum flow during the study period (i.e., 0.20 $m^3 s^{-1}$) occurred in autumn, although the river never dried up. Floods usually occurred during spring (i.e., snowmelt at spring), and especially late summer and autumn (i.e., localized thunderstorms). Although absolute maxima generally occur in autumn, the largest peak ever recorded at the basin outlet took place in summer (August 1963), reaching 370 $m^3 s^{-1}$ (Q_{90}, estimated from the instantaneous maximum discharge series using the Gumbel method for the period 1951-2005, where Q_i is the discharge associated to a *i* return period in years). Mean annual discharge at the Capella gauging station, located at the basin outlet (Fig. 1c) for the entire period of record (1945-2008) is 4.1 $m^3 s^{-1}$ (σ = 2.2 $m^3 s^{-1}$, where σ is the standard deviation of the observations). The mean annual water yield is 177 hm^3 (σ = 92 hm^3), a value that represents ca. the 1.5% of the Ebro basin total runoff.

The Isábena belongs to the Tremp-Graus geological basin. In the headwaters, the river flows through narrow valleys which incise Cretaceous limestones. In the middle reaches, erosion have left the calcareous materials, partially karstified, at the highest levels of the massifs, with Eocene marls presenting badland structures, shaping run-down reliefs (Verdú et al., 2006). These badland areas are the most important source of sediment during storm periods (see locations in Fig. 1c), although encompassing less than the 1% of the entire catchment. In the lower part, the basin is mainly formed by Cretaceous chalks together with Tertiary clay rocks and conglomerates.

2.2. Silting of the Barasona Reservoir

The Barasona Reservoir (Fig. 1c) was built during the 1930s, being later expanded in the 1970s. The reservoir supplies water to the canal of Aragon and Catalunya, which provides irrigation to more than 70,000 ha. Barasona has experienced acute siltation problems since its construction (e.g., Avendaño et al., 1997a; Avendaño et al., 1997b, Navas et al., 1998). The mean load transported by the Isábena to the reservoir has been estimated at around 0.36 $hm^3 yr^{-1}$, a value that represents more than 0.4% of the original reservoir capacity (López-Tarazón et al., 2009) and more than 4% of the total sediment sluiced down during maintenance operations carried out in the 1990s (ca. 9 hm^3: Palau, 1998; Avendaño et al., 2000). The sediment load transported by the River Isábena, in

addition to that transported by the Ésera, explains the historical siltation of the Barasona reservoir.

High sediment loads originate in the badland areas, which are composed mainly of marls that occupy the middles reaches of those two catchments. In the case of the Isábena, the badlands contribute the majority of sediment transported through the drainage network (Francke et al., 2008a, Francke et al., 2008b). Suspended sediment concentrations span five orders of magnitude, occasionally attaining instantaneous values in excess of 300 g l^{-1} at the Capella gauging station (López-Tarazón et al., 2009).

3. METHODS

3.1. In-channel storage

The amount of fine sediment stored in the channel bed of the Isábena was determined using the method developed by Lambert and Walling (1988). Field data provides information on the amount of sediment stored on the bed of the channel at specific sites that can be subsequently extrapolated to hydraulically and morphologically equivalent areas. Sediment storage is commonly temporarily and spatially variable, and may be remobilised during high flow periods. In this study, we obtained sediment storage data over a one year period (2007-2008) which allowed comparison with measurements of sediment exports from the catchment.

The sampling of sediment storage was done at four different cross-sections located in the lower part of the basin (between 1 and 4 km upstream from the Capella gauging station, see locations in Fig. 1b). Monitoring sections were selected based on i) their location downstream from the main tributaries to include the total discharge and sediment transport from the basin and ii) their representativeness of the morphological characteristics of the lower Isábena mainstem channel (i.e., riffle-pool system in typical low gradient gravel-bed river). In summary, sections 1 (S1) and 4 (S4) represent multichannel reaches, with point and central bars, while sections 2 (S2) and 3 (S3) are mostly plain-bed reaches flanked by alternative gravel bars (see plates in Fig. 2).

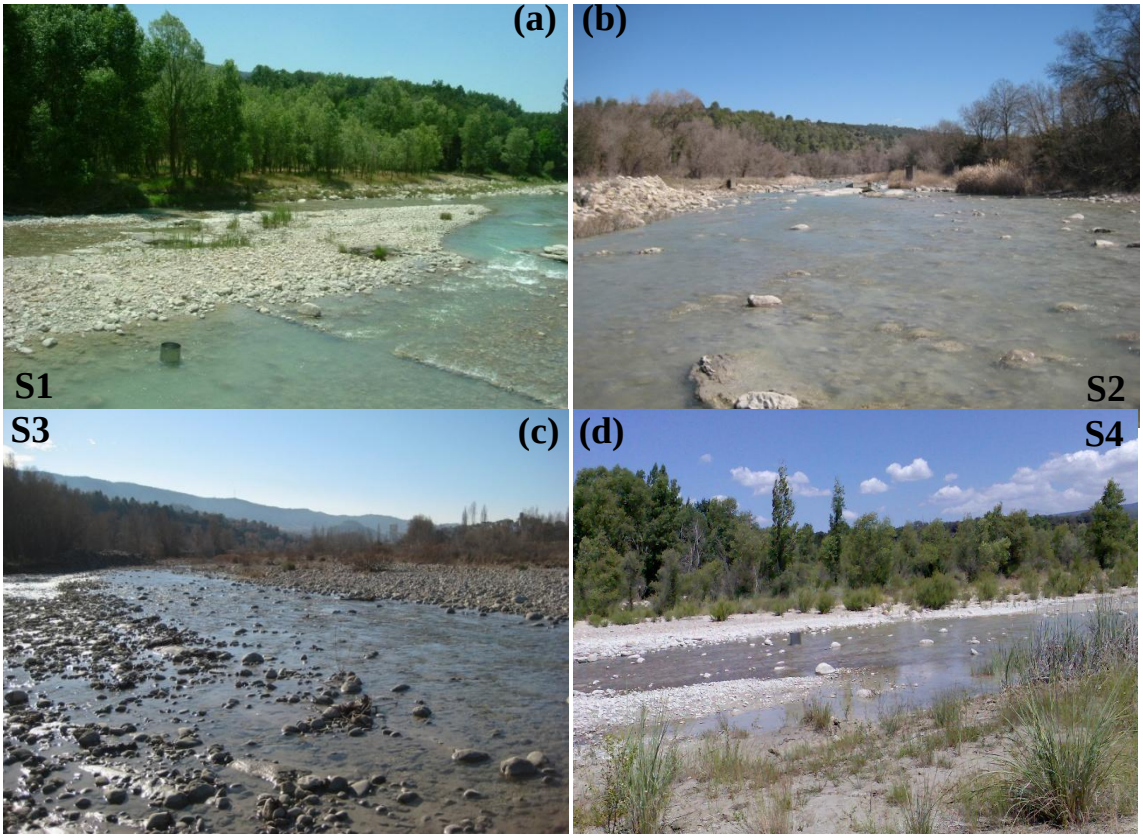

Figure 2. Images of the sampling sections: a) S1, b) S2, c) S3 and c) S4. Main geomorphic characteristics of the sites (i.e. gravel-bed channel, bars, etc.) can be seen in the photographs. Photographs were taken mostly during low flows by the first and second authors in July-2007 (S1 and S4), November-2007 (S3) and April-2008 (S2). Arrow indicates flow direction.

The sampling methodology is as follows: a metal cylinder (diameter of 0.25 m, surface area 0.20 m^2, and height 0.6 m) was carefully lowered into the water until it rested on the channel bed (avoiding disturbance of the fine sediment) and then slowly rotated to create a seal with the gravels, thereby establishing the exact bed area to be sampled. Next, the channel bed was manually disturbed (i.e., using a rod), in order to re-suspend the fine sediment and, thus, estimate the sediment storage. The disturbance was done following two consecutive steps:

a) first, only the water column contained in the cylinder was agitated to re-suspend just the sediment stored on the surface of the bed (i.e., level of agitation: N1).

b) second, the top 10 cm of bed (i.e., gravel coarse surface layer D_{50}=54 mm, D_{90}= 125 mm) was vigorously agitated to re-suspend both the remaining fine sediment on the bed surface together with the fines contained in the upper bed sediment matrix (i.e., level of agitation: N2). Although the surface of the bed was vigorously agitated

during this procedure, special attention was given to avoid the agitation of the subsurface material. 1-liter replicated samples of water and suspended sediment were taken for each of the two steps. Apart from these samples, two complementary water samples were collected before the agitation process, to use them as a blank (i.e., later subtracting these concentrations from the corresponding concentrations of the agitated samples).

The cylinder was positioned at different points in every section. The location of these points was selected aiming to capture the transversal sediment storage variability that was observed in the field. The number of sampling points in each section was three sites in S2 and S4 and five sites in S1 and S3. Sampling locations were kept at the same exact locations for the whole study period (subsequent field campaigns). A total of 4 sampling campaigns (one per season) were performed. Samples were taken to the laboratory to determine their suspended sediment concentration [$C(t)_i$, in g l^{-1}] by filtering or decanting the water samples (depending on the amount of sediment) using the procedures described by López-Tarazón et al. (2009). The amount of sediment released from the bed per unit surface area at a given point i [$B(t)_i$, in g cm^{-2}] was obtained as:

$$B(t)_i = \frac{C(t)_i W(t)_i}{A} \quad (1)$$

where the volume of the water [$W(t)_i$, in l] contained into the cylinder is calculated from the depth of the column water above the bed and the surface area of the cylinder [A, in cm^2]. Sediment storage at a given section, period and agitation level was then calculated by the average of the amount of sediment released from the bed at the different sampling points.

3.2. Suspended sediment transport

Water stage is continuously measured and recorded every 15 minutes at the Capella gauging station (i.e., EA047, see location in Fig. 1c). The station is operated by the Ebro Water Authority. Water stage is later transformed to discharge (Q) using the rating curve developed by the authors (López-Tarazón et al., 2010). In addition, we measure

turbidity by means of a high-range backscattering Endress+Hauser Turbimax W CUS41 turbidimeter (with a measuring range up to 300 g l^{-1}). Turbidity readings were taken at 5-sec intervals while logging was performed at 15-min intervals (thus recording the average value of the samples between log intervals). The turbidimeter was linked to a Campbell CR-510 data-logger. Turbidity records were transformed into suspended sediment concentration (i.e., *C*) by means of the calibration curve developed by the authors (for more information of the sampling and calibration procedures see López-Tarazón et al., 2009; López-Tarazón et al., 2010). Figure 3 represents the discharge and the suspended sediment concentration during the study period (June 2007-June 2008).

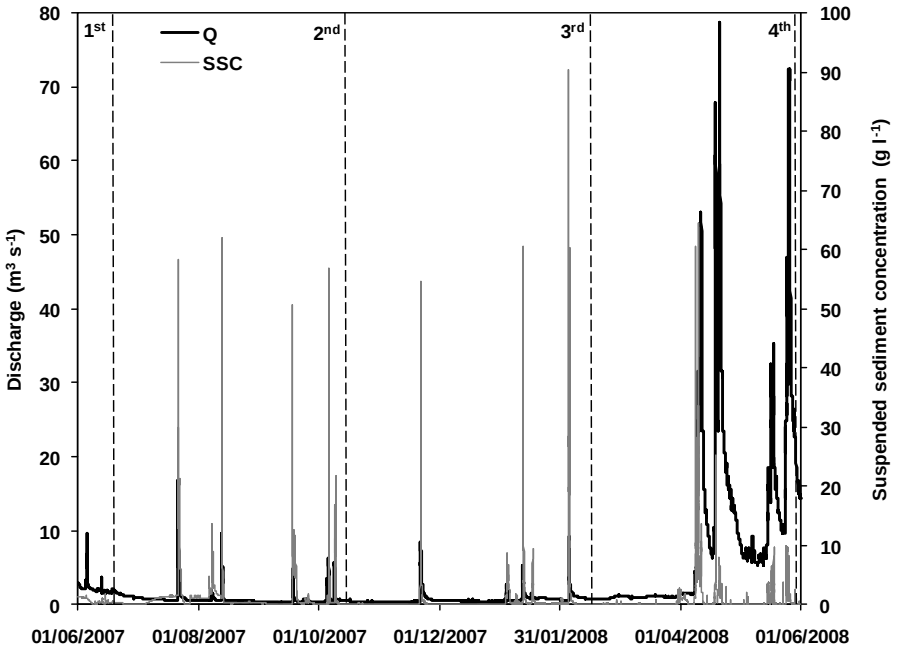

Figure 3. Discharge and suspended sediment concentration of the Isábena River measured at the Capella gauging station (EA047; see Fig. 1c for location) over the study period (June 2007 – June 2008). The vertical dashed lines show the dates when the in-channel storage sampling was carried out.

4. IN-CHANNEL BED STORAGE

It is usual that fine-grained sediment settles into gravel beds during flood recession when the energy to maintain it in suspension decreases. Under such conditions an ephemeral mantle of few *mm* to *cm* covers the bed surface and sediment infiltrates into the channel bed, becoming incorporated within the gravel matrix (Walling et al., 1998).

This process reaches remarkable intensity in rivers like the Isábena where enormous amounts of fine sediment are typically supplied during floods and may be transferred further downstream during low flow conditions (for more details on the role of baseflows in the sediment transport and yield in the Isábena see López-Tarazón et al., 2009). Fine sediment remains in the channel until a competent discharge re-suspends particles again and the river-bed acts as a temporary store of sediment that controls the temporal dynamics of the river's sediment yield. The magnitude and effective role of this control remains unknown in most rivers, largely due to the paucity of measurements.

In this study it is assumed that the amount of sediment re-suspended during individual sampling is a representative estimation of the fine sediment accumulated in the channel bed of the sampling sections at the time of sampling (i.e., the results provide a snap-shot of the in-channel sediment storage at each section). It is also hypothesized that channel accumulations will be at their maximum during periods of low flows and during small floods. The majority of that sediment will be remobilised during high flows typically occurring during late spring, late summer and autumn. However, due to the Mediterranean condition of the Isábena (i.e., irregularity of the rainfall, persistence of dry periods) this process may not occur yearly, but will depend on the precipitation characteristics (and its spatial concentration) and generation of competent discharges.

Table 1 and Figure 4 show the results for the measurements of the fine-grained sediment storage in the channel bed for each sampling site and seasonal sampling expressed in g cm^{-2}. We are aware of operational problems due to the manual nature of the methodology and some other field limitations that may produce a bias in the estimation of the stored material. For example, field observations indicated that during the agitation process sediment losses may occur due to an imperfect sealed between the cylinder and the bed or because of the rapid sedimentation of the fine-grained materials. Despite the sampling limitations, there are some consistent trends in the data. First, considerable variations in sediment storage between sites and for both levels of agitation can be seen, reflecting the high variability in both bed material and in-channel sediment storage (e.g., Lambert and Walling, 1988). Moreover, there is a clear seasonal pattern in the mean amount of sediment stored for every sampling site and both

agitation levels, which increases progressively from summer to winter and shows a marked reduction in spring, the season during which most floods occur.

Table 1. Average seasonal fine sediment storage in the channel bed for each sampling site in the lower reach of the River Isábena (n = 5 for S1 and S3; n = 3 for S2 and S4; where n is the number of points in each sampling site; see Fig. 1c for location details), as determined by the two levels of bed disturbance (see text for further description).

Season	Section	N1[a] (g cm^{-2})	N2[b] (g cm^{-2})	Mean (g cm^{-2})	σ[c] (g cm^{-2})	CV[d] (%)
Summer 2007	**S1**	0.005	0.049	0.027	0.032	117
	S2	0.009	0.053	0.031	0.031	100
	S3	0.007	0.078	0.043	0.050	117
	S4	0.006	0.215	0.111	0.147	133
	Mean	0.007	0.099	0.053	0.065	117
	σ	0.002	0.079	0.039	0.055	13
Autumn 2007	**S1**	0.013	0.128	0.070	0.081	115
	S2	0.006	0.056	0.031	0.035	115
	S3	0.009	0.162	0.085	0.108	127
	S4	0.004	0.092	0.048	0.063	131
	Mean	0.008	0.109	0.059	0.072	122
	σ	0.004	0.046	0.024	0.031	8
Winter 2007-08	**S1**	0.362	1.130	0.746	0.543	73
	S2	0.016	0.101	0.059	0.060	102
	S3	0.057	0.255	0.156	0.140	90
	S4	0.034	0.844	0.439	0.572	130
	Mean	0.118	0.583	0.350	0.329	99
	σ	0.164	0.485	0.309	0.267	24
Spring 2008	**S1**	0.023	0.030	0.026	0.005	19
	S2	0.045	0.055	0.050	0.007	15
	S3	0.007	0.107	0.057	0.071	124
	S4	0.009	0.104	0.057	0.067	119
	Mean	0.021	0.074	0.047	0.038	69
	σ	0.017	0.038	0.014	0.036	60

[a] Water agitation
[b] Water and bed agitation
[c] Standard deviation
[d] Coefficient of Variation

Results in Table 1 illustrate that the amount of sediment re-suspended in the water column and the top 10 cm of the channel bed is substantially greater than when only the water is agitated. This observation is consistent across all the sampling points and reflects a similar phenomenon to that reported by Lambert and Walling (1988) and Walling et al. (1998). It shows the relatively high amount of fine sediment stored within the channel bed surface sediment matrix. N1 (i.e., water column agitation level) is considered to represent fine sediment that may be re-suspended during relatively small floods, whereas N2 (i.e., remaining surface sediment plus sediment contained in the top layer of the bed) represents fine sediment that may only be removed during higher

floods when the gravel-bed matrix becomes unstable. In the present study there is insufficient field information to define thresholds of fine sediment resuspension associated with flood magnitude, thus we cannot precisely identify which level of bed agitation is the most appropriate for inferring the annual sediment storage at the sampling sites. For that reason we have used the average of the two (N1, N2) in further calculations. Table 1 also indicates that the values of sediment storage obtained at all sampling sites exhibit a considerable both spatial and temporal variability, ranging from 0.026 to 0.44 g cm^{-2}. These values provide an interesting comparison with those reported in other rivers. For example, Lambert and Walling (1998) found that the range of the average amount of sediment stored in the channel bed of the River Exe, UK, varied between 0.017 (N1, water agitation) and 0.04 g cm^{-2} (N2, water and bed agitation). Walling et al. (1998) found a considerable variability in the average fine sediment storage ranging from 0.017 (N1) to 0.92 g cm^{-2} (N2) in four rivers in Yorkshire, UK. Further, Walling and Quine (1993) reported very high variations in the bed storage along the course of the River Severn, UK, ranging from 0.063 to 8.0 g cm^{-2}. Finally, Droppo and Stone (1994) estimated that channel bed storage fluctuated between 0.066 and 0.22 g cm^{-2} in three rivers in SW Ontario, Canada.

The results for each site have been extrapolated to the total surface area of the ~3-km study reach in order to estimate the total amount of fine-grained sediment stored in the channel (S_s in tonnes). This extrapolation has been done using the following equation:

$$S_s = \sum_{i=1}^{n} \left(\frac{R_i + R_{i+1}}{2}\right) \left(\frac{L_i + L_{i+1}}{2}\right) D \qquad (2)$$

where, R_i is the average sediment released at a given site i (t m^{-2}), L_i is the width of the channel bed at site i (m) and D is the representative distance of each section (middle distance between consecutive sections, in m). Results are presented in Table 2 and Figure 5 and, once expressed per unit length of channel (i.e., t km^{-1}), suggest an increasing trend in sediment storage in the downstream direction, with just two exceptions: S3 in autumn and S2 in winter. This spatial trend may be related to the downstream increase of the channel width, thus widening flows and decreasing transport capacity, which may in turn enhance sediment deposition and storage per unit

surface area. Another trend appears evident from field data: sediment storage in the channel bed (per unit length of channel) increases seasonally from summer to winter and reduces strongly in spring, after a period of high floods (Fig. 3). This observation suggests that the River Isábena may reach maximum flow capacity during certain periods of the year (i.e., snowmelt season, that transported ca. 80% of the total water yield and generated the highest discharge peak of 79 $m^3 s^{-1}$ during the study period) and that fine sediment is deposited and accumulated at channel locations where flow conditions are not competent to keep it in suspension. Comparison of data from the Isábena with results reported by Walling et al. (1998) for the River Ouse (UK), where storage of fine sediment represents an important component of the sediment budget, shows that average in-channel storage for the Isábena is 55 t km^{-1} with a section-maximum of 297 t km^{-1}, while in the Ouse the average was 48 t km^{-1} with a maximum of 204 t km^{-1}.

5. THE ROLE OF IN-CHANNEL STORAGE ON THE SEDIMENT YIELD

Estimation of channel storage allows comparison with the sediment yield at the outlet of the catchment for a specific hydrological year (i.e., 2007-2008, average runoff conditions and water yield). Before attempting such comparison it is important to consider the temporal and spatial representativeness of in-channel sediment storage estimate. Storage has been derived by sampling sediment re-suspended from the river bed once at the end of each season with no inter-flood sampling (i.e., cylinder cannot be operated during high flows), so seasonal storage data should be interpreted as net values reflecting the sequence of flow events that re-suspend sediment and low flow accumulation periods over each season. The exact depth to which sediment is stored within the bed matrix is not precisely known and thus is not clear how representative the different levels of agitation are for estimating sediment bed storage. Furthermore, experiments were carried out in three to five sampling sites in four different sections of the lower part of the River Isábena that covers a fraction of the total channel length (i.e., 3.125 km, the length immediately upstream from the Capella section). We know that sediment yield encompasses contributions from further upstream and, as the results show, that spatial variability can be considerable. Several studies (e.g., Duijsings, 1986; Lambert and Walling, 1988; Diplas and Parker, 1992; Meade, 1994; Walling et al.,

1998) have also documented large and complex temporal and spatial variations in channel bed storage, so extrapolation of the storage data presented in the present study to the rest of the channel network must treated with caution. To estimate the channel bed storage in the entire catchment channel length, we have extrapolated the average sediment storage per unit of channel length to the 45-km mainstem river.

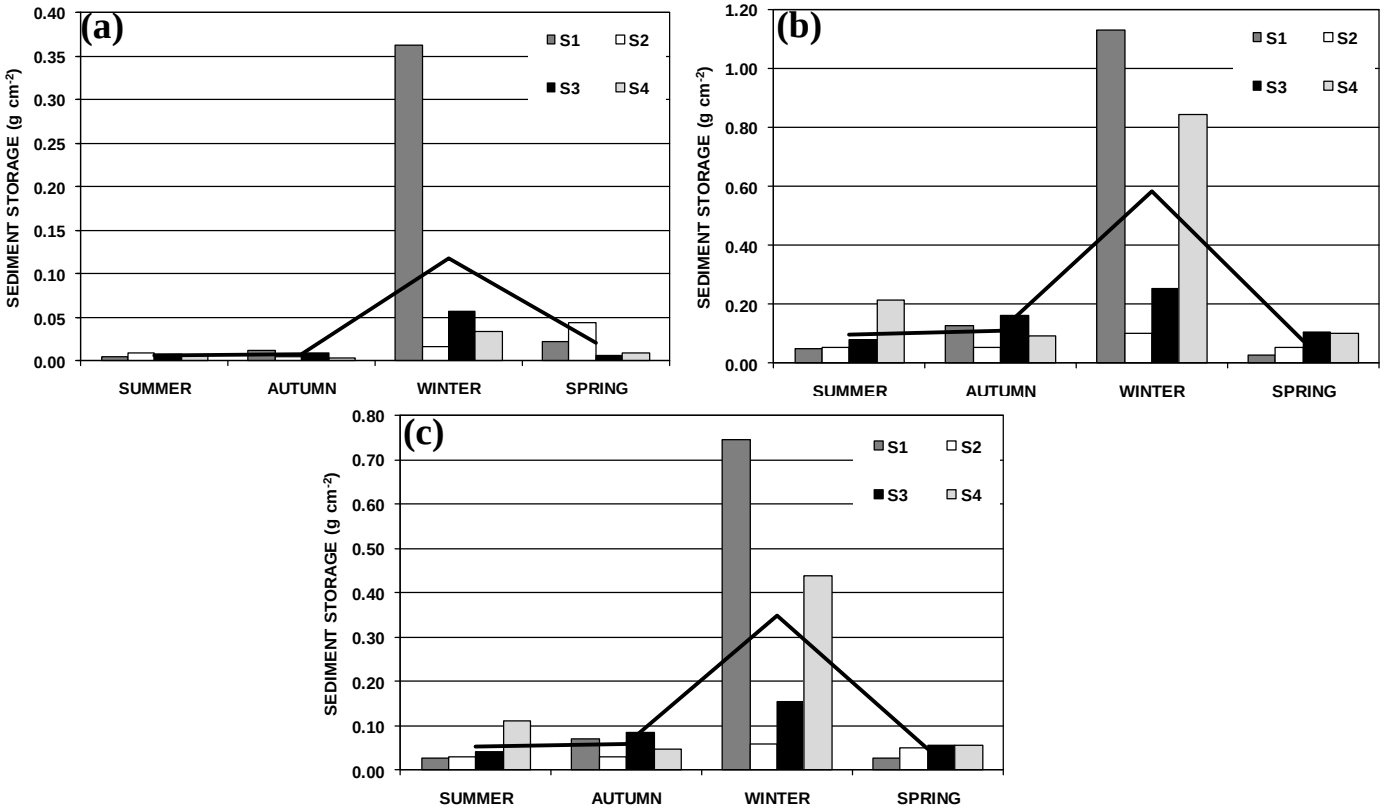

Figure 4. Results obtained from the fine-grained sediment storage measurements at each season and for each sampling section (S1, S2, S3 and S4; see Fig. 1c for specific locations). (A) Results obtained for the first level of agitation (i.e., N1); (B) Results obtained after the second level of agitation (i.e., N2); (C) Average results for both agitation levels (see text for more details). In all cases, the black line represents the average value for all sampling sections and for each season

The suspended sediment load has been calculated by means of the multiplication of 15-min resolution discharge (*Q*) and suspended sediment concentration (*SSC*) datasets (for more information see López-Tarazón et al., 2009) for the sampling period (June 2007 – June 2008). The mean annual discharge at the basin outlet for the study period was 3.2 $m^3 s^{-1}$ (σ = 7.3 $m^3 s^{-1}$), with a maxima of 79 m^3 registered on the 20th of April, 2008. The mean annual water yield was 100 hm^3, a value that can be considered as moderately dry comparing it with the mean long-term annual water yield (i.e., 177 hm^3 for the period

1945-2008) but average in relation to the Isábena recent monitoring period (94 hm^3 y^{-1} for the monitoring period 2005-2008, for details see López-Tarazón et al., 2009). The mean *SSC* for the study period was 0.8 g l^{-1} (σ = 3.1 g l^{-1}), with a maxima of 90 g l^{-1}, recorded on the 4th of February 2008, during a relatively low magnitude flood (i.e., peak discharge of 9.2 m^3 s^{-1}, for a return period of 0.6 years; see Fig. 3). The annual suspended sediment load was 209,559 t and can also be considered representative of average conditions over recent years (i.e., 180,000 t y^{-1} for the period May 2005 to May 2008; López-Tarazón et al., 2009).

Table 2. Total storage of fine-grained sediment in the channel bed of the lower part of the River Isábena for each sampling season. Sediment storage (calculated following equation 2) is presented in absolute terms (t) but also relatively to the channel length (t km^{-1}). The maximum discharge registered in each season and its respective return period has been added as a reference of seasonal flood magnitude.

Season	Section	Storage (t)	Storage (t km^{-1})	Q_{max} (m^3 s^{-1})	Return period (y)
Summer 2007	**S1**	5	11	16.72	0.61
	S2	20	16		
	S3	44	40		
	S4	17	67		
	Total	87	28		
Autumn 2007	**S1**	9	20	8.43	0.54
	S2	35	27		
	S3	44	39		
	S4	8	32		
	Total	96	31		
Winter 2007-08	**S1**	70	159	9.22	0.55
	S2	65	50		
	S3	199	177		
	S4	74	297		
	Total	408	131		
Spring 2008	**S1**	7	15	78.74	1.46
	S2	33	25		
	S3	39	35		
	S4	10	40		
	Total	88	28		
	Average	170	55	3.16	0.51

Table 3 compares the values of fine sediment channel storage at the study reach and the extrapolations made to the whole channel length with the suspended sediment yield calculated at the EA047 gauging station (see locations in Figure 1c), both per season and for the whole study period. Progressive accumulation of fine sediment in the entire channel bed can be seen as the year progresses (Figure 6) due to the absence of rainfall generating high flows and the relatively high sediment supply. Accumulation was

rapidly reduced to a level similar to that measured at the start of sampling once high flows occurred (i.e., spring 2008). According to field data, it appears that the in-channel storage in the River Isábena follows a cyclical pattern; sediment that is continuously produced in the badland areas it is episodically exported and deposited on the channel bed mostly during relatively low flows (e.g., inter-flood periods, small floods, baseflows, flood recessions) until high flows re-suspends and transports it downstream. Due to the Mediterranean characteristics of the catchment (i.e., irregular distribution of the precipitation during and between years), the cycle may not be regular in time and it may be difficult to establish during which seasons sediment accumulation or re-suspension dominates. Despite this limitation, the data shows how the main river channel acts as an intermediate temporal sediment compartment (with marked sink-source dynamics) between source areas and the basin outlet. This process seems to modulate river transport and associated conveyance capacity, as well as the sediment yield in mesoscale catchments, where sources are located far from the outlet and sediment supply is high.

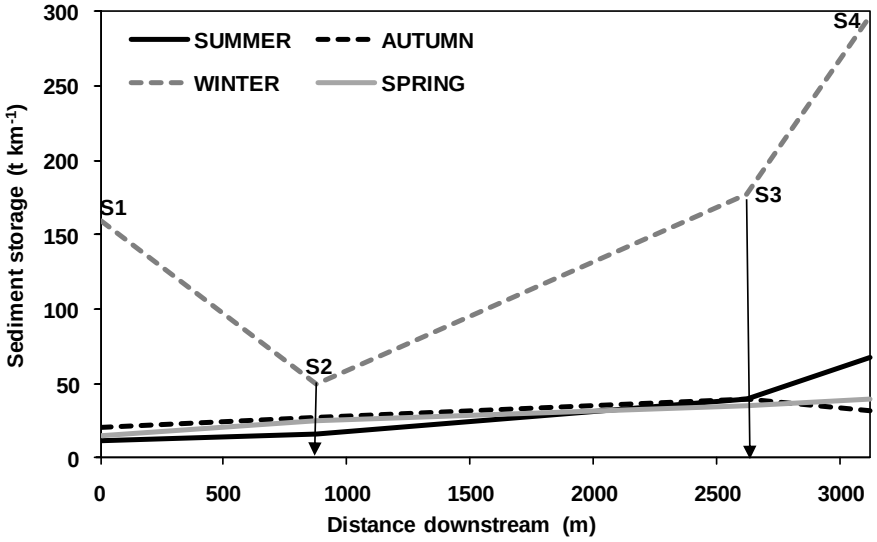

Figure 5. Average sediment storage per unit length of channel for each sampling site (S1, S2, S3 and S4) and distance downstream from the first studied section (i.e., presented values for each site are based on the mean of results provided for both levels of agitation).

In our case, sediment seasonally stored in the ~3-km of channel length equates to up to almost 4% (i.e., winter 2007-08) of the sediment load transported at the outlet of the

basin and 0.3% of the total load of the year. Extrapolation to the whole channel length (45 km, river mainsteam) suggests that sediment stored increases more than an order of magnitude, attaining ca. 55 % of the winter 2007-08 sediment yield and ca. the 5 % of the total annual load.

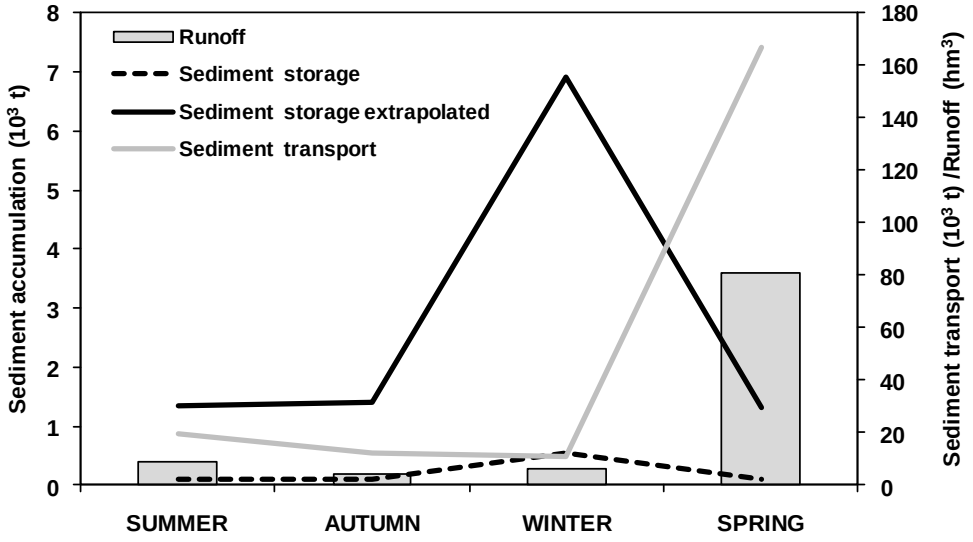

Figure 6. Comparison of the estimated seasonal sediment storage in the study reach, the sediment storage extrapolated to the whole channel, and the sediment yield and runoff for the study period in the Isábena basin.

The channel storage data presented in this study is comparable to the level of storage reported in other catchments. For instance, Duijsings (1986) estimated that 9% of the sediment load may have been seasonally stored in the channel bed for the Schrondweilerbaach River in Luxembourg, while Lambert and Walling (1988) calculated that channel bed storage represented around 2% of the annual suspended sediment load for the River Exe in the UK. Walling and Quine (1993) reported, for the River Severn in the UK, that channel bed storage represented around 2% of the sediment load, while Walling et al. (1998) found channel storage equated to 10% of the annual suspended sediment load for the Ouse and Wharfe basins in the UK.

Table 3. Comparison of channel-bed sediment storage estimation in the River Isábena with the suspended sediment yield measured at the basin outlet (Capella gauging station, EA047, see Fig. 1c for location details).

Season	Suspended sediment load (t)	Channel bed storage[a] (t) / (t km^{-1})	Storage / Load ratio[b] (%)	Total channel bed storage[c] (t)	Storage / Load relation[d] (%)
Summer 07	19,617	87 / 28	0.44	1,260	6.42
Autumn 07	12,327	96 / 31	0.78	1,395	11.32
Winter 07-08	10,827	408 / 131	3.77	5,895	54.45
Spring 08	166,788	88 / 28	0.05	1,260	0.76
Total	209,559	679 / 217	0.32	9,810	4.68

[a]Absolute and relative values obtained at the sampled 3.125-km channel length.
[b]Relation between the total suspended sediment load and the storage values calculated for the sampled sites.
[c]Values obtained after extrapolation to the whole channel-length (45 km) of the results estimated for the sampled sites.
[d]Relation between the total suspended sediment load and the storage values for the total channel length (45 km, mainstem river).

6. SUMMARY AND CONCLUSIONS

The amount of fine-grained sediment stored in the channel bed of a ca. 3-km length reach of the lower River Isábena has been estimated using field measurements during an average hydrological year to examine channel storage magnitude and seasonal variability. Despite extrapolation uncertainties, results highlight that fine-grained sediment stored on the channel is an important component of the suspended sediment budget of the basin. A series of conclusions can be drawn up from the results:

1) The total storage in the channel bed for the study period was 679 t (representing a 0.32% of the annual suspended sediment load at the basin's outlet, which was 209,559 t). This storage varied from 88 t in spring 2008 to 408 t in winter 2007-08, representing a 0.05% and 3.77% of these seasons sediment load, respectively.

2) Average seasonal values obtained in the monitored channel reach extrapolated to the whole channel length (i.e., 45 km) show that the total storage may equate to 9,810 t (i.e., 4.68 % of the total load), while the storage would increase up to 1,260 t in spring 2008 and to 5,895 t in winter 2007-08 (i.e., 0.76 and 64.45 % of the season sediment load, respectively).

3) In-channel sediment storage is rather variable in space and time; however, two interesting trends can be pointed out: a) a clear tendency for the stored sediment to

increase in the downstream direction, probably due to the increase in both the width of the channel and the likelihood of sediment deposition; and b) a continuous year-round sediment accumulation mostly during low-flow periods (which lack sufficient competence to entrain fines). However, a general pattern is difficult to establish due to rainfall irregularity (which precludes any long-term extrapolation) and also because of the short length of the study period.

4) Finally, field observations suggest that the average residence time of the sediment stored in the channel bed is relatively short, probably less than 1 year. Storage has thus important implications for both the routing of sediment through the fluvial system and for the determination and interpretation of downstream sediment fluxes and export.

This study emphasises the need to further investigate the use of field measurements to quantify sediment storage and routing in basins like the Isábena, where basin size as well as the type and spatial extent of sediment sources are likely to enhance the proportion of sediment stored in the channel, thus impacting on the frequency and magnitude of sediment yields. Because of the scale-dependency of geomorphological processes described in this paper, studies conducted at a range of different spatial scales should be promoted to improve understanding of catchment sediment pathways and connectivity.

Acknowledgements

The first author has a grant funded by the Catalan Government and the European Social Fund. Research has been carried out within the framework of the project "Sediment Export from Large Semi-Arid Catchments: Measurements and Modelling" (SESAM), funded by the *Deutsche Forschungsgemeinschaft* (DGF). The authors wish to thank the Ebro Water Authorities for the permission to install the equipment at the Capella gauging station and for providing hydrological data. We also thank Álvaro Tena, Alberto Sánchez, Sabina Márquez and Nuria Bonastre for their assistance in fieldwork and during the process of samples in the laboratory. Special thanks are given to Hugh Smith for a first review of the manuscript.

REFERENCES

Acornley, R.M., Sear, D.A., 1999. Sediment transport and siltation of brown trout (*Salmo trutta* L.) spawning gravels in chalk streams. *Hydrological Processes*, **13**: 447–458.

Avendaño, C., Cobo, R., Sanz, M.E., Gómez, J.L., 1997a. Capacity situation in Spanish reservoirs. *Proceedings of the Nineteenth Congress on Large Dams***, 74:** 849–862.

Avendaño, C., Sanz, M.E., Cobo, R., Gómez, J.L., 1997b. Sediment yield at Spanish reservoirs and its relationships with the drainage basin area. *Proceedings of the Nineteenth Congress on Large Dams***, 74:** 863–874.

Avendaño, C., Sanz, M.E., Cobo, R., 2000. State of the art of reservoir sedimentation management in Spain. In: *Proceedings of the International Workshop and Symposium on Reservoir Sedimentation Management*, Tokyo, Japan, pp. 27–35.

Clarke, S.J., Wharton, G., 2001. Sediment nutrient characteristics and aquatic macrophytes in lowland English rivers. *The Science of the Total Environment*, **266**: 103–112.

Collins, A.L., Walling, D.E., 2007. Fine-grained bed sediment storage within the main channel systems of the Frome and Piddle catchments, Dorset, UK. *Hydrological Processes*, **21**: 1448–1459.

Diplas, P., Parker, G., 1992. Deposition and removal of fines in gravel-bed streams. In: Billi, P., Thorne, C.R., Tacconi, P. (eds.): *Dynamics of Gravel-bed rivers*. Wiley, Chichester, pp. 313-329.

Droppo, L.G., Stone, M., 1994. In-channel surficial fine-grained sediment laminae, Part I. Physical characteristics and formation processes. *Hydrological Processes*, **8**: 101-111.

Duijsings, J.J.H.M., 1986. Seasonal variation in the sediment delivery ratio of a forested drainage basin in Luxembourg. In: Hadley, R.F. (ed.): *Drainage Basin Sediment Delivery*. IAHS Publication 159, IAHS Press, Wallingford, pp. 153-164.

Francke, T., López-Tarazón, J.A., Schröder, B., 2008a. Estimation of suspended sediment concentration and yield using linear models, random forests and quantile regression forests. *Hydrological Processes*, **22**:4892–4904.

Francke, T., López-Tarazón, J.A., Vericat, D., Bronstert, A., Batalla, R.J., 2008b. Flood-based analysis of high-magnitude sediment transport using a non-parametric method. *Earth Surface Processes and Landforms*, **33**: 2064–2077.

Hodgkins, R., Cooper, R., Wadham, J., Tranter, M., 2003. Suspended sediment fluxes in a high-Artic glacierised catchment: implications for fluvial sediment storage. *Sedimentary Geology*, **162**: 105–177.

Jordan, P., Slaymaker, O., 1991. Holocene sediment production in Lillooet River basin, British Columbia: a sediment budget approach. *Géographie physique et Quaternarie*, **45**: 45–57.

Lambert, C.P., Walling, D.E., 1988. Measurements of channel storage of suspended sediment in a gravel-bed river. *Catena*, **15**: 65–80.

López-Tarazón, J.A., Batalla, R.J., Vericat, D., Francke, T., 2009. Suspended sediment transport in a highly erodible catchment: The River Isábena (Southern Pyrenees). *Geomorphology*, **109**: 210–221.

López-Tarazón, J.A., Batalla, R.J., Vericat, D., Balasch, J.C., 2010. Rainfall, runoff and sediment transport relations in a mesoscale mountainous catchment: The River Isábena (Ebro basin). *Catena*, **82**: 23– 34.

Loughran, R.J., Campbell, B.L., Shelley, D.J., Elliot, G.L., 1992. Developing a sediment budget for a small drainage basin in Australia. *Hydrological Processes*, **6**: 145–158.

Meade, R.H., 1994. Suspended sediment of the modern Amazon and Orinocco Rivers. *Quaternary International*, **21**: 29–39.

Navas, A., Valero, B., Machín, J., Walling, D., 1998. Los sedimentos del embalse Joaquín Costa y la historia de su depósito. *Limnética*, **14:** 93–112.

Owens, P.N., Walling, D.E., He, Q., Shanahan, J., Foster, I.D.L., 1997. The use of caesium-137 measurements to establish a sediment budget for the Start catchment, Devon, UK. *Hydrological Sciences Journal*, **42**: 405–423.

Packman, A.I., Mackay, J.S., 2003. Interplay of stream-subsurface exchange, clay deposition and stream bed evolution. *Water Resources Research*, **39**: 41–49.

Palau, A., 1998. Estudio limnológico del ecosistema fluvial afectado por los vaciados del embalse de Barasona. *Limnética*, **14**: 1–15.

Phillips, J.D., 1991. Fluvial sediment budgets in the North Carolina Piedmont. *Geomorphology*, **4**: 231–241.

Quinn, J.M., Davies-Colley, R.J., Hickey, C.W., Vickers, M.L., Ryan, P.A., 1992. Effects of clay discharge on streams, 2: benthic invertebrates. *Hydrobiologia*, **248:** 235–247.

Smith, H.G., Dragovich, D., 2008. Sediment budget analysis of slope-channel coupling and in-channel sediment storage in an upland catchment, southeastern Australia. *Geomorphology*, **101:** 643–654.

Trimble, S.W., 1983. A sediment budget for Croon Creek basin in the Driftless area, Wisconsin, 1853-1977. *American Journal of Sciences*, **283**: 454–474.

Verdú, J.M., Batalla, R.J., Martínez-Casasnovas, J.A., 2006. Estudio hidrológico de la cuenca del río Isábena (Cuenca del Ebro). I: Variabilidad de la precipitación. *Ingeniería del Agua*, **13**(4): 321–330.

Walling, D.E.,1983. The sediment delivery problem. *Journal of Hydrology*, **65:** 209–237.

Walling, D.E., Amos, C.M., 1999. Source, storage and mobilisation of fine sediment in a chalk stream system. *Hydrological Processes*, **13**: 323–340.

Walling, D.E., Quine, T.A., 1993. Using Chernobyl-derived radionuclides to investigate the role of downstream conveyance losses in the suspended sediment budget of the River Severn, United Kingdom. *Physical Geography*, **14**: 239–253.

Walling, D.E., Owens, P.N., Leeks, G.J.L., 1998. The role of channel and floodplain storage in the suspended sediment budget of the River Ouse, Yorkshire, UK. *Geomorphology*, **22**: 225–242.

Wilson, A.J., Walling, D.E., Leeks, G.J.L., 2004. In-channel storage of fine sediment in rivers of southwest England. In: Golosov, V., Belyaev, V., Walling, D.E. (eds.): *Sediment transfer through the fluvial system*. IAHS Publication 288, pp. 291–299.

Wood, P.J., Armitage, P.D., 1997. Biological effects of fine sediment in the lotic environment. *Environmental Management*, **21**: 203–217.

CHAPTER 6

SEDIMENT BUDGET

INDEX CHAPTER 6: SEDIMENT BUDGET

Figure captions in the paper

Figure 1. (A) Location of the Ebro and Isábena basins in the Iberian Peninsula. (B) Location of the Cinca, Ésera and Isábena basins in the Ebro basin. (C) General map of the Isábena catchment, showing locations of the main badlands areas, the Barasona Reservoir and the sampling sites.

Figure 2. Examples of the instrumentation installed at the monitored sub-basins: (A) Cabecera, (B) Lascuarre. Note that the capacitive water stage sensors (Trutrack WT-HR) are installed inside the grey PVC tubes.

Figure 3. Variable importance of *SSC* predictions for each sub-basin normalized to 100%. Abbreviations are shown in Table 2. Note that in the case of Villacarli, values correspond just to the periods in which modeling was possible.

Figure 4. Close-up-view of runoff and suspended sediment concentration (*SSC*) measured and predicted by using *RF* for one flood at each of the measuring sections.

Figure 5. Suspended sediment yield of the whole basin for the study period.

Figure 6. Water and sediment sub-catchment contributions to the Isábena basin for the study period: (A) 2007-2008 year, (B) 2008-2009 year and (C) whole study period. Inside the arrows there is shown the contribution (%) of each sub-basin and at each period.

Figure 7. Schematic sediment budget for the Isábena catchment

Figure 8. The relations between sediment delivery ratio and catchment area shown by the Isábena catchment and data reported for catchments in the United States by Roehl (1962) and Williams and Berndt (1972).

Table captions in the paper

Table 1. Physical parameters and sampling data of the main sub-basins and the entire Isábena catchment.

Table 2. Summary of the ancillary predictors used to model the sedigraphs and their meaning (see equations (1) and (2) for the definition of temporal shifts).

Table 3. Performance of *SSC* prediction using *RF*/*QRF* in comparison with traditional sediment rating curves.

Table 4. Summary of measured discharge (*Q*), specific discharge (Q_s) and suspended sediment concentration (*SSC*) data at the 6 monitored sections during the study period.

Table 5. Villacarli's water yield (*WY*), modeled sediment load (*SSL*), number of flood-events and maximum peak discharge (Q_{max}) registered at the periods where data was available. Comparison with the results obtained at the other sub-basins.

Table 6. Summary of the seasonal and total precipitation (*P*), water yield (*WY*) and suspended sediment load (*SSL*) at the whole basin and its sub-basins during the study period.

Table 7. Specific suspended sediment yield (*SSY*s) of each sub-basin and the total catchment. In the case of Villacarli, the calculation of the *SSY*s has been done using its basin size, assuming as negligible the paper of the ungauged catchment's areas over the sediment load.

Table 8. Water and sediment budget of the Isábena basin. The contribution of each sub-basin is represented as its percentage over the total water and sediment load.

1. INTRODUCTION

This chapter reports on the water and suspended sediment budget of the Isábena basin for the period 2007-2009. For this purpose the non-parametrical statistical techniques (*Random Forests, Quantile Regression Forests*) developed for the Isábena basin were used to interpolate continuous sedigraphs from ancillary hydrological data. To undertake this we present a paper submitted analysing this issue. Paper is presented maintaining its original structure; its format has been adapted to the general format of the present volume.

The paper was submitted to *Geomorphology* in December 2010. It examines the contribution of the main sub-basins to the total water and suspended sediment loads for a quasi-average period (2007-2009). The non-parametric extrapolation could be applied to all the sub-basin with the exception of Villacarli, in which the discontinuous discharge records impeded that. Extrapolations showed regular to good agreement at the sub-basins. Results suggest that Cabecera sub-basin controls the hydrology of the Isábena basin while Villacarli and Lascuarre sub-basins generate the most of the suspended sediment load (related to Objective 4). Finally, it establishes the sediment budget of the catchment, together with the denudation rates and the residence time of the sediment within the basin.

2. SEDIMENT BUDGET

López-Tarazón, J.A., Batalla, R.J., Vericat, D., Francke, T., 2010. The sediment budget of a highly dynamic catchment. An approach based on field data and non-parametric statistics (submitted to *Geomorphology*).

The sediment budget of a highly dynamic catchment. An approach based on field data and non-parametric statistics.

Abstract

A sediment budget is a quantitative description of the sediment generation and movement through a single landscape unit, and it includes the identification of storage sites, the transport processes, and linkages among them, and the quantification of stored volumes and rates of transport processes. Establishing a sediment budget provides a means of clarifying the link between upstream erosion and downstream sediment yield and the role of sediment storage. Within this context, the suspended sediment budget of the Isábena basin for the period July 2007 - July 2009 has been estimated applying a methodology that allows the interpolation of intermittent measurements of suspended sediment concentrations, estimates confidence intervals of these estimations and enables a subsequent calculation of sediment loads. To calculate the budget, the suspended sediment yield of all the sub-basins as well as that of the basin outlet were calculated. The results have been compared to define the hydro-sedimentological contribution of each sub-basin to the total water and sediment delivery of the Isábena catchment. The annual suspended sediment load was 225,822 t for the 2007-2008 and 243,524 t for the 2008-2009. In terms of specific sediment yields, the results obtained suggest a very high sediment activity, especially in the case of Villacarli and Lascuarre. The specific sediment yield obtained for the entire Isábena catchment is 527 t km^{-2} and can be considerate as high. Finally, the sediment budget of the basin has been established, quantifying a sediment delivery ratio (i.e., relation between sediment input and export) of 52%, while in-channel storage represents the 4% and losses on the conveyance system the 44% of the sediment introduced in the basin mainly by the badland areas. These results show the high sediment dynamics of the Isábena catchment and the short (< 2 years) residence time of the sediment within the basin.

Keywords: sediment budget, sediment transport, fieldwork, non-parametrical statistical techniques, random forests, quantile regression forests, River Isábena, Ebro basin.

1. SEDIMENT BUDGETS. THE ROLE OF HIGHLY ERODIBLE AREAS

A sediment budget is a quantitative assessment of the sediment generation and movement through a landscape unit. This assessment includes the identification of erosion and storage zones (i.e., sediment sources and sinks), the sediment delivery and transfer processes (including connectivity and fluvial sediment transport) and the linkages among them (Dietrich and Dunne, 1978; Swanson and Friedriksen, 1982; Golosov et al., 1992; Nelson and Booth, 2002). Establishing a sediment budget provides thus a mean of clarifying the link between upstream erosion and downstream sediment yield and the role of sediment storage under different temporal scales (Walling, 1983, 1999; Dunne, 1994; Trimble, 1995; Trimble and Crosson, 2000; Slaymaker, 2003; Walling et al., 2006). Despite the obvious scientific and applied advances provided by the sediment budgets, it remains difficult to assemble the necessary information for anything other than small (e.g., <10 km^2) drainage basins (Walling et al., 2006). Still, traditional techniques available to investigate sediment mobilization by erosion and sediment storage, within a catchment, are hampered by significant spatial and temporal sampling constraints (Peart and Walling, 1988; Loughran,1989; Phillips, 1991; Collins and Walling, 2004), numerous operational problems and the costs incurred inassembling representative datasets (Slaymaker, 2003). Nevertheless, some works on in-channel suspended sediment storage can be stressed, estimating that the sediment stored in the channel represents between the 2% to the 10 % of the total suspended sediment load (Duijsings, 1986; Lambert and Walling, 1988; Walling and Quine, 1993; Walling et al., 1998). Besides that, some more interesting information can be derived from the sediment budgets calculations, as can be the sediment delivery ratios (i.e., relation between the sediment inputs and the sediment exported out of the basin) or the residence time (i.e., the time that a sediment particle needs to leave the basin). Regarding to the former, it is usually shown a scale effect, with an inverse trend between the sediment delivery ratio and the drainage area, ranging from a delivery ratio of ca 100% at microscale basins (i.e., <0.1 km^2; Porto et al, 2010) to values <10% in mesoscale basins (i.e., 100-1000 km^2; Roehl, 1962; Williams and Berndt, 1972; Porto et al, 2010); whilst the latter is quite variable, ranging from the daily scale (i.e., 50-80 days, Matisoff et al., 2005), to the decadal scale (i.e., 10 years, Swanson and Friedriksen, 1982; 28 years, Batalla et al., 1995; 30 years, Douglas et al., 2009) to the

centurial scale (i.e., 164 years, Rovira et al., 2005; several centuries, Hart and Schurger, 2005) or even more (i.e., 10,000 years, Dietrich and Dunne, 1978).

Suspension is the major transferring mechanism of particulate material in streams worldwide (Wood, 1977; Webb et al., 1995), typically attaining more than 90% of the annual load in alluvial streams (Meade et al., 1990). This is the main reason why sediment yields are often based purely on suspended load data. In addition, research on sediment transport in catchments draining highly erodible materials (e.g., soft marls, badlands) has become of interest due to the possibility of setting maximum thresholds and magnitudes of sediment transport, and also allowing model calibration and validation in extremely active geomorphic environments (e.g., Mamede et al., 2006; López-Tarazón et al., 2009; López-Tarazón et al., 2010b). Badlands are considered to be characteristic of arid regions but they also occur in wetter climates with high intensity storm events such as in the Mediterranean (Gallart et al., 2002). The so-called humid badlands are found in mountainous areas such as the Southern Alps (e.g., Mathys et al., 2005) and the Pyrenees (e.g., Clotet et al., 1988). There, mean annual precipitation is around 700 mm or higher. Rainfall mostly occurs in the form of high intensity storm events. Vegetation growth is no longer limited by water availability but by the high erosion rates and freezing on north exposed slopes (e.g., Regüés et al., 2000b). The extremely high suspended sediment loads delivered by the badlands, which result in increased turbidity and reduced light penetration as well as the siltation of fish habitat spawning gravels, the accumulation of sediment within channel and channel-margin habitats, and the presence of increased sediment-associated nutrient and contaminant loadings, have frequently been cited as important contributors to the degradation of fluvial ecosystems (i.e., UK Biodiversity Action Plan Steering Group for Chalk Rivers, 2004). Sedimentation problems compound their negative impacts on both environmental and socio-economical issues. The first is focused mainly on macrophyte communities (Clarke and Wharton, 2001), invertebrate biodiversity (Scullion, 1983) and fish populations (Acornley and Sear, 1999), whilst the latter refers especially to reservoir siltation, that causes water quality problems and, especially, a progressive reduction in dam impoundment capacity, which creates serious problems for water management, especially near dam outlets (e.g., Owens et al., 2005), Francke et al., 2008a, b).

This is the case of the River Isábena basin, a 445 km² catchment located in the Southern Central Pyrenees that drains extensive areas of badlands that have been identified as the main source of the sediment deposited in the downstream Barasona Reservoir (Valero-Garcés et al., 1999). The Barasona Reservoir supplies the region with water for drinking and irrigation. The large amount of sediment input coming from the badlands leads to a severe reduction in the storage capacity of the reservoir. Developing an improved understanding of the fine sediment dynamics in such important highly erodible catchments, including sediment sources, sediment mobilization, transfer and storage, and sediment yields, must be seen as a key requirement to inform the development and implementation of improved sediment control strategies, and catchment and reservoir management policies.

Within this context, this study aims to calculate the suspended sediment budget of the Isábena basin for the period July 2007 - July 2009. For this purpose, we have applied a methodology that allows the interpolation of intermittent measurements of suspended sediment concentrations, estimates confidence intervals of these estimations and enables a subsequent calculation of sediment loads. To calculate the budget, we have estimated the suspended sediment yield of all the sub-basins as well as that at the basin outlet upstream the Barasona Reservoir, together with the sediment that is stored in the main course channel or lost in the conveyance system. Results have been examined to define the contribution of each sub-basin to the total water and sediment delivery of the Isábena catchment. The findings provide a rationale to link sediment sources and production from the badlands with sedimentation in the reservoirs, and insights into the temporal dynamics and magnitude of sediment transport and its driving forces. The present paper is based on previous works done by Francke et al. (2008a, b) and López-Tarazón et al. (2009; 2010a, b).

2. THE ISÁBENA BASIN

The study was carried out in the Isábena basin, a mountainous catchment located in the Central Pyrenees, NE of the Iberian Peninsula (Fig. 1a).The River Isábena, together with the River Ésera, are the main tributaries of the River Cinca, in turn the second

largest tributary of the River Ebro (Fig. 1b). The Isábena basin is characterised by heterogeneous relief, vegetation and soil characteristics. Elevation varies from 450 m a.s.l. at the outlet to 2,720 m a.s.l. in the northern part of the basin (headwaters). The catchment is composed by 5 main sub-basins: Cabecera (146 km^2, representing the 33% of the total catchment area, draining the main Isábena catchment), Villacarli (42 km^2, 9%), Carrasquero (25 km^2, 6%), Ceguera (28 km^2, 6%) and Lascuarre (45 km^2, 10%) (Fig. 1c; Table 1). The climate is typical of Mediterranean mountainous areas (e.g., Continental Mediterranean climate), with mean annual precipitation of 767 mm (ranging from 450 at the lower part and 1600 mm at the summits) and an average potential evapotranspiration rate of 550 to 750 mm, both showing a strong south-north gradient due to topography (Verdú, 2007a). Mean temperature varies from 11ºC to 14 ºC in the southern part and between 9ºC to 11ºC in the northern zone, following the south-north gradient cited above too (Verdú, 2007b). Vegetation is mainly composed by deciduous woodland, agriculture, pasture and bushes in the valley bottoms, evergreen oaks, pines and bushes in the higher areas. Regarding to geology and lithology, the Northern parts are composed by Paleogene and Cretaceous sediments and the southern lowlands are mainly dominated by Eocene continental sediments.These areas consist of easily erodible materials (marls, sandstones), leading to the formation of badlands and making them the major source of sediment within the catchment, as have been previously described (Fargas et al., 1997; Francke et al., 2008b). Badlands can mainly be found in the Villacarli and Carrasquero sub-basins (6% and 2% of their total area, respectively), and at a lower degree in the Ceguera and Lascuarre sub-basins (1% and 0.4% of their total area, respectively); they are almost absent in the largest sub-basin, representing <0.01 % of the Cabecera's total area (Table 1, see the extension of badlands in Fig. 1c).

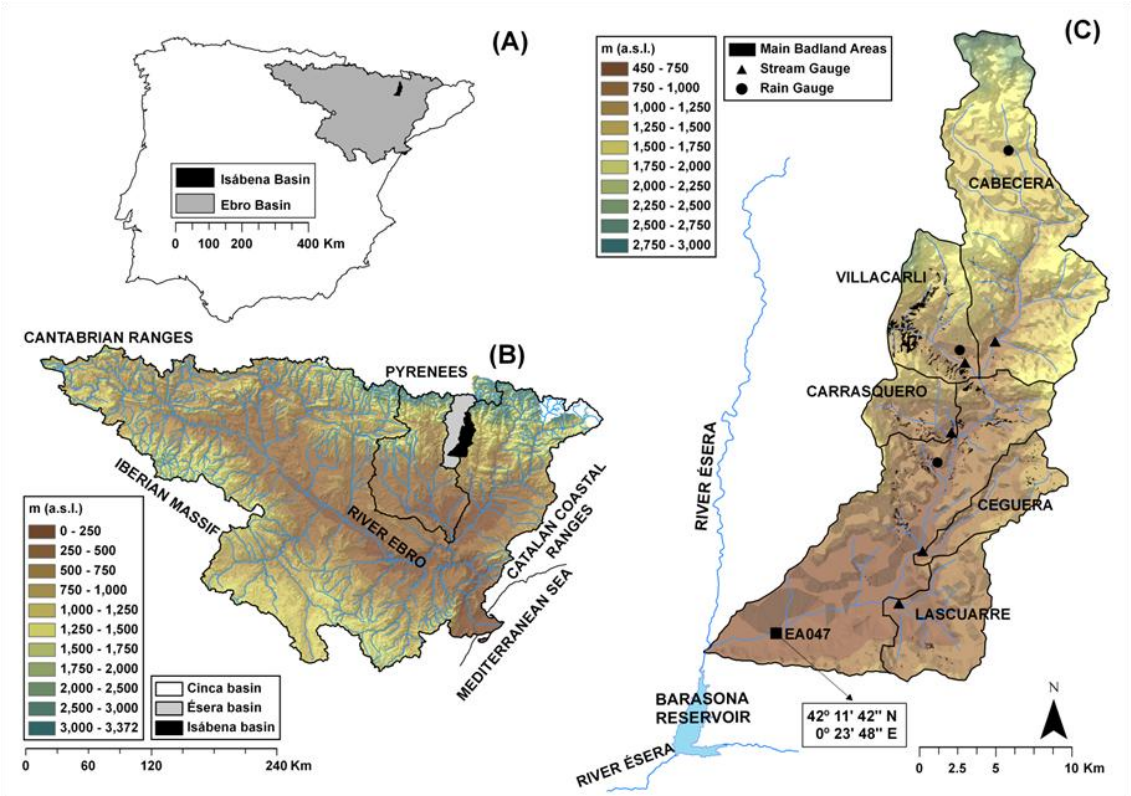

Figure 1. (A) Location of the Ebro and Isábena basins in the Iberian Peninsula. (B) Location of the Cinca, Ésera and Isábena basins in the Ebro basin. (C) General map of the Isábena catchment, showing locations of the main badlands areas, the Barasona Reservoir and the sampling sites.

The hydrology of the basin is characterized by a rain-snow fed regime. Floods typically occur in spring (due to the snowmelt) and, especially, in late summer and autumn as a consequence of localised thunderstorms. Minimum flows (~ 0.20 $m^3 s^{-1}$) typically occur in summer, but the river never dries up. Absolute maximum flows normally occur in autumn; however, the largest peak ever recorded at the basin outlet (i.e., Capella gauging station, EA047, see Fig. 1c) took place in summer (August 1963), reaching 370 $m^3 s^{-1}$ (a discharge with a return period of 86 years, calculated from the series of annual maximum instantaneous discharges by the Gumbel method for the period 1951-2008). The mean annual discharge at the basin outlet for the entire period of record (1945-2009) is 4.1 $m^3 s^{-1}$ (P_{10} = 2.14 $m^3 s^{-1}$ and P_{90}= 8.21 $m^3 s^{-1}$, where P_i is the i percentile of the observations). The mean annual water yield is 177 hm^3 (P_{10} = 68 hm^3 and P_{90}= 259 hm^3, 1 hm^3 = 1 x 10^6 m^3), a value that represents ~1.5% of the Ebro basin's total runoff.

The River Isábena flows into the Barasona Reservoir (Fig. 1c) at its confluence with the River Ésera. The dam closing the reservoir (i.e., Joaquín Costa Dam) was constructed in the early 1930s for an original capacity of 71 hm^3, and it was later enlarged in 1972 reaching a total capacity of 92 hm^3. The reservoir supplies water mainly to the Aragón and Catalunya Channel, irrigating more than 100,000 ha in the lowland. For almost 75 years, the reservoir has been progressively silting up at a rate of between 0.3 and 0.5 hm^3 of sediment deposited per year (Francke et al., 2008a). Engineering works during 1990s to release sediment through the dam bottom outlets resulted in around 9 hm^3 of sediment being sluiced through the dam (Palau, 1998; Avendaño et al., 2000). Nowadays, the reservoir capacity equals again that of 1990 (i.e., 76 hm^3) (Mamede, 2008).

Table 1. Physical parameters and sampling data of the main sub-basins and the entire Isábena catchment.

Sub-basin	Area (km^2)	Area[a] (%)	Badlands[b] (%)	Slope[c] (%)	T_c[d] (h)	Discharge record[e]	Total Gauges[f]	Total manual SS samples[g]	Total automatic SS samples[h]
Cabecera	146	32.8	0.01	4.4	3.2	14/09/2006-30/09/2009[i]	13	119	63
Villacarli	42	9.4	5.57	9.2	1.2	14/09/2006-30/09/2009[j]	12	145	23
Carrasquero	25	5.6	1.95	7.6	0.7	14/06/2007-30/09/2009	2	42	9
Ceguera	28	6.3	0.93	3.2	1.7	22/09/2007-30/09/2009[k]	3	32	17
Lascuarre	45	10.1	0.36	2.8	1.2	13/06/2007-30/09/2009	3	46	80
Isábena basin[l]	445	100.0	0.83	0.4	8.6	01/01/1945-nowadays	5	280	1177

[a] Percentage of the sub-basin area in relation to the total catchment area.
[b] Percentage of the total area covered by badlands.
[c] Mean longitudinal slope.
[d] Concentration time.
[e] Period of discharge sampling.
[f] Total gauges done at the measuring sections by means of an electromagnetic current meter (Valeport).
[g] Manual suspended sediment samples taken manually by means of a depth-integrated sampler US DH59.
[h] Automatic suspended sediment samples taken by the water stage samplers at the sub-basins or by an ISCO automatic sampler in the case of Capella (i.e., EA047).
[i] No data recorded during the period 28/01/2007-13/06/2007.
[j] No data recorded during the periods 28/01/2007-02/03/2007, 08/06/2007-16/11/2007 and 26/04/2008-30/09/2009.
[k] No data recorded during the periods 16/11/2007-18/12/2007 and 19/06/2008-30/10/2008.
[l] All data referred to sampling correspond to the Capella gauging station (i.e., EA047).

3. SAMPLING STRATEGY, FIELD METHODS AND DATA PROCESSING

3.1. Sampling strategy and field instrumentation

Suspended sediment transport dynamics have been studied in the Isábena basin since 2005. The instrumentation of the basin was made in two phases: initially, the Capella gauging station (i.e., EA047) was monitored in order to estimate the suspended sediment load at the basin outlet (Fig. 1c). This gauging station is operated by the Ebro Water Authorities (hereafter CHE). Sampling strategy was based on continuous records

of discharge (provided by CHE) and suspended sediment concentration (from turbidity records calibrated using direct concentrations obtained during low flows and flood events). Main results (including probe calibrations) have been presented by López-Tarazón et al., 2009 and López-Tarazón et al., 2010b. In 2006 and 2007 new equipments were installed, which increased the spatial and temporal resolution and precision of the measurements, including such at EA047. We monitored the five main sub-basins for discharge and sediment transport and installed a new set of rain-gauges (specific details of the sampling strategy are provided below). The location of all the instrumentation can be seen in figure 1c, while plates in figure 2 show examples of two of the monitoring sections.

Discharge

Discharge is measured by means of capacitive water stage sensors/loggers (Trutrack WT-HR) installed at suitable cross sections in the sub-catchments (in river constriction below bridges where available, in exception to EA047 where the CHE operates the station) (Fig. 2). Sensor bias (<10%) was estimated by comparing real field measured and sensor sampled water stages obtained during field visits that were performed weekly for instrument-maintenance and episodically for sampling during flood events. These measurements were used to calibrate the stage records under different flow and sediment transport conditions. Flow stage was recorded at a 5-min interval and was later converted into discharge by means of the derived water stage-discharge rating curves of each location. These rating curves were obtained by combination of the stage-mean velocity and stage-area methods as being more robust for extrapolation (Mosley and McKerchar et al., 1993). To calibrate them, repeated discharge measurements (e.g., gauges) were made at each tributary (Table 1) using an electromagnetic flow meter (Valeport 801) and completed with cross section surveys (Geodimeter total station). Water depth, at the catchment outlet (EA047), was recorded at a 15-min time interval and then transformed into discharge by the calibrated stage-discharge rating curve developed by the authors (López-Tarazón et al., 2010b).

Sediment Transport

Suspended sediment transport at EA047 is recorded continuously as turbidity using a high-range backscattering Endress+Hauser Turbimax W CUS41 turbidimeter (with a measuring range up to 300 g l^{-1}). The turbidity probe is linked to a Campbell CR-510 data logger. Turbidity reading was set up at 5-sec intervals while the logging recorded at 15-min intervals (thus recording the average value of the samples between log intervals). Turbidity records have been calibrated by means of suspended sediment concentrations obtained from water samples (for more details see López-Tarazón et al., 2009). Mixing was assumed complete. Further, at each of the monitored basins, suspended sediment was discrete sampled using water stage samplers (Fig. 2); they were designed and built following the methodology initially developed by Schick (1967). Samplers' height ranged between 1 and 2 meters and they never were over-flooded. The distance between bottle intakes was between 6 and 10 cm (i.e., 1 water sample per each 6-10 cm stage increment). In addition, manual samples were taken and stored in 1-litre-bottles during flood events and routinely (weekly or fortnightly), mostly during low flows. Due to the highly turbulent flow conditions, mixing was also assumed complete and none spatial or depth variability correction factor was applied. Overall, data collection resulted in a total of 1089 samples of suspended sediment over the five sub-basins and the entire catchment (EA047: 544; Cabecera: 182; Villacarli: 168; Carrasquero: 51; Ceguera: 49; Lascuarre: 126). Samples were vacuum filtered (Millipore, 0.045 mm pore size) or decanted when concentrations were above 2 g l^{-1}, oven-dried and weighted to determine the suspended sediment concentration.

Rainfall

Precipitation was measured by the CHE by means of 2 tipping-bucket rain gauges located in Les Paules (Cabecera sub-basin, Fig. 1c) and EA047 (Fig. 1c). To complete the rainfall record across the basin, we installed two Campbell ARG100 tipping-bucket rain gauges in the villages of Villacarli (Villacarli sub-basin, Fig. 1c) and Roda de Isábena (located downstream of the Carrasquero and Isábena confluence, Fig. 1c). Both were connected to a Campbell CR-200 data-logger, setting-up the measurements at 1-min intervals. To improve model performance (i.e., non-parametric statistical models

were selected to produce continuous sedigraphs for each sub-basin; see following section for a complete description), four additional tipping-bucket rain gauges located within less of 10 km from the Isábena water division), were also incorporated in the data acquisition design (for more details, see López-Tarazón et al., 2010b). All rain gauges operated by CHE registered accumulated rainfall values every 15 minutes.

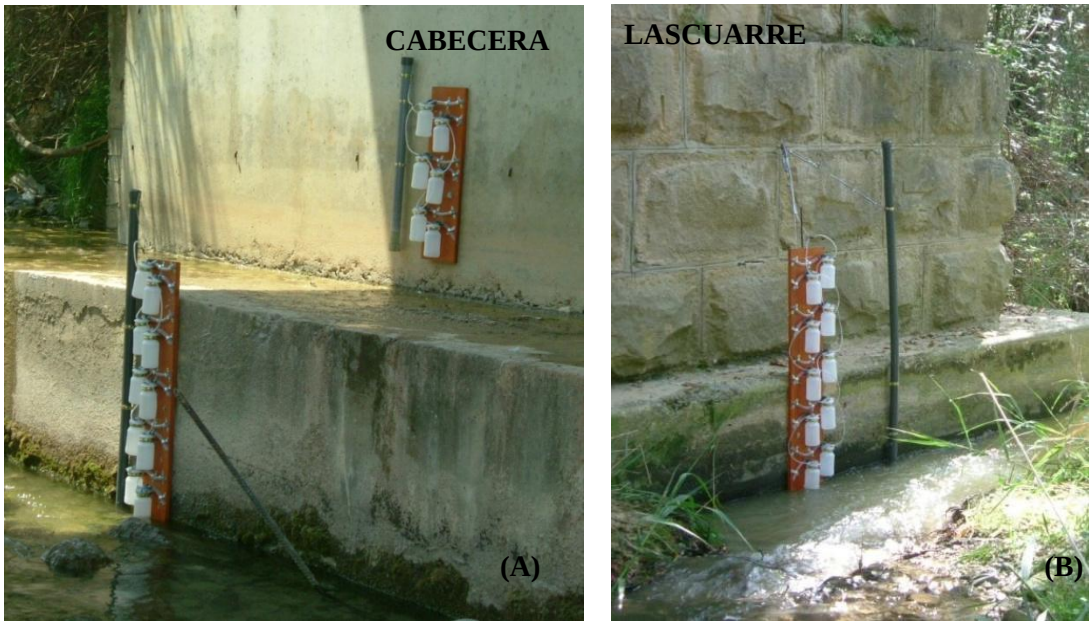

Figure 2. Examples of the instrumentation installed at the monitored sub-basins: (A) Cabecera, (B) Lascuarre. Note that the capacitive water stage sensors (Trutrack WT-HR) are installed inside the grey PVC tubes.

3.2. Interpolation of the suspended sediment concentration

The use of traditional Flow Duration Curve methods (Walling, 1984) to estimate sediment yields was not possible due to the poor statistical relations founded between discharge (hereafter *Q*) and suspended sediment concentration (hereafter *SSC*) at all the monitoring sections (for more details see table 2). *SSC*s for a given discharge could oscillate up to five orders of magnitude (see Lopez-Tarazon et al., 2009 for an example at Capella). Instead of that, continuous sedigraphs were derived for all the sites using Random Forest and Quantile Regression Forest models (hereafter *RF* and *QRF*, respectively) allowing, this way, the estimation of sediment yields from ancillary data. The *QRF* (Meinshausen, 2006) is a non-parametric multivariate regression technique that builds on *RF* regression tree ensembles (Breiman et al., 1984). Regression trees (i.e., CARTs, Breiman et al., 1984) are constructed by recursive data partitioning, which

can include both categorical and continuous data from ancillary datasets. *RF* and *QRF* employ an ensemble of these trees, each one grown on a random subset of the training data. In *RF*, model estimates are based on the mean of all tree predictions, whereas *QRF* employs the whole distribution of tree predictions and hence, offers the possibility to assess the accuracy and precision of model estimates (Meinshausen, 2006; Table 2). The advantage of both *RF* and *QRF* is their ability to perform favourably when dealing with nonlinearity, imply no assumptions about the distribution of the data and are robust and capable of handling non-additive behaviour and non-Gaussian data, which makes these techniques particularly suited for *SSC* modelling (see more details in Francke et al., 2008a,b).

Table 2. Summary of the ancillary predictors used to model the sedigraphs and their meaning (see equations (1) and (2) for the definition of temporal shifts).

General Predictor	Example	Meaning
Limb$_i$	Limb$_1$	Change in discharge for an *i* timestep
Sin	Sin	Day of the year (following the Julian calendar) in a sinusoidal form
P$_{x\text{-}i}$	P$_{Capella\text{-}135}$	Cumulated rainfall at a determinate location and temporal shift
Q$_{x\text{-}i}$	P$_{Capella\text{-}135}$	Cumulated discharge at a determinate location and temporal shift

Suspended sediment transport in the monitored Isábena sub-basins was analyzed thus using data obtained from this modeling approach. To construct continuous sedigraphs, we have modeled the suspended sediment at 15-min resolution (considered a high temporal frequency), predetermined by the maximum resolution of our rainfall and discharge data. To run the model we used ancillary predictors from rainfall and discharge data (P_n, Table 3) derived from their primary predictors P (e.g., rainfall and discharge) by using increasing temporal shifts (a_0) and window sizes (S_n) and keeping correlation between the derived predictors as low as possible:

$$S_n = \begin{cases} a_0 \sum_{k=0}^{n} q^k & \forall n \geq 0 \\ 0 & n = -1 \end{cases} \quad (1)$$

$$P_n(t) = \sum_{i=S_{n-1}+a_0}^{S_n} P(t+1) \quad (2)$$

where a_0 denotes the temporal resolution of the rainfall and discharge time series, q is the growth factor for the temporal shifts and window sizes, and n denotes the respective time period. For our *SSC* predictions we used 8 levels of S_n (n=0, 1, 2…7) for rainfall

and discharge, which corresponds with pre-event periods of 22 days, 18 hours and 45 minutes (given q=3, and a_0=15 min), respectively. The ancillary datasets were selected according to the perceived capability of representing (i.e., drive) relevant processes as, for example, sediment production on slopes or in the riverbed, exhaustion of sediment supply on slopes or within the riverbed and dilution (e.g., Schnabel and Maneta, 2005). As additional predictors, we used the day of year (i.e., Julian calendar) to capture the pronounced seasonality and the change in discharge as a useful indicator for intra-event dynamics. The procedure to obtain ancillary variables described above yields predictors that contain discrete portions of information, which reduces multi-collinearity and allows a clearer identification of variable importance.

We assessed the variable importance, *VI*, with a permutation-based measure (Liaw and Wiener, 2002). The *VI* is calculated as the difference in mean square error (*MSE*) on the out of bag data (*OOB*, data not used for modeling) for each tree t, with $t \in \{1,...,ntree\}$, and the *MSE* also using the *OOB* data but with permuted values of a predictor (P^*). The differences in *MSE* are then averaged over all trees and normalized by the standard error:

$$VI = \frac{\frac{1}{ntree}\sum_{n=1}^{ntree} d}{\frac{\sigma(d)}{\sqrt{ntree}}} \quad (3)$$

$$d = MSE_{OOB}^{t,P^*} - MSE_{OOB}^{t,P} \quad (4)$$

$$MSE_{OOB} = \frac{\sum_{i=1}^{n}[SSC_{obs}(i) - SSC_{mod}(i)]^2}{n} \quad (5)$$

where SSC_{obs} and SSC_{mod} refer to observed and modeled *SSC* values. Predictors with low importance have a low impact on model quality, and hence show relatively small *VI* values. In order to compare the influence of predictors among all monitoring sites we normalized them to 100% (Fig. 3). Model building and statistical analyses were conducted using the statistic software R (R-Team Development Core, 2006) with the Random Forest (Liaw and Wiener, 2002) and quantregForest (Meinshausen, 2007) packages.

Table 3. Performance of *SSC* prediction using *RF*/*QRF* in comparison with traditional sediment rating curves.

Sampling site	Model	*n*	R^2	V (%)[a]
Cabecera	*SSC* – *Q*	161	0.04	-
	log(*SSC*) – log(*Q*)		0.06	-
	RF		-	41
	QRF		-	26
Villacarli	*SSC* – *Q*	138	0.11	-
	log(*SSC*) – log(*Q*)		0.09	-
	RF		-	52
	QRF		-	23
Carrasquero	*SSC* – *Q*	45	0.08	-
	log(*SSC*) – log(*Q*)		0.16	-
	RF		-	57
	QRF		-	28
Ceguera	*SSC* – *Q*	33	0.16	-
	log(*SSC*) – log(*Q*)		0.16	-
	RF		-	29
	QRF		-	18
Lascuarre	*SSC* – *Q*	118	0.13	-
	log(*SSC*) – log(*Q*)		0.15	-
	RF		-	60
	QRF		-	50

[a] Explained variability

3.3. Sedigraph prediction and estimation of sediment yield

By applying the most appropriated model to the data of the complete monitoring period (July 2007 - July 2009) *SSC* data for each time step and each study site was derived; this way, three *SSC* values for each time step and site were calculated: i) a 'best estimate', for both *RF* and *QRF*, being the value predicted by the model and used afterwards for the estimation of the total loads, and ii) a lower and upper value (just for *QRF*) comprising the 95% confidence interval for prediction. Finally, the suspended sediment yield (hereafter *SSY*) for each time step (15-min) was obtained by multiplying *SSC* (i.e., *SSC* transformed from the turbidity record in the case of Capella, for more details see López-Tarazón et al., 2009; the *SSC*s modelled in the case of the sub-basins) and the associated discharge value. The Gaussian shape of the *SSY* distributions were confirmed in all cases. Despite that the uncertainties implicitly included at *QRF* are bigger than in *RF*, we decided to use the latter consistently instead of the former because of the better performance given by *RF* (Table 2).

The random drawing of predicted *SSC* values described above implies the assumption of uncorrelated model errors (e.g., e) defined here as the absolute differences between

observed and predicted values. We verified this assumption by analyzing the temporal correlation of e using variograms. For a detailed description of variogram modeling in the temporal domain we refer to the work of Zimmermann et al. (2009).

In the case of the Villacarli sub-basin and due to the inconsistency of the hydrological dataset (i.e., *Q*) it was not possible to model the continuous 15-min sedigraph using the non-parametrical techniques for the whole period. Data acquisition was interrupted mainly because of vandalism and technical problems (i.e., at-a-site extreme sedimentation). Due to such problems the capacitive sensor had to be replaced five times during the monitoring period (the exact period of sampling of each sub-basin can be seen in Table 1). Villacarli's sediment loads had to be thus estimated as the difference between the sum of the modeled sediment load of the others sub-catchments and the sediment load calculated at the outlet of the basin (i.e., EA047). The sediment load resulting from this subtraction corresponds to the sum of Villacarli's load and the rest of the ungauged areas of the basin (altogether 201 km^2, the 45% of the entire catchment area). However, based on field observations and due to a) the relatively high abundance of badlands in the Villacarli sub-catchment in comparison to other parts of the basin (i.e., up to 6% of its total area), b) the differences in precipitation (i.e., the highest rainfall intensities and total amounts of precipitation were always registered at the Villacarli's rain gauge), c) the relief gradient (i.e., with a longitudinal slope >9%, the largest of the basin; Table 1), d) the relatively modest area and e) the ephemeral flows typically present in the other creeks, we hypothesize that the most of the sediment comes directly from Villacarli. This assumption allows us to clarify the interpretation of the Isábena sediment budget and to discuss the role of badland areas in the total sediment load. Despite this limitation, modeling in Villacarli could still be applied for some weeks when the station stayed in operation (i.e., 23 weeks, from 16th of November 2007 to 1st of April 2008). This period forms part of the study period presented in this paper; but, in addition, water and sediment load had been measured before (i.e., 28 weeks, from 1st of October 2006 to the 28th of January 2007 and from 2nd of March 2007 to the 8th June 2007). *SSC*s for those periods were estimated by applying the above described modeling approach. Results could be then compared with those obtained in the other monitored sections for the same period of time. Results were then used to

compare patterns observed in Villacarli in relation to the neighboring sub-catchments, the main channel and the whole basin.

4. RESULTS AND DISCUSSION

4.1. Discharge and suspended sediment concentration

Table 4 summarizes *Q* and *SSC* measurements at the six monitoring sections. The maximum *Q* increases with increasing catchment size. The smallest sub-catchments (e.g., Carrasquero and Ceguera, size area of 25 and 28 km^2 respectively) showed the smallest *Q* peaks (e.g., 2.02 and 3.25 $m^3\ s^{-1}$, respectively) during the study period. Almost all sub-basins showed a flashy behaviour, with a time response of just 1 to 2 hours after a heavy rainfall (i.e., >20 mm h^{-1} at a 15-min interval, which is the minimum estimated value to consider the infiltration excess surface flow as "Hortonian overland flow"; Selby, 1982) and recessions usually lasting more than one day. Cabecera, as the largest sub-basin draining the headwaters of the main Isábena, experienced the highest *Q*, with a maximum recorded value of 63 $m^3\ s^{-1}$. There, the onset of floods was, on average, seven hours later than that observed in the rest of the sub-catchments, although water stage roused sharply. Both, this delay and the much flatter recession limb suggest a considerably less flashy runoff regime than that in the other sub-basins. *Q* at Capella (i.e., EA047, the catchment outlet) is mainly controlled by the input from Cabecera which, on average, yielded the 68% of the runoff of the entire catchment (very similar to values reported by Verdú et al., 2007b). The delay of the basin's response to floods in Capella, when compared with the sub-basins, varied greatly (e.g., 7 hours between Villacarli and Capella, and 2 hours between Lascuarre and Capella); and occasionally even preceded some of them, showing the effect of the flashy tributaries located downstream (e.g., Ceguera and Lascuarre) and the heterogeneity of the rainfall distribution. The irregular distribution of rainfall and the different runoff responses are also reflected in the occurrence of floods at each of the sub-catchments; i.e., 21 flood events occurred in Cabecera, 24 occurred in Carrasquero, 31 in Ceguera and 33 floods in Lascuarre. Further downstream, at the Capella gauging station, 30 floods have been observed. As previously described, it has not been possible to determine the number of floods that occurred at Villacarli due to the inconsistency of the *Q* record. Nevertheless,

if we compare the periods with available *Q* data at Villacarli and at the rest of the gauging sections, it appears that the total number of floods at each sub-basin is very similar, keeping the magnitude differences on the flood-peaks as explained above (Table 5). A total of 8 floods were register in Villacarli, Cabecera and Capella (i.e., the monitored basins at that moment) during the period September 2006 - January 2007; further, for the period March 2007 – June 2007, 5 floods were registered in Villacarli and 6 in Capella (i.e., the rest of the sub-basins were not instrumented and the instrumentation of Cabecera was broken down); finally, 6 floods were registered in Villacarli, Lascuarre and Capella, 5 were recorded in Ceguera and 4 happened in Cabecera and Carrasquero, during the period November 2007 – April 2008 (when instrumentation was fully operative in the whole basin).

Table 4. Summary of measured discharge (*Q*), specific discharge (Q_s) and suspended sediment concentration (*SSC*) data at the 6 monitored sections during the study period.

Sections	***Q*** **($m^3 s^{-1}$)**			***Q_s*** **($l s^{-1} km^{-2}$)**			***SSC*** **($g l^{-1}$)**		
	Min	**Mean**	**Max**	**Min**	**Mean**	**Max**	**Min**	**Median**	**Max**
Cabecera (n= 182)	0.73	2.94	63.06	5.00	20.14	431.92	0.001	0.18	45.87
Villacarli (n= 168)	*N/A*	*N/A*	*N/A*	*N/A*	*N/A*	*N/A*	0.001	0.77	277.85
Carrasquero (n= 51)	0.04	0.15	2.02	1.60	6.00	80.80	0.001	0.03	106.54
Ceguera (n= 49)	0.00	0.50	3.25	0.00	17.96	116.07	0.002	0.31	140.63
Lascuarre (n= 126)	0.00	0.20	21.25	0.00	4.40	472.22	0.001	31.05	396.22
Capella (n= 544)	0.21	4.02	101.55	0.47	9.03	228.21	0.002	1.35	89.18

Suspended sediment concentration follows a different behaviour: the largest sub-basin (i.e., Cabecera) yielded the lowest sediment concentrations. In the smallest sub-basins (e.g., Carrasquero and Ceguera), concentrations varied from 0.001 g l^{-1} to 107 and 141 g l^{-1}, respectively, while in Villacarli and Lascuarre concentrations ranged from 0.001 g l^{-1} to 278 and 396 g l^{-1}, respectively. In all cases, *SSC* ranged over a 5 orders of magnitude. The return of *SSC* to pre-flood levels is usually quicker than the recession of the hydrograph (independently of the rainfall intensity), a fact that may suggest a certain exhaustion of sediment in the catchments; decline of *SSC* during flood recession can be interrupted by rainbursts (e.g., the flood registered at Lascuarre in April 11th 2009, in which a second peak at the sedigraph was delayed 7 hours from the peak of the hydrograph, during the flood recession). In the case of Cabecera (the largest sub-basin) and Capella (the entire catchment), *SSC* varied from 0.001 g l^{-1} to 46 and 89 g l^{-1}, respectively, covering 4 orders of magnitude. *SSC* is generally one order of magnitude

lower than those measured in the other 4 sub-basins during the study period; nevertheless, it is worth to mention that higher instantaneous *SSC* (i.e., > 300 g l^{-1}) has been obtained at the Capella gauging station during a flood event recorded before the period analysed in this paper (López-Tarazón et al, 2009). Sediment dynamics appear to be mainly influenced by local rainbursts (e.g., flood event sampled at Capella in September 28th 2006), which often produce *SSC* peaks long before maximum discharge is reached. This behaviour (i.e., counterclockwise hysteresis loops) confirms the patterns found by López-Tarazón et al. (2009), in which the 60% of the 73 analysed floods followed that loop-shape. This pattern is driven by the relatively high sediment availability in the river channel near the outlet of the basin (see López-Tarazón et al., 2010a, for a complete discussion of the role of in-channel sediment storage on suspended sediment transport patterns). Flood peaks and related sediment concentrations decreased in direct relation to rainfall magnitude, as reported by López-Tarazón et al. (2010b).

Table 5. Villacarli's water yield (*WY*), modeled sediment load (*SSL*), number of flood-events and maximum peak discharge (Q_{max}) registered at the periods where data was available. Comparison with the results obtained at the other sub-basins.

Sub-basin		**Period**		
		09/2006 - 01/2007	**03/2007 - 06/2007**	**11/2007 - 04/2008**
Capella	*WY* (hm^3)	60.4	60.0	10.4
	SSL (t)	174,128	35,883	18,094
	Floods (n)	8	6	6
	Q_{max} (m^3 s^{-1})	88.6	70.8	78.6
Cabecera	*WY* (hm^3)	34.5	*N/A*	12.9
	SSL (t)	22,026	*N/A*	520
	Floods (n)	8	*N/A*	4
	Q_{max} (m^3 s^{-1})	43.4	*N/A*	39.8
Villacarli	*WY* (hm^3)	6.5	3.5	2.4
	SSL (t)	74,392	25,244	6,908
	Floods (n)	8	5	6
	Q_{max} (m^3 s^{-1})	21.2	1.8	24.0
Carrasquero	*WY* (hm^3)	*N/A*	*N/A*	1.0
	SSL (t)	*N/A*	*N/A*	102
	Floods (n)	*N/A*	*N/A*	4
	Q_{max} (m^3 s^{-1})	*N/A*	*N/A*	0.6
Ceguera	*WY* (hm^3)	*N/A*	*N/A*	2.4
	SSL (t)	*N/A*	*N/A*	168
	Floods (n)	*N/A*	*N/A*	5
	Q_{max} (m^3 s^{-1})	*N/A*	*N/A*	3.6
Lascuarre	*WY* (hm^3)	*N/A*	*N/A*	0.1
	SSL (t)	*N/A*	*N/A*	191
	Floods (n)	*N/A*	*N/A*	6
	Q_{max} (m^3 s^{-1})	*N/A*	*N/A*	6.6

4.2. Modelling *SSC*s: Defining Predictors

Our analysis of variable importance (Fig. 3) indicates that, with the exception of Cabecera, predictors containing hydrological information from a time span of less than 1 hour prior the *SSC* prediction are the most influential. This fact reflects the fast hydrological response to rainfall in most of the study basins. In the case of Cabecera (the largest sub-basin), the most influential predictors are those related to a previous rainfall from a time span of 2 hours to more than 22 days, revealing that the hydrosedimentological response of this sub-basin is, overall, less flashy than in the other sub-basins, probably due to the size, vegetation cover (e.g., humid forests, in contrast to the Mediterranean vegetation and agricultural areas in the lower Isábena) and geology (e.g., badlands are not present). Finally, other important variables found were the day of the year (e.g., Day), that is related to annual water and sediment dynamics, and abrupt changes in the shape of the hydrograph (e.g., Limb), that can be related to the magnitude and energy of the floods.

The explanatory power of the variable importance procedure has its limitations because the importance of a variable may result from complex interactions with other variables (Liaw and Wiener, 2002). It remains thus difficult to assess the influence of the predictors in a greater detail. Due to the likely influence of such interactions, we did not attempt to reduce the number of variables but omitted those showing lower importance.

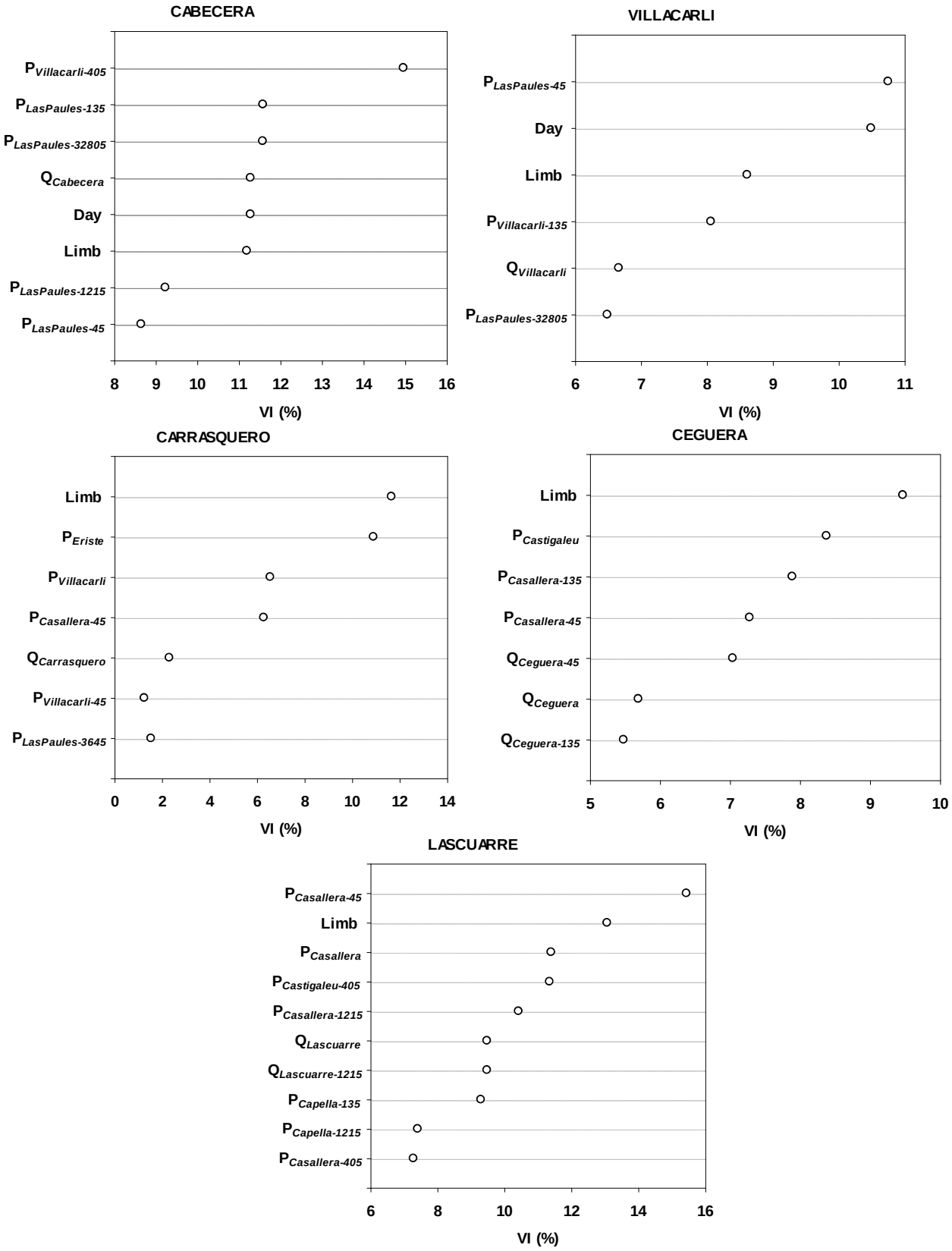

Figure 3. Variable importance of *SSC* predictions for each sub-basin normalized to 100%. Abbreviations are shown in Table 2. Note that in the case of Villacarli, the values correspond just to the periods in which modeling was possible.

4.3. Modelling *SSC*s: Prediction of sedigraphs

The modelled sedigraphs show moderate agreement with the observed data (Table 2, Fig.4); we see this fact a step forward taking in account the highly complex hydro-sedimentary response of the catchments as explained before. Variability explained by the modelled data after validation with real data differs considerably between sub-basins varying, in the case of *RF*, from the 29% in Ceguera to the 60% in Lascuarre. Obviously, the sub-basin with less sample availability (i.e., Ceguera, 33 samples) was the one which performed the worst; nevertheless, the sub-basin with the highest sample availability (i.e., Cabecera, 161 samples) did not perform the best, remarking its highly dynamic hydro-sedimentological response. High *SSC* values, mainly at the beginning of the observational period, are underestimated: up to 60% of difference between modelled and real data was observed during the 2 first monitoring months; this value was quickly reduced, achieving differences <10% from the 3rd monitoring month. This underestimation could be due, probably, to the limited number of observations, especially at the beginning of the study period. At some of the monitoring sections (e.g., Cabecera, Lascuarre and Ceguera) *SSC* values tend to be underestimated during flood peaks, especially at the beginning of the observational period and at the same order of magnitude explained above (e.g., up to 60% during the initial monitoring months; <10% for the rest of the monitoring period, increasing until the 25% during floods of a high or very high magnitude); this effect may lead to a slight underestimation of the initial sediment yields (i.e., summer 2007) but, due to the low runoffs recorded during that period the phenomena can be considered negligible.

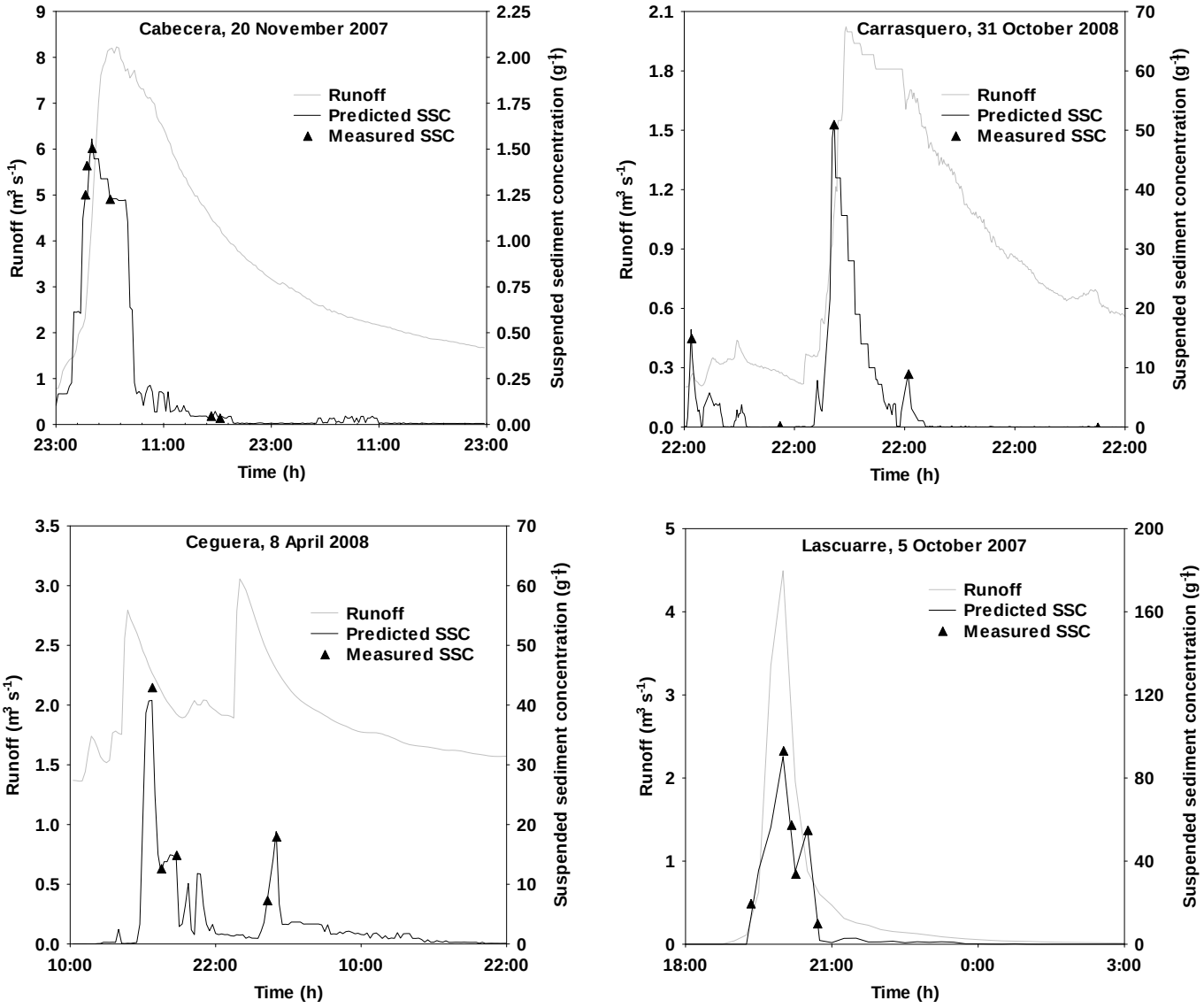

Figure 4. Close-up-view of runoff and suspended sediment concentration (*SSC*) measured and predicted by using *RF* for one flood at each of the measuring sections.

4.4. The sediment budget of the Isábena catchment

The information provided by the individual components of the data collection programme described above has been synthesized to establish a seasonal and annual suspended sediment yield for each studied sub-catchment and, finally, a total catchment budget for the period 2007-2009. For several elements of the sediment budget, and due to some technical problems (e.g., Villacarli), this synthesis has involved several assumptions and extrapolations as has been fully explained in section 3. As a result, the

final budgets necessarily involve a number of uncertainties. Despite limitations, results are seen as providing an important advance in the current understanding of the key features of the sediment budgets of such high erodible areas in Mediterranean mountainous catchments.

The distinct role of the Villacarli sub-basin and the in-channel sediment storage

In the case of Villacarli, water and sediment yields could be modelled just for few periods (i.e., when the discharge record was available); comparison with the other sub-catchments was done just for those periods when common data was available (see Table 5 for details). These values show a first approximation to the sediment patterns of the Isábena catchment: the sediment load in Villacarli is always much higher than in the other sub-catchments, constituting the most important fraction of the load exported at Capella (e.g., varying from 40% during the third period to 70% in the second one); water yield is, however, very low in relation to Cabecera and Capella but in the same order of magnitude than that in the other sub-basins.

It is also important to mention the role of the in-channel suspended sediment storage that, besides from the direct sediment delivery from the sub-catchments, has been identified as one of the main sediment sources during flood events (López-Tarazón et al., 2010a). An additional calculation to those of López-Tarazón et al., (2010a) has been made for the period for which all monitoring stations were fully in operation. In that period (November 2007 – April 2008, Table 5), the difference between the sediment transported in Capella and the sum of the sediment transported in each sub-basin is ca.10,000 t (e.g., a value that represents the 56% of the total load passing through the Capella gauging station); this observation indicates that the channel clearly acted as a net source of sediment, corroborating thus our previous results (i.e., role of the in-channel storage over the total sediment load of the basin can account for up to the 55% during given periods). Moreover, that particular season was the driest during the whole study period, with no significant flood events; this fact remarks the role of the in-channel contribution to the suspended sediment transport during periods of low flows, as reported by López-Tarazón et al. (2010a).

Sub-catchments runoff and sediment load

Table 6 presents the summary of the seasonal and annual water and sediment yields of the entire basin and the sub-catchments. At the basin scale, both years behave similarly: average precipitation in 2007-2008 was 745 mm while in 2008-2009 was 730 mm; water yield was 130.8 hm^3 for the first year and 139.9 hm^3 for the second. These values can be considered as moderately dry comparing them with the mean long-term annual water yield (i.e., 177 hm^3 for the period 1945-2008) but they are average in relation to the ones obtained during the last 5 years, since the Isábena is being monitored (121 hm^3 $y^{-1}$for the period 2005-2010). The annual suspended sediment load at the basin outlet was 225,800 t for the 2007-2008 and 243,500 t for the 2008-2009. These values are in the range of those obtained by López-Tarazón et al., (2009) for the period 2005-2008 (i.e., average of 180,000 t y^{-1} for the period May 2005 to May 2008).

Table 6. Summary of the seasonal and total precipitation (*P*), water yield (*WY*) and suspended sediment load (*SSL*) at the whole basin and its sub-basins during the study period.

Period	Basin	Capella		Cabecera		Villacarli[a]		Carrasquero		Ceguera		Lascuarre	
	P (mm)	*WY* (hm^3)	*SSL* (t)	*WY* (hm^3)	*SSL* (t)	*WY* (hm^3)	*SSL* (t)	*WY* (hm^3)	*SSL* (t)	*WY* (hm^3)	*SSL* (t)	*WY* (hm^3)	*SSL* (t)
Summer 07	99	8.5	19,429	6.3	116	1.6	11,507	0.4	29	0.0	0	0.2	7,776
Autumn 07	86	8.9	10,044	6.9	696	1.3	8,430	0.6	33	0.1	175	0.1	711
Winter 08	109	13.4	11,032	9.1	305	1.2	10,094	0.7	74	2.4	336	0.1	223
Spring 08	451	100.0	185,317	63.5	23,888	29.2	108,352	0.5	308	4.5	8,304	2.3	44,465
Summer 08	106	10.5	11,612	8.4	569	1.5	6,095	0.4	34	0.0	0	0.2	4,913
Autumn 08	235	26.9	67,922	18.8	29,275	2.1	12,395	1.8	1,417	3.3	6,561	0.8	18,275
Winter 09	130	44.7	35,577	28.4	2,237	4.0	17,342	2.6	474	6.3	7,297	3.4	8,227
Spring 09	259	57.8	128,413	42.2	15,861	1.9	29,628	2.4	1,216	6.0	15,519	5.3	66,189
2007-2008	745	130.8	225,822	85.7	25,005	33.4	138,382	2.1	444	7.0	8,815	2.6	53,175
2008-2009	730	139.9	243,524	97.8	47,942	9.5	65,461	7.3	3,141	15.6	29,377	9.7	97,603

[a] Water and sediment yield correspondent to the Villacarli sub-basin and the ungauged catchment's area.

At a sub-basin scale, and confirming the results obtained by Verdú et al. (2007b), it becomes clear that Cabecera controls the hydrology of the Isábena basin while Villacarli and Lascuarre contribute with most of the suspended sediment load (*SSL*). Carrasquero and Ceguera yield very low water and *SSL* (Table 6). Water yield of the year 2007-2008 was of 85.7 hm^3 in Cabecera, while Carrasquero, Ceguera and Lascuarre generated 2.1, 7 and 2.6 hm^3 respectively. Villacarli yielded 33.4 hm^3 of water; however, Villacarli values were estimated by subtracting the sum of all sub-catchments estimations to the values obtained at the outlet of the basin, so an overestimation may be expected. Water

yield during the 2008-2009 followed a similar pattern: Cabecera yielded 97.8 hm^3, while Villacarli, Carrasquero, Ceguera and Lascuarre yielded 9.5, 7.3, 15.6 and 9.7 hm^3 respectively.

Regarding to the suspended sediment load, Villacarli and Lascuarre recorded the highest values at both seasonal and annual scales (Table 6; Figure 5). *SSL* for the year 2007-2008 was 138,400 t in Villacarli and 53,200 t in Lascuarre, while in Cabecera, Carrasquero and Ceguera was 25,000, 444 and 8,815 t respectively. Spring 2008 (e.g., the wettest season of the study period) was also the season with the largest *SSL* at the Villacarli monitoring station: 108,350 t were estimated, a value that represents the 78% of the Villacarli's sediment load and 48% of the Isábena basin's sediment load of that year. Lascuarre lead the sediment yield for the year 2008-2009, with a total value of 97,600 t for the 65,500 t that were estimated for Villacarli. Cabecera registered 47,950 t, while Carrasquero and Ceguera accounted for 3,141 and 29,377 t, respectively. Besides owing for most of the badlands in the whole catchment, the contribution of Villacarli and Lascuarre to the total sediment yield in the basin was probably driven also by the distribution of the rain (total amount and intensity) across the basin. During the first year, the precipitations were rather uniformly distributed along the whole Isábena basin (i.e., <15% of difference between all the rain gauges) while during the second year the most intense events (i.e., those exceeding the limit to generate the "Hortonian overland flow"; Selby 1982) succeeded mainly in the lower Isábena, where Lascuarre is located. This issue can be also applied to Ceguera (e.g., located at the lower Isábena as well), and Carrasquero (e.g., located at the medium Isábena) whose runoff during the second year was more than double than during the first study year. Results in table 6 confirm the sedimentary behaviour reported by López-Tarazón et al. (2010b) i.e., the sediment transport in the Isábena basin is mainly controlled by the precipitation; that is, the highest sediment yield values were always registered at the wettest seasons.

Suspended sediment loads were related to each sub-catchment area to calculate average specific sediment yields (hereafter *SSYs*). Average *SSY*s for the entire monitoring period range for over an order of magnitude between basin sub-catchments, varying from 72 t km^{-2} in Carrasquero, 250 t km^{-2} in Cabecera, 682 t km^{-2} in Ceguera, 1,675 t km^{-2} in Lascuarre and 2,427 t km^{-2} in Villacarli (Table 7). In this case, the calculations of

Villacarli have been obtained using its basin size (42 km^2) instead of using the size of the whole ungauged catchment's area assuming than almost all sediment is exported directly from Villacarli's basin and the contribution of the rest of the ungauged area is minimum (see sediment export from Carrasquero as surrogate of the other small sub-catchments). Values from Villacarli and Lascuarre are in the range of those obtained on similar landscape (i.e., presenting highly erodible areas) such as Vallcebre in the Western Pyrenees (2,800 t km^{-2} y^{-1}, 5 years of monitoring, Regüés et al., 2000a,), despite of being more than 40 times larger in area. The *SSYs* obtained for the entire Isábena catchment at Capella is 527 t km^{-2}. This number plots above the 350 t km^{-2} y^{-1} yield for the entire Ésera catchment (e.g., 1,600 km^2) reported by Sanz Montero et al. (1996) and ranks high in relation to data for 44 Mediterranean catchments given by de Vente et al. (2006), both being long-term estimates derived from reservoir siltation. The notable difference in *SSYs* between sub-catchments in the Isábena underlines the influence of different hydrological response and, especially, the predominant role of badlands as the primary sediment source. Figure 6 and table 8 present the spatial distribution of the water and sediment contribution of each sub-catchment to the whole basin.

Table 7. Specific suspended sediment yield (*SSYs*) of each sub-basin and the total catchment. In the case of Villacarli, the calculation of the *SSYs* has been done using its basin size, assuming as negligible the paper of the ungauged catchment's areas over the sediment load.

Period	Capella		Cabecera		Villacarli		Carrasquero		Ceguera		Lascuarre	
	SSL (t)	*SSYs* (t km^{-2})	*SSL* (t)	*SSYs* (t km^{-2})	*SSL* (t)	*SSYs* (t km^{-2})	*SSL* (t)	*SSYs* (t km^{-2})	*SSL* (t)	*SSYs* (t km^{-2})	*SSL* (t)	*SSYs* (t km^{-2})
Summer 07	19,429	44	116	1	11,507	274	29	1	0	0	7,776	173
Autumn 07	10,044	23	696	5	8,430	201	33	1	175	6	711	16
Winter 08	11,032	25	305	2	10,094	240	74	3	336	12	223	5
Spring 08	185,317	416	23,888	164	108,352	2,580	308	12	8,304	297	44,465	988
Summer 08	11,612	26	569	4	6,095	145	34	1	0	0	4,913	109
Autumn 08	67,922	153	29,275	201	12,395	295	1,417	57	6,561	234	18,275	406
Winter 09	35,577	80	2,237	15	17,342	413	474	19	7,297	261	8,227	183
Spring 09	128,413	289	15,861	109	29,628	705	1,216	49	15,519	554	66,189	1,471
2007-2008	225,822	507	25,005	171	138,382	3,295	444	18	8,815	315	53,175	1,182
2008-2009	243,524	547	47,942	328	65,461	1,559	3,141	126	29,377	1,049	97,603	2,169
Average	234,673	527	36,474	250	101,922	2,427	1,793	72	19,096	682	75,389	1,675

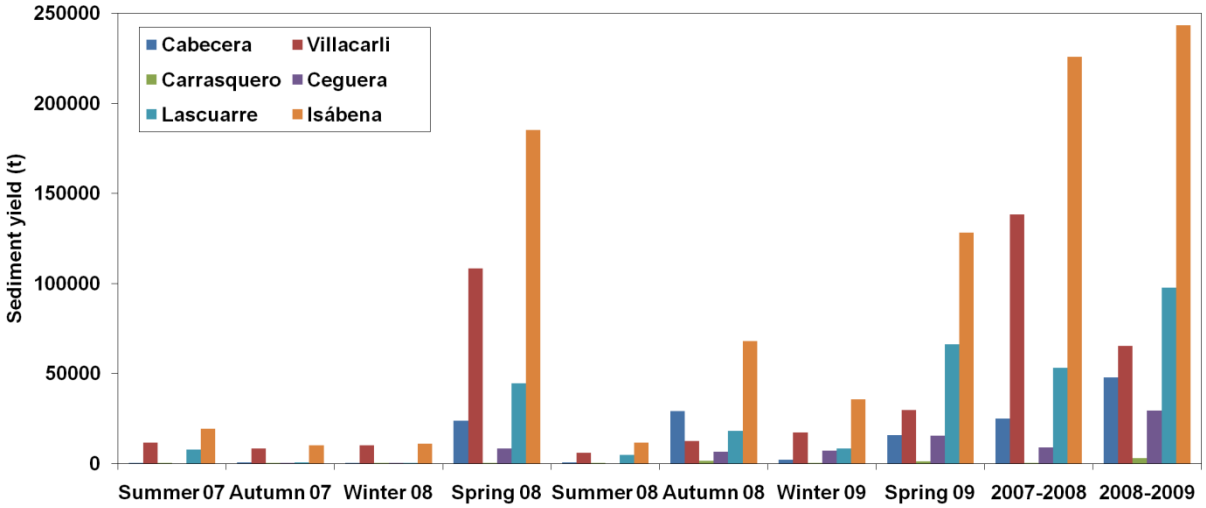

Figure 5. Suspended sediment yield of the whole basin for the study period.

Table 8. Water and sediment budget of the Isábena basin. The contribution of each sub-basin is represented as its percentage over the total water and sediment load.

Period	Basin	Cabecera		Villacarli[a]		Carrasquero		Ceguera		Lascuarre	
	P (mm)	*WY* (%)	*SSL* (%)	*WY* (%)	*SSL* (%)	*WY* (%)	*SSL* (%)	*WY* (%)	*SSL* (%)	*WY* (%)	*SSL* (%)
Summer 07	99	74.0	0.6	19.3	59.2	5.0	0.2	0.0	0.0	1.7	40.0
Autumn 07	86	77.1	6.9	14.9	83.9	6.4	0.3	0.9	1.7	0.7	7.1
Winter 08	109	67.9	2.8	9.2	91.5	5.0	0.7	17.5	3.1	0.4	2.0
Spring 08	451	63.5	12.9	29.2	58.5	0.5	0.2	4.5	4.5	2.3	24.0
Summer 08	106	80.1	4.9	14.1	52.5	4.3	0.3	0.0	0.0	1.6	42.3
Autumn 08	235	69.9	43.1	8.0	18.2	6.7	2.1	12.4	9.7	3.1	26.9
Winter 09	130	63.6	6.3	8.9	48.7	5.8	1.3	14.1	20.5	7.7	23.1
Spring 09	259	73.0	12.4	3.3	23.1	4.2	0.9	10.4	12.1	9.1	51.5
2007-2008	745	65.5	11.1	25.6	61.3	1.6	0.2	5.3	3.9	2.0	23.5
2008-2009	730	69.9	19.7	6.8	26.9	5.2	1.3	11.2	12.1	6.9	40.1
Total	1475	67.8	15.5	15.9	43.4	3.5	0.8	8.3	8.1	4.5	32.1

Residence time and denudation rates

The mean residence time of a given particle in the drainage system can be assessed by dividing the mass or volume of the sediment storage within the system by the annual transport or erosion rate (Dietrich and Dunne, 1978; Malmon et al, 2002; Phillips et al, 2007). Although sediment storage may play an important role on sediment transport processes, little research has been devoted to this issue. In our particular case, in-channel storage plays an important role in controlling basin's sediment yield (see López-Tarazón et al., 2010a). Nevertheless, due to the difficulties to estimate the total fine-sediment stored in the basin, an estimate was obtained by comparing the total sediment produced at the sources (e.g., badlands) and the total sediment exported at the

outlet for a given period. This way, it was assumed that all the sediment produced and not transported out of the basin is accumulated and rests available to be moved down during later floods. An investigation on the erosion rates at the badlands formation was done by Francke et al. (2008b). It was carried out by means of erosion pins whose exposed height was frequently measured to calculate the mean erosion rate, in combination with topographical surveys and digital elevation models. The total sediment eroded from the badland was quantified at around 96,710 t km^{-2} y^{-1}. Taking this figure as a representative value of the sediment contribution from badlands all over the catchment (4.75 km^2), total yield would results in around 456,000 t y^{-1}. If we compare this value to the mean sediment load measured at the outlet for the study period (e.g., 239,000 t y^{-1}), the mean residence time of a fine particle within the fluvial system would be around 2 years. This estimate matches to that predicted by López-Tarazón et al. (2010a) from field observations of in-channel sediment storage showing, this way, the high activity in the sediment production areas, and the quick transfer and transport processes in the Isábena basin. Swanson and Friedriksen (1982) assessed that the stored volume of sediment in the channel is commonly more than 10 times the average annual export of total particulate sediment, while in the same is less than 2. Batalla et al. (1995) reported a value of 28 years as mean residence time of a particle in the Arbúcies river-channel, in this case applied to bed-material transport.

Besides that, a significant geomorphological implication that can be derived from the previous investigations is the estimation of the denudation rate for the basin. Assuming a uniform contribution over the whole Isábena catchment area of the sediment exported out of the basin, the long-term denudation rate is estimated to be 0.2 m × 10^3 y^{-1}, using a bedrock density of 2.61 t m^{-3} measured by the authors and a mean sediment contribution of 239,000 t y^{-1}. Denudation rate plots remarkably higher than studies by Dietrich and Dunne in a basin in Oregon (0.03 m × 10^3 y^{-1}) and by Batalla et al., (1995) in the Mediterranean basin of Arbúcies (0.02 m × 10^3 y^{-1}); both showing a rather high degree of equilibrium between sediment contribution from hillslopes and sediment export; in contrast, the Isábena is controlled by a high sediment production from the badlands and a high connectivity between sources and the fluvial network, thus showing extreme geomorphic activity.

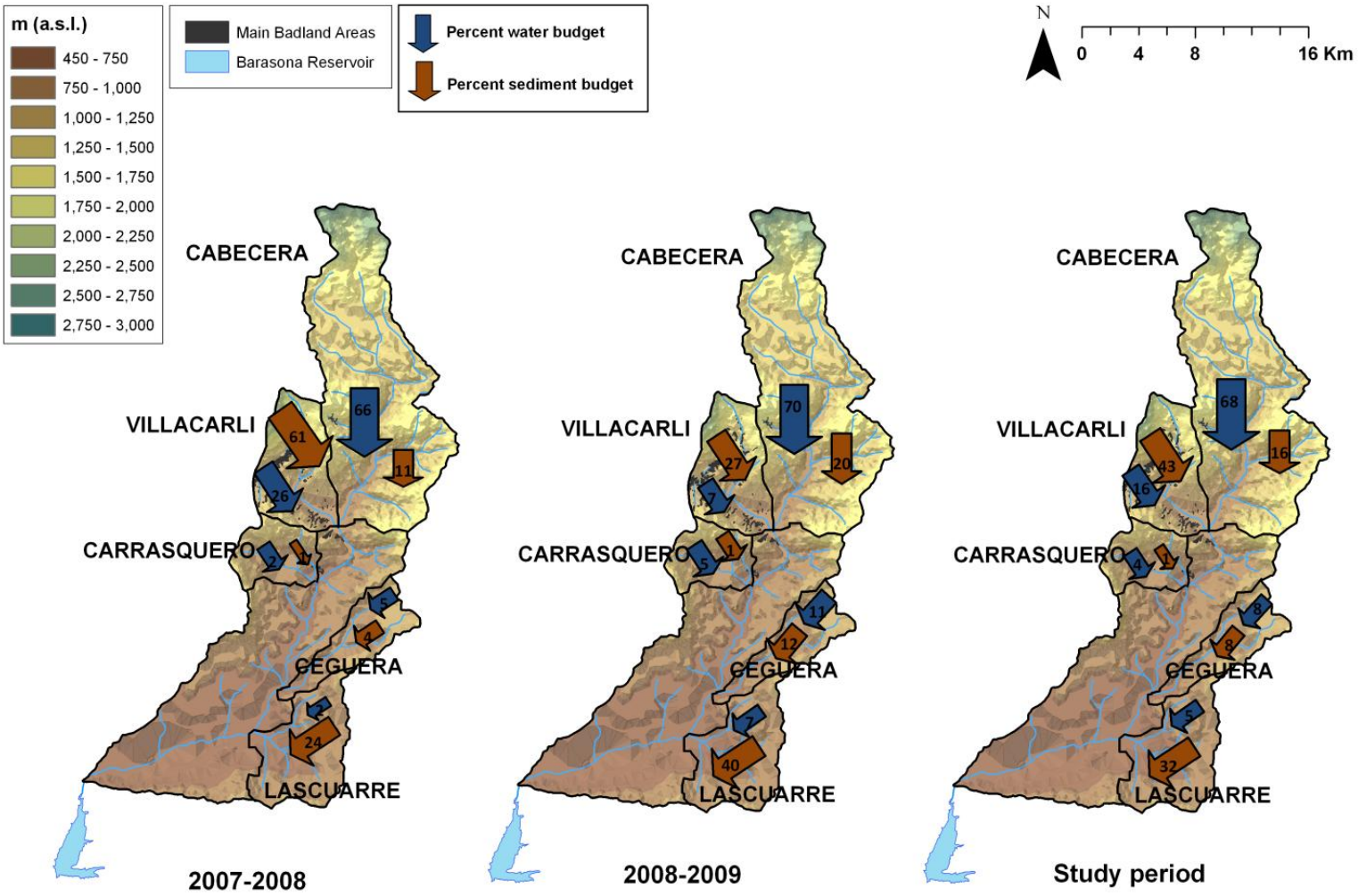

Figure 6. Water and sediment sub-catchment contributions to the Isábena basin for the study period: (A) 2007-2008 year, (B) 2008-2009 year and (C) whole study period. Inside the arrows there is shown the contribution (%) of each sub-basin and at each period.

Sediment delivery ratios

The sediment budget of the study basin is presented in Figure 7 by a schematic representation. To facilitate comparison between the different parts of the budget structure, the estimates of erosion and deposition depicted in Figure 7 have been expressed as annual sediment load and deposition (t y^{-1}); and, in order to emphasize the contrasts between them, the sediment inputs and outputs have been represented by arrows with a proportional width to their contribution. Budget has been constructed as follows: the suspended sediment input was calculated by the contributions to the basin of a badland formation (e.g., the same explained previously) that was monitored by the

authors (Francke et al. 2008b). Suspended sediment contribution of the badland formation to the main system resulted in 456,000 t y^{-1}. The storage in the active bed of the main channel (i.e., channel storage) was estimated using the results obtained by López-Tarazón et al. (2010a) (e.g., 5% of the total load transported at the catchment outlet, i.e., 12,000 t y^{-1}). Sediment output was estimated as the mean suspended sediment yield measured at the Capella gauging station (e.g., 239,000 t y^{-1}) for the study period. As a result, a component of sediment deposition and storage can be expected to occur in low order streams and the main valley floodplain; this conveyance loss or deposition (e.g., 205,000 t y^{-1}) has been estimated as the difference between the sediment input, the in-channel storage and the measured sediment output from the catchment.

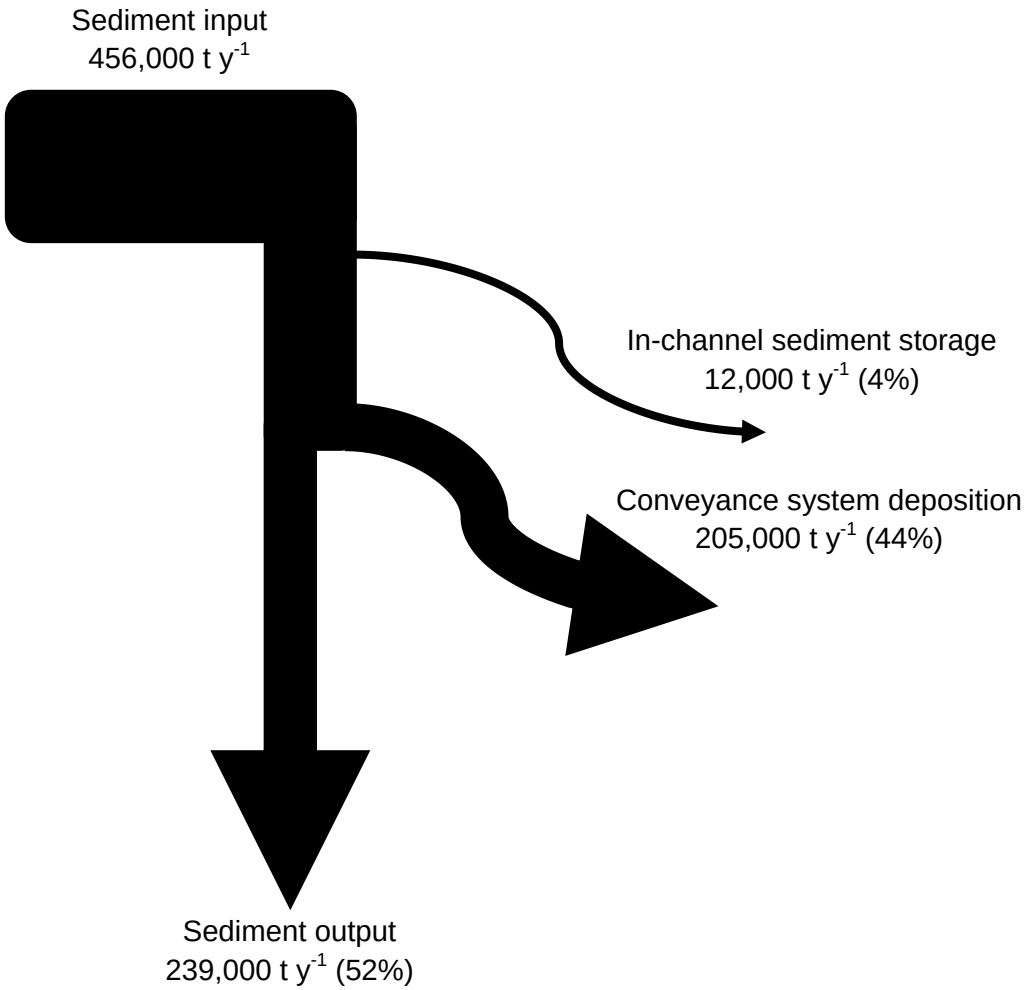

Figure 7. Schematic sediment budget for the Isábena catchment

Figure 7 clearly demonstrates the important differences between the sediment input, the in-channel storage, the sediment conveyance and the sediment output in the basin. In terms of absolute magnitudes it is clear that the sediment output is the most important component (i.e., arrow) in the figure. It indicates that a large part of the sediment mobilized from the catchment slopes reaches the catchment outlet, providing a sediment delivery ratio of 52%. Sediment conveyance losses also account for an important part of the sediment supply from the catchment (44%). This result is the consequence of the size of the basin (e.g., with a relatively low longitudinal gradient) and the frequent presence of a relatively well-developed valley floor where sediment is accumulated. The in-channel sediment storage represents a small part of the sediment budget, with ca. 4% of the sediment input, but constitutes an important factor in controlling the seasonal variability of the sediment load (i.e., ranging from 5 to 55% of the seasonal sediment yield, López-Tarazón et al., 2010a) and the high loads tipically transported during baseflows (López-Tarazón et al., 2009).

Figure 8 plots the relations between the estimated sediment delivery ratio and the catchment area for the present study and by data reported by other workers (e.g., Roehl, 1962; Williams and Berndt, 1972). The results obtained in these studies follow the same pattern: it appears clear the inverse trend between both variables, which largely reflects the increasing opportunity for sediment deposition and storage as catchment area increases. Nevertheless, in the case of the Isábena, this pattern is not seen; the Isábena, despite its size, matches with the sediment delivery ratios calculated for smaller basins (<10 km^2), showing the high sediment dynamics of the basin and the short residence time of the sediment within the basin.

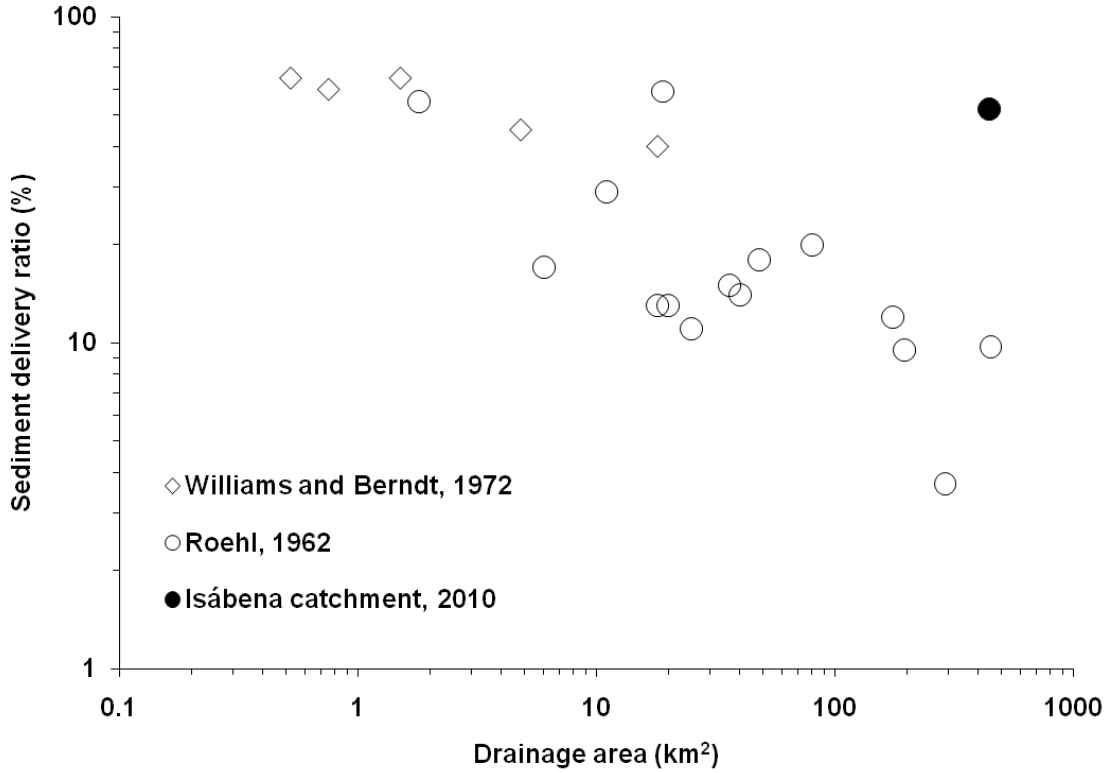

Figure 8. The relations between sediment delivery ratio and catchment area shown by the Isábena catchment and data reported for catchments in the United States by Roehl (1962) and Williams and Berndt (1972).

5. SUMMARY AND CONCLUSIONS

This paper has presented the sediment budget of the Isábena river basin, a mesoscale mountainous catchment located in the Central Pyrenees that generates unusually high sediment loads. The work has been focused on the description and quantification of the hydro-sedimentological dynamics of the five main sub-basins (where most active sediment sources i.e., badlands, are located), as well as of the entire catchment (basin outlet). The study period (2007-2009) is considered moderately dry in comparison to the long-term water yield (1945-2009). The suspended sediment transport series at the main sub-basins have been obtained from field work (i.e., data acquisition) and modelling (i.e., data extrapolation). Modelling was performed by using a non-parametric multivariate regression technique (Random Forest); this procedure allowed the estimation of sediment yields at the monitoring sections of each sub-basin. Overall, the

reconstructed sedigraphs show moderate agreement with the observed data, despite of the limited number of samples. Our results illustrate the predictive power of the non-parametrical statistical techniques and their value in producing continuous sediment transport time-series. Finally, results have been compared to those obtained at the basin outlet and the estimates of sediment storage in the main channel, in order to establish the total sediment budget. A summary of results together with the main conclusions are drawn up as follows:

1) The annual sediment load was 226,000 and 243,500 tonnes for 2007-2008 and 2008-2009, respectively. Despite their relatively small area, Villacarli and Lascuarre sub-catchments, supply most of the sediment (102,000 and 75,000 t y^{-1}; 43 and 32% of the total load of the Isábena, respectively).

2) Specific sediment yields reach almost 2,500 t km^{-2} in Villacarli and 1,675 t km^{-2} in Lascuarre, illustrating the high sedimentary activity (i.e., sediment production and supply) that takes place in the badland areas. Yields decrease to below 600 t km^{-2} in the other sub-basins, owing to the less presence of erodible areas. The specific sediment yield obtained for the entire Isábena catchment is 530 t km^{-2}, a value that is considered high for a basin of such an area. A mean sediment residence time of two years and a denudation rate for the entire catchment of 0.2 m × 10^3 y^{-1} corroborate the intensity of sediment production, delivery and transfer process in the Isábena basin.

3) A large part of the sediment mobilized from the catchment slopes reaches the basin outlet, resulting in a delivery ratio above 50%, illustrating the high connectivity between the source of sediment and the channel network. Sediment conveyance losses also account for an important part of the sediment supply (44%) at the outlet of the basin. The in-channel sediment storage represents a small but significant part of the sediment budget (i.e., controlling sediment dynamics and temporal variability at the basin outlet), and overall accounting for the 4% of the annual sediment yield.

4) A small part (1%) of the area controls most of the catchment's gross sediment load. The high connectivity between sediment sources (badlands) and transfer paths (streamcourses) exacerbates the influence of the sediment production that occurs at the

local scale on the global catchment's sediment yield; this fact is remarkable here by its magnitude, and not typically found in the literature for basins of such scale. In addition, the in-channel sediment storage exerts a notable control on the temporal dynamics and magnitude of the sediment transport, showing the need of taking this key geomorphic element into account in the estimation of sediment budgets at the mesoscale.

Together with the Ésera, the River Isábena delivers water and sediments into the Barasona Reservoir. Overall, the River Isábena's suspended load for the study period nearly reached half a million tonnes, which represents 0.30 hm^3 (from a sediment density of 1.52 g cm^{-3}, Mamede 2008). This value represents ca. 0.4% of the original reservoir capacity and 4% of the total sediment sluiced down during maintenance operations carried out in the 1990s (Palau, 1998; Avendaño et al., 2000). In its middle sections, both catchments shear a highly active badland stripe that forms on exposed Eocene marls; results, in its order of magnitude, on sediment production, transfer and yield obtained in the Isábena can be thus extrapolated to the Ésera with a certain degree of confidence, altogether explaining the historical severe siltation observed in the reservoir.

Acknowledgements

The first author has a grant funded by the Catalan Government and the European Social Fund. Research has been carried out within the framework of the project "Sediment Export from Large Semi-Arid Catchments: Measurements and Modelling (SESAM)", funded by the German Science Foundation (*Deutsche Forschungsgemeinschaft*, DFG). The authors wish to thank the Ebro Water Authorities for the permission to install our measuring equipment at the Capella gauging station and for providing hydrological data. Special thanks are due to Álvaro Tena for his assistance in the field and in the laboratory.

References

Acornley, R.M., Sear, D.A., 1999. Sediment transport and siltation of brown trout (SalmoTrutta L.) spawning gravels in chalk streams. *Hydrological Processes*, **13**: 447–458.

Avendaño, C., Sanz, M.E., Cobo, R., 2000. State of the art of reservoir sedimentation management in Spain. In: Proceedings of the International Workshop and Symposium on Reservoir Sedimentation Management, Tokyo, Japan, pp. 27-35.

Batalla, R. J., Sala, M., Werrity, A., 1995. Sediment budget focused in solid material transport in a subhumid Mediterranean drainage basin. *Zeitschrift für Geomorphologie*, **39**(2): 249–269.

Breiman, L.M., Friedman, J., Olshen, R., Stone, C., 1984. Classification and regression trees. Wadsworth: Belmont, CA.

Clarke, S.J., Wharton, G., 2001. Sediment nutrient characteristics and aquatic macrophytes in lowland English rivers. *The Science of the Total Environment*, **266**: 103–112.

Clotet, N., Gallart, F. and Balasch, C., 1988. Medium–term erosion rates in a small scarcely vegetated catchment in the Pyrenees. *Catena Supplement*, **13**: 37 – 47.

Collins, A.L., Walling, D.E., 2004. Documenting catchment suspended sediment sources: problems, approaches and prospects. *Progress in Physical Geography*, **28:** 159–196.

de Vente, J., Poesen, J., Bazzoffi, P., Van Rompaey, A., Verstraeten, G., 2006. Predicting catchment sediment yield in Mediterranean environments:the importance of sediment sources and connectivity in Italian drainage basins. *Earth Surface Processes and Landforms*,**31**: 1017–1034.

Dietrich, W., Dunne, T., 1978. Sediment budget for a small catchment in mountanious terrain. *Zeitschrift für Geomorphologie N.F. Suppl. Bd.*, **29**: 191-206.

Douglas, G., Caitcheon, G., Palmer, M., 2009. Sediment source identification and residence times in the Maroochy River estuary, southeast Queensland, Australia. *Environmental Geology*, **57**: 629-639.

Duijsings, J.J.H.M., 1986. Seasonal variation in the sediment delivery ratio of a forested drainage basin in Luxembourg. In: Hadley, R.F. (ed.): *Drainage Basin Sediment Delivery*. IAHS Publication 159, IAHS Press, Wallingford, pp. 153-164.

Dunne, T., 1994. Hydrogeomorphology: an introduction. *Transactions Japanese Geomorphological Union,***15A**: 1–4.

Estrany, J., Garcia, C., Batalla, R.J., 2009. Suspended sediment transport in a small Mediterranean agricultural catchment. *Earth Surface Processes and Landforms*, **34**: 929-940.

Fargas, D., Martínez-Casasnovas, J.A., Poch, R., 1997. Identification of Critical Sediment Source Areas at Regional Level. *Physics and Chemistry of the Earth*, **22**(3-4): 355-359.

Francke, T., López-Tarazón, J.A., Schröder, B., 2008a. Estimation of suspended sediment concentration and yield using linear models, random forests and quantile regression forests. *Hydrological Processes*, **22**: 4892–4904.

Francke, T., López-Tarazón, J.A., Vericat, D., Bronstert, A., Batalla, R.J., 2008b. Flood-based analysis of high-magnitude sediment transport using a non-parametric method. *Earth Surface Processes and Landforms*, **33**: 2064–2077.

Gallart, F., Llorens, P., Latron, J., Regüés, D., 2002. Hydrological processes and their seasonal controls in a small Mediterranean mountain catchment in the Pyrenees. *Hydrology and Earth System Sciences*, **6**(3): 527–537.

Golosov, V.N., Ivanova, N.N., Litvin, L.F., Sidorchuk, A.Yu., 1992. Sediment budget in river basins and small river aggradation. *Geomorphologiya*, **4**: 62–71.

Harrell, F.E., 2001. Regression modeling strategies with applications to linear models, logistic regression, and survival analysis. Springer: New York.

Hart, E.A., Schurger, S.G., 2005. Sediment storage and yield in an urbanized karst watershed. *Geomorphology*, **70**: 85-96.

Lambert, C.P., Walling, D.E., 1988. Measurements of channel storage of suspended sediment in a gravel-bed river. *Catena*, **15**: 65–80.

Liaw, A., Wiener, M., 2002. Classification and Regression by randomForest. *R News*, **2**(3): 18-22.

López-Tarazón, J.A., Batalla, R.J., Vericat, D., 2010a. In-channel sediment storage in a highly erodible catchment: the River Isábena (Ebro basin, Southern Pyrenees). *Zeitschrift für Geomorphologie* (*in press*).

López-Tarazón, J.A., Batalla, R.J., Vericat, D., Balasch, J.C., 2010b. Rainfall, runoff and sediment transport relations in a mesoscale mountainous catchment: The River Isábena (Ebro basin). *Catena*, **82**: 23-34.

López-Tarazón, J.A., Batalla, R.J., Vericat, D., Francke, T., 2009. Suspended sediment transport in a highly erodible catchment: The River Isábena (Southern Pyrenees). *Geomorphology*, **109**: 210-221.

Loughran, R.J., 1989. The measurement of soil erosion. *Progress in Physical Geography*, **13:** 216–233.

Malmon, D.V., Dunne, T., Reneau, S.L., 2002. Predicting the fate of sedimentand pollutants in river floodplains. *Environmental Science and Technology*, **36**: 2026–2032.

Mamede, G., 2008. Reservoir sedimentation in dryland catchments: modelling and management. Unpublished PhD Thesis, Universität Potsdam, Germany.

Mamede, G.L., Bronstert, A., Francke, T., Müller, E., deAraújo, J.C., Batalla, R.J., Güntner, A., 2006. 1D Process-based modelling of reservoir sedimentation: a case study for the Barasona Reservoir in Spain. In: Conference Proceeding River Flow 2006. International Conference on Fluvial Hydraulics, Lisbon, September 06 - 08, 2006.

Mathys, N., Klotz, S., Esteves, M., Descroix, L., Lapetite, J.M., 2005. Runoff and erosion in the Black Marls of the French Alps: Observations and measurements at the plot scale. *Catena*, **63**: 261-281.

Matisoff, G., Wilson, C.G., Whiting, P.J., 2005. The $^{7}Be/^{210}Pb_{xs}$ ratio as an indicator of suspended sediment age or fraction new sediment in suspension. *Earth surface processes and landforms*, **30**: 1191-1201.

Meade, R.H., Yuzyk, T.R., Day, T.J., 1990. Movement and storage of sediment in rivers of the United States and Canada. In: Wolman, M.G., Riggs, H.C. (eds), Surface Water Hydrology, The Geology of North America, vol. O-1. Geological Society of America: Boulder, Columbia, United States of America, 255–280.

Meinshausen, N., 2006. Quantile Regression Forests. *Journal of Machine Learning Research*, 7: 983-999.

Meinshausen, N., 2007. quantregForest: Quantile Regression Forests; R package version 0.2-2.

Mosley, M.P., McKerchar, A., 1993. Streamflow. In:Maidment, D.R. (ed): Handbook of Hydrology. McGraw-Hill: New York; 8.1-8.39.

Nelson, E.J., Booth, D.B., 2002. Sediment sources in an urbanizing mixed land-use watershed. *Journal of Hydrology*, **264**: 51–68.

Owens, P.N., Batalla, R.J., Collins, A.J., Gomez, B., Hicks, D.M., Horowitz, A.J., Kondolf, G.M., Marden, M., Page, M.J., Peacock, D.H., Petticrew, E.L., Salomons, W., Trustrum, N.A., 2005. Fine-grained sediment in river systems: environmental significance and management issues. *Journal of River Research and Applications*, **21** (8): 1-25.

Palau, A., 1998. Estudio limnológico del ecosistema fluvial afectado por los vaciados del embalse de Barasona. *Limnética*, **14**: 1-15.

Peart, M.R., Walling, D.E., 1988. Techniques for establishing suspended sediment sources in two drainage basins in Devon, UK: a comparative assessment. In: Bordas, M.P., Walling, D.E. (eds): Sediment Budgets, IAHS Publ. No. 174. IAHS Press, Wallingford, pp. 269–279.

Phillips, J.D., 1991. Fluvial sediment budgets in the North Carolina piedmont. *Geomorphology*, **4**: 231–241.

Phillips, J.D., Marden, M., Gomez, B., 2007. Residence time of alluvium in an aggrading fluvial system. *Earth Surface Processes and Landforms*, **32**: 307–316.

Porto, P., Walling, D.E., Callegari, G., 2010. Using 137Cs measurements to establish catchment sediment budgets and explore scale effects. *Hydrological Processes* (*in press*), DOI: 10.1002/hyp.7874.

Regüés, D., Balasch, J.C., Castelltort, X., Soler, M., Gallart, F., 2000a. Relación entre las tendencias temporales de producción y transporte de sedimentos y las condiciones climáticas en una pequeña cuenca de montaña mediterránea (Vallcebre, Eastern Pyrenees). *Cuadernos de Investigación Geográfica*, **26**: 24–41.

Regüés, D., Guardia, R., Gallart, F., 2000b. Geomorphic agents versus vegetation spreading as causes of badland occurrence in a Mediterranean subhumid mountainous area. *Catena*, **25**: 199–212.

Roehl, J.E., 1962. Sediment source areas, and delivery ratios influencing morphological factors. *IAHS Publication*, **59**: 202–213.

Rovira, A., Batalla, R.J., 2006. Temporal distribution of suspended sediment transport in a Mediterranean basin: the lower Tordera (NE Spain). *Geomorphology*, **79**: 58–71.

Rovira, A., Batalla, R.J., Sala, M., 2005. Fluvial sediment budget of a Mediterranean river: the lower Tordera (Catalan Coastal Ranges, NE Spain). *Catena*, **60**: 19-42.

R-Team Development Core, 2006. R: a Language and Environment for Statistical Computing. R Foundation for Statistical Computing: Vienna.

Sanz-Montero, M., Cobo-Rayán, R., Avendaño-Salas, C., Gómez-Montaña, J., 1996. Influence of the drainage basin area on the sediment yield toSpanish reservoirs. In: *Proceedings of the First European Conference and Trace Exposition on Control Erosion.*

Selby, M.J., 1982. *Hillslope Materials and Processes*. Oxford University Press. 264 pp.

Schick, A.P., 1967. Gerlach troughs, overland flow traps, Field methods for the study of slope and fluvial processes. *Revue de Géomorphologie Dynamique*, **4**: 170- 172.

Schnabel, S., Maneta, M., 2005. Comparison of a neural network and a regression model to estimate suspended sediment in a semiarid basin. In: Batalla, R.J., Garcia, C., (eds): *Geomorphological Processes and Human Impacts in River Basins*. IAHS Publication 299, 91-100.

Scullion, J., 1983. Effects of impoundments on downstream bed materials of two upland rivers in mid-Wales and some ecological implications. *Archiv für Hydrobiologie*, **96**: 329–344.

Slaymaker, O., 2003. The sediment budget as conceptual framework and management tool. *Hydrobiologia*, **494:** 71–82.

Swanson, F.J., Fredriksen, R.L., 1982. Sediment routing and budgets: implications for judging impacts on forestry practices. In: Swanson, F.J., Janda, R.J., Dunne, T., Swanston, D.N. (eds.): *Sediment budgets and routing in forested drainage basins*, USDA Forest Service General Technical Report PNW-141, 129-137.

Trimble, S.W., 1995. Catchment sediment budgets and change. In: Gurnell, A.M., Petts, G., (eds): *Changing River Channels*. Wiley, Chichester, pp. 201–215.

Trimble, S.W., Crosson, P., 2000. U.S. soil erosion rates: myth and reality. *Science*, **289**: 248–250.

UK Biodiversity Action Plan Steering Group for Chalk Rivers, 2004. *The State of England's Chalk Rivers*. Environment Agency, Bristol.

Valero-Garcés, B.L., Navas, A., Machín, J., Walling, D.E., 1999. Sediment sources and siltation in mountain reservoirs: a case study from the Central Spanish Pyrenees. *Geomorphology*, **28**: 23–41.

Verdú, J.M., Batalla, R.J., Martínez-Casasnovas, J.A., 2007a. Estudio hidrológico de la cuenca del río Isábena (Cuenca del Ebro). I: Variabilidad de la precipitación. *Ingeniería del Agua*, **13**(4): 321-330.

Verdú, J.M., Batalla, R.J., Martínez-Casasnovas, J.A., 2007b. Estudio hidrológico de la cuenca del río Isábena (Cuenca del Ebro). II: Respuesta hidrológica. *Ingeniería del Agua*, **13**(4):331-343.

Vericat, D., Batalla, R.J., 2006. Sediment transport in a large impounded river: the lower Ebro, NE Iberian Peninsula. *Geomorphology*, **79**: 72–92.

Walling, D.E., 1983. The sediment delivery problem. *Journal of Hydrology*, **65:** 209–237.

Walling, D.E., 1984. Dissolved loads and their measurements. In: Hadley, R.F., Walling, D.E, (eds): *Erosion and sediment yield: Some methods of measurements and modelling*. Geo Books: London; 111-177.

Walling, D.E., 1999. Linking land use, erosion and sediment yields in river basins. *Hydrobiologia*, **410:** 223–240.

Walling, D.E., Quine, T.A., 1993. Using Chernobyl-derived radionuclides to investigate the role of downstream conveyance losses in the suspended sediment budget of the River Severn, United Kingdom. *Physical Geography*, **14**: 239–253.

Walling, D.E., Owens, P.N., Leeks, G.J.L., 1998. The role of channel and floodplain storage in the suspended sediment budget of the River Ouse, Yorkshire, UK. *Geomorphology*, **22**: 225–242.

Walling, D.E., Collins, A.L., Jones, P.A., Leeks, G.J.L., Old, G., 2006. Establishing fine-grained sediment budgets for the Pang and Lambourn LOCAR catchments, UK. *Journal of Hydrology*, **330**: 126-141.

Webb, B.W., Foster, I.D.L., Gurnell, A.M., 1995. Hydrology, water quality and sediment behaviour. In: Foster, I., Gurnell, A., Webb, B. (eds): *Sediment and Water Quality in River Catchments*. John Wiley and Sons Ltd., Chichester, pp. 1-30.

Williams, J.R., Berndt, H.D., 1972. Sediment yield computed with universalequation. *Journal of the Hydraulics Division*, **98**(12): 2087–2098.

Wolman, M.G., Miller, W.P., 1960. Magnitude and frequency of forces in geomorphic processes. *Journal of Geology*, **68**: 54–74.

Wood, P.A., 1977. Controls of variation in suspended sediment concentration in the River Rother, West Sussex, England. *Sedimentology*, **24**: 437-445.

Zimmermann, A., Zimmermann, B., Elsenbeer, H., 2009. Rainfall redistribution in a tropical forest: Spatial and temporal patterns. *Water Resources Research*, **45**, W11413, doi: 10.1029/2008WR007470.

CHAPTER 7
DISCUSSION AND CONCLUSIONS

INDEX CHAPTER 7: DISCUSSION AND CONCLUSIONS

Table captions in the chapter

Table captions in the chapter

1. DISCUSSION

Reservoirs experience siltation worldwide. This fact is especially severe in areas under variable climatic conditions, such as the Mediterranean mountains, with long dry periods in which sediments are produced and storms of high rainfall intensity that detach and export them. In these regions, the life-time of reservoirs may be reduced by decades due to siltation. Therefore, it is necessary to manage sediment as well as water to achieve a sustained long-term use of these vital infrastructures. Siltation is even more severe where runoff occurs over highly erodible unconsolidated sediments on bare slopes (i.e., badlands on marls, mudstones or shales). Under such conditions, erosion rates are very high, creating large suspended sediment loads in the river network that reach the lowland areas and the reservoirs (Francke et al., 2008). This is the case of the Isábena basin, whose suspended sediment loads threaten seriously the storage capacity of the Barasona Reservoir.

Mean annual runoff for the whole study period (2005-2009) in the River Isábena was 114 hm^3 y^{-1} (σ = 23 hm^3 y^{-1}, being σ the standard deviation of the dataset). Annual runoff for each of the studied years was below the long-term mean (i.e., 177 hm^3 y^{-1} for the period 1945-2009; σ = 92 hm^3 y^{-1}). We consider a very dry year that in which the annual runoff is lower than the long-term mean minus one σ (i.e., 92 hm^3 y^{-1}). Based on this assumption, just the first study year can be classified as very dry (i.e., 82 hm^3); the rest of the years can be considered simply as dry because annual runoff is just slightly lower (i.e., 0.5 σ) than the long-term mean annual value. Due to the complex hydrological response, no clear seasonal patterns in runoff were observed but late summer-autumn (i.e., due to localised convective thunderstorms) and spring (i.e., effects of snowmelt) tend to be the wettest seasons. Hydrologically, the Isábena is a very dynamic river having, on average, more than 30 flood events per year (i.e., flood peaks exceeding 100 m^3 s^{-1}), remarking the torrential and the mountainous Mediterranean characteristics of the basin.

Mean annual suspended sediment load for the whole study period was 202,512 t y^{-1} (σ = 75,443 t y^{-1}). This value is in the same order of magnitude of these estimated by others authors based on remote sensing techniques (i.e., spatially distributed soil erosion and sediment delivery modelling, Alatorre et al., 2010). These authors have reported a

mean annual suspended sediment load, for the period May 2005-May 2008, of 192,741 t y^{-1} (σ = 74,890 t y^{-1}). Specific sediment yield in the Isábena averaged 455 t km^{-2} y^{-1} (with a maximum of 550 t km^{-2} y^{-1} in 2006-2007). This is in the same order of magnitude as those reported for the Ésera basin (1,250 km^2, including the Isábena catchment) by Sanz-Montero et al. (1996) estimated from the Barasona Reservoir sedimentation data (350 t km^{-2} y^{-1}). De Vente et al. (2006) reported data on sediment yield for 44 Mediterranean basins, within which the Isábena would fall within the moderate to high values. For instance, Rovira and Batalla (2006) reported values in the order of 50 t km^{-2} y^{-1} for the 900 km^2 Tordera catchment. Oeurng et al. (2010) estimated a mean value of 43 t km^{-2} y^{-1} for the 1110 km^2 Save catchment. Most studies (e.g., Mathys et al., 2005; Gallart et al., 2005) showing a similar range of specific sediment yield are restricted to small mountainous catchments (<1 km^2), where sediment eroded off the slopes is readily available to be transported and exported out of the catchment during floods. Mathys et al. (2005) reported 800 t km^{-2} y^{-1} for the Brusquet catchment, a 1 km^2 basin located in the French Alps; Gallart et al. (2005) presented an average of 535 t km^{-2} y^{-1} for the Ca l'Isard basin (1.3 km^2 in the southeastern Pyrenees). Worth to remember at this point that values obtained in the mesoscale Isábena catchment were observed during dry years, well below the average rainfall-runoff activity in the catchment as discussed previously.

Floods are responsible of the majority of the sediment transport in the catchment (i.e., 90% of the annual yield is transported during the 25% of the time, on average), illustrating both the torrential character of this mesoscale catchment and the high availability of sediment, whether it is primarily confined in badlands or stored within the drainage network. Other studies in the Mediterranean area have shown the same pattern for basins with sizes comparable to the Isábena (Batalla et al., 1995; Rovira and Batalla, 2006). Recently, Estrany et al. (2009) reported that 90% of the load was transported in just 1% of the time in a small agricultural catchment on the Balearic Islands. Nevertheless, results also indicate that the Isábena has a more constant sediment transport in comparison with its regional counterparts (i.e., illustrated by the high suspended sediment concentrations observed even during base flows; mean concentration for the whole period = 1 g l^{-1}). In other words, overall sediment yield is strictly dependent upon floods, but base flows, and even daily fluctuations in the flow

and small floods play remarkably important roles in the export of sediment from the catchment.

A seasonal pattern in suspended sediment transport (as in the case of runoff) is not evident. The highest loads usually correlate well with periods of high rainfall, being late summer-autumn and spring the periods with the highest values. Nevertheless, there are some periods without direct relations between rainfall and runoff. This may indicate that exhaustion phenomena can occur after periods with a very high sediment load; besides that, this fact can also occur during periods in which the discharge is dominated by the Cabecera sub-catchment input, without sediment contributions. No linear relation was either found between the annual runoff and the suspended sediment loads. Data suggest that a small increment in the annual runoff can trigger a large increment in the total load; this way, relatively high runoff activities can cause a large sediment contribution that was not completely exported but retained in the channel during previous floods.

Statistically significant relationships between discharge and suspended sediment concentration were not found for the complete period. The suspended sediment concentrations may be up to 5 orders of magnitude for the same discharge (i.e., ranging from 0.01 g l^{-1} to 357 g l^{-1}). That scatter, besides not allowing the application of traditional techniques to calculate sediment transport (e.g., flow duration curves), may indicate that suspended sediment concentration is not only hydraulically dependent (i.e., it does only increase as discharge increases during floods), a fact that may suggest that fine sediment may also be available and easily removed, even during base flows.

As underlined in previous sections, the role of in-channel storage of sediment has been identified as one of the main controls on suspended sediment transport during interflood periods of stable flow (e.g., Walling and Amos, 1999; Smith and Dragovich, 2008); this phenomenon was studied in a ~3-km of channel reach, equating up to almost the 0.3% of the total load transported during the year 2007-2008. Extrapolation to the whole channel length (45 km, river mainsteam) suggests that sediment stored increases more than an order of magnitude, attaining ca. the 5 % of the total annual load. These results are comparable to the level of storage reported in other catchments; Duijsings (1986) estimated that 9% of the sediment load may have been seasonally stored in the channel bed for the Schrondweilerbaach River in Luxembourg, while Lambert and Walling

(1988) calculated that channel bed storage represented around 2% of the annual suspended sediment load for the River Exe in the UK. Walling and Quine (1993) reported, for the River Severn in the UK, that channel bed storage represented around 2% of the sediment load, while Walling et al. (1998) found channel storage equated to 10% of the annual suspended sediment load for the Ouse and Wharfe basins in the UK. Nevetheless, it must be considered that estimates of channel storage were derived by resuspending fine sediment from the river's bed and there is no temporal control for these data, representing an instantaneous measure of storage at the time of sampling.

No statistically significant relations were found between the runoff, the sediment transport and the rainfall intensity factors, whereas the hydro-sedimentological response was strongly correlated with the antecedent and the total precipitation. This behaviour indicates that the total amount of precipitation and the antecedent moisture conditions have an important role in determining the hydro-sedimentological response of the catchment. Even more, the highest suspended sediment loads are produced, to a great extend, by the highest runoff volumes. This indicates that such events are the only ones capable of entraining and resuspending the large amounts of sediment previously accumulated in the channel, supplied from the badlands to the system through small events that not reach the basin outlet. Such non-linear hydro-sedimentological responses have been observed and reported in other Mediterranean catchments (e.g., Ceballos and Schnabel, 1998; Cosandey et al., 2005; Latron et al., 2008).

The application of statistical techniques as *Random Forest*, and *Quantile Regression Forest* has been proved capable to simulate sedigraphs in basin such dynamic as the Isábena. In our case, it was possible to apply these techniques to all but one of the sub-basins, due to the lack of a continuous discharge record. Owing to the obtained results, it was seen that the maximum discharge peak increase with increasing sub-catchment size, whereas suspended sediment concentration follows an opposite pattern: the largest sub-basins produced the lowest concentrations. Water and suspended sediment budgets seem to have an aswer for this: the Cabecera sub-basin seems to control the hydrology of the Isábena whole basin (183.5 hm^3, 68% of the total runoff) while Villacarli and Lascuarre sub-basins control the sediment load (203,843 and 150,778 t, 43 and 32% of the total sediment transport, respectively). The role of Carrasquero (i.e., yielding less than the 1% and the 4% of the sediment load and runoff respectively) and Ceguera (i.e.,

representing around the 8% of both sediment and water yields) are much less relevant. The specific sediment load for each sub-catchment reveals a clear distinct pattern for areas where badlands are predominant and areas where its presence is likely negligible: the monitoring period of 250 t km^{-2} y^{-1} for Cabecera, 2,427 t km^{-2} y^{-1} for Villacarli, 72 t km^{-2} y^{-1} for Carrasquero, 682 t km^{-2} y^{-1} for Ceguera and 1,675 t km^{-2} y^{-1} for Lascuarre. Villacarli and Lascuarre values suggest a very high sedimentary activity and can be compared with mean annual sediment yields of similar catchments such as those in the Vallcebre area with badlands (2,800 t km^{-2} y^{-1}, Regüés et al., 2000, 5 years of monitoring), despite of being more than 40 times larger in area.

A mean residence time of a fine particle within the fluvial system of around 2 years has been estimated. This estimate matches to that predicted by López-Tarazón et al. (2010) from field observations of in-channel sediment storage showing, this way, the high activity in the sediment production areas, and the quick transfer and transport processes in the Isábena basin. Swanson and Friedriksen (1982) assessed that the stored volume of sediment in the channel is commonly more than 10 times the average annual export of total particulate sediment, while in the same is less than 2. Batalla et al. (1995) reported a value of 28 years as mean residence time of a particle in the Arbúcies river-channel, in this case applied to bed-material transport. Besides that, the long-term denudation rate is estimated to be 0.2 m × 10^3 y^{-1}. Denudation rate plots remarkably higher than studies by Dietrich and Dunne in a basin in Oregon (0.03 m × 10^3 y^{-1}) and by Batalla et al., (1995) in the Mediterranean basin of Arbúcies (0.02 m); both showing a rather high degree of equilibrium between sediment contribution from hillslopes and sediment export; in contrast, the Isábena is controlled by a high sediment production from the badlands and a high connectivity between sources and the fluvial network, thus showing extreme geomorphic activity.

Important differences between the sediment input, the in-channel storage, the sediment conveyance and the sediment output in the basin have been observed. In terms of absolute magnitudes it is clear that the sediment output is the most important component of the sediment budget, providing a sediment delivery ratio of 52%. Sediment conveyance losses also account for an important part of the sediment supply from the catchment (44%). This result is the consequence of the size of the basin (e.g., with a relatively low longitudinal gradient) and the frequent presence of a relatively well-

developed valley floor where sediment is accumulated. The in-channel sediment storage represents a small part of the sediment budget, with ca. 4% of the sediment input, but constitutes an important factor in controlling the seasonal variability of the sediment load (i.e., ranging from 5 to 55% of the seasonal sediment yield, López-Tarazón et al., 2010) and the high loads tipically transported during baseflows (López-Tarazón et al., 2009). It is worth to remark that both conveyance losses and in-channel sediment storage do not create permanent accretions on the catchment (i.e., based on field observations); they rest available to future floods, becoming another sediment source. This fact may increase the sediment budget and, surely, the sediment delivery ratio as well so, if we extend the study to some more years we could appreciate that almost the whole sediment input delivered by the badlands moves out of the basin.

Finally, the Isábena represents one-third of the catchment area of the Barasona Reservoir. The suspended sediment load for the entire 4-year period exceeds 800,000 t. Assuming a dry density of the sediment of 1.52 g cm^{-3} (Mamede, 2008), the total load transported by the Isábena to the reservoir can be estimated at around 0.53 hm^3 (e.g., more than 0.13 hm^3 y^{-1}). This value that represents ca. 0.6% of the original reservoir capacity, and around the 6% of the total sediment sluiced down during maintenance operations carried out in the 1990s (ca. 9 hm^3). We can compare these values with those extrapolated by Nadal-Romero and Regüés (2010) regarding to the contributions of the badland areas developed in the Inner Depression in the Central Pyrenees to the Yesa reservoir; these authors estimated the suspended sediment load in 0.69 hm^3, that represents an annual reduction of about 0.15% of the reservoir. Regüés et al., (2009) argue that this loss of capacity is not enough to represent a problem at short to medium term, unless the extent and the geomorphological activity of badlands are notably increased

2. SUMMARY OF RESULTS AND CONCLUSIONS

This thesis works out the **sediment transport and budget** of the Isábena river basin, a mesoscale mountainous catchment located in the Central Pyrenees that generates unusually high sediment loads. The work has been focused on the description and quantification of the hydro-sedimentological dynamics of the entire catchment and in the five main sub-basins, where most active sediment sources (i.e., badlands) are located. Study years (2005-2009) are considered as moderately-dry compared to with the long-term annual water yield (1945-2009). The suspended sediment transport data has been obtained mainly from field work (continuous measurements and regular sampling); whereas data extrapolation using a non-parametric multivariate regression technique (Random Forest) has been applied to those sections where only discrete sampling was performed. In particular, non-parametric regression techniques allowed the estimation of sediment yields at the monitoring sections of each sub-basin. Finally, results have been compared to those obtained at the basin outlet and the estimates on sediment storage in the main channel, to establish the total sediment budget.

A **summary of results** is presented next:

1) Suspended sediment **concentrations** at the basin outlet span five orders of magnitude, occasionally attaining instantaneous values in excess of 300 g l^{-1}. Mean concentration at the basin outlet for the whole period attained 1 g l^{-1} (σ = 7.11 g l^{-1}; *CV* = 720%). Concentrations do not show a direct relationship with flow discharge (i.e., they are not solely hydraulically dependent). This fact indicates, between others, that sediments sources are not uniformly distributed (a fact illustrated by the intense hysteretic activity during floods) and that temporal in-channel sediment storage exerts an important control on sediment yield.

2) **Floods** dominate the sediment transport and yield. However, sediment transport is much more constant through time than observed in other basins; this can be attributed to the role of **baseflows** and even small discharge fluctuations, which entrain fine sediment stored in the channel and force the river to carry high sediment concentrations (i.e., typically in the order of 0.5 g l^{-1}, even under minimum flow conditions).

3) The **sediment load** for the period 2005-2009 was 203,000 t y^{-1}. Despite their relatively small area, the Villacarli and Lascuarre sub-cachments supplied the most of the sediment (102,000 and 75,000 t y^{-1}; 43 and 32% of the total Isábena load for the period 2007-2009, respectively).

4) **Specific sediment yields** reach almost 2,500 t km^{-2} in Villacarli and 1,675 t km^{-2} in Lascuarre, illustrating the high sedimentary activity (i.e., sediment production and supply) that takes place in the badland areas. Yields decrease to below 600 t km^{-2} in the other sub-basins, owing to the less presence of erodible areas. The specific sediment yield obtained for the entire Isábena catchment is 530 t km^{-2}, a value that is considered high for a basin of such an area. A mean sediment **residence time** of two years and a **denudation rate** for the entire catchment of 0.2 m × 10^3 y^{-1} corroborate the intensity of sediment production, delivery and transfer process in the Isábena basin.

Main conclusions of the work are presented next:

a) A small part (1%) of the area controls most of the catchment's gross sediment load. The high **connectivity** between sediment sources (badlands) and transfer paths (channel network) exacerbates the influence of the sediment production that occurs at the local scale on the global catchment's sediment yield; this fact is remarkable here by its magnitude, and not typically found in the literature for basins of such scale. In addition, the **in-channel sediment storage** exerts a notable control on the temporal dynamics and magnitude of the sediment transport, showing the need of taking this key geomorphic element into account in the estimation of sediment budgets at the mesoscale.

b) A large part of the sediment mobilized from the catchment slopes reaches the basin outlet, resulting in a **delivery ratio** above 50%. Sediment conveyance losses also account for an important part of the sediment supply (44%). The in-channel sediment storage represents a small but significant part of the sediment budget (i.e., controlling sediment dynamics and temporal variability at the basin outlet); and overall accounting for the 4% of the annual sediment yield.

c) Overall, **sediment load** in the Isábena does not follow a direct relation with discharge. Hypothetically, **floods** coming mostly from Villacarli and Lascuarre with no

major runoff contribution from Cabecera would result in an increase of in-channel sediment storage; whereas floods in which Cabecera plays the major role, runoff would be able to **transfer** most of the sediment supplied from tributaries as well as re-suspending and exporting (part of) the fine material previously accumulated in the main channel. Despite the results of the investigation point out to this direction, a thorough analysis (i.e., sediment sources, fingerprinting) on the relation between spatial sources and sediment yield would be necessary to assess this hypothesis further.

d) For the methodological point of view it is worth to mention that the **reconstructed sedigraphs** using Random Forest show moderate agreement with the observed data, despite of the low number of sediment samples. This fact illustrates the predictive power of the non-parametrical statistical techniques used here and their value assisting in the production of continuous sedigraphs.

Finally, some further considerations shall be added regarding research **uncertainties** as well as on the potential use of our results to inform **sediment management** actions in the Isabena-Ésera / Barasona hydrosedimentary system:

The results of this thesis are a synthesis of numerous working steps, some of which are subject to simplifying **assumptions** and/or a certain degree of **error** that cannot always be quantified. Due to the characteristics of the time-series, a certain degree of serial correlation in the data must be expected, which could not be investigated due to the limited number of temporally close *SSC* samples. Although we are confident of having captured virtually the entire range of *SSC* conditions, we cannot exclude the possibility of having missed the absolute maximum in *SSC*. The resulting effect of underestimation of peak concentrations and overestimation of low *SSC* has also been observed with linear regression and *ANN* models and may lead to an underestimation of *SSC* variability.

The **Isábena** represents one-third of the catchment area of the **Barasona** Reservoir. The total suspended load for the study period (2005-2009) attained ca. 750,000 t. Assuming a dry density of the sediment of 1.52 g cm^{-3} (Mamede, 2008), the total load transported by the Isábena to the reservoir can be estimated at around 0.5 hm^3, a value that represents ca. 0.7% of the original reservoir capacity and the ca. 6% of the total

sediment sluiced down during maintenance operations carried out in the 1990s (ca. 9 hm^3).The sediment load transported by the River Isábena, in addition to that transported by the Ésera, explains the historical siltation of the Barasona Reservoir. The present work together with joint previous research in the Isábena catchment (Mamede, 2008; Francke, 2009) can inform **mitigation actions** to ameliorate the impact of sedimentation in the reservoir. On one side, location of sediment sources in specific sub-basins, degree of sedimentary activity in relation to catchment's hydrology and magnitude of the sediment supply are now well-know and quantified. On the other, the relation between sources and yield, and the temporal dynamics of sediment reaching the reservoir has also been assessed in a precise way. Altogether, this type of information can be used to design conservation measures and sediment management actions (both in the catchment and in the reservoir) at the short and medium term. Within this context, two proposals on potential sediment management actions are presented:

i) Design and construction of a large **sediment retention pond** at the backwater zone of the reservoir that may capture an important part of the fine sediment load regularly entering the lake. Magnitude and temporal dynamics supplied here shall be of use to inform both the construction and the further management of the pond and auxiliary installations. The pond should be accessible to allow regular emptying. Permanent disposal sites should also be specified (e.g., perhaps in lateral ephemeral creeks) as a semi-permanent storage for dredged sediments. No major chemical problems are expected associated to the incoming sediments. Economic value and local use of fine sediment should be also evaluated.

ii) Model and implementation of a **sediment pass-through system** in the lake and the dam. The Ésera and the Isábena rivers have regular frequent floods. Floods may supply the necessary energy to route part of the sediment until the dam, to be subsequently released to downstream reaches. A specific dam operation programme should be developed and implemented to facilitate sediment routing and pass. A minimum pool is however required for this practice; therefore this management action might not be feasible in all years and at all times of the year, indistinctly; but it should be planned in relation to catchment hydrology in previous years (i.e., volume of stored water) and the yearly updated irrigation needs.

3. LIMITATIONS OF THE THESIS AND FUTURE WORK

Limitations in the suspended sediment measuring (i.e., continuous versus discrete), together with the in-channel storage sampling, can be seen as some of the main limitations of the monitoring work carried out in this Thesis but, at the same time, it can be taken as the bases to propose future work related to sediment transport in high-erodible catchments such as the Isábena. In addition, it is worth to remember that that study has been carried out in a dry or very dry periods. To quantify the real suspended sediment transport and dynamics in the Isábena basin a continued monitoring until an averaged hydrological year happens should be pursued.

Chapter 5 reports on the in-channel suspended sediment storage based on a 1-year sampling campaign in the lower Isábena. To include the whole variability of the sediment accumulation, sampling campaigns should be extended both spatially and temporally. To include the temporal variability, sampling should be extended to the longest possible period. To include the spatial variability, sampling should be extended to the entire main channel together with the main sub-catchments. This way, extrapolations to the whole catchment from data coming from a 3-km channel reach would be less uncertain. Some hydraulic modeling approaches would be also studied to decreases field sampling efforts.

Chapter 6 estimates the water and sediment budget of the Isábena basin by using the *Random Forest* and *Quantile Regression Forest* statistical techniques. In order to enhance model performance more suspended sediment concentration data at the sub-catchments would be needed. To obtain these data it would be necessary to continue monitoring the sub-catchments by means of the current sampling techniques (i.e., water stage samplers) and/or improving these techniques by means of the installation of automatic electronic samplers and high-range turbidimeters. This way, continuous suspended sediment records would be then generated for each of the sub-basin. The main problem associated to the application of the statistical techniques was the lack of a continuous discharge records in the Villacarli sub-catchment. This fact may be avoided in the future by building a regular gauging station with measuring specification related to high density flows.

Additionally to these, other important source of errors associated with experimental design can be summarized as follows:

(a) Errors associated to data collection: capacitive water stage samplers can generate measuring errors derived from high suspended sediment concentrations. In addition, water stage samplers and turbidimeters can have considerable source of bias on the suspended sediment transport estimations and further computations due to problems reported in Chapters 2 and 3.

(b) Errors associated to equipment calibration and discharge calculations; all installed instruments needed to be calibrated. Therefore, total errors on the estimates are the cumulative sum of standard errors associated not only to sampling and postprocessing but also to the statistical adjustment of the calibrations. Although most surveyed sections have remain to be stable over time, in the case of the discharge estimations, natural changes on channel topography and grain size distribution after floods can alter the calculated rating curves water height-discharge (i.e., h/Q). Continuous topographical surveys and grain size distribution samplings at the measuring sections can reduce this bias.

At the light of the limitations that have arisen during the course of this thesis, several aspects need to be considered before defining future work on suspended sediment transport in the Isábena basin or similar fluvial environments. A summary is presented next:

(a) To improve the measurement of sediment transport at each sub-basin:

- Improve discharge and suspended sediment records at the sub-catchments by the installation of more precise water stage samplers and continuous direct or indirect water samplers providing suspended sediment transport estimates (i.e., electronic automatic samplers, high-range turbidimeters).

(b) To improve the study of the in-channel sediment storage:

- Increase sampling at a spatial (i.e., including the river's whole mainsteam and the main tributaries) and temporal scales (i.e., sampling seasonally and during several years).
- Study of the relations between the channel geomorphology and the in-channel storage.

(c) To improve the analysis and model of suspended sediment transport and budget:

- Deeply study of the relations between discharge and suspended sediment transport at different time scales (e.g., flood events, daily, monthly, seasonally, annually) to determine the exact hysteretic patterns of the Isábena basin.
- Determine the exact location and contributions of sediment sources, as well as the residence time of the sediment within the basin by applying fingerprinting techniques (e.g., radionuclides, mineral magnetism, geochemistry, colourimetry).
- Upgrading of the statistical techniques used to model suspended sediment transport by the application of different model approaches such Artificial Neural Networks.
- Study of the relations between bedload and suspended sediment transport, especially the interactions between bedload entrainment and fine sediment re-suspension.

4. REFERENCES

Alatorre, L.C., Beguería, S., García-Ruiz, J.M., 2010. Regional scale modeling of hillslope sediment delivery: A case study in the Barasona Reservoir watershed (Spain) using WATEM/SEDEM. *Journal of Hydrology*, **391**: 109-123.

Batalla, R.J., Sala, M., Werrity, A., 1995. Sediment budget focused in solid material transport in a subhumid Mediterranean drainage basin. *Zeitschrift für Geomorphologie*, **39**(2): 249-269.

Ceballos, A., Schnabel, S., 1998. Hydrological behaviour of a small catchment in the dehesa landuse system (Extremadura, SW Spain). *Journal of Hydrology*, **210**:4-14.

Cosandey, C., Andréassian, V., Martin, C., Didon-Lescot, J.F., Lavabre, J., Folton, N., Mathys, N., Richard, D., 2005. The hydrological impact of the Mediterranean forest: a review of French research. *Journal of Hydrology*, **301**:235-249.

de Vente, J., Poesen, J., Bazzoffi, P., Van Rompaey, A., Verstraeten, G., 2006. Predicting catchment sediment yield in Mediterranean environments: the importance of sediment sources and connectivity in Italian drainage basins. *Earth Surface Processes and Landforms*, **31:** 1017-1034.

Dietrich, W., Dunne, T., 1978. Sediment budget for a small catchment in mountanious terrain. *Zeitschrift für Geomorphologie N.F. Suppl. Bd.*, **29**: 191-206.

Duijsings, J.J.H.M., 1986. Seasonal variation in the sediment delivery ratio of a forested drainage basin in Luxembourg. In: Hadley, R.F. (ed.): *Drainage Basin Sediment Delivery*. IAHS Publication 159, IAHS Press, Wallingford, pp. 153-164.

Estrany, J., Garcia, C., Batalla, R.J. (2009): Suspended sediment transport in a small Mediterranean agricultural catchment. *Earth Surface Processes and Landforms*, **34** (7): 929-940

Francke, T., López-Tarazón, J.A., Vericat, D., Bronstert, A., Batalla, R.J., 2008. Flood-based analysis of high-magnitude sediment transport using a non-parametric method. *Earth Surface Processes and Landforms*, **33**: 2064-2077.

Gallart, F., Balasch, J.C., Regüés, D., Soler, M., Castelltort, F., 2005. Catchment dynamics in a Mediterranean mountain environment: the Vallcebre research basins (southeastern Pyrenees). II: Temporal and spatial dynamics of erosion and stream sediment transport. In: García, C., Batalla, R.J. (Eds.), *Catchment Dynamics and River Processes: Mediterranean and Other Climate Regions*. Developments in Earth Surface Processes, Publication 7, Elsevier, Amsterdam, The Nederlands, pp. 17-29.

Lambert, C.P., Walling, D.E., 1988. Measurements of channel storage of suspended sediment in a gravel-bed river. *Catena*, **15**: 65–80.

Latron, J., Soler, M., Llorens, P., Gallart, F., 2008. Spatial and temporal variability of the hydrological response in a small Mediterranean research catchment (Vallcebre, Eastern Pyrenees). *Hydrological Processes*, **22**: 775-787.

López-Tarazón, J.A., Batalla, R.J., Vericat, D., 2010. In-channel sediment storage in a highly erodible catchment: the River Isábena (Ebro basin, Southern Pyrenees). *Zeitschrift für Geomorphologie* (*in press*).

López-Tarazón, J.A., Batalla, R.J., Vericat, D., Francke, T., 2009. Suspended sediment transport in a highly erodible catchment: The River Isábena (Southern Pyrenees). *Geomorphology*, **109**: 210-221.

Mamede, G., 2008. Reservoir sedimentation in dryland catchments: modelling and management. Unpublished PhD Thesis, Universität Potsdam, Germany.

Mathys, N., Klotz, S., Esteves, M., Descroix, L., Lapetite, J.M., 2005. Runoff and erosion in the Black Marls of the French Alps: observations and measurements at the plot scale. *Catena,* **63**: 261-281.

Nadal-Romero, E., Regüés, D., 2010. Geomorphological dynamics of subhumid mountain badland areas weathering, hydrological and suspended sediment transport processes: A case study in the Araguás catchment (Central Pyrenees) and implications for altered hydroclimatic regimes. *Progress in Physical Geography*, **34** (2): 123-150.

Oeurng, C., Sauvage, S., Sánchez-Pérez, J.M., 2010. Dynamics of suspended sediment transport and yield in a large agricultural catchment, southwest France. *Earth Surface Processes and Landforms*, **35**: 1289-1301.

Regüés, D., Nadal-Romero, E., Latron, J., Martí-Bono, C., 2009. Producción y transporte de sedimento en cárcavas desarrolladas en la Depresión Interior Altoaragonesa (Cuenca de Araguás, Pirineo Central). *Cuadernos de Investigación Geográfica*, **35**: 263–88.

Regüés, D., Balasch, J.C., Castelltort, X., Soler, M., Gallart, F., 2000. Relación entre las tendencias temporales de producción y transporte de sedimentos y las condiciones climáticas en una pequeña cuenca de montaña mediterránea (Vallcebre, Eastern Pyrenees). *Cuadernos de Investigación Geográfica*, **26**: 24–41.

Rovira, A., Batalla, R.J., 2006. Temporal distribution of suspended sediment transport in a Mediterranean basin: the lower Tordera (NE Spain). *Geomorphology*, **79**: 58-71.

Sanz-Montero, M., Cobo-Rayán, R., Avendaño-Salas, C., Gómez-Montaña, J., 1996. Influence of the drainage basin area on the sediment yield to Spanish reservoirs. In: *Proceedings of the First European Conference and Trade Exposition on Control Erosion*, International Erosion Control Association IECA, Sitges, Spain.

Smith, H.G., Dragovich, D., 2008. Sediment budget analysis of slope-channel coupling and in-channel sediment storage in an upland catchment, southeastern Australia. *Geomorphology*, **101**: 643-654.

Swanson, F.J., Fredriksen, R.L., 1982. Sediment routing and budgets: implications for judging impacts on forestry practices. In: Swanson, F.J., Janda, R.J., Dunne, T., Swanston, D.N. (eds.): *Sediment budgets and routing in forested drainage basins*, USDA Forest Service General Technical Report PNW-141, 129-137.

Walling, D.E., Amos, C.M., 1999. Source, storage and mobilisation of fine sediment in a chalk stream system. *Hydrological Processes*, **13** (3): 323-340.

Walling, D.E., Quine, T.A., 1993. Using Chernobyl-derived radionuclides to investigate the role of downstream conveyance losses in the suspended sediment budget of the River Severn, United Kingdom. *Physical Geography*, **14**: 239–253.

Walling, D.E., Owens, P.N., Leeks, G.J.L., 1998. The role of channel and floodplain storage in the suspended sediment budget of the River Ouse, Yorkshire, UK. *Geomorphology*, **22**: 225–242.

5. PUBLICATION STATUS OF THE PAPERS

This Thesis is composed by a series of papers published in international peer-reviewed journals. Four papers presented as thesis chapters are meant to be evaluated while other two are presented in the annexes as complementary materials. The actual status of the papers is as follows:

Table 1. Publication status of the papers presented in this Thesis (January 3rd, 2011)

Chapter	Journals	State
3. Sediment transport	GEO[a]	Published
4. Hydro-sedimentological response	CAT[b]	Published
5. In-channel sediment storage	ZfG[c]	Accepted, in press
6. Suspended sediment budget	GEO	Submitted
Annex 1. Model development	HP[d]	Published
Annex 2. Model application	ESPL[e]	Published

[a] *Geomorphology*
[b] *Catena*
[c] *Zeitschrift für Geomorphologie*
[d] *Hydrological Processes*
[e] *Earth Surface Processes and Landforms*

ANNEXES

ANNEX 1
SUSPENDED SEDIMENT MODEL DEVELOPMENT

INDEX ANNEX 1: SUSPENDED SEDIMENT MODEL DEVELOPMENT

Francke, T., López-Tarazón, J.A., Vericat, D., Schröder, B., 2008. Estimation of suspended sediment concentration and yield using linear models, random forests and quantile regression forests. *Hydrological Processes*, **22**: 4892-4904.

Figure captions in the paper

Figure 1. Isábena catchment with monitored subcatchments and rain gauges (C: Capella; L: Laspaules; S: Serraduy, T: Torrelaribera, V: Villacarli).

Figure 2. Monte-Carlo-simulation of *SSC*. Dots represent single realizations of the simulation and the continuous line their mean *SSC*-value (example from Torrelaribera, flood 12).

Figure 3. Distribution of Torrelaribera sediment yield computed by Monte Carlo method using 70 realisations (dashed: fitted normal distribution, dotted: 95 % confidence interval).

Figure 4. Close-up-view of rainfall, discharge and *SSC* (measured and modelled) for two floods at Villacarli.

Figure 5. Hydrograph (top), sediment yield of flood (bars and whiskers) and interflood (whiskers only) periods at Villacarli. The whiskers comprise the 95 % *CI*. The grey bars underlying the hydrograph depict the numbering of the floods.

Figure 6. Variable importance for application of *RF* model. Equivalent predictors in the *RF* model (log_disch~discharge, cum_q_all~julian_day) have been omitted (see Table 3 for abbreviations).

Figure 7a, b. Effect of changes in *SSC* per change in discharge for different conditions of daily rainfall and season. The continuous line marks the moving average (example from Torrelaribera).

Figure 8. Hysteresis loops for (a) a monitored and (b) an unmonitored flood corresponding to floods 5 and 4 at Cabecera, respectively.

Table captions in the paper

Table 1. Summary of measured discharge and *SSC* data.

Table 2. Ancillary data used for regression (see Table 3 for abbreviations).

Table 3. Abbreviations used in the text.

Table 4. Results of predictor selection (for abbreviations see Table 3 and Table 5).

Table 5. Performance of models used for *SSC* prediction.

Table 6. Total sediment yield with 95 % confidence interval for the different gauges within the observation period (calculated with the *QRF* model).

1. INTRODUCTION

This annex develops the non-parametrical statistical techniques (*Random Forest*, *Quantile Regression* Forest) applied to model the continuous sedigraphs from ancillary data. The development of the model includes the explanation of the statistical basis and the programming procedures utilized to extrapolate the suspended sediment register. For this purpose we present a paper analysing the development of an statistical model to obtain a continuous sedigraph from ancillary hydrological data. Paper is presented maintaining its original structure; its format has been adapted to the general format of the present volume.

The paper was published by *Hydrological Processes* in December 2008; it presents a comparison of the applicability of traditional sediment rating curves, generalised linear models (*GLM*) and non-parametric regression using *Random Forests* (*RF*) and *Quantile Regression Forests* (*QRF*) applied to a dataset of suspended sediment concentration obtained for three subcatchments and the entire Isábena basin. All proposed *GLM*s showed an inferior performance, whereas *RF* and *QRF* proved to be very robust and performed favourably for reproducing sediment dynamics. *QRF* additionally provides estimates on the accuracy of the predictions and thus allows the assessment of uncertainties in the estimated sediment yields that is not commonly found in other methods. The capabilities of *RF* and *QRF* concerning the interpretation of predictor effects are also outlined.

2. SUSPENDED SEDIMENT MODEL DEVELOPEMENT

Francke, T., López-Tarazón, J.A., Vericat, D., Schröder, B., 2008. Estimation of suspended sediment concentration and yield using linear models, random forests and quantile regression forests. *Hydrological Processes,* **22**: 4892-4904

Estimation of suspended sediment concentration and yield using linear models, random forests and quantile regression forests

Abstract

For sediment yield estimation, intermittent measurements of suspended sediment concentration (*SSC*) have to be interpolated to derive a continuous sedigraph. Traditionally, sediment rating curves (*SRC*s) based on univariate linear regression of discharge and *SSC* (or the logarithms thereof) are used but alternative approaches (e.g. fuzzy logic, artificial neural networks, etc.) exist. This paper presents a comparison of the applicability of traditional *SRC*s, generalised linear models (*GLM*s) and non-parametric regression using Random Forests (*RF*) and Quantile Regression Forests (*QRF*) applied to a dataset of *SSC* obtained for four subcatchments (0.08, 41, 145 and 445 km²) in the Central Spanish Pyrenees. The observed *SSC*s are highly variable and range over six orders of magnitude. For these data, traditional *SRC*s performed inadequately due to the over-simplification of relating *SSC* solely to discharge. Instead, the multitude of acting processes required more flexibility to model these non-linear relationships. Thus, alternative advanced machine learning techniques that have been successfully applied in other disciplines were tested. *GLM*s provide the option of including other relevant process variables (e.g. rainfall intensities, temporal information) but require the selection of the most appropriate predictors. For the given datasets, the investigated variable selection methods produced inconsistent results. All proposed *GLM*s showed an inferior performance, whereas *RF* and *QRF* proved to be very robust and performed favourably for reproducing sediment dynamics. *QRF* additionally provides estimates on the accuracy of the predictions and thus allows the assessment of uncertainties in the estimated sediment yields that is not commonly found in other methods. The capabilities of *RF* and *QRF* concerning the interpretation of predictor effects are also outlined.

Keywords: suspended sediment concentration, sediment rating curve, generalised linear model, Random Forests, Quantile Regression Forests.

1. INTRODUCTION

Understanding the transport of sediment by streams is an important aspect related to issues of sediment-water quality interactions, reservoir siltation, water pollution, channel navigability, soil erosion and soil loss, fish and invertebrate habitat, malfunctioning of hydropower plants, instream mining, river restoration, river aesthetics, etc. (Walling, 1977; Williams, 1989). In addition, in the context of climate change, with the possibility of the progressive aridification of the climate in the Mediterranean, improving and adapting water resources management strategies is essential. For this purpose, accurate estimations of the sediment volume carried by rivers are necessary to prevent, as much as possible, problems derived from suspended sediment load circulating in rivers, especially in relation to the loss of water storage in reservoirs and water quality.

Rivers transport water and sediment from headwaters to the deposition areas, being responsible for the equilibrium between fluvial and marine processes in deltaic and coastal zones (e.g. Vericat and Batalla, 2006). Sediment can be carried downstream as bed load (particles that move along the river bed by rolling, skipping, or sliding) or as suspended load (supported by fluid flow and maintained by fluid turbulence). Bed load is flow dependent and generally accounts for around 10 % of a river's total solid transport. In alluvial streams, bed load can contribute as little as 1 % to the total annual load, while in mountain streams it may account for more than 70 % (Meade, Yuzyk and Day, 1990). In contrast, suspended load is typically source-dependent, i.e. wash-load. It is mostly composed by particles finer than 0.062 mm in diameter, although may also include bed-material particles i.e. sand fractions, during high flows. Suspended load is the major transporting mechanism in streams worldwide. Thus sediment yields are often based on data concerning the suspended load only (Wood, 1977). However, their computation, especially when based on a limited number of measurements, is not a trivial task.

1.1. Methodological issues –state of the art

In contrast to the measurement of discharge, measurements of suspended sediment concentration (*SSC*) or sediment flux are relatively intricate. Besides the direct determination of *SSC* from water samples in the lab, various indirect *in situ* (i.e. quasi-continuous) methods such as optical, X-ray or acoustic backscatter, attenuation or laser diffraction, etc. exist.

Direct measurements, however, remain the benchmark against which other methods are calibrated (Wren, Barkdoll, Kuhnle and Derrow, 2000). They are widely used where logistic, administrative or financial issues or *SSC*-range inhibit the use of *in-situ* measurements. But direct measurement of *SSC* demands sampling, which requires manual labour or automatic water samplers and thus can only produce intermittent data. Consequently, the estimation of sediment loads requires the integration of the continuous discharge data with discrete measurements of *SSC*, i.e. estimates of *SSC* between the observations have to be made. According to Holtschlag (2001), two approaches can be distinguished:

i) time-averaging methods / interpolators: *SSC* between observations is estimated from nearest neighbour, linear or spline interpolation. This method is apparently suitable when *SSC* is measured at high frequency compared to *SSC* variability. For less-frequent sampling, this method may fail to reproduce *SSC* dynamics; for unmonitored events, no *SSC*-prediction can be made at all. The estimations thus obtained are consistent with the data at the times of measurement, but do not allow for the estimation of uncertainty (Holtschlag, 2001). Sivakumar and Wallender (2005) advocate using a non-linear deterministic dynamic model that builds upon a local approximation in multi-dimensional phase-space. This method yielded promising results when used with comparatively densely sampled data but is also not suitable to predict values of unmonitored events.

ii) flow weighting methods / regression estimators: *SSC* is estimated by regression on ancillary variables. This approach generally does not exactly reproduce the observations

but can provide a formal measure for uncertainty. Commonly, linear regression on discharge data is used for this purpose (traditional 'sediment rating curve', *SRC*; Walling, 1984), but also other predictors can be included in multiple regression models (e.g. Cohn et al., 1992; Schnabel and Maneta, 2005). Regression is often carried out on log-transformed data to improve linearity between *SSC* and discharge and reduce heteroscedasticity (Smith and Croke, 2005). The resulting bias often requires a correction (Crawford, 1991; Asselman, 2000) that in turn may generate additional uncertainty (Smith and Croke, 2005). The nonlinearity of the underlying processes has also been dealt with by using second and third order polynomials or power and exponential functions (Schnabel and Maneta, 2005).

However, it is generally accepted that there is no simple discharge-*SSC* relationship which can be addressed by a single sediment rating curve (*SRC*). This issue has been dealt with by fitting different curves according to season or discharge range (Sivakumar and Wallender, 2005) or using moving rating curves for sediment flux estimation (van Dijk et al., 2005). Since soil loss is also highly related to other variables such as rainfall intensity (Schnabel and Maneta, 2005), especially for small ephemeral streams, accommodating these variables in models capable of using multiple predictors can greatly improve performance.

Generally, established regression estimators can also be applied for periods when no *SSC* observations are available as long as the necessary predictor data has been recorded (Holtschlag, 2001). *State-space-estimators* (e.g. Holtschlag, 2001) further extend this concept by considering autoregressive error components. These models can have high predictive performance (Holtschlag, 2001) but are conceptually more demanding. They require the estimation of additional parameters such as the covariances of process and measurement errors. Kisi et al. (2006) employed fuzzy logic to predict SSC from discharge. For *SSC* prediction from a set of predictors, Schnabel and Maneta (2005) applied polynomial regression and artificial neural networks. Nagy et al. (2002) trained artificial neural networks using stream-hydraulic parameters as predictors, which bridges the gap towards physically based approaches. Both FL and artificial neural networks are designed to address the issues of nonlinearity and have recently

experienced much attention. Both approaches are non-parametric and produce range-conservative predictions but no error estimations. Fuzzy logic is more interpretable and transparent than artificial neural networks but requires a subjective or automated calibration procedure (Kisi et al. 2006). Kisi (2005) demonstrated the inclusion of multiple predictors (discharge and SSC of preceding time step) with fuzzy logic and artificial neural networks and obtained slightly better performance with fuzzy logic, which was also reported by Lohani et al. (2007).

Instead of predicting *SSC*, Regüés et al. (2000) perform multivariate linear regression on flood-related sediment yields. Though being more direct and presumably more robust in the context of yield estimations, this approach requires a comparatively large database for calibration, because multiple *SSC*-measurements during a flood are integrated into a single value – a process that in itself requires high-frequency sampling or one of the methods presented above.

Thus, in the context of *SSC* prediction and sediment yield reconstruction for intermittently monitored sites, a method should be applied that deals adequately with the non-linear nature of the subject, includes multiple predictors and provides a measure for the uncertainty of predicted values. In the presented study, we explore the applicability of multivariate linear regression by means of generalised linear models (*GLM*s) and ensemble forecasting by regression trees for *SSC* predictions for four sites compared to traditional methods. The characteristics of the techniques employed are briefly outlined in the following section.

2. REGRESSION METHODS

2.1. (Generalised) linear regression models (GLMs)

Linear regression refers to relating a response variable Y to a set of predictors x_i in the form (e.g. Chatterjee and Price, 1991):

$$Y = b_{0+}b_1 \cdot x_1 + b_2 \cdot x_2 + \cdots + b_p \cdot x_p \quad (1)$$

where the coefficients b_i are adjusted to obtain an optimum fit. Each predictor x_i may consist of an unmodified or transformed value, such as the logarithm of the discharge. An advantage of linear regression is its easy implementation: in the univariate case, the model can be set up in most spreadsheet application; multivariate regression may require slightly advanced software. The obtained regression coefficients allow the interpretation of the predictors' influence. Linear regression models are computationally efficient and can also predict confidence intervals for the obtained coefficients and the predicted data, if the underlying statistical assumptions are met. These include normal distribution of error terms, homoscedasticity, independence of observations, (i.e. absence of autocorrelation) and absence of multicollinearity (e.g. Quinn and Keough, 2002). In practice, however, these assumptions often do not hold (e.g. Asselman, 2000; Holtschlag, 2001), which impedes an analysis of the uncertainties in parameters and predictions (Smith and Croke, 2005).

Generalised linear models (*GLM*s), in contrast, extend this concept by transforming the response variable with a link function and accommodating response variables with non-normal conditional distributions (e.g. Fox, 2002).

Therefore, applying an appropriate link function that ensures at least some of the above mentioned prerequisites (homoscedasticity, appropriate distribution of error terms) can potentially remedy these limitations. Furthermore, when applying the model for prediction, suitable link functions can confine the range of predictions to a reasonable interval (e.g. positive *SSC*s only), inhibiting physically implausible results.

2.2. Regression trees, Random Forests, Quantile Regression Forests

Classification and regression trees (*CART*s) are a non-parametric statistical technique for classification and regression problems (Breiman et al., 1984). A *CART* is a rule-based classifier that partition observations into groups having similar values for the response variable, based on a series of binary rules (splits) constructed from the predictor variables (Hastie et al. 2001). It is constructed as a binary decision tree by

recursive data partitioning, which can include both categorical and continuous data. In case of continuous response variables, i.e. regression trees, model predictions are obtained by calculating the average of the response variable in the respective terminal leaf of the tree. Model selection usually is carried out by crossvalidation which also yields a realistic estimate of model performance. Advantages of regression trees include the ability to deal with nonlinearity and interactions as well as their interpretability. Regression trees imply no assumptions about the distribution of the data. They are capable of handling non-additive behaviour, for which linear models require pre-specified interactions (De'ath and Fabricius, 2000). A disadvantage of regression trees is their instability with respect to small changes in the training data. To overcome this problem, bootstrap aggregation techniques such as bagging can be applied (Breiman 1996). In bagging, one takes a large number of bootstrap samples from the data set and fits a single tree to each bootstrap sample. To receive predictions for new data each of the fitted trees is used and their predictions are averaged (Prasad et al., 2006). Predictive performance is evaluated on those parts of the data that are not considered in the bootstrap samples (out-of-bag data, *OOB*). Usually, aggregated trees outperform single trees.

Random forests (*RF*, Breiman 2001) are a modified version of bagged trees (De'ath 2007). They employ an ensemble prediction of regression trees, i.e. a "forest" of trees is grown on the bootstrap samples. In contrast to bagging, a random subset of the predictors is used for each tree and at each node (Meinshausen 2006). This procedure results in a robust model that also yields internal error estimates and measures variable importance (Breiman, 2001). *RF*s include effective methods to handle missing values when training the model.

These ideas have been extended by Meinshausen (2006). Quantile Regression Forests (*QRF*) are a generalisation of *RF*s. For each node in each tree, *RF*s keep only the mean of the observations that fall into this node and neglect all other information. In contrast, *QRF*s keep the value of all observations in this node, not just their mean (Meinshausen 2006). Thus, *QRF*s consider the spread of the response variable. This allows the construction of prediction intervals which cover new observations with high probability.

Regression trees, *RF* and *QRF*-models do not allow easy interpretation of the effects of single predictors although there are some methods regarding the relative variable influence and partial dependency plots (cf. De'ath 2007). They are generally far more demanding in computational power than linear regression models. Because predictions are made from a weighted average of the training data, the model predictions will always be within the range of the observations: this precludes implausible values but inhibits extrapolation.

Our study compares the capability of traditional *SRC*s (i.e. simple linear regression models), *GLM*s, *RF* and *QRF*-models for *SSC* prediction using data from a flood season of four catchments of different size. Ancillary data (e.g. precipitation) is used to increase the predictive power. All models are tested using a bootstrapping approach. For each catchment, the best model is applied to the entire flood season which allows the calculation of flood-based sediment yields. Eventually, the advantages and problems associated with the different models are discussed.

3. STUDY AREA, INSTRUMENTATION AND DATABASE

This study uses data collected during a three-month observation period (September – December 2006) in the Isábena catchment (445 km²) and two of its sub-basins located in the Central Spanish Pyrenees (Fig. 1). The catchment is characterised by strong heterogeneity in relief, vegetation and soil characteristics, with elevation ranging from 450 m to 2,720 m asl in the northern parts (*Axial Pyrenees*, Valero-Garcés et al., 1999). The climate is a typical Mediterranean mountainous type with mean annual precipitation rates of 450 to 1600 mm, showing a strong south–north gradient due to topography (Verdú, 2007). Miocene continental sediments dominate the lower parts of the catchment with easily erodible materials (marls, sandstones, carbonates), leading to the formation of badlands and making them the major source of sediment within the catchment (Fargas et al., 1997).

Discharge and SSC were monitored (Tab. 1) in the Isábena catchment (Fig. 1) at time intervals of 2 minutes at Torrelaribera, 5 minutes at Villacarli and Cabecera gauge and 15 minutes at Capella (Fig. 3). SSC was measured within a flood-based sampling scheme by means of manual samples in Torrelaribera, Cabecera and Villacarli. Because of the shallow river and the highly turbulent flow, vertical mixing could be assumed complete at these locations. For Capella, automatic (ISCO 3700 automatic sampler) and manual sampling (i.e. DH-59 depth integrated sampler) was employed. In addition, turbidity was recorded every 15 minutes up to 3000 NTU (i.e. 3 g/l) in Capella. The total number of SSC measurements was 122 for Torrelaribera, 104 for Villacarli, 66 for Cabecera and 319 for Capella (for more details on instrumentation, see Francke et al., in press). The measured SSCs show great variability within up to five orders of magnitude (Table 1). 15-min rainfall data for three close-by rain gauges were included into the dataset.

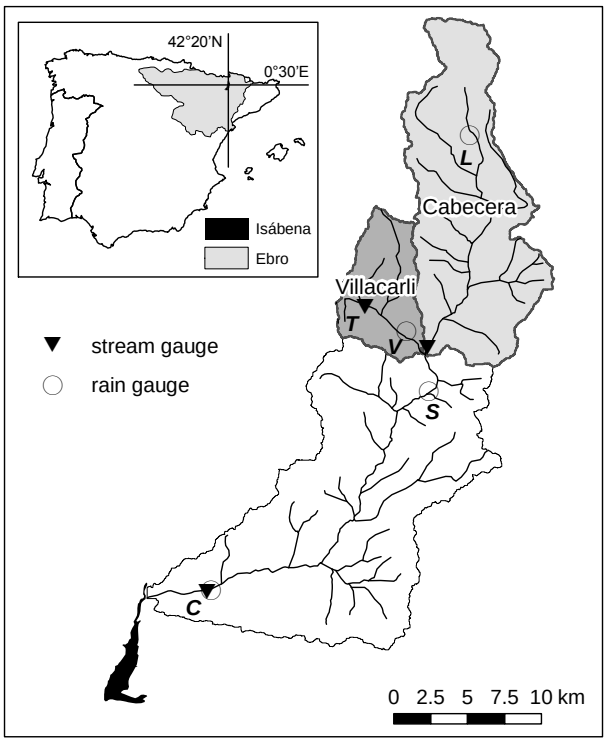

Figure 1. Isábena catchment with monitored subcatchments and rain gauges (C: Capella; L: Laspaules; S: Serraduy, T: Torrelaribera, V: Villacarli).

Table 1. Summary of measured discharge and *SSC* data

Subcatchment	Discharge [$m^3 s^{-1}$]			*SSC* [$g l^{-1}$]		
	min	mean	max	min	median	max
Torrelaribera (n=122)	0	0.002	0.68	0.001	2.8	240.6
Villacarli (n=104)	0.10	0.65	21.2	0.001	1.3	277.9
Cabecera (n=66)	0.91	3.77	43.4	0.002	0.1	30.5
Capella (n=331)	0.5	5.6	64.3	0.0005	1.2	99.6

4. METHOD

4.1. Model generation

Multiple models aimed at predicting *SSC* (our response variable) from ancillary data were set up. Ancillary datasets were selected according to the perceived capability of representing relevant processes (Table 2) and their continuous availability (cf. Schnabel and Maneta, 2005). Discharge data were included directly and log-transformed (*log_disch*), following common practice in sediment rating curve estimation. Further predictors are the Julian day, the sum of rainfall for 15 minutes, 60 minutes and 1 day registered at the three gauges Villacarli, Laspaules and Capella (denoted e.g. as *rain_capella15*), the respective USLE (Wischmeier and Smith, 1978) erosivity factors for 60 minutes and 1 day (denoted e.g. as *r_capella1d*), the cumulated discharge of the previous one, five hours and the entire observation period (denoted as e.g. *cum_q_5h*) and the rate of change in discharge (*limb_dec*).

4.1.1. Setup of traditional sediment rating curves (SRCs)

Traditional sediment rating curves resulted from fitting a linear relationship between *SSC* and discharge or log(*SSC*) and log(discharge), respectively. The extent of the Capella data set additionally also allowed performing the latter process separately for single floods (denoted s*SRC* hereafter).

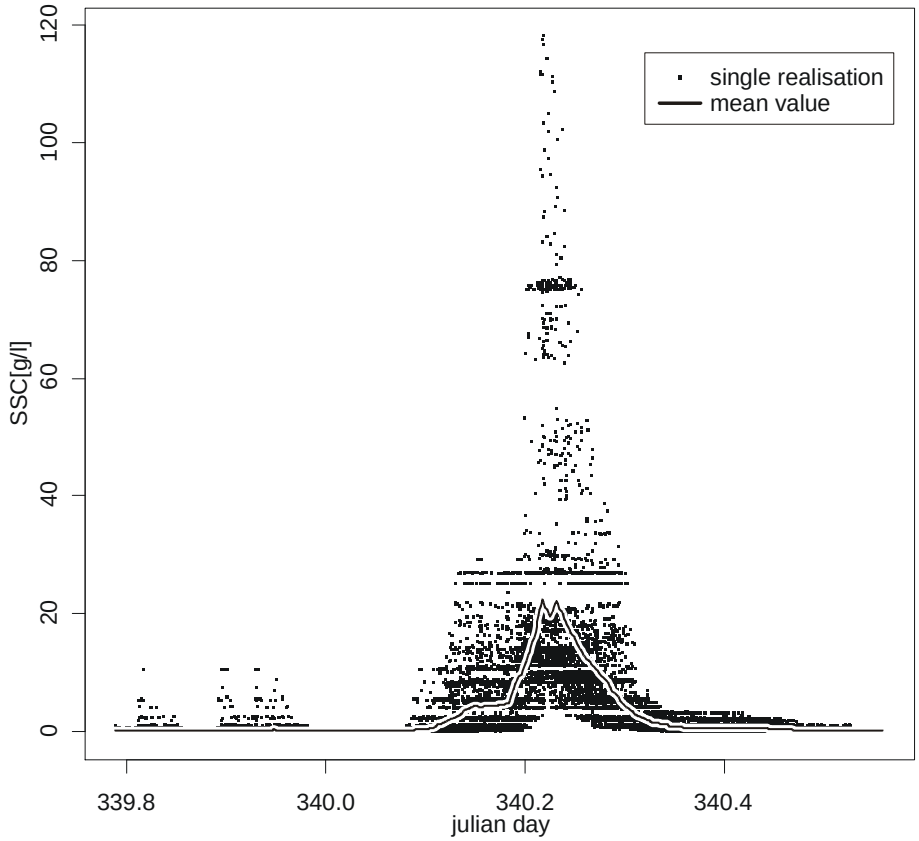

Figure 2. Monte-Carlo-simulation of SSC. Dots represent single realizations of the simulation and the continuous line their mean SSC-value (example from Torrelaribera, flood 12)

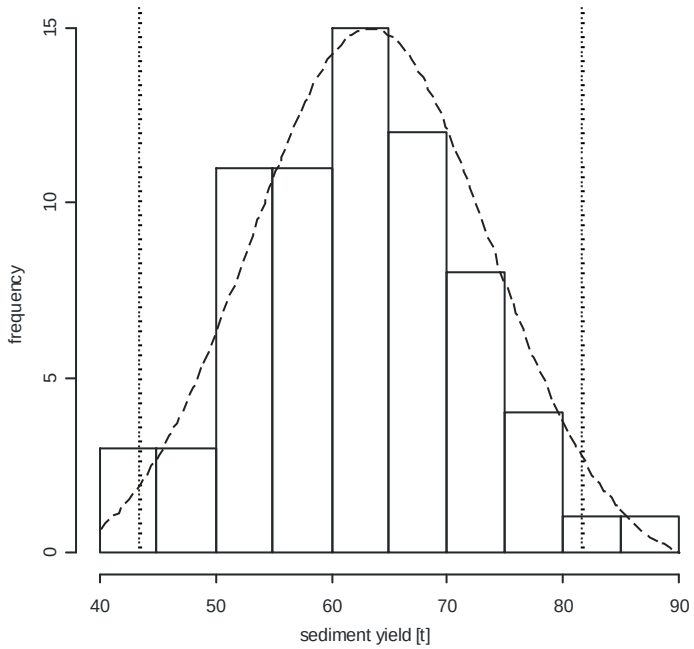

Figure 3. Distribution of Torrelaribera sediment yield computed by Monte Carlo method using 70 realisations (dashed: fitted normal distribution, dotted: 95 % confidence interval)

Table 2. Ancillary data used for regression (see Table 3 for abbreviations).

Presumably approximated process				
Sediment production on slopes	**Sediment production/re-mobilisation in riverbed**	**Exhaustion of sediment supply on slopes**	**Exhaustion of sediment supply within riverbed**	**Dilution**
rain_x15 rain_x60 rain_x1d r_x60 r_x1d	discharge rain1d cum_q_1h cum_q_5h	julian_day rain_x1d cum_q_1h cum_q_5h r_x1d	julian_day limb_dec cum_q_1h cum_q_5h	discharge rain_x15 rain_x60 rain_x1d cum_q_1h cum_q_5h

Table 3. Abbreviations used in the text

Abbreviation	**Meaning**
rain_*x*15	Cumulated rainfall of 15 min recorded in *x*
rain_*x*60	Cumulated rainfall of 60 min recorded in *x*
rain_*x*1d	Cumulated rainfall of 1 day recorded in *x*
r_*x*60	Hourly rainfall recorded in *x*
r_*x*1d	Daily rainfall erosivity recorded in *x*
cum_q_1h	Cumulated discharge during 1 hour
cum_q_5h	Cumulated discharge during 5 hours
cum_q_all	Cumulated discharge for entire observation period
log_disch	Log-transformed discharge data
limb_dec	Rate of change in discharge

4.1.2. Setup of generalised linear models (GLMs)

GLM-regression was performed using the Box-Cox-transformation (Box and Cox, 1964) (Equation (2)) and logit-transformation (Equation (3)) as link functions. The Box-Cox-parameter λ was selected by maximum-likelihood estimation (Fox, 2002). The logit-transformation was performed on *SSC*/*maxval*, where the value for *maxval* was manually adjusted to achieve normality in the response variable. Both link functions were chosen because of their potential to reduce heteroscedasticity and their effect of constraining model predictions to positive values.

$$Y^* = \begin{cases} \frac{Y^\lambda - 1}{\lambda} for\ \lambda \neq 0 \\ ln(Y)\ for\ \lambda = 0 \end{cases} \quad (2)$$

$$Y^* = ln\left(\frac{Y/maxval}{1-Y/maxval}\right) \quad (3)$$

where Y^* is the transformed variable, Y is the untransformed variable (*SSC*) and λ is the

maxval transformation parameter.

We performed predictor variable selection to find the minimum adequate model and obtain concise robust models by preventing overfitting and eliminate collinearity in the predictors (e.g. Harrell, 2001). Since most of the predictors included are related to rainfall-runoff processes, many of them are correlated. Collinearity in the predictors can be problematic when interpreting coefficients or for prediction if the correlation structure is not constant (Fox, 2002). For all locations, the predictors could be grouped into roughly three independent classes. Therefore, in the reduced models, only three not strongly correlated predictors (i.e. |Spearman correlation coefficient|<0.6) were included. Because there is no established "standard" procedure for variable selection (Crawley, 2002), three different methods were used:

- *Best subset regression* (e.g. Chatterjee and Price, 1991) performs an exhaustive search of all combinations of (in our case up to 3) predictors. We then selected the best model (according to Mallow's *Cp* criteria) with uncorrelated predictors.

- In *hierarchical partitioning* (Mac Nally and R., 1996), the independent predictive power of each predictor is computed. We selected the three predictors with the highest percentage of independent effects, making sure they are uncorrelated.

- The *stepwise procedure on bootstrapped dataset* (Harrell, 2001) generates a bootstrap sample of the full dataset, select the minimum adequate *GLM* by a "stepwise"-algorithm employing Bayes Information Criterion (BIC) as a selection criterion (which is stricter than the commonly used Akaike Information Criterion, AIC, cf. e.g. Reineking and Schröder, 2006). This procedure was repeated 1000 times. We chose the predictors that had been selected most often in the 1000 repetitions, making sure they are uncorrelated.

4.1.3. Setup of RF and QRF models

Starting with the full set of predictors, the optimum number of selected predictors used for splitting at each node (parameter *mtry*) was selected according to the lowest out-of-bag error E_{OOB} for the *RF* model: For each tree *i*, the mean squared error $E_{OOB,i}$ for the *OOB*-data is computed. E_{OOB} is calculated from the average error of all $E_{OOB,I}$ (Breiman, 2001). For *QRF*, the same *mtry* was used. The minimum size of terminal nodes (*nodesize*) was set to five in both approaches.

4.2. Model comparison and selection

To assess the reliability and robustness of the employed models, validation was performed using a bootstrapping approach (n = 1000), where bootstrapped training data sets were generated and model performance was assessed on the remaining test data. We then used the Spearman correlation coefficient R_{Sp} between modelled and observed *SSC*, averaged over all bootstrap runs, as a measure of goodness-of-fit. $R_{Sp,full}$ for the full dataset is calculated as:

$$\overline{\mathrm{R}_{\mathrm{Sp,full}}} = \mathrm{mean}\left[\mathrm{cor}_{\mathrm{Sp}}\left(\mathrm{SSC}_{\mathrm{mod,SSC}_{\mathrm{obs}}}\right)\right] \quad (4)$$

$R_{Sp,test}$ for the test dataset is computed as:

$$\overline{R_{Sp,test}} = mean\left[cor_{Sp}\left(SSC_{mod}^{test}, SSC_{obs}^{test}\right)\right] \quad (5)$$

Optimism in R_{Sp} (Harrell, 2001) can be written as:

$$O_{R_{Sp}} = \overline{R_{Sp,train}} - \overline{R_{Sp,test}} \quad (6)$$

with:

$$\overline{R_{Sp,train}} = mean\left[cor_{Sp}\left(SSC_{mod}^{train}, SSC_{obs}^{train}\right)\right] \quad (7)$$

where *SSC* denotes suspended sediment concentration, subscripts "*obs*" and "*mod*" meaning "observed" or "modelled" values, respectively. Superscripts "*full*", "*train*" and "*test*" refer to the entire, training or test dataset, respectively.

R_{Sp} is more suited to deal with nonlinear models and the range of the data over several orders of magnitude than the traditionally used coefficient of determination R^2. The "optimism" in R_{Sp} gives information on the dependency of the model structure on the subset of the training data and therefore its robustness.

4.3. Sedigraph prediction and calculation of sediment yield

For each of the datasets, the most appropriate model was applied to data of the complete monitoring period, i.e. 10. September – 12. December. The obtained sedigraph data contained three values for each time step: a "best estimate", being the value predicted by the model, and a lower and upper value comprising the 95 % confidence interval for prediction.

Sediment yields for flood and inter-flood periods were computed using a Monte Carlo approach: For each time step, we randomly drew a *SSC* value from the 95 % confidence interval, according to its probability. Subsequently, the sediment yield for the current time span (flood or inter-flood period) was obtained by multiplying with the discharge data. Repeating the previous two steps *n* times yielded a distribution of sediment yield estimates, from which we computed the 95 % confidence interval for the population (see examples in Figures 2 and 3).

Model building and statistical analyses were conducted using R (R-Team Development Core, 2006) with the packages *car* (Fox, 2006), *leaps* (Miller and Lumley, 2006), *MASS* (Venables and Ripley, 2002), *randomForests* (Liaw and Wiener, 2002), and *quantregForest* (Meinshausen, 2007).

5. RESULTS AND DISCUSSION

5.1. Model building and predictor selection

For all datasets, optimum transformations of the response variable to achieve normal distribution were obtained either by logit or Box-Cox transformation with parameters

maxval=300 and $\lambda = 0$, respectively.

The three methods of predictor selection propose different subsets as being most suitable for further consideration (see Table 4). In four cases, variable selection by bootstrapping did not show any preference, making this method the least dependable for the given datasets. For the Villacarli and Capella datasets, best subset and regression and hierarchical partitioning lead to the same subset of predictors, while the results of both methods differ when applied to the datasets of Torrelaribera and Cabecera. Moreover, for the Capella dataset, predictor selection by bootstrapping differs from the other methods only in choosing daily erosivity instead of daily rainfall values as predictor.

Table 4. Results of predictor selection (for abbreviations see Table 3 and Table 5)

	Transformation	Selection Method	Predictors	Code
Torrelaribera	boxcox	best subset	log_disch, r_villacarli1d, cum_q_all	GLM_T1
		hier. part.	log_disch, julian_day, rain15	GLM_T2
		bootstrap	*no preference*	-
	logit	best subset	log_disch, rain15, cum_q_all	GLM_T3
		hier. part.	log_disch, julian_day, rain15	GLM_T4
		bootstrap	*no preference*	-
Villacarli	boxcox	best subset	log_disch, rain60, cum_q_all	GLM_V1
		hier. part.	log_disch, rain60, cum_q_all	
		bootstrap	rain15, limb_dec, rain1d	GLM_V2
	logit	best subset	log_disch, rain60, cum_q_all	
		hier. part.	log_disch, rain60, cum_q_all	GLM_V3
		bootstrap	*no preference*	-
Cabecera	boxcox	best subset	rain15, rain1d, rain_laspaules60	GLM_Cb1
		hier. part.	rain1d, julian_day, discharge	GLM_Cb2
		bootstrap	rain15, rain_laspaules1d, julian_day	GLM_Cb3
	logit	best subset	julian_day, rain1d, rain_laspaules60	GLM_Cb4
		hier. part.	rain1d, julian_day, discharge	GLM_Cb5
		bootstrap	*no preference*	-
Capella	boxcox	best subset	log_disch, rain1d, cum_q_all	GLM_Cp1
		hier. part.	log_disch, rain1d, cum_q_all	
		bootstrap	log_disch, r_villacarli1d, cum_q_all	GLM_Cp2
	logit	best subset	log_disch, rain1d, cum_q_all	GLM_Cp3
		hier. part.	log_disch, rain1d, cum_q_all	
		bootstrap	log_disch, r_villacarli1d, cum_q_all	Cp4

For Torrelaribera, log-transformed discharge is contained in all selected model structures. The predictors *julian_day*, *rain15* and *cum_q_all* have been selected twice each. For Villacarli, hierarchical partitioning and best subset search yielded the same combination of predictors for both transformations, which also included the log-transformed discharge.

Discharge (or log thereof) is an important predictor for all locations except Cabecera where it has only been selected twice. Instead, *julian_day* and rainfall-related predictors are included, indicating that discharge apparently plays a minor role for *SSC* here. In all but two predictor sets, *julian_day* or *cum_q_all* is contained. Since both are increasing monotonically, this suggests a systematic trend in *SSC* during the observation period.

5.2. Comparison of model performance

Table 5 compares the model performances in terms of Spearman rank correlations, *RMSE* and optimism. For the traditional *SRC*-approaches of relating *SSC* to discharge or the respective log-transformations, differences cannot be observed with regard to R_{Sp}. For Torrelaribera and Capella, the log-transformation reduces the *RMSE*, but for Villacarli and Cabecera the untransformed version outperforms the regression of log-transformed values in terms of *RMSE*.

The *GLM*s including more variables generally show a better performance (higher R_{Sp}, lower *RMSE*) than the traditional *SRC*s, especially for Capella. Considerable differences among the *GLM*s exist for Villacarli and Cabecera, which is particularly pronounced in the case of V2 with poor performance. Except for the Cp1-4, the *GLM*s show comparatively high values for optimism in R_{Sp}. This notion of low robustness of the *GLM*s is also apparent in the numerical instability: during the bootstrapping, for some *GLM*s in up to 95 % of the bootstrap cycles (e.g. Cp3) the model could not be fitted to the training data.

RF and *QRF* models deliver the best performance in $R_{Sp,full}$ and $R_{Sp,train}$ except for *RF* of Cabecera. The *RF*s feature the lowest *RMSE*-values, those of *QRF* are slightly higher but generally lower than those of the *GLM*s. Optimism of the *RF*s and *QRF*s is also low (if not the lowest) among all investigated models. The best overall R_{Sp} values range from 0.85 to 0.95, except for Cabecera, where only 0.65 to 0.67 are achieved.

In addition to the models listed in Table 5, a traditional *SRC* was fitted for each flood separately, yielding a set of *SRC*s specific for each event (s*SRC*). When applied to the

full dataset, the s*SRC* model achieves an *RSME* of 10.4, making it only marginally better than the *GLM*s, and being clearly outperformed by the *RF* and *QRF* models with *RMSE*s of 5.3 and 6.9, respectively.

Because of their favourable properties, the *RF* and *QRF* models will be used for the future analyses for all gauges.

Table 5. Performance of models used for *SSC* prediction

	Model	**Full dataset**	**OOB data**		
		$R_{Sp,full}$	**$R_{Sp,test}$**	***RMSE***	**Optimism R_{Sp}**
Torrelaribera	*SSC*~discharge	0.75	0.74	29.98	0.25
	log(*SSC*)~log(log_disch)	0.75	0.74	27.02	**0.18**
	*GLM*_T1	0.79	0.71	28.61	0.80
	*GLM*_T2	0.77	0.72	**26.95**	0.55
	*GLM*_T3	0.77	0.71	33.21	0.95
	*GLM*_T4	0.68	0.69	33.23	0.90
	Random Forests	**0.88**	**0.83**	**26.46**	0.46
	Quantile Regression Forests	**0.91**	**0.87**	27.48	**0.22**
Villacarli	*SSC*~discharge	0.64	0.64	25.85	**0.24**
	log(*SSC*)~log(log_disch)	0.64	0.63	25.98	0.25
	*GLM*_V1	0.68	0.65	**25.65**	0.93
	*GLM*_V2	0.42	0.04	30.57	0.89
	*GLM*_V3	0.69	0.63	33.33	1.19
	Random Forests	**0.85**	**0.76**	**24.24**	0.24
	Quantile Regression Forests	**0.89**	**0.83**	27.09	**0.09**
Cabecera	*SSC*~discharge	0.40	0.39	5.73	0.24
	log(*SSC*)~log(log_disch)	0.40	0.39	6.06	0.29
	*GLM*_Cb1	0.38	0.62	4.28	0.64
	*GLM*_Cb2	0.63	**0.65**	3.56	0.55
	*GLM*_Cb3	0.59	0.62	4.23	1.03
	*GLM*_Cb4	0.58	0.59	**4.18**	0.96
	*GLM*_Cb5	0.63	0.59	3.95	0.76
	Random Forests	**0.65**	0.58	**3.89**	**0.23**
	Quantile Regression Forests	**0.67**	**0.67**	5.09	**0.09**
Capella	*SSC*~discharge	0.14	0.13	17.15	**0.02**
	log(*SSC*)~log(log_disch)	0.14	0.14	14.08	**0.00**
	*GLM*_Cp1	0.75	0.73	**11.73**	0.07
	*GLM*_Cp2	0.76	0.75	12.04	0.06
	*GLM*_Cp3	0.75	0.75	12.76	0.27
	*GLM*_Cp4	0.76	0.75	13.05	0.24
	Random Forests	**0.94**	**0.84**	**8.30**	0.07
	Quantile Regression Forests	**0.93**	**0.88**	12.21	0.07

5.3. Sedigraph prediction and calculation of sediment yield

The reconstructed sedigraphs show good agreement with the observed data (e.g., Fig. 4). However, high *SSC* values, especially at the beginning of the observation period, are partially underestimated, probably resulting from the low number of observations of this kind and the characteristics of conservative estimation of *QRF*.

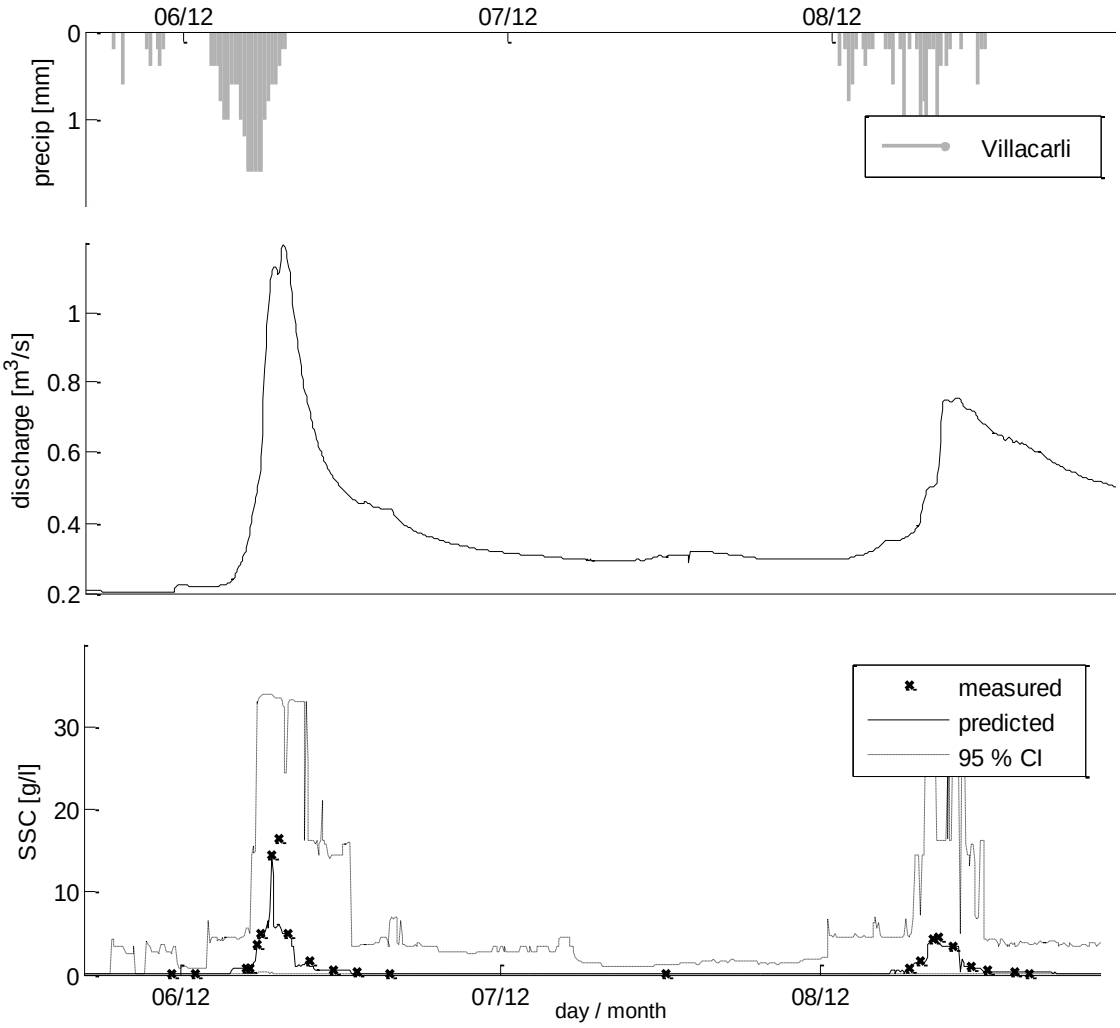

Figure 4. Close-up-view of rainfall, discharge and *SSC* (measured and modelled) for two floods at Villacarli

The confidence bounds are quite narrow shortly after the event and during low flows but widen considerably during periods of high dynamics, reflecting a higher level of uncertainty in these estimates. For Torrelaribera, Villacarli and Capella, *SSC*-values tend to be somewhat overestimated during the low-flow periods at the beginning of the observation. For Villacarli and Capella with continuous runoff, this effect may lead to a

slight overestimation of the early inter-flood sediment yields, while it is irrelevant for Torrelaribera because of the ephemeral runoff regimen.

The Monte Carlo simulation for calculating sediment yield has been performed on a flood-basis to analyze the effect of individual floods. Figure 5 shows the respective results for Villacarli. The greatest absolute uncertainties are related to the large flood events in September, where the confidence interval increases to 20 % of the value of best estimate. For later floods, the absolute range of the confidence intervals decreases. During low-flows, they are relatively narrow due to the low variability of *SSC* during these periods.

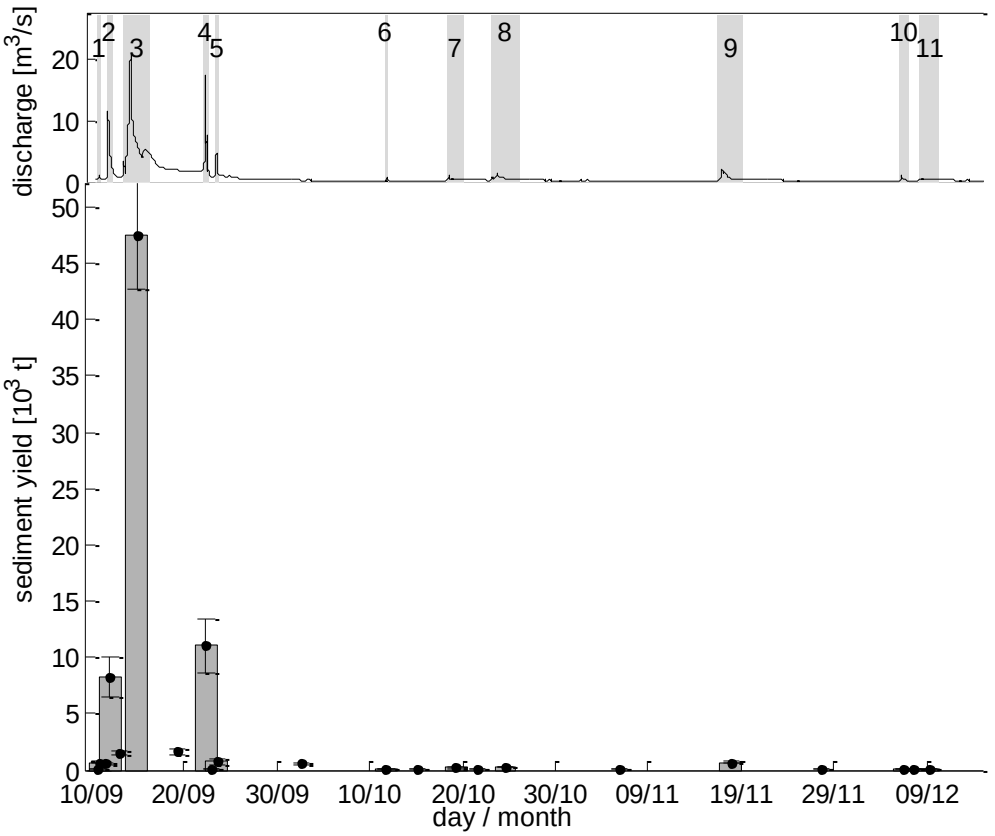

Figure 5. Hydrograph (top), sediment yield of flood (bars and whiskers) and interflood (whiskers only) periods at Villacarli. The whiskers comprise the 95 % *CI*. The grey bars underlying the hydrograph depict the numbering of the floods.

For the sediment yield of the entire observation period, the relative size of the confidence interval ranges from 9 to 18 % of the mean value. Apparently, the large

relative confidence intervals are associated with large *RMSE* values of the underlying model (Table 6).

Table 6. Total sediment yield with 95 % confidence interval for the different gauges within the observation period (calculated with the *QRF* model).

Gauge	**Total sediment yield [t]**	***CI*-95% [t]**	**Coefficient of variation [%]**
Torrelaribera	509	419-599	8.9
Villacarli	74,103	63,971-84,235	6.9
Cabecera	20,087	18,340-21,832	4.4
Capella	173,706	149,100-197,702	7.1

5.4. Analysis of effects of predictors, reproduction of hysteresis loops

Figure 6 depicts the variable importance of the 12 most important predictors for the *RF*-models. For each predictor, the loss of model performance (expressed as increase in Mean Squared Error, IncMSE) is quantified when it is omitted from the model. Thus, the explanatory power of each predictor can be assessed. For Torrelaribera, *SSC* is mainly explained by the predictors *discharge*, rate-of-change in discharge *limb_dec* and daily rainfall *rain1d*. Whereas *discharge* (or *log_disch*, respectively) has also been identified as an important predictor for the *GLM*s (see Table 4), this is not the case for the latter two predictors favoured by *RF*.

For Villacarli, *discharge*, *julian_day* and *limb_dec* have the highest explanatory power. The former two are also included in four of the five *GLM*s as *log_disch* and *cum_q_all*; the latter appears only in one *GLM* (see Table 4). For Cabecera and Capella, the predictive explanatory power is more concentrated in few predictors: the Cabecera-model relies mostly on *rain1d*, *julian_day* and *r_laspaules60*. The predictive power of the former two has also been identified by the variable selection methods for the *GLM*s, resulting in their inclusion in four of five *GLM*s.

At Capella, *SSC* dynamics are mostly reflected in the predictor *julian_day* which could be a result of the high number of temporally close samples of the automatic sampler and their relative similarity in *SSC*. Thus, *RF* shows its capability of taking advantage of

higher sampling frequency when combined with a rather steady evolution of the response variable. Apart from this effect which essentially builds on interpolation in time, the predictors *discharge* and its cumulative sums over one and five hours hold some explanatory power for the *RF*-model, although not very distinct. The latter two are not included in any of the *GLM*s, whereas *rain1d*, favoured by four of the six *GLM*s, only ranks among the least important predictors for *RF*.

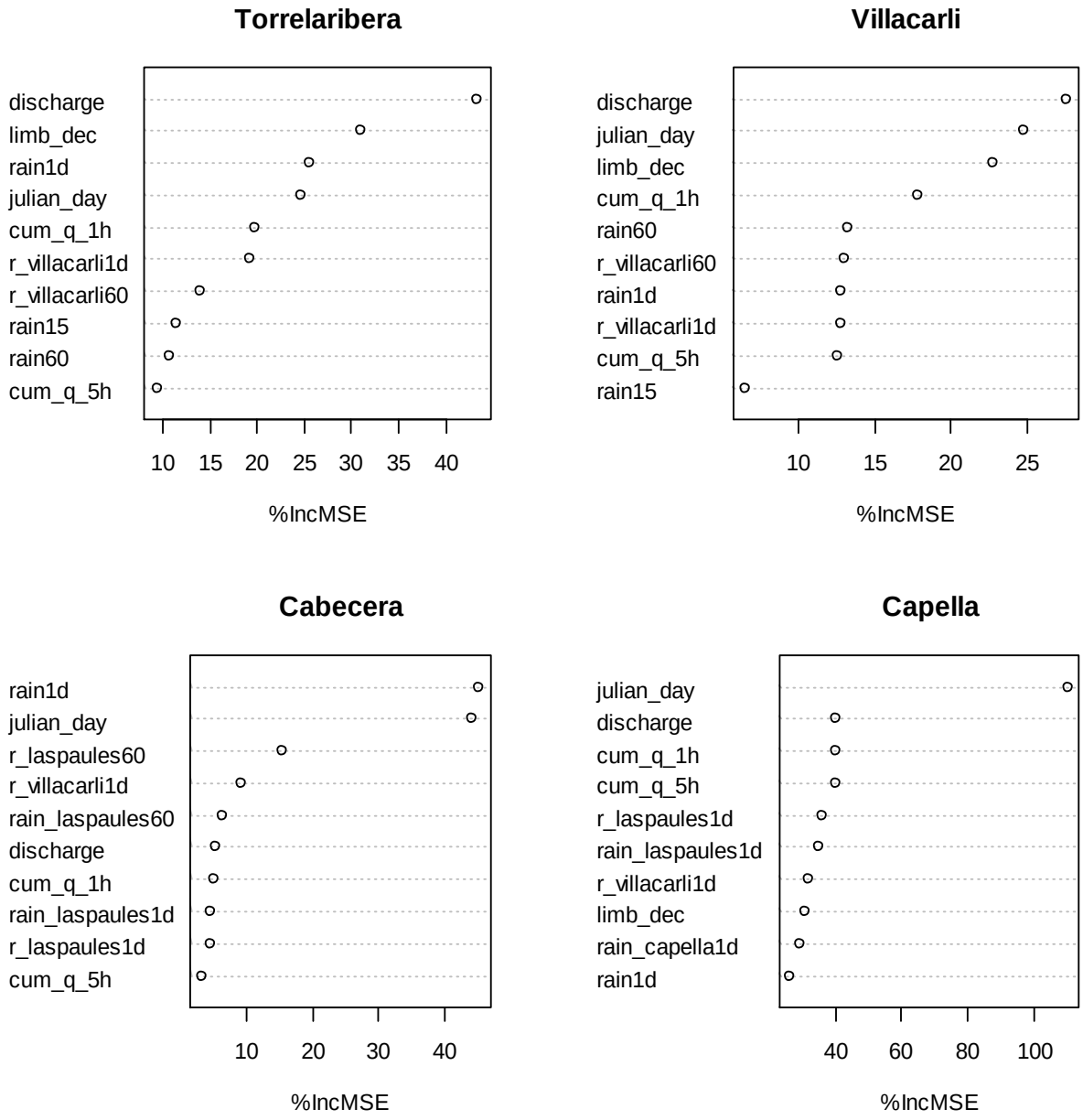

Figure 6. Variable importance for application of *RF* model. Equivalent predictors in the *RF* model (log_disch~discharge, cum_q_all~julian_day) have been omitted (see Table 3 for abbreviations).

In contrast to *GLM*s, regression trees and Fuzzy Logic, where the influence of each predictor can be interpreted from coefficients, tree structure or rules respectively, *RF* and *QRF* do not provide easy insight. Nevertheless, where interactions are not too complex, the qualitative effect of important predictors can still be revealed by suitable plots.

In a simple traditional *SRC* (*SSC* ~ *Q*), the slope *S* of the *Q*-*SSC*-relation (*S=dSSC/dQ*) is a constant, usually positive, value. When using log-transformed data (*logSSC~logQ*), *S* is a function of *Q* itself. We analysed *S* for the *RF* model. In Figure 7 each dot represents *S* for one record in the dataset, with one of the predictors (plotted along the x-axis) varied throughout its entire range. As with traditional *SRC*s, *S* is positive regardless of daily rainfall and the Julian day, but may vary considerably (from almost zero to 2.5), reflecting the effects of other predictors. On average (Figure 7*Figure* a, black line), however, *S* decreases gradually for very high amounts of daily rainfall (>40 mm). This suggests that changes in discharge have progressively less effect under conditions of much prior rainfall. Analogously, Figure 7b depicts a similar effect for the advancing season.

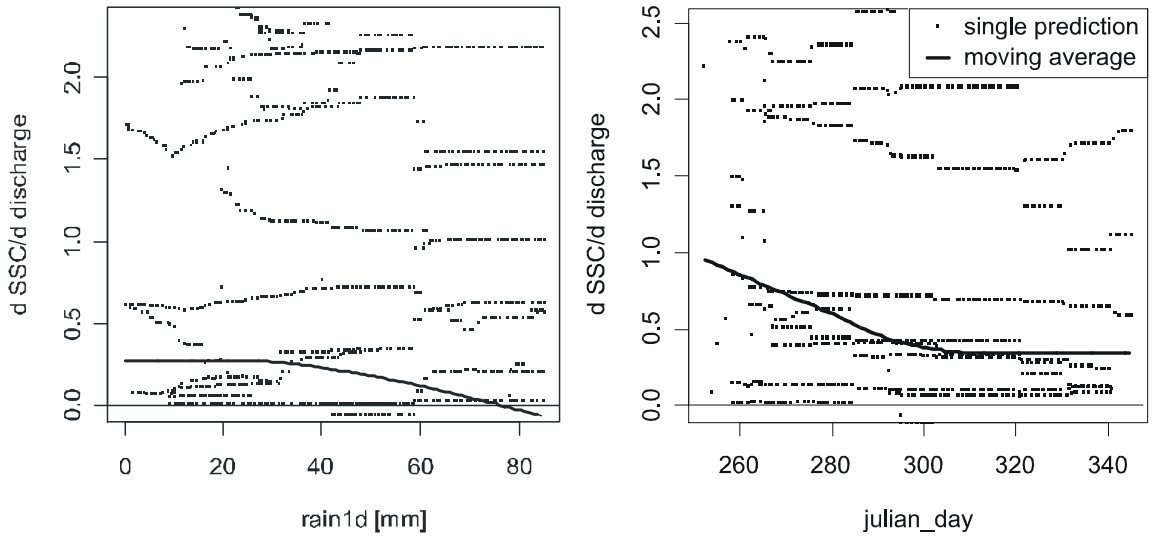

Figure 7a, b. Effect of changes in *SSC* per change in discharge for different conditions of daily rainfall and season. The continuous line marks the moving average (example from Torrelaribera).

5.4.1. Hysteresis

Hysteresis is a common feature of the discharge-SSC relationship during a flood (Williams, 1989). This effect cannot be reproduced by traditional SRCs and most other univariate approaches, but requires advanced methods (e.g. fuzzy logic, artificial neural networks, Lohani et al., 2007). RF and QRF also provide this capability. For a monitored flood, the observed values with clockwise hysteresis are closely reproduced (Figure 8a). For a completely unmonitored event, a plausible characteristic with a clockwise hysteresis is also predicted, although somewhat spiky in some parts (Figure 8b).

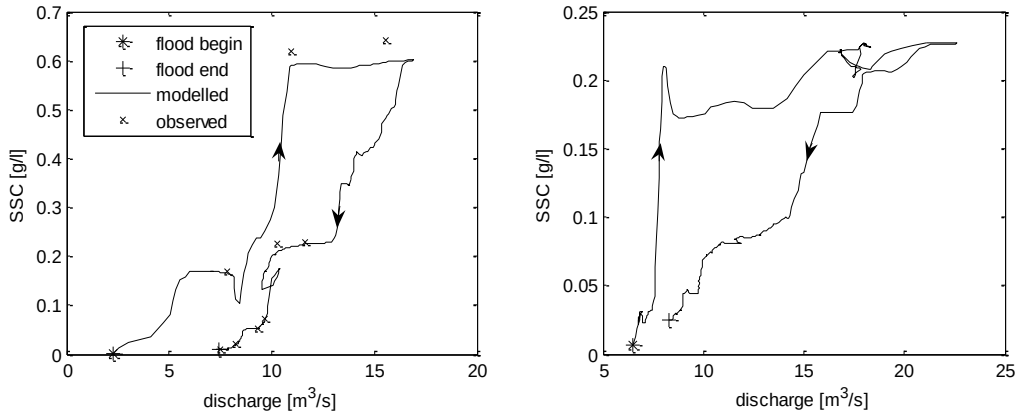

Figure 8. Hysteresis loops for (a) a monitored and (b) an unmonitored flood corresponding to floods 5 and 4 at Cabecera, respectively.

6. DISCUSSION OF MODEL PROPERTIES, SHORTCOMINGS

For the given datasets, the tested models showed pronounced differences in their performance in predicting *SSC*. Traditional *SRC*s performed poorly in reproducing *SSC*-variability. Since discharge as the only predictor is insufficient, the application of multivariate models is indicated. In the case of *GLM*s, this requires the choice of the appropriate link functions, and the best set of predictors to prevent overfitting. The three different methods for predictor selection yielded inconclusive results, which only converged slightly for the data set with the largest sample size (Cabecera, see Table 4). The performance of the analysed *GLM*s deteriorated strongly on the test data set. This

suggests that, despite all efforts, an apparently good fit on the training data was partially caused by overfitting the models using more degrees of freedom. The investigated *GLM*s do not include any interactions between predictors and no predictor can have a non-linear effect, which also contributes to their inferiority when compared to *RF* and *QRF* that can implicitly account for these effects.

The good performance of *RF* / *QRF* and their favourable properties make them a promising technique for *SSC* prediction. Moreover, the results illustrated in Figure allow plausible conclusions for the underlying processes: Figure a suggests that changes in discharge have progressively less effect under conditions of much prior rainfall, which is presumably a result of the exhaustion of sediment supplies due to depletion. Analogously, Figure b can be interpreted as a similar effect for the advancing season, probably also because of sediment exhaustion or, implicitly, decreasing rainfall intensity as the season progresses. These findings confirm the perception based on field-observation of a relatively intricate system of sediment delivery, where various processes of sediment production, temporal storage and conveyance interact.

As well as the errors that are related to instrumentation and monitoring setup (Francke et al., 2008), the following limitations of the proposed methods must be noted.

Regression analysis as performed here assumes independent observations. Due to the time-series characteristics of the matter, however, a certain degree of serial correlation must be expected. The limited number of temporally-close samples suggests that short term variability on the scale of 30 min is considerable for the headwater catchments, but autocorrelation at Capella is apparently an issue.

The applied *QRF*-method can be seen as an adaptive neighbourhood regression procedure: Each prediction is computed from a weighted mean of all observations, restricting the range of the predictions to the range of the observations. The resulting effect of underestimating peak concentrations on one hand and the overestimation of low *SSC* on the other hand has also been observed with linear regression and *ANN* models (Schnabel and Maneta, 2005; Lohani et al., 2007) and may eventually lead to an

underestimation of *SSC* variability.

The regression was performed using samples of an observation period of only three months. This restricts the applicability of the derived models to this time span. For temporal extrapolation, sampling of longer time period is mandatory. Regarding the high inter-annual variability rainfall and, thus, of sediment transport processes, temporal extrapolation is especially problematic as annual yields may be subject to major variability of up to an order of magnitude (Regüés et al., 2000). Therefore, the training data must contain a wide range of observations. Furthermore, for longer time spans, the definitions of the supplementary variables such as Julian day and cumulated runoff have to be replaced by cyclic predictors such as the seasonality indices used by Holtschlag (2001).

The Monte Carlo method for assessing the confidence intervals of the sediment yield calculation assumes uncorrelated data in time, otherwise the prediction interval is likely to be underestimated (Meinshausen, personal communication, 2007). As mentioned before, this point could not be properly investigated.

In spite of these limitations, the presented methodology clearly performs better than traditionally used *SRC*s, because additional influential processes can be accounted for. The use of *GLM*s was problematic because the choice of the optimum set of predictor variables turned out to be strongly dependent on the variable selection method and thus not robust. Only for the largest dataset (Capella) did the variable selection methods produce comparable results, while in general the selected variables differed. Predictor selection by bootstrapping proved to be the least robust method because it was not able to designate important predictors for some cases or returned combinations of relative poor performance.

7. CONCLUSION

Predicting suspended sediment concentrations from auxiliary data is often performed using models of different complexity. Especially in small catchments with high *SSC*

dynamics and a multitude of involved processes, the traditional sediment rating curve-approach of relating *SSC* to discharge is unsatisfactory. We employed traditional sediment rating curves (*SRC*), generalised linear models (*GLM*), Random Forests (*RF*) and Quantile Regression Forests (*QRF*) techniques and included ancillary predictor data to improve the predictive power. While *GLM*s could generally reproduce observed *SSC* better than traditional *SRC*s, the choice of the most suitable predictors remains problematic because of the different results produced by the variable-selection methods employed. Furthermore, some *GLM*s tended to be numerically unstable and all of them showed a considerable drop in performance when used on independent test data not included in the training.

In contrast to the *GLM*s, the non-parametric *RF* and *QRF* models provided the best performance and, in the case of *QRF*, allowed the calculation of confidence intervals for the predictions, which enabled the computation of sediment yields and the associated uncertainties. The proposed method identifies predictors with high explanatory power. Multiple interactions of predictors can be accounted for without prior knowledge, and in the case of simple interactions, these can be interpreted. These advantages, which cannot be found combined in any of the established methods, provide potential for tackling questions of suspended sediment transport in rivers in a qualitative and quantitative way, especially when based on a limited number of samples.

Acknowledgements

This research was carried out within the SESAM-project (Sediment Export from Semi-Arid catchments: Measurement and Modelling) funded by the German Science Foundation (Deutsche Forschungsgemeinschaft, DFG). The second author has a research grant from the Catalan Government and the European Social Fund. Rainfall data were obtained from the Spanish National Institute of Meteorology (INM) and the Ebro Water Authorities (SAIH). Hydrological data were supplied by the Ebro Water Authorities (SAIH). The Ebro Water Authorities also provided logistic support for using the Capella gauging station. We would like to thank Ramon J. Batalla and Damià Vericat for the installation of the sampling equipment in Capella and to the students of the University of Potsdam assisting in the field and in the laboratory.

REFERENCES

Asselman, N.E.M., 2000. Fitting and interpretation of sediment rating curves. *Journal of Hydrology*, **234**(3-4): 228 - 248.

Box, G.E.P., Cox, D.R., 1964. The analysis of transformations (with discussion). *Journal of the Royal Statistics Society*, **26**: 211-252.

Breiman, L., 1996. Bagging predictors. *Machine Learning*, **24**: 123-140.

Breiman, L., 2001. Random Forests. *Machine Learning*, **45**(1): 5-32.

Breiman, L.M., Friedman, J., Olshen, R., Stone, C., 1984. *Classification and regression trees.* Wadsworth: Belmont, CA.

Chatterjee, S., Price, B., 1991. *Regression analysis by example*. Wiley: New York.

Cohn, T., Caulder, D., Gilroy, E., Zynjuk, L., Summers, R., 1992. The Validity of a Simple Statistical Model for Estimating Fluvial Constituent Loads: An Empirical Study Involving Nutrient Loads Entering Chesapeake Bay. *Water Resources Research*, **28**: 2353-2363.

Crawford, C.G., 1991. Estimation of suspended-sediment rating curves and mean suspended-sediment loads. *Journal of Hydrology*, **129**(1-4): 331 - 348.

Crawley, M.J., 2002. *Statistical computing an introduction to data analysis using S-Plus*. Wiley: Chichester.

De'ath, G., 2007. Boosted trees for ecological modeling and prediction. *Ecology*, **88**: 243–251.

De'ath, G., Fabricius, K.E., 2000. Classification and regression trees: a powerful yet simple technique for the analysis of complex ecological data. *Ecology*, **81**(11): 3178-3192.

Fargas, D., Martínez-Casasnovas, J., Poch, R., 1997. Identification of Critical Sediment Source Areas at Regional Level. *Physics and Chemistry of the Earth*, **22**(3-4): 355-359.

Fox, J., 2002. *An R and S-PLUS companion to applied regression*. Sage: Thousand Oaks, CA.

Fox, J., 2006. *car: Companion to Applied Regression, R package version 1.2-1*. http://www.r-project.org.

Francke, T., López-Tarazón, J.A., Vericat, D., Bronstert, A., Batalla, R.J., 2008. Flood-Based Analysis of High-Magnitude Sediment Transport Using a Non-Parametric Method. *Earth Surface Processes and Landforms*, **33**: 2064-2077.

Harrell, F.E., 2001. *Regression modeling strategies : with applications to linear models, logistic regression, and survival analysis*. Springer: New York, NY.

Hastie, T., Tibshirani, R., Friedman, J.H., 2001. *The elements of statistical learning: data mining, inference, and prediction.* Springer: New York.

Holtschlag, D.J., 2001. Optimal estimation of suspended-sediment concentrations in streams. *Hydrological Processes*, **15**: 1133-1155.

Kisi, O., 2005. Suspended sediment estimation using neuro-fuzzy and neural network approaches. *Hydrological Sciences Journal*, **50**(4): 683-696.

Kisi, O., Emin-Karahan, M., Sen, Z., 2006. River suspended sediment modelling using a fuzzy logic approach. *Hydrological Processes*, **20**(20): 4351-4362.

Liaw, A., Wiener, M., 2002. Classification and Regression by Random Forests. *R News*, **2**(3): 18-22.

Lohani, A.K., Goel, K., Bhatia, K.K.S., 2007. Deriving stage–discharge–sediment concentration relationships using fuzzy logic. *Hydrological Sciences Journal*, **52**(4): 793-807.

MacNally, R., 1996. Hierarchical partitioning as an interpretative tool in multivariate inference. *Australian Journal of Ecology*, **21**: 224-228.

Mallows, C.L., 1973. Some comments on Cp. *Technometrics*, **15**: 661-675.

Meade, R.H., Yuzyk, T.R., Day, T.J., 1990. Movement and storage of sediment in rivers of the United States and Canada. In: Wolman, M.G., Riggs, H.C. (eds): *Surface Water Hydrology, The Geology of North America*, vol. O-1. Geological Society of America, Boulder, CO, 255–280.

Meinshausen, N., 2006. Quantile Regression Forests. *Journal of Machine Learning Research*, **7**: 983-999.

Meinshausen, N., 2007. *quantregForest: Quantile Regression Forests; R package version 0.2-2*. http://www.r-project.org.

Miller, T., Lumley, A., 2006. *leaps: regression subset selection; R package version 2.7*. http://www.r-project.org.

Nagy, H.M., Watanabe, K., Hirano, M., 2002. Prediction of Sediment Load Concentration in Rivers using Artificial Neural Network Model. *Journal of Hydraulic Engineering*, **128**(6): 588-595.

Prasad, A.M., Iversion, L.R., Liaw, A. 2006. Newer classification and regression tree techniques: bagging and random forests for ecological prediction. *Ecosystems*, **9**: 181–199.

Quinn, G.P., Keough, M.J., 2002. *Experimental design and data analysis for biologists*. Cambridge Univ. Press: Cambridge.

Regüés, D., Balasch, J.C., Castelltort, X., Soler, M., Gallart, F., 2000. Relación entre las tendencias temporales de producción y transporte de sedimentos y las condiciones climáticas en una pequeña cuenca de montaña mediterránea (Vallcebre, Eastern Pyrenees). *Cuadernos de Investigación Geográfica*, **26**: 24-41.

Reineking, B., Schröder, B., 2006. Constrain to perform: Regularization of habitat models. *Ecological Modelling*, **193**(3-4): 675-690.

Schnabel, S., Maneta, M., 2005. Comparison of a neural network and a regression model to estimate suspended sediment in a semiarid basin. In: Batalla, RJ, Garcia, C. (eds): *Geomorphological Processes and Human Impacts in River Basins*. *IAHS Publication* 299, 91-100.

Sivakumar, B., Wallender, W.W., 2005. Predictability of river flow and suspended sediment transport in the Mississippi River basin: a non-linear deterministic approach. *Earth Surface Processes and Landforms*, **30**(6): 665-677.

Smith, C., Croke, B., 2005. Sources of uncertainty in estimating suspended sediment load. In: Horowitz, A.J., Walling, D.E. (eds): Sediment Budgets 2. IAHS: 136-143.

R-Team Development Core. 2006. *R: A Language and Environment for Statistical Computing*. R Foundation for Statistical Computing: Vienna, Austria.

Valero-Garcés, B.L., Navas, A., Machín, J., Walling, D.E., 1999. Sediment sources and siltation in mountain reservoirs: a case study from the Central Spanish Pyrenees. *Geomorphology*, **28**: 23–41.

Venables, W.N., Ripley, B.D., 2002. *Modern Applied Statistics with S*. Springer: New York.

Verdú, J.M., Batalla, R.J., Martínez-Casasnovas, J.A., 2006. Estudio hidrológico de la cuenca del río Isábena (Cuenca del Ebro). I: Variabilidad de la precipitación. *Ingeniería del Agua*, **13**(4): 321-330.

Vericat, D., Batalla, R.J., 2006. Balance de sedimentos en el tramo bajo del Ebro. *Cuaternario y Geomorfología*, **20**(1-2): 79-90.

Walling, D.E., 1977. Limitations of the rating curve technique for estimating suspended sediment loads, with particular reference to British rivers. In: *Erosion and Solute Matter Transport in Inland Waters*. *International Association of Hydrological Sciences. Publication no*. **122**: 34-38.

Walling, D.E., 1984. Dissolved loads and their measurements. In: Hadley R.F., Walling D.E. (eds): *Erosion and sediment yield: Some methods of measurements and modeling*. Geo Books: London; 111-177.

Williams, G.P., 1989. Sediment concentration versus water discharge during single hydrologic events in rivers. *Journal of Hydrology*, **111**: 89-106.

Wischmeier, W.H., Smith, D.D., 1978. *Predicting rainfall erosion losses. Agriculture Handbook 537*. USDA. Agricultural Research Service, Washington, DC.

Wood, P.A., 1977. Controls of variation in suspended sediment concentration in the River Rother, West Sussex, England. *Sedimentology*, **24**: 437-445.

Wren, D.G., Barkdoll, B.D., Kuhnle, R.A., Derrow, R.W., 2000. Field Techniques for Suspended-Sediment Measurement. *Journal of Hydraulic Engineering*, **126**(2): 97-104.

ANNEX 2
SUSPENDED SEDIMENT MODEL APPLICATION

INDEX ANNEX 2: SUSPENDED SEDIMENT MODEL APPLICATION

Francke, T., López-Tarazón, J.A., Vericat, D., Bronstert, A., Batalla, R.J., 2008. Flood-based analysis of high-magnitude sediment transport using a non-parametric method**.** *Earth Surface Processes and Landforms*, **33**: 2064-2077.

Figure captions in the paper

Figure 1. Isábena catchment and monitored subcatchments Villacarli and Cabecera (C: Capella;Cb: Cabecera; L: Las Paules; S: Serraduy, T: Torrelaribera).

Figure 2. Variable importance for prediction of *SSC* (for details cf. section 3.2)

Figure 3. Close-up-view of rainfall, discharge and *SSC* (measured and modelled) for two floods at Villacarli (*CI*: 95 % confidence interval).

Figure 4. Sediment yield of flood (bars and whiskers) and interflood (whiskers only) periods. The whiskers comprise the 95 % *CI*. The grey bars underlying the hydrograph depict the numbering of the floods.

Figure 5. Duration curves of water and sediment fluxes. Cabecera+Villacarli (C+V) denotes the simulated properties of the confluence of subcatchments Villacarli and Cabecera.

Figure 6. Combined sediment yield of Villacarli and Cabecera compared to sediment yield at Capella. Note the different scale for flood 1-3; “n.d.” denotes “no data”.

Table captions in the paper

Table 1. Summary of subcatchment characteristics.

Table 2. Ancillary data used for regression analysis (abbreviations explained in the text).

Table 3. Mean, upper and lower quartile (*q*25%, *q*75%) of monthly rainfall and maximum daily rainfall recorded at INM-station Serraduy (9853) 1988-2005 compared to data measured during observation period (2006).

Table 4. Summary of measured discharge (*Q*) and suspended sediment concentration (*SSC*) data.

Table 5. Performance of *SSC*-prediction using *QRF* in comparison with traditional sediment rating curves.

Table 6. Flood based sediment yields. Note that the flood numbers are not related between locations.

Table 7. Total and specific sediment yield for observation period (95 % confidence interval in brackets).

1. INTRODUCTION

This annex reports on the application and the capability of the non-parametrical statistical techniques (*Random Forest*, *Quantile Regression* Forest) applied to model the continuous sedigraphs from ancillary data to an extremely rainy season with extremely high taxes of sediment transport in 2 of the mains sub-basins and the entire Isábena basin. For this purpose we present a paper analysing the application of the non-parametrical regressions to obtain a continuous sedigraph from ancillary hydrological data. Paper is presented maintaining its original structure; its format has been adapted to the general format of the present volume.

The paper was published by *Earth Surface Processes and Landforms* in November 2008; it presents the results of the monitoring, a method for the calculation of a sedigraph from intermittent measurements and the derived sediment yields at the Isábena catchment outlet and two adjacent sub-catchments during a three-month period. The observed suspended sediment concentrations (*SSC*) demonstrate the role of badlands as sediment sources, but *SSC* displayed only a loose correlation with discharge, inhibiting the application of a simple sediment rating curve. Instead, ancillary variables acting as driving forces or proxies for the processes were included in a quantile regression forest model to explain the variability in *SSC*. The variables with most predictive power vary between the sites, suggesting the predominance of different processes. Finally, relating upland sediment production to yield at the outlet suggests considerable effects of sediment storage within the river channel.

2. SUSPENDED SEDIMENT MODEL APPLICATION

Francke, T., López-Tarazón, J.A., Vericat, D., Bronstert, A., Batalla, R.J., 2008. Flood-based analysis of high-magnitude sediment transport using a non-parametric method**.** *Earth Surface Processes and Landforms*, **33**: 2064-2077

Flood-based analysis of high-magnitude sediment transport using a non-parametric method

Abstract

Upland erosion and the resulting reservoir siltation is a serious issue in the Isábena catchment (445 km², Central Spanish Pyrenees). During a three-month period, water and sediment fluxes have been monitored at the catchment outlet (Capella), two adjacent subcatchments (Villacarli, 41 km²; Cabecera, 145 km²) and the elementary badland catchment Torrelaribera (8 ha). This paper presents the results of the monitoring, a method for the calculation of a sedigraph from intermittent measurements and the derived sediment yields at the monitored locations. The observed suspended sediment concentrations (*SSC*) demonstrate the role of badlands as sediment sources: *SSC* of up to 280 g/l were encountered for Villacarli, which includes large badland areas. *SSC* at the Cabecera catchment, with great areas of woodland, barely exceeded 30 g/l. *SSC*s directly at the sediment source (Torrelaribera) were comparable to those at Villacarli, suggesting a close connection within this subcatchment. At Capella, *SSC*s of up to 99 g/l were observed. For all sites, *SSC* displayed only a loose correlation with discharge, inhibiting the application of a simple sediment rating curve. Instead, ancillary variables acting as driving forces or proxies for the processes (rainfall energy, cumulative discharge, rising/falling limb data) were included in a quantile regression forest model to explain the variability in *SSC*. The variables with most predictive power vary between the sites, suggesting the predominance of different processes. The subsequent flood-based calculation of sediment yields attests high specific sediment yields for Torrelaribera and Villacarli (6,277 and 1,971 t km^{-2}) and medium to high yields for Cabecera and Capella (139 and 410 t km^{-2}) during the observation period. In all catchments, most of sediment was exported during intense storms of late summer. Later flood events yield successively less sediment. Relating upland sediment production to yield at the outlet suggests considerable effects of sediment storage within the river channel.

Keywords: suspended sediment, sediment yield, sediment rating curve, quantile regression forest, Isábena.

1. INTRODUCTION

Reservoirs face siltation worldwide. However, siltation is accelerated in areas where runoff occurs over highly erodible unconsolidated sediments on bare slopes (i.e. badlands on marls, mudstones or shales) under severe climatic conditions, such as in the Mediterranean mountains, with long dry periods and storms of high rainfall intensity. There, most sediment is detached and eroded during short high magnitude rainfall events. Under such circumstances erosion rates are very high, creating high-density flows in the river network that reach the lowlands, even in large catchments. Quite often sediments are deposited in reservoirs located at the basin outlet. Sedimentation in reservoirs is not only an environmental issue but also a socio-economic problem, since it causes water quality problems and, especially, a progressive reduction in dam impoundment capacity, which creates serious problems for water management, especially near dam outlets.

Badlands are considered to be characteristic of arid regions but they also occur in wetter climates with high intensity storm events such as in the Mediterranean (Gallart *et al.*, 2002). The so-called humid badlands are found in mountainous areas such as the Southern Alps (e.g. Mathys *et al.*, 2005) and the Pyrenees (e.g. Clotet *et al.*, 1988). There, mean annual precipitation is around 700 mm or higher. Rainfall mostly occurs in the form of high intensity storm events. Vegetation growth is no longer limited by water availability but by the high erosion rates and freezing on north exposed slopes (Regüés *et al.*, 2002). This is the case for the Isábena River basin, a 445 km² catchment located in the Central Pyrenees that drains extensive areas of badlands that have been identified as the main source of the sediment deposited in the downstream Barasona Reservoir (Valero-Garcés *et al.*, 1999). Instantaneous concentrations of suspended sediment of up to 300 g/l have been measured at the basin outlet (López-Tarazón, 2006). The Barasona Reservoir supplies the region with water for drinking and irrigation. The large amount of sediment input coming from the badlands leads to a severe reduction in the storage capacity of the reservoir. Therefore, intense monitoring and specific modelling are needed to gain a better understanding of the magnitude and frequency of erosion and sediment transport in these particular fluvial environments which will help with

informing management decisions in relation to the long-term availability and quality of water resources.

Within this context, this study aims to quantify flood-based sediment yields in two highly active headwater catchments in the upper Isábena River. The results are compared with the sediment delivery from a zero-order badland catchment and the sediment yield at the outlet of the basin, upstream of the reservoir. The findings provide insights into the magnitude and temporal dynamics of sediment delivery and its driving forces. For this purpose, a novel regression approach is applied that allows the interpolation of intermittent measurements of suspended sediment concentrations, computes confidence intervals for these estimates and enables the calculation of sediment loads. Sediment fluxes are quantified at a range of spatial scales and catchments units (i.e. badland, headwater tributaries, river mainstem, lowland). Sediment yields and improved process understanding aid calibration and contribute to improvements in a numerical hydrological and sediment transport model (Bronstert et al., 2007) as well as the development of a 1D-model of reservoir sedimentation (Mamede et al. 2006). The paper develops a comprehensive conceptual framework to couple river channel with wider catchment processes; specifically, it links particle detachment and soil erosion to in-channel sediment transport and downstream sedimentation. Thus, it provides new data and methods relevant to studies of sediment transport in highly erodible montane catchments, many of which are experiencing increasing frequency of extreme flows and high rates of sediment loss as a result of environmental change.

2. STUDY AREA

This study was carried out in the Isábena catchment (Central Spanish Pyrenees) and two of its main sub-basins Villacarli and Cabecera (Figure 1). The catchment has an area of 445 km² and is part of the Ebro Basin. It is characterised by heterogeneous relief, vegetation and soil characteristics. Elevation increases from 450 m a.s.l. in the southern and central parts of the catchment (i.e. Intermediate Depression and Internal Ranges) to up to 2,720 m a.s.l. in the northern part (i.e. Axial Pyrenees). The climate is typical of

Mediterranean mountainous areas, with mean annual precipitation of 767 mm (from 450 to 1600 mm) and an average potential evaporation rate of 550 to 750 mm, both rates showing a strong south–north gradient due to topography (Verdú et al, 2006a). Vegetative cover includes deciduous woodland, agriculture, pasture and *matorral* in the valley bottoms, evergreen oaks, pines and *matorral* in the higher areas. The Northern parts are composed of Paleogene and Cretaceous sediments and the southern lowlands are mainly dominated by Miocene continental sediments. These areas consist of easily erodible materials (marls, sandstones), leading to the formation of badlands and making them the major source of sediment within the catchment (Fargas *et al.*, 1997). Badlands can mainly be found in the Villacarli sub-basin (6 % of total area), while they are almost absent in the adjacent Cabacera sub-basin (<0.1 % of total area). Within the former, the areal fraction of badlands may be as high as 30 %, as it is the case for the zero-order badland catchment Torrelaribera.

The Isábena River drains into the Barasona Reservoir (Figure 1). The dam was constructed in the early 1930s for an original capacity of 71 hm^3 and it was enlarged in 1972 reaching a total capacity of 92 hm^3. The reservoir supplies water mainly to the Aragón and Catalunya canal that irrigates an area of ca. 70,000 ha. For almost 75 years the reservoir has been progressively silting up at a rate of between 0.3 and 0.5 hm^3 of sediment deposited per year. Engineering works during the 1990s released sediment through the dam bottom outlets resulting in around 5 hm^3 of sediment being sluiced through the dam. Nowadays the reservoir capacity equals that of 1993 (76 hm^3).

Table 1. Summary of subcatchment characteristics.

Subcatchment	**Area (km^2)**	**Lithology**	**Dominant landuse**
Torrelaribera	0.08	Mesozoic marls	Matorral Badlands (30 %)
Villacarli	41	Mesozoic marls, limestone, sandstone	Forest Matorral Pasture Badlands (6 %)
Cabecera	145	Conglomerates, Limestone	Forest Pasture [Badlands (<0.1 %)]
Isábena (Capella gauging station)	445	as in Villacarli and Cabecera plus quaternary deposits	Forest Matorral Pasture Agriculture [Badlands (<0.02 %)]

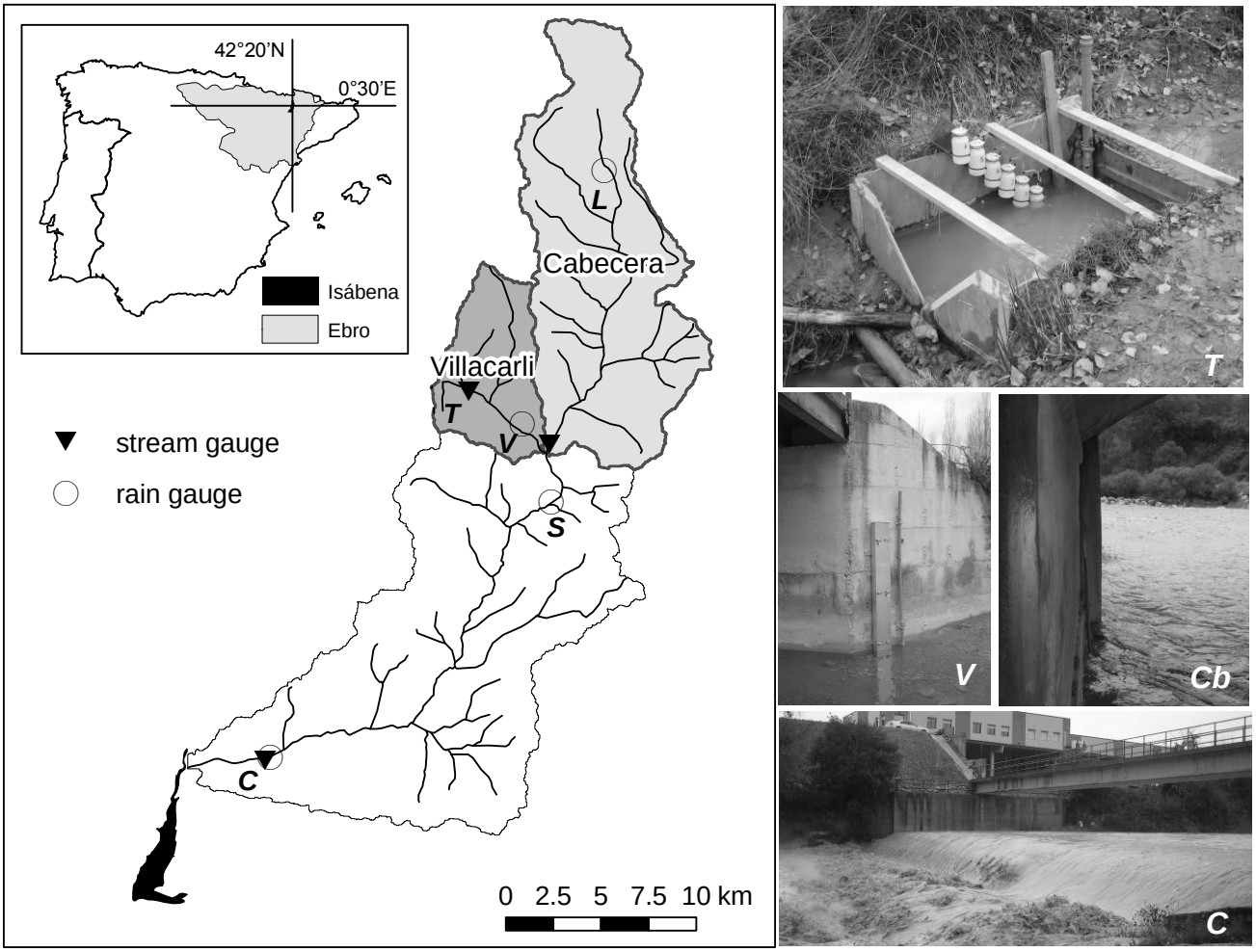

Figure 1. Isábena catchment and monitored subcatchments Villacarli and Cabecera (C: Capella;Cb: Cabecera; L: Las Paules; S: Serraduy, T: Torrelaribera).

2. METHODOLOGY

2.1. Instrumentation

During a three-month observation period (September – December 2006), discharge (hereafter *Q*) and suspended sediment concentration (hereafter *SSC*) were monitored at four sites in the Isábena catchment (Table 1, Figure 1). Late summer and autumn is when most thunderstorms and rainfall events take place, therefore this study focussed on this time of the year. The discharge was measured using a capacitive water stage sensors/loggers (Trutrack WT-HR) installed at suitable cross sections at the Torrelaribera, Villacarli and Cabecera subcatchments (Figure 1). Flow stage was

recorded at a 2 to 5 minute interval. At Torrelaribera, a sharp-crested V-notch weir provided a constant cross section, while at Villacarli and Cabecera the river constriction below bridges were employed. Repeated discharge measurements were made using the volumetric technique, current meter (OTT C2) transects and tracer dilution (NaCl) completed with cross section surveys (Geodimeter total station). During high water stages and for safety reasons, flow velocity was measured at the water surface only (Villacarli) and at a wider section (Cabecera). Water stage-discharge rating curves were derived by combining the stage-mean velocity and stage-area methods as being more robust for extrapolation (Mosley and McKerchar *et al.*, 1993). Water depth was recorded at a 15 minute time interval at the Capella gauging station at the basin outlet. This station is operated by the Ebro Water Authorities whose stage-discharge rating curve was used for discharge calculation.

Suspended sediment was manually sampled and stored in 1-litre-bottles at a frequency of 20 to 90 minutes during flood events and routinely during low flows. Due to highly turbulent flow conditions, mixing was assumed complete. Additionally, a total of six samples originate from rising stage sediment samplers at Torrelaribera and Villacarli (Figure 1). At the Capella station, samples were obtained by means of an ISCO automatic sampler and manual sampling; in addition, turbidity is recorded every 15 minutes up to 3000 NTU (i.e. 3 g/l). A calibration equation was developed to convert turbidity to *SSC* using 490 pairs of values gained from water samples (*SSC [g/l]=0.0012 NTU+0.0605;* r^2*=0.82*). Out of the data set obtained from the turbidimeter, twelve measurements (weekly interval) were used in the analysis to represent the otherwise undersampled low-flow periods, complementing the measurements obtained from the automatic sampler. The data collection resulted in 611 values of SSC over the four study sites (Torrelaribera:122; Villacarli:104; Cabecera: 66; Capella: 331). Samples were vacuum filtered (Millipore, 0.045 mm pore size) or decanted when concentrations were (approximately) above 4 g/l, oven-dried and weighed to determine *SSC*.

Precipitation was measured using a tipping-bucket rain gauge installed in Villacarli. In addition, 15-minute rainfall data for the Cabecera and the Isábena catchments were

obtained from the rain gauges at Las Paules and Capella (Ebro Water Authorities P030 and P047, respectively, see Figure 1).

3.2. Interpolation of SSC measurements

Discharge and *SSC* show poor statistical relationships in all the study sites, impeding the use of the traditional Flow Duration Curve method (Walling, 1984) to calculate the sediment yield. A continuous sedigraph was produced allowing the calculation of sediment yields from ancillary data using a Quantile Regression Forests model (hereafter *QRF*). *QRF* (Meinshausen, 2006) are a non-parametric multivariate regression technique that builds on Random Forests (*RF*) regression tree ensembles (Breiman., 2001). Regression trees (a.k.a. CARTs, Breiman *et al.*, 1984) are constructed by recursive data partitioning, which can include both categorical and continuous data from ancillary datasets. *RF* and *QRF* employ an ensemble of these trees, each one grown on a random subset of the training data. Model predictions are obtained from the mean of the prediction of each single tree (*RF*) or based on the distribution of these single-tree predictions (*QRF*). *RF* and *QRF* perform favourably when dealing with nonlinearity, imply no assumptions about the distribution of the data and are robust and capable of handling non-additive behaviour, which makes them particularly attractive for the problem at hand. Furthermore, measures of variable importance are calculated: For each predictor, the loss of model performance (expressed as increase in Mean Squared Error, IncMSE) is quantified when it is omitted from the model. Thus, the explanatory power of each predictor can be assessed (see Figure 2 below for example).

For the use as additional predictors, ancillary datasets (Table 2) were selected according to the perceived capability of representing relevant processes (cf. Schnabel and Maneta, 2005) and their continuous availability. These predictors include the Julian day, the sum of rainfall for 15 minutes, 60 minutes and 1 d registered at the three gauges Villacarli, Laspaules and Capella (denoted e.g. as *rain_capella15*), the respective USLE erosivity factors for 60 minutes and 1 day (denoted e.g. as *r_capella1d*), the cumulative discharge of the previous one and five hours (denoted as e.g. *cum_q_5h*) and the rate of change in discharge (*limb_dec*).

Table 1. Ancillary data used for regression analysis (abbreviations explained in the text).

Presumably approximated process				
Sediment production on slopes	**Sediment production/re-mobilisation in riverbed**	**Exhaustion of sediment supply on slopes**	**Exhaustion of sediment supply within riverbed**	**Dilution**
(discharge) rain_x15 rain_x60 rain_x1d r_x60 r_x1d	discharge rain1d cum_q_1h cum_q_5h	julian_day rain_x1d cum_q_1h cum_q_5h r_x1d	julian_day limb_dec cum_q_1h cum_q_5h	discharge rain_x15 rain_x60 rain_x1d cum_q_1h cum_q_5h

To assess the reliability and robustness of the employed models, validation was performed using a bootstrapping approach (n=1000), where bootstrapped training data sets were generated and model performance on the remaining test data assessed. The Spearman correlation coefficient R_{Sp} between modelled and observed *SSC*, averaged over all bootstrap runs, was used as a measure of goodness-of-fit. $R_{Sp,full}$ for the full dataset is calculated as:

$$\overline{R_{Sp,full}} = \mathrm{mean}\left[\mathrm{cor}_{Sp}\left(\mathrm{SSC}_{mod,\mathrm{SSC}_{obs}}\right)\right]$$

$R_{Sp,test}$ for the test dataset is computed as:

$$\overline{R_{Sp,test}} = mean\left[cor_{Sp}\left(SSC_{mod}^{test}, SSC_{obs}^{test}\right)\right]$$

Optimism in R_{Sp} (Harrell (2001) is estimated as:

$$O_{R_{Sp}} = \overline{R_{Sp,train}} - \overline{R_{Sp,test}}$$

with

$$\overline{R_{Sp,train}} = mean\left[cor_{Sp}\left(SSC_{mod}^{train}, SSC_{obs}^{train}\right)\right]$$

where subscripts "*obs*" and "*mod*" mean "observed" or "modelled" values, respectively. Superscripts "*full*", "*train*" and "*test*" refer to the entire, training or test dataset, respectively. R_{Sp} is more suited to deal with nonlinear models and the range of the data

over several orders of magnitude than the traditionally used coefficient of determination R^2. The "optimism" in R_{Sp} gives information on the dependency of the model structure on the subset of the training data and thus for the models robustness.

3.3. Sedigraph prediction and calculation of sediment yield

By applying the calibrated models to data of the complete monitoring period (September 10 to December 15, 2006) in the temporal resolution of the discharge dataset, *SSC* data for each timestep was estimated (i.e. values for best estimate, lower and upper limit of the 95 % Confidence Interval for prediction, hereafter *CI*). Subsequently, flood-based sediment yields and their confidence intervals were computed using a Monte-Carlo-approach: For each time-step, random *SSC*-value was randomly drawn from the 95 % *CI*, according to its probability. From these values, the flood-based sediment yields were computed. Repeating this process 70 times allowed the calculation of the *CI* for the sediment yield of each flood.

Model building and statistical analyses were conducted using the statistic software R (R-Team Development Core, 2006) with the randomForest (Liaw and Wiener, 2002) and quantreg-Forest (Meinshausen, 2007) packages.

4. RESULTS

4.1. Primary data

Rainfall was unusually strong in September 2006 (Table 3). The monthly total of 252 mm is almost three times the 20-year average value at the station of Serraduy that is located 2 km downstream from the confluence of the Villacarli and Cabecera torrents (Figure 1). The September precipitation surpassed the previous maximum recorded September rainfall by more than 70 mm. The maximum daily rainfall of 57 mm also ranks among the highest within the record. From October to December 2006, rainfall characteristics were close to average (within the interquartile range). At Capella rain gauge station (Figure 1), the September precipitation of 2006 was 202 mm compared to

a mean of 92 mm and a previous maximum of 149 mm (10 years of data). Similar conditions were encountered at the rain gauge located in Las Paules (10 years of data), with percentile values of 100 and 90 for monthly rainfall and maximum daily rainfall in September, respectively, confirming that September 2006 was unusually wet over the entire catchment.

Table 3. Mean, upper and lower quartile (*q*25%, *q*75%) of monthly rainfall and maximum daily rainfall recorded at INM-station Serraduy (9853) 1988-2005 compared to data measured during observation period (2006).

Month	**Monthly rainfall [mm]**		**Max daily rainfall [mm]**	
	Mean 1988-2005 (q25%-q75%)	*Year 2006 (percentile)*	*Mean 1988-2005 (q25%-q75%)*	*Year 2006 (percentile)*
September	87 (67-94)	252 (>94)	32 (25-36)	57 (94)
October	80 (24-117)	42 (39)	24 (12-34)	13 (33)
November	61 (21-84)	26 (37)	21 (10-26)	22 (74)
December	55 (23-72)	40 (63)	23 (11-30)	22 (63)

4.2. Discharge and suspended sediment concentration

Table 4 summarises *Q* and *SSC* measurements at the four monitored sections. The continuity of discharge increases with increasing catchment size. The smaller catchment, Torrelaribera (Figure 1), shows an ephemeral character with relatively high discharges of up to 0.68 m^3/s quickly following summer thunderstorms and drying up within hours thereafter. Late in the season, discharge becomes more persistent with baseflows of less than 1 l/s. The surrounding Villacarli valley (Figure 1) still showed flashy behaviour with a response time of one to two hours after heavy rainfall, resulting in peak discharges as high as 21 m^3/s, with recessions usually lasting one day. Discharge reached values as low as 0.1 m^3/s but never ceased completely. Cabecera, as the largest of the headwater subcatchments, experienced the highest discharges. The maximum recorded *Q* of 44 m^3/s equals ten times the mean discharge over the study period, evidence of less variability than in the smaller subcatchments. The onset of

floods was on average seven hours later than at Villacarli while water stage would also rise abruptly within a very short time. This delay and the much flatter recession limb testify to a considerably less flashy runoff regime than that at Villacarli. Discharge at Capella (i.e. the catchment outlet) is quantitatively mainly controlled by the behaviour of Cabecera, which, on average, yielded two-thirds of the runoff of the entire catchment, while Villacarli only represents one fifth (Verdú et al., 2006b). The delay of the onset of the floods at Capella when compared to Villacarli varied greatly and even preceded the latter for some cases, showing the effect of small downstream flashy tributaries and heterogeneous rainfall distribution. Approximately, this delay is 10 hours between Torrelaribera and Capella, 7 hours between Villacarli and Capella and 5 hours between Cabecera and Capella. The different runoff response characteristics are also reflected in the occurrence of floods in the subcatchments. Whereas 13 and 11 flood events were identified in Torrelaribera and Villacarli, respectively, only 8 flood events occurred in Cabecera. Moreover, the latter floods are considerably delayed with regard to Villacarli and in one case are not related to a corresponding flood at all. Further downstream at the Capella station, only 10 floods have been observed.

Suspended sediment concentration follows a pattern similar to the discharge. In Torrelaribera, the observed concentrations range from a few milligrams to 240 g/l, covering six orders of magnitude. The recession of *SSC* to pre-flood level is usually quicker than the recession of the hydrograph but can be interrupted by rainbursts. This behaviour could also be observed in Villacarli, where the measured range of *SSC* is even larger (for more details see Table 4). Maximum *SSC* at Cabecera station reached 30 g/l registered during September floods. However, after this month the maximum observed *SSC* decreased to less than 2 g/l. Thus, *SSC* is generally one order of magnitude lower than those measured in Torrelaribera and Villacarli. Dynamics appear mainly influenced by local rainbursts, which often produce *SSC* peaks long before maximum discharge is reached. At the Capella section, *SSC* during September floods frequently exceeded 50 g/l, decreasing to peak values of approximately 8 g/l during late autumn floods. At all observation sites, the magnitude of discharge and *SSC* decreased from the end of the summer throughout the autumn: the onset of heavy storm events after the summer dry period (September) caused the most extreme values of both

discharge and *SSC*. As rainfall as the driving force decreased (Table 3), so did the magnitude of the flood events and the related sediment concentrations.

Table 4. Summary of measured discharge (*Q*) and suspended sediment concentration (*SSC*) data.

Subcatchment	***Q***						***SSC***		
	[m^3 s^{-1}]			*[l (s ha)$^{-1}$]*			*[g l^{-1}]*		
	min	mean	max	min	mean	max	min	median	max
Torrelaribera (n=122)	0	0.002	0.68	0	0.25	85	0.001	2.8	240.6
Villacarli (n=104)	0.1	0.65	21.2	0.02	0.16	5.17	0.001	1.3	277.9
Cabecera (n=66)	0.91	3.77	43.4	0.06	0.26	2.99	0.002	0.1	30.5
Capella (n=331)	0.5	5.6	64.3	0.01	0.13	1.46	0.0005	1.2	99.6

Table 5. Performance of *SSC*-prediction using *QRF* in comparison with traditional sediment rating curves.

	model	R_{Sp}		**Optimism in R_{Sp}**
		full dataset	**test data**	
Torrelaribera	*SSC* ~ *Q*	0.75	0.74	0.25
	log(*SSC*) ~ log(*Q*)	0.75	0.74	0.18
	QRF	0.91	0.87	0.22
Villacarli	*SSC* ~ *Q*	0.64	0.64	0.24
	log(*SSC*) ~ log(*Q*)	0.64	0.63	0.25
	QRF	0.89	0.83	0.09
Cabecera	*SSC* ~ *Q*	0.40	0.39	0.24
	log(*SSC*) ~ log(*Q*)	0.40	0.39	0.29
	QRF	0.67	0.67	0.09
Capella	*SSC* ~ *Q*	0.16	0.16	0.02
	log(*SSC*) ~ log(*Q*)	0.16	0.16	0.00
	QRF	0.95	0.88	0.05

4.3. Interpolation of SSC measurements

For the four headwater monitoring sections, the traditional application of a rating curve model (hereafter *SRC*) in the form of log(*SSC*)~log(*Q*) performs unsatisfactorily (Table 5), especially with regard to the temporal dynamics and general trend of seasonal decline in *SSC*s. For all observation sites, the *QRF* model provides a better goodness of fit, especially for Cabecera and Capella. For Villacarli and Cabecera, the *QRF*

furthermore shows lower values for optimism in R_{Sp}, making the model more robust and less dependent on single measurements.

Figure 2 plots the variable importance of the 12 most important predictors for the *QRF*-models. The results confirm that discharge is insufficient for *SSC* prediction if not supplemented by other ancillary predictors. The important role of the Julian day underlines the strong seasonal dependence of sediment dynamics. For Cabecera, discharge is not even among the most appropriate predictors, suggesting that areas of major discharge generation do not coincide with the major sediment sources.

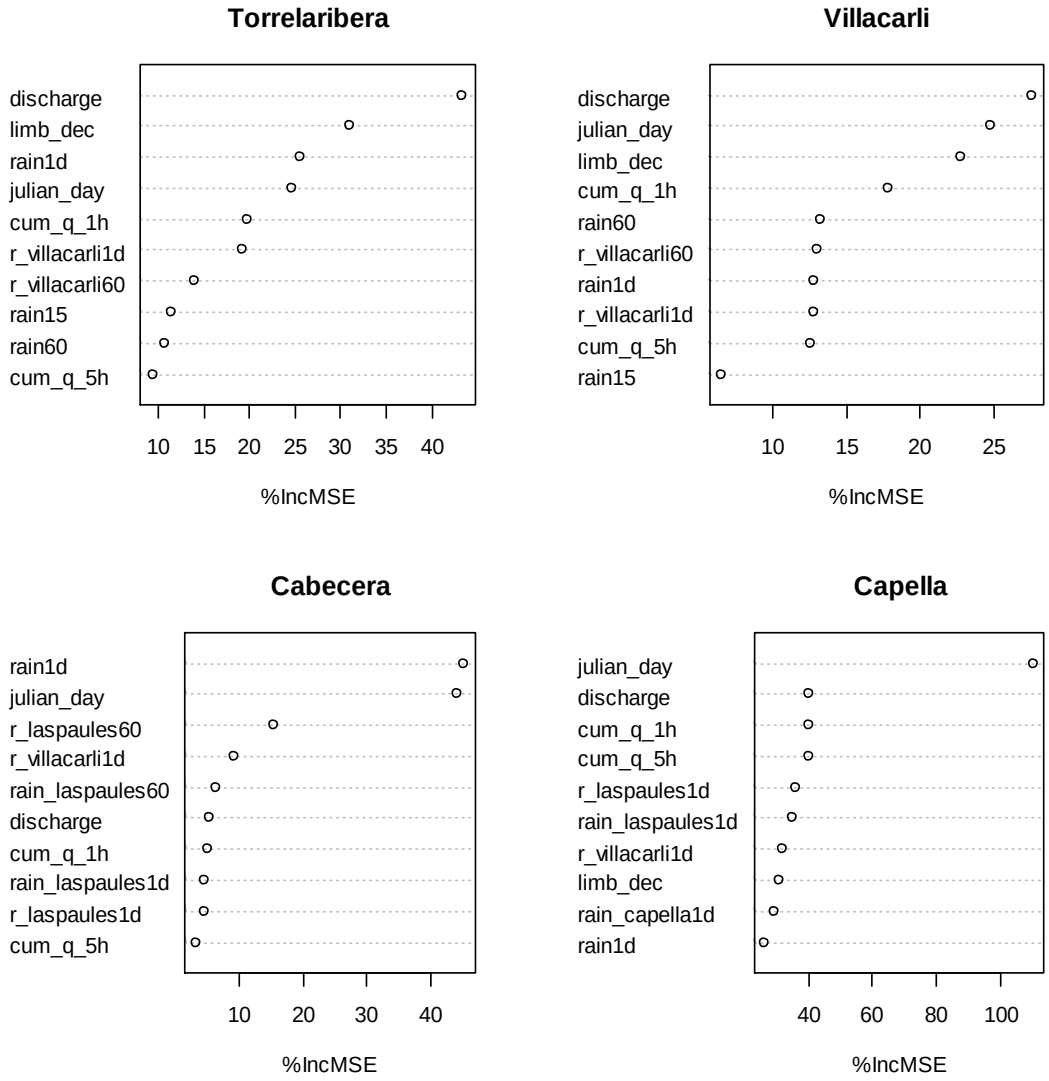

Figure 2. Variable importance for prediction of *SSC* (for details cf. section 3.2)

4.4. Sedigraph prediction

The reconstructed sedigraphs show moderate to good agreement with the observed data (Table 5, Figure 3). However, high *SSC* values, especially at the beginning of the observation period, are partially underestimated, probably resulting from the low number of observations of this kind and the characteristics of conservative estimation of *QRF*. The confidence bounds are quite narrow shortly after the peak of the event and during low flows, but widen considerably during periods of high dynamics, reflecting a higher level of uncertainty in these estimates. At the Torrelaribera and Villacarli stations *SSC* values tend to be somewhat overestimated during low-flow periods at the beginning of the observation period. For Villacarli with continuous runoff, this effect may lead to a slight overestimation of the early inter-flood sediment yields, while it is irrelevant for Torrelaribera because of the ephemeral runoff regimen.

4.5. Sediment yield

Mean flood-based sediment yields for Torrelaribera (see Figure 4 and Table 6) range from 0.2 to 161 t, with *CI* 95 % ranging from 6 % (flood 4) to 39 % (flood 7) of the estimated value. Interflood periods are generally negligible in terms of sediment yield, with the low-flow period between flood 4 and 5 being the exception with an export budget of 2.1 t. During the entire observation period, 99.5 % of the sediment export occurred during floods.

At Villacarli station (see Figure 4 and Table 6), mean flood-based sediment yields varied from 57 to 47,500 t, with *CI* 95 % ranging from 10 % (flood 3) to 38 % (flood 5). Even between floods, significant amounts of sediment (i.e. 6% of the total sediment yield of the study period) were exported from the catchment, especially at the beginning of the observation period. Interflood periods preceding floods 2 and 6 yielded several hundred tons, exceeding greatly the yield of the late autumn periods. The concentration of sediment export in late summer and early autumn is much more pronounced than for Torrelaribera, which hints at the importance of flushing effects and depletion of temporary sediment storage.

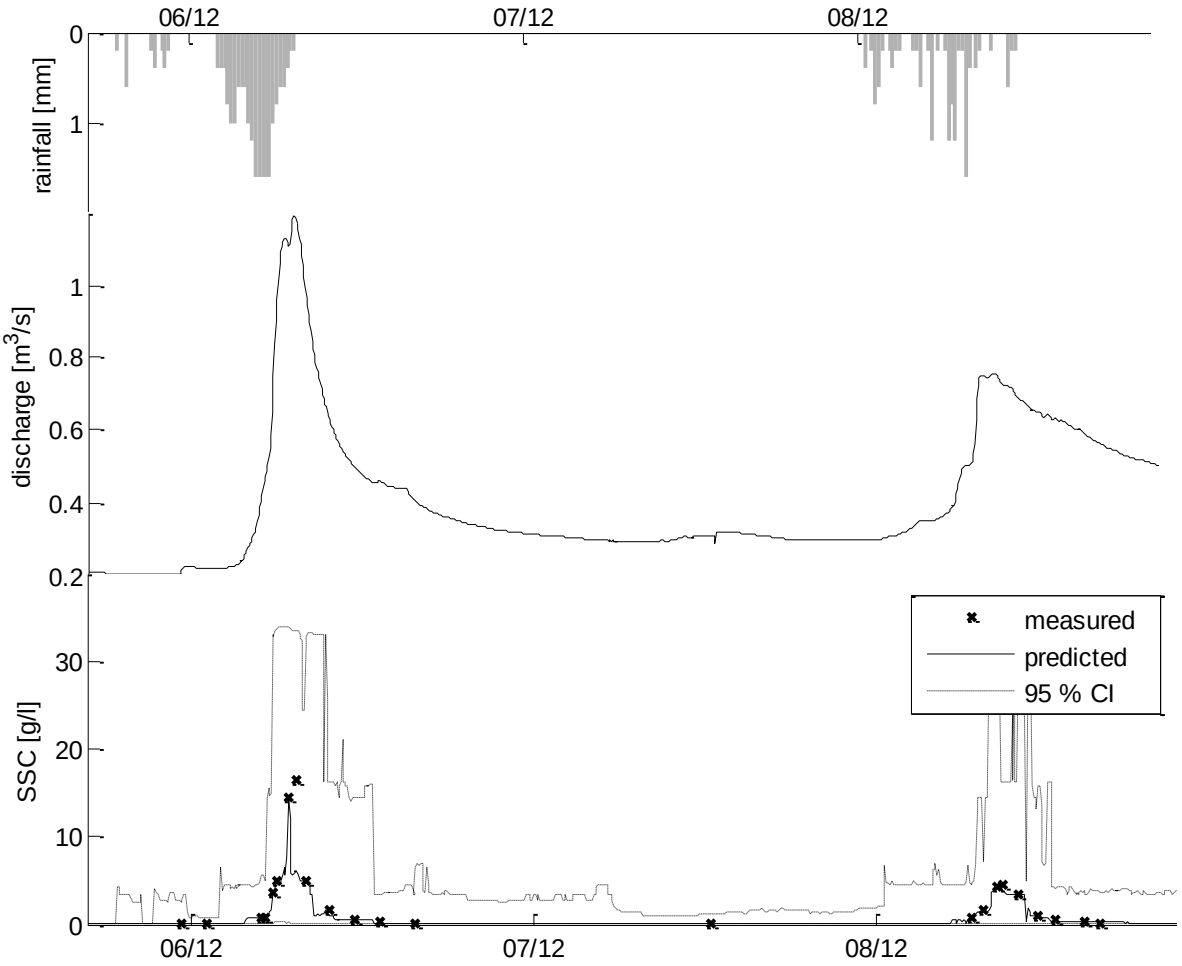

Figure 3. Close-up-view of rainfall, discharge and *SSC* (measured and modelled) for two floods at Villacarli (*CI*: 95 % confidence interval).

Mean flood-based sediment yields at Cabecera (see Figure 4 and Table 6) varied from 33 to 16,073 t, with *CI* 95 % ranging from 7 % (flood 1) to 26 % (flood 4) of the estimated value. Apparently, sediment concentration is less variable at Cabecera, enabling better predictability and narrower *CI*, in comparison with Torrelaribera and Villacarli. Interflood periods yielded several hundred tons in the early observation period and thus exceeded those of the late autumn floods. The total contribution of interflood periods is 5 % of the overall sediment yield. The seasonal trend of decreasing sediment yield is even more pronounced than for Villacarli: sediment transport (flood and interflood periods) mainly took place during the first floods after summer, later floods contribute only very little to the overall yield. Overall export rates are considerably lower than those at Villacarli, despite the larger catchment area (see

discussion below).

At the catchment outlet in Capella the highest sediment yield could be observed during the September floods, which exported up to 84,000 t from the catchment (see Figure 4 and Table 6). Thus, the two strong September floods 4 and 5 accounted for nearly 77 % of the total suspended load for the whole study period. Later floods of similar water yield produced only a fraction of this amount, producing yields in the order of the interflood periods only. However, looking at the entire observation period, low flows contributed to 6 % of the overall sediment transport. Only one *SSC* sample is available for the low flow period in early September. This seemed to lead to an implausibly high estimate of *SSC* and yield during that period. Therefore, that period has been excluded from analysis.

For all locations, the highest sediment export rates from the catchment could be observed during the first floods of late summer and early autumn. During that period, the overall amount of rainfall was highest and the most intense storms occurred, which generated much runoff. For Torrelaribera and Villacarli, the sediment yield is closely related to the overall runoff of the floods. This effect could not be observed for Cabecera and Capella where sediment is exported virtually completely during the first two major floods (i.e. 98 and 77 % of the total yield, respectively); successive floods contribute only with minor yields.

5. DISCUSSION AND FINAL REMARKS

The length of the observation period confined to 3 months and the unusual wet September greatly limit the long-term representativity of the obtained values. Thus, even though late summer/autumn is presumably the season of highest sediment export rates of more than 70 % of the annual yield (Gallart et al., 2005; López-Tarazón, 2006) and are therefore responsible for a major part of the annual sediment yield, the given values may not be representative of the long term average. This temporal extrapolation is especially problematic as annual yields may be subject to major variability of up to an order of magnitude (Regüés *et al.*, 2000).

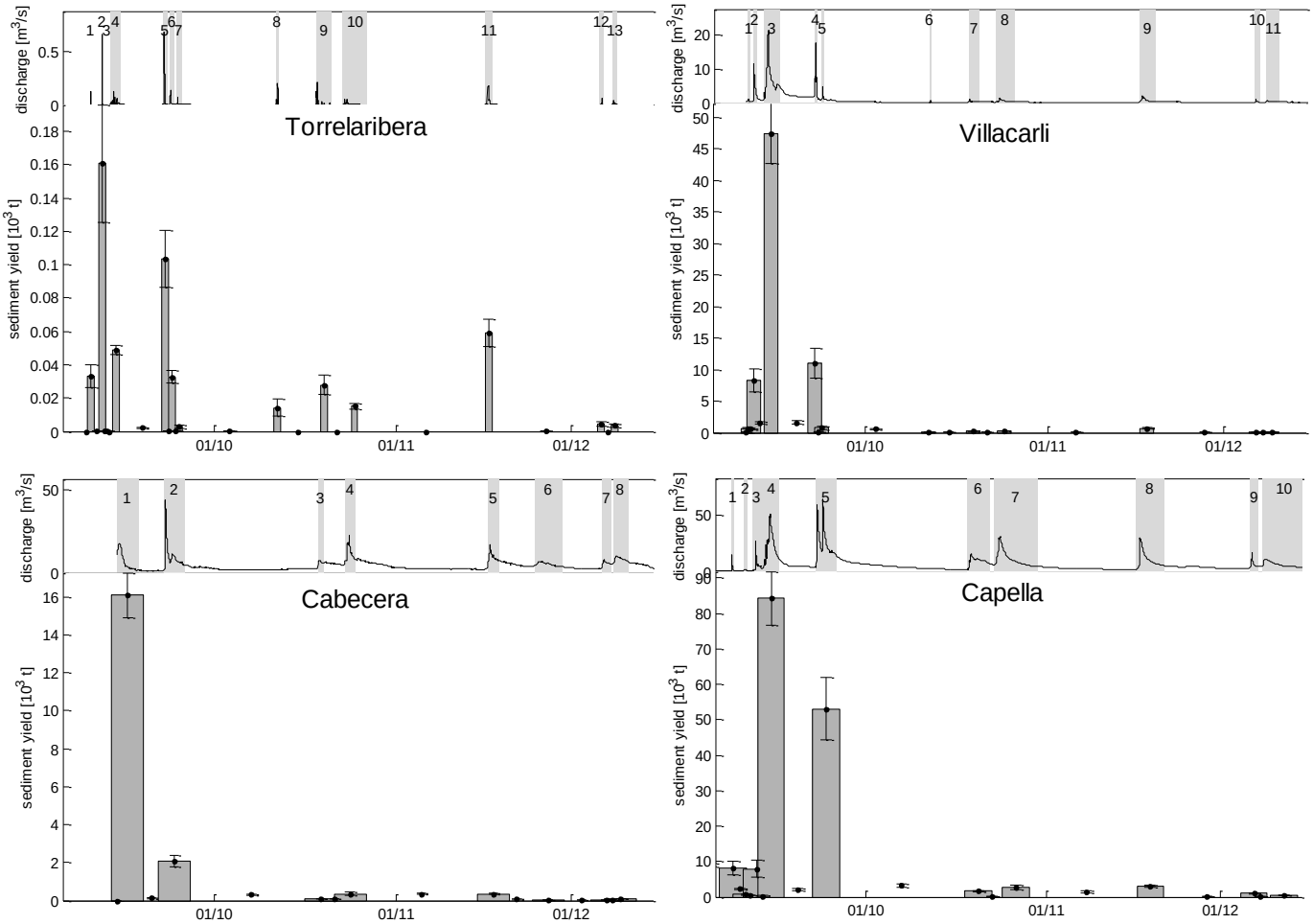

Figure 4. Sediment yield of flood (bars and whiskers) and interflood (whiskers only) periods. The whiskers comprise the 95 % *CI*. The grey bars underlying the hydrograph depict the numbering of the floods.

During the observation period, approximately 74,100 t of suspended sediment were exported from the Villacarli catchment (41 km^2). The Cabecera catchment (145 km^2) yielded around 20,000 t in the same period (Table 7). Relating these numbers to the catchment area results in specific sediment yields (hereafter *SSY*) for the monitoring period of 1971 and 139 t km^{-2}, respectively. The above-mentioned limitations notwithstanding, the former value suggests a very high sediment activity and compares with mean annual sediment yields of similar catchments such as those in the Vallcebre area with badlands (2800 t km^{-2} a^{-1}, Regüés *et al.*, 2000, 5 year of monitoring), despite being 40 times larger in area. The *SSY* obtained for the entire Isábena catchment at Capella is 410 t km^{-2}. This number is slightly above the 350 t km^{-2} a^{-1} yield for the entire

Ésera catchment by Sanz Montero *et al.* (1996) and ranks as moderate to high in relation to data for 44 Mediterranean catchments given by de Vente *et al.* (2006), both being long-term estimates derived from reservoir siltation. The great difference in *SSY* between the adjacent catchments of Villacarli and Cabecera underlines the influence of different hydrological response and, especially, the predominant role of badlands (covering 6 % of the Villacarli subcatchment) as the primary sediment source for the Villacarli torrent, a geological formation that is almost absent in the Cabecera catchment (<0.1 % of area).

Table 6. Flood based sediment yields. Note that the flood numbers are not related between locations.

Location	Flood number	Begin	Duration [h]	Rainfall [mm]	Total runoff [m^3]	Sediment yield [t]	CI sediment yields [t]
Torrelaribera	1	09.09.	3	9	478	33.1	26.2 - 40.0
	2	11.09.	2	13	2,170	160.8	125.5 - 196.1
	3	12.09.	2	6	8	0.2	0.1 - 0.2
	4	13.09.	39	107	1,771	48.7	45.9 - 51.4
	5	22.09.	17	53	3,391	103.4	86.2 - 120.6
	6	23.09.	22	28	1,590	32.6	29.0 - 36.3
	7	24.09.	19	9	392	2.8	1.7 - 3.9
	8	11.10.	8	11	331	14.3	9.4 - 19.2
	9	18.10.	62	34	1,082	28.0	22.3 - 33.7
	10	22.10.	96	32	1,182	15.1	13.3 - 17.0
	11	16.11.	30	49	2,235	58.9	50.9 - 67.0
	12	05.12.	19	22	295	4.5	3.2 - 5.7
	13	08.12.	18	14	350	3.5	2.5 - 4.6
Villacarli	1	10.09.	10	4	27,039	683	582 - 784
	2	11.09.	17	21	268,505	8,263	6,445 – 10,081
	3	13.09.	68	99	1,696,951	47,447	42,665 – 52,230
	4	22.09.	12	54	281,243	11,019	8,669 – 13,369
	5	23.09.	9	27	77,422	743	457 – 1,029
	6	11.10.	8	12	12,064	57	41 - 74
	7	18.10.	42	31	78,311	194	157 - 232
	8	23.10.	74	31	176,044	301	254 - 347
	9	16.11.	67	43	201,012	643	553 - 733
	10	06.12.	23	20	39,905	111	79 - 143
	11	08.12.	52	14	89,263	65	53 - 76

Location	Flood number	Begin	Duration [h]	Rainfall [mm]	Total runoff [m^3]	Sediment yield [t]	CI sediment yields [t]
Cabecera	1	14.09.	88	49	2041,727	16,073	14,874 – 17,272
	2	22.09.	83	96	3,220,319	2,081	1,787 – 2,376
	3	18.10.	23	39	539,922	70	62 - 78
	4	23.10.	40	31	1,703,302	359	265 - 453
	5	16.11.	45	50	1,561,124	359	302 - 417
	6	24.11.	110	12	2,007,849	43	40 - 47
	7	06.12.	38	16	807,548	34	30 - 38
	8	08.12.	60	13	1,799,918	77	70 - 84
Capella	2	10.09.	13	8	65,475	653	6,306 – 10,104
	3	11.09.	43	30	778,536	9,244	504 - 783
	4	13.09.	66	107	5,392,881	84,066	5,669 – 10,283
	5	22.09.	82	85	7,650,513	49,979	76,492 – 91,848
	6	11.10.	11	8	302,157	299	44,336 – 61,906
	7	18.10.	92	41	3,179,673	1671	1,400 – 1,879
	8	23.10.	176	27	6,783,747	2783	2,222 – 3,270
	9	16.11.	119	43	4,395,069	3053	2,718 – 3,384
	10	06.12.	35	21	815,382	1052	932 – 1,154
	11	08.12.	182	12	3,845,718	399	443 - 560

Table 7. Total and specific sediment yield for observation period (95 % confidence interval in brackets).

Gauge	Total sediment yield [t]	Specific sediment yield[t/km^2]
Torrelaribera	509	6,277
	(419-599)	(5,166-7,388)
Villacarli	74103	1,970
	(63,971-84,235)	(1,701-2,240)
Cabecera	20,087	139
	(18,341-21,832)	(127-151)
Capella	173,705	409
	(149,710-197,702)	(353-466)

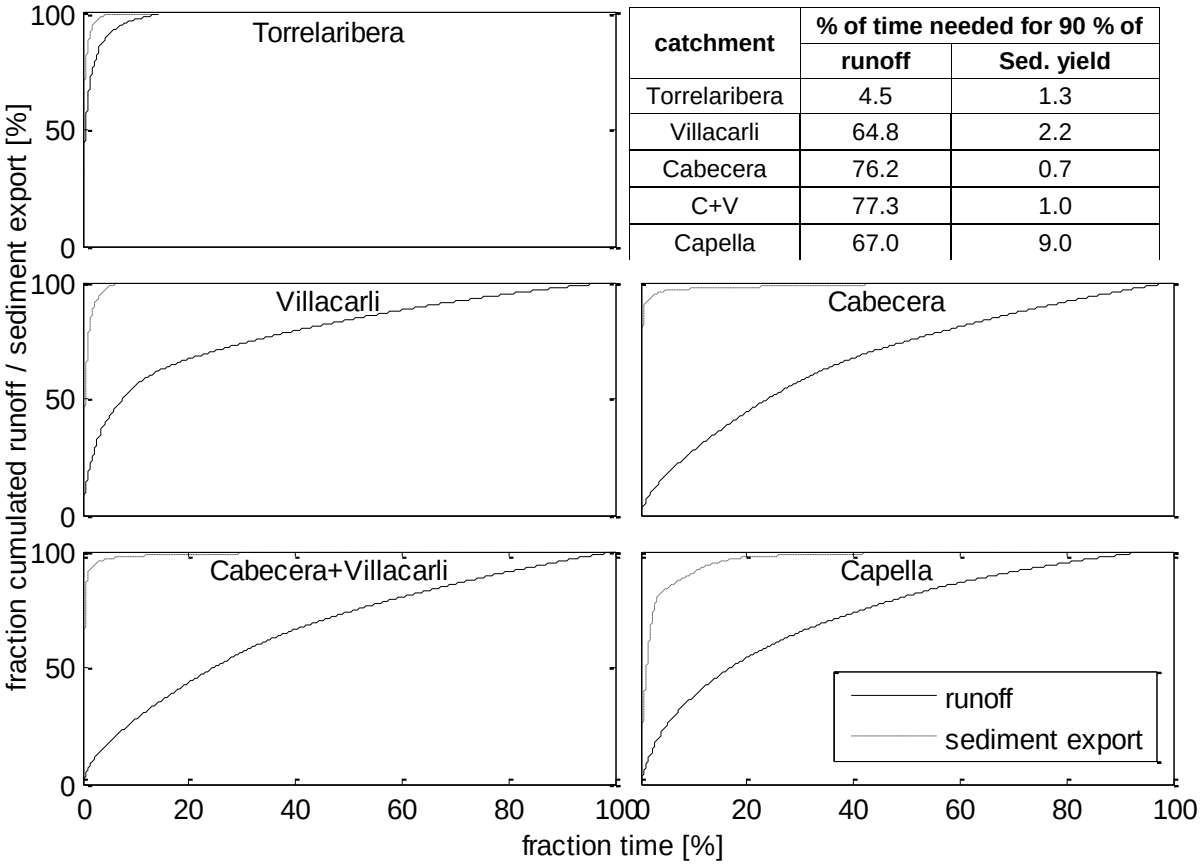

catchment	% of time needed for 90 % of	
	runoff	Sed. yield
Torrelaribera	4.5	1.3
Villacarli	64.8	2.2
Cabecera	76.2	0.7
C+V	77.3	1.0
Capella	67.0	9.0

Figure 5. Duration curves of water and sediment fluxes. Cabecera+Villacarli (C+V) denotes the simulated properties of the confluence of subcatchments Villacarli and Cabecera.

The elementary catchment of Torrelaribera has the highest *SSY* of the three monitored areas. The value of 6277 t km^{-2} falls somewhat short of the 30200 t km^{-2}a^{-1} reported by Martínez-Casasnovas and Poch (1997) and 60000 t km^{-2}a^{-1} reported by Regüés *et al.* (2000) for badland plots in the Vallcebre catchment (5 years of monitoring). This may be attributed to the fact that only 30 % of the Torrelaribera catchment is composed of bare badland slopes. Its special settings result in a sediment delivery ratio of ~70 %, based on the survey of a dateable sediment trap and erosion pin measurements. Thus, using the portion of the basin occupied by such slopes instead of the whole catchment, the *SSY* value is close to the above mentioned values.

As shown in the previous section, most of the sediment load is transported during flood periods, underlining the importance of the temporal distribution of water and sediment

fluxes between flood and interflood periods. This temporal concentration is especially pronounced in Torrelaribera, where less than 1 % of the sediment load is transported during low flow, due to the ephemeral behaviour of the catchment. The pronounced flashiness of Torrelaribera is expressed in the fact that 90 % of water and sediment fluxes occur in only 4 % of the time (Figure 5). For Villacarli and Cabecera, the fraction of sediment transported during low flows is 6.1 and 4.9 %, respectively. The water fluxes from Villacarli, Cabecera and their combined outflow (C+V, i.e. calculated as the sum of the values of each) become successively more balanced with time. In contrast, sediment flux is highly concentrated in time. For C+V, 90 % of the sediment is transported in approximately 1% of the time (i.e. 2.2 % for Villacarli). Further downstream at Capella, sediment flux is somewhat more evenly distributed in time (90% of sediment in 9 % of the time), although the catchment keeps its flashy behaviour with regard to runoff.

Relatively high sediment fluxes even during low flows have also been observed by López-Tarazón (2006) in the lower Isábena. In the relatively dry year of 2005, up to 70 % of the time was required to transport 90 % of the sediment. Although Fargas *et al.* (1997) also identified further sediment sources downstream of the Villacarli-Cabecera confluence, it is unlikely that these provide an asynchronous sediment input to cause a more continuous sediment flux downstream at Capella. This phenomenon is presumably a result of the effect of sediment storage in the river channel, which is supported by field observations, although no quantitative data are available to support this hypothesis yet.

Figure compares the sediment yield calculated for the headwater catchments and the catchment outlet. During the early floods (floods 1 and 2), the headwater catchments, namely Villacarli, release 67 – 100 % of the sediment yield observed at the outlet, suggesting a high degree of sediment connectivity within the river network. During the smaller successive flood in late autumn, the headwater catchments provide only 9-27 % of the sediment loads measured at the outlet. This could be explained by the increasing role of the downstream tributaries as the flood season progresses or the riverbed with temporary sediment deposits as a source for the sediments leaving the catchment.

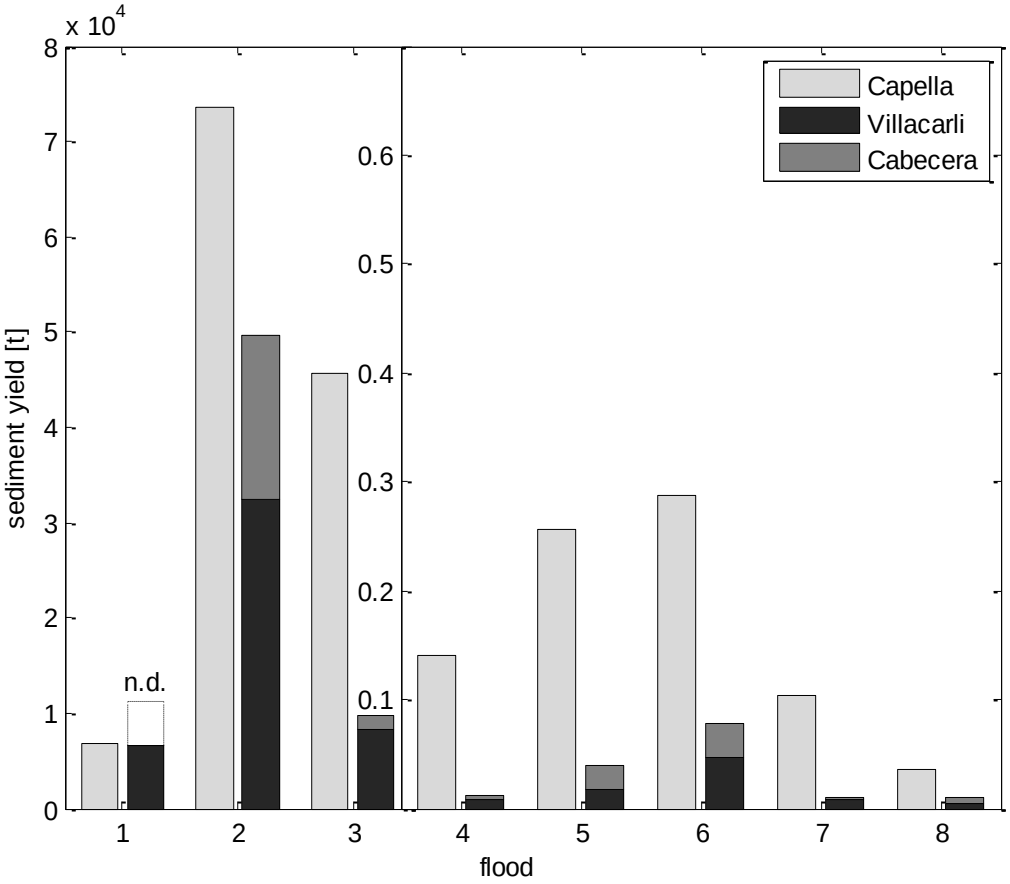

Figure 6. Combined sediment yield of Villacarli and Cabecera compared to sediment yield at Capella. Note the different scale for flood 1-3; "n.d." denotes "no data".

The results of this paper are a synthesis of numerous working steps, some of which are subject to simplifying assumptions and/or a certain degree of error that cannot always be quantified. The major source of error during measurements is related to the water stage–discharge conversion in non-regular cross sections that suffer scour and fill processes during floods. In addition, the higher discharge values are more uncertain because of the extrapolation of the rating curve (i.e. *Q* measurements were increasingly difficult during high flow). Since high sediment fluxes usually coincide with high discharge, errors in the upper part of the rating curve can certainly influence the subsequent calculation of the sediment yield. However, due to the time-series characteristics of the measurements, a certain degree of serial correlation in the data must be expected, which could not be investigated due to the limited number of temporally-close *SSC*-samples. Effectively, the *QRF*-method computes each prediction from a weighted mean of all observations, restricting the range of the predictions to the

range of the observations. Although we are confident of having captured virtually the entire range of *SSC*-conditions, we cannot exclude the possibility of having missed the absolute maximum in *SSC*. The resulting effect of underestimation of peak concentrations and overestimation of low *SSC* has also been observed with linear regression and *ANN* models (Schnabel and Maneta, 2005) and may lead to an underestimation of *SSC* variability. Due to the limited time-span of monitoring and the employed predictor Julian Day, the method cannot be applied. With regard to the inter-annual variability of sediment transport processes and the unusually wet month of September, the obtained results cannot be extrapolated.

The findings of this study reveal the magnitude of the sediment transport processes and their temporal and spatial complexity that require methods of analysis beyond the simple use of traditional rating curves. Further instrumentation is planned to elucidate the role of temporary sediment storage in the river and the contribution of downstream tributaries. The results will be used to validate whether the current process-based modelling approach in the river is appropriate. Alternatively, the use of a more empirical approach using the shape of the sediment duration curves as a function of the catchment size is to be considered.

Acknowledgements

This research was carried out within the SESAM-project (Sediment Export from Semi-Arid catchments: Measurement and Modelling) funded by the German Science Foundation (Deutsche Forschungsgemeinschaft, DFG). The second author has a research grant funded by the Catalan Government and the European Social Fund. Rainfall data were obtained from the Spanish National Institute of Meteorology and the Ebro Water Authorities (SAIH). Hydrological data were supplied by the Ebro Water Authorities (SAIH). The Ebro Water Authorities also provided logistic support for using the Capella gauging station. Thanks are due to the students of the University of Potsdam assisting in the field and in the laboratory.

REFERENCES

Breiman, L. 2001. Random Forests. *Machine Learning*, **45**(1): 5-32.

Breiman, L.M., Friedman, J., Olshen, R., Stone, C., 1984. *Classification and regression trees*. Wadsworth: Belmont, CA.

Bronstert, A., Batalla, R.J., de Araújo, J.C., Francke, T., Güntner, A., Mamede, G., Müller., E., 2007. Investigating erosion and sediment transport from head-waters to catchments to reduce reservoir siltation in drylands. In: *Reducing the Vulnerability of Societies to Water Related Risks at the Basin Scale* (Proceedings of the third International Symposium on Integrated Water Resources Management, Bochum, Germany, September 2006). IAHS Publ. 317

Clotet, N., Gallart, F., Balasch, J.C., 1988. Medium-term erosion rates in a small scarcely vegetated catchment in the Pyrenees. In: Imeson, A.C. (ed): *Geomorphic processes in environments with strong seasonal contrasts*, Vol. 2. *Catena*, **13**: 37-47.

Fargas, D., Martínez-Casasnovas, J., Poch, R., 1997. Identification of Critical Sediment Source Areas at Regional Level. *Physics and Chemistry of the Earth*, **22**(3-4): 355-359.

Gallart, F., Balasch, J.C., Regüés, D., Soler, M., Castelltort, X., 2005. Catchment dynamics in a Mediterranean mountain environment: the Vallcebre research basins (southeastern Pyrenees) II: temporal and spatial dynamics of erosion and stream sediment transport. In: Garcia, C., Batalla, R.J. (eds): *Catchment Dynamics and River Processes: Mediterranean and Other Climate Regions*. Elsevier: 17-29.

Gallart, F., Llorens, P., Latron, J., Regüés, D., 2002. Hydrological processes and their seasonal controls in a small Mediterranean mountain catchment in the Pyrenees. *Hydrology and Earth System Sciences*, **6**(3): 527-537.

Harrell, F.E., 2001. *Regression modeling strategies with applications to linear models, logistic regression, and survival analysis*. Springer: New York.

Liaw, A., Wiener, M., 2002. Classification and Regression by randomForest. *R News*, **2**(3): 18-22.

López-Tarazón, J.A., 2006, Transport de sediment en suspensió al riu Isàbena (conca de l'Ebre). *Unpublished Master-thesis*, Universitat de Lleida.

Mamede, G.L., Bronstert, A., Francke, T., Müller, E., de Araújo, J.C., Batalla, R.J., Güntner, A., 2006. 1D Process-based modelling of reservoir sedimentation: a case study for the Barasona Reservoir in Spain. In: *Conference Proceedings River Flow 2006*. International Conference on Fluvial Hydraulics, Lisbon, September 06-08, 2006.

Martínez-Casasnovas, J., Poch, R., 1997. *Estado de conservación de los suelos de la cuenca del embalse 'Joaquín Costa'*. Zaragoza.

Mathys, N., Klotz, S., Esteves, M., Descroix, L., Lapetite, J.M., 2005. Runoff and erosion in the Black Marls of the French Alps: Observations and measurements at the plot scale. *Catena*, **63(**2-3): 261-281.

Meinshausen, N., 2006. Quantile Regression Forests. *Journal of Machine Learning Research*, **7**: 983-999.

Meinshausen, N., 2007. *quantregForest: Quantile Regression Forests*, R package version 0.2-2.

Mosley, M.P., McKerchar, A., 1993. Streamflow. In: Maidment, D.R. (ed): *Handbook of Hydrology*, McGraw-Hill: New York; 8.1-8.39.

Regüés, D., Balasch, J.C., Castelltort, X., Soler, M., Gallart, F., 2000. Relación entre las tendencias temporales de producción y transporte de sedimentos y las condiciones climáticas en una pequeña cuenca de montaña mediterránea (Vallcebre, Eastern Pyrenees). *Cuadernos de Investigación Geográfica*, **26**: 24-41.

Regüés, D., Guardia, R., Gallart, F., 2000. Geomorphic agents versus vegetation spreading as causes of badland occurrence in a Mediterranean subhumid mountainous area. *Catena*, **25**: 199 – 212.

R-Team Development Core. 2006. *R: A Language and Environment for Statistical Computing*. R Foundation for Statistical Computing: Vienna, Austria.

Sanz-Montero, M., Cobo-Rayán, R., Avendaño-Salas, C., Gómez-Montaña, J., 1996. Influence of the drainage basin area on the sediment yield to Spanish reservoirs. In: *Proceedings of the First European Conference and Trace Exposition on Control Erosion.*

Schnabel, S., Maneta, M., 2005. Comparison of a neural network and a regression model to estimate suspended sediment in a semiarid basin. In: Batalla, R.J., Garcia, C., (eds): *Geomorphological Processes and Human Impacts in River Basins*, IAHS Publication 299, 91-100.

Valero-Garcés, B.L., Navas, A., Machín, J., Walling, D.E., 1999. Sediment sources and siltation in mountain reservoirs: a case study from the Central Spanish Pyrenees. *Geomorphology*, **28**: 23–41.

de Vente, J., Poesen, J., Bazzoffi, P., Van Rompaey, A., Verstraeten, G., 2006. Predicting catchment sediment yield in Mediterranean environments: the importance of sediment sources and connectivity in Italian drainage basins. *Earth Surface Processes and Landforms,* **31**: 1017–1034.

Verdú, J.M., Batalla, R.J., Martínez-Casasnovas, J.A., 2006a. Estudio hidrológico de la cuenca del río Isábena (Cuenca del Ebro). I: Variabilidad de la precipitación. *Ingeniería del Agua*, **13**(4): 321-330.

Verdú, J.M., Batalla, R.J., Martínez-Casasnovas, J.A., 2006b. Estudio hidrológico de la cuenca del río Isábena (Cuenca del Ebro). II: Respuesta hidrológica. *Ingeniería del Agua*, **13**(4): 331-343.

Walling, D.E., 1984. Dissolved loads and their measurements. In: Hadley, R.F., Walling, D.E. (eds): *Erosion and sediment yield: Some methods of measurements and modeling*. Geo Books: London; 111-177.